Spring 3-28-2022

OCEAN QUAHOG (ARCTICA ISLANDICA) POPULATION DYNAMICS: SEX-BASED DEMOGRAPHICS AND REGIONAL COMPARISONS IN THE NORTHWEST ATLANTIC

Kathleen M. Hemeon

OCEAN QUAHOG (ARCTICA ISLANDICA) POPULATION DYNAMICS: SEX-BASED DEMOGRAPHICS AND REGIONAL COMPARISONS IN THE NORTHWEST ATLANTIC

by

Kathleen M. Hemeon

A Dissertation
Submitted to the Graduate School,
the College of Arts and Sciences
and the School of Ocean Science and Engineering
at The University of Southern Mississippi
in Partial Fulfillment of the Requirements
for the Degree of Doctor of Philosophy

Approved by:

Dr. Eric N. Powell, Committee Chair
Dr. M. Zachary Darnell
Dr. John Klinck
Dr. Roger Mann
Dr. Wei Wu

May 2022

Published by the Graduate School

THE UNIVERSITY OF SOUTHERN MISSISSIPPI

ABSTRACT

Arctica islandica (ocean quahog) is the longest-lived bivalve on Earth. Individuals on the deep continental shelf of the Mid-Atlantic (US) can survive for centuries, and when found in the colder, boreal waters of Iceland, ages over 500 years can be reached. The ocean quahog is important in the US, yet very little is known about the resiliency of the ocean quahog stock to fishing activity, and ocean quahog recruitment patterns over time. To quantify and constrain age-reader error prior to age analysis, a triple-method error protocol was developed for *A. islandica* that included age-reader bias, precision, and error frequency. The error protocol was implemented for samples collected in 2017 from Georges Bank (GB) and Long Island (LI) in the US Mid-Atlantic. Assumptions of prolonged lapses in recruitment were not substantiated for either the GB or LI populations, yearly cohorts were observed for the past century, and both populations presented recruitment pulses in regular 8-y periods. The oldest animal at GB was a 261-year-old male, and the oldest animal at LI was a 310-year-old male. Estimated ages from this study are older than previously reported for the US Mid-Atlantic. Total mortality was higher at GB than LI, and higher for GB females than GB males. Constructed ALKs were reliable but not interchangeable between sexes or populations. The population sex ratio at GB was 1.1.1 (F:M), whereas LI was 1:1.4 and relatively deficient in fishery-sized females. The Modified Tanaka growth model was the best fit growth function for *A. islandica* age-length data from the Mid-Atlantic, and growth models changed over time dependent on birth year. Indexed growth from both populations expressed significant 31-y frequency periods, where GB growth lagged behind LI between 1760-1950. Growth rates of *A. islandica* from both populations have

continuously increased since the mid-1800s, female growth rates are faster than males, and growth rates at GB are generally faster than those at LI. Females dominated large size classes, males dominated small size classes, and evidence strongly suggests that this species is sexually dimorphic.

ACKNOWLEDGMENTS

First, I would like to thank my advisor, Dr. Powell, for his dedicated mentorship and patience while I learned the ins and outs of fishery population dynamics and associated statistics. Committee member Dr. Mann provided bivalve expertise and access to his Molluscan Ecology Lab at the Virginia Institute of Marine Science where over 1,500 *Arctica* samples were processed for this dissertation. Wavelet analyses would not have been possible without the expert guidance of Dr. Klinck to direct me through this complex analysis. Committee members Dr. Wu contributed statistical assistance and encouragement throughout the dissertation process, and Dr. Darnell provided outside ecological perspective to this project.

I would also like to acknowledge the Seawatch International crew from the F/V E.S.S. Pursuit for their assistance in collecting field samples and the use of their industry gear and personnel. Additionally, the Northeast Fisheries Science Center Fishery Biology Program and Population Dynamics Branch (particularly Dr. Hennen and Eric Robillard) who provided expert training in ocean quahog management and the development of age-reader error analysis. Finally, I would like to recognize the contributions of my colleagues in the Dr. Powell and Dr. Mann labs who were essential to the ongoing development of age-reader error protocols and aging methodologies for *Arctica islandica*.

This research was financially supported by the National Science Foundation (NSF) and the Science Center for Marine Fisheries (SCEMFIS) under NSF awards 1266057 and 1841112, through membership fees provided by the SCEMFIS Industry Advisory Board, and an NSF non-academic research internship.

DEDICATION

This dissertation is dedicated to:

My parents Frank and Jennifer

My husband Jacob

My desk companions Luna, Momo, and Fox

A dissertation written during the time of covid would not have been as successful, or nearly as fun, without your love and support.

TABLE OF CONTENTS

LIST OF TABLES

LIST OF FIGURES

LIST OF ABBREVIATIONS

USM	The University of Southern Mississippi
SCEMFIS	Science Center for Marine Fisheries
GB	Georges Bank
LI	Long Island
ALK	Age-length key
CV	Coefficient of variation
ACV	Average coefficient of variation
AMO	Atlantic Multi-decadal Oscillation
NAO	North Atlantic Oscillation
MAB	Mid-Atlantic Bight

CHAPTER I INTRODUCTION

1.1 Species Description

Ocean quahogs (*Arctica islandica*, Linnaeus 1767) are boreal bivalves that have an expansive range in the North Atlantic, and currently occupy cold shelf waters from the White Sea at northern latitudes, through the Norwegian Sea, around the British Isles to Iceland, and finally from Newfoundland Canada as far south as southern Virginia, US (Dahlgren et al. 2000). The last extant species of the family Arcticidae, *A. islandica* grow optimally in water temperatures between 6-16ºC (Golikov & Scarlato 1973, Merrill et al. 1969) and at depths conducive to cool waters, typically between 21-61m (Merrill & Ropes 1969, Serchuk et al. 1982). When conditions are suboptimal, such as during extreme temperatures, storm events, or limited food availability, this species can burrow into the sediment to a mean maximum depth of 85 mm (± 17 mm) and remain buried for up to seven days while metabolic activity is drastically curtailed (Taylor 1976, Oeschger 1990, Strahl et al. 2011, Sosnowska et al. 2014, Ragnarsson & Thorarinsdóttir 2020).

This species is remarkable in that maximum observed ages exceed 500 y and, in the Mid-Atlantic, ages of up to 200 y have been estimated (Butler er al. 2013, Pace et al. 2017a,b). The causation of such longevity is widely debated, but it has been postulated that longevity may be associated with reduced metabolism during deep burial that may suspend aging due to suppressed reactive oxygen production and oxidative stress (Ungvari et al. 2011), elevated antioxidant capacity (Abele et al. 2008), accumulation of nucleic acid oxidation (Gruber et al. 2015), and low somatic maintenance energy demands (Ballesta-Artero et al. 2019) possibly due to low cell turnover rates (Strahl & Abele 2009) during such burrowing behavior; although, telomere-length maintenance has

also been considered (Gruber et al. 2014). Regardless of the underlying causal mechanism for this extreme longevity, *A. islandica* survive for centuries in comparatively the same location and, due to poikilothermic energetics, grow in synchrony with benthic cycles (temperature, salinity, phytoplankton abundance, physical disturbance events) and act as biorecorders to describe greater paleochronologies (Schöne et al. 2005, Butler et al. 2010, Schöne 2013, Marali & Schöne 2015, Mette et al. 2016, Begum et al. 2019, Poitevin et al. 2019).

Three traditional methods exist to age a bivalve that include counts of concentric annual growth bands (annuli) on the external shell valve (see Stevenson & Dickie 1954), counts of annuli in the hinge ligament (Merrill et al. 1966), and internal annuli counts of a cross sectioned valve using acetate peels (see Ropes et al 1984) or high-resolution imaging (Pace et al. 2017a). Due to the longevity of *A. islandica,* annuli at the outer shell edge are compacted and difficult to age ("edge effect"). Therefore, this species of bivalve requires that the shell be cross sectioned to expose internal annuli, and either acetate peels must be taken of the exposed hinge plate (see Ropes et al. 1984) to be viewed optically, or highly-polished cross-sectioned hinge plates must be imaged with a high-resolution camera and compound microscope (Figure 1.1) (see Pace et al. 2017a). Both methods display clear annuli differentiation at the growing edge. Whether an acetate peel or images are applied for age estimations, the processes used to age *A. islandica* are expensive and time consuming and with hundreds of possible age classes, high reader error rates can occur.

Arctica islandica age is measured as the sum of the internal annuli in the hinge plate, and annual growth is measured as the length of light carbonate deposited between

hinge plate annuli (Figure 1.2). Growth in the hinge plate is proportional to growth on the outer shell valve; therefore annual hinge plate growth can be extrapolated to annual valve growth to obtain annual growth rates in relation to the total shell length of an individual (Thompson et al. 1980a). Light carbonate growth deposition initiates in March-April with rapid growth in the late spring and early summer, followed by slower growth from approximately July-August during the warmest months (Jones 1980). The dark annuli bookmark the lighter carbonate growth are deposited in late fall, commencing in September for many individuals, with slowest annuli growth during the coldest months (Jones 1980). Spawning typically occurs in tandem with the formation of annuli, where ripe and spent gonadal stages transpire between September-December (Jones 1980); however, spawning timing and duration are highly variable for this species and is greatly dependent on oceanographic conditions of that year (Jones 1981). Also highly variable are the growth rates between *A. islandica* cohorts that coexist in contemporary populations (Pace et al. 2018). As growth is dependent on features such as temperature, food availability, and salinity, the conditions experienced by each cohort determine the time needed to reach a particular size (growth rate). With each cohort reaching size classes at different ages, the age compositions within a single 5-mm size class can span hundreds of years and restrict any meaningful prediction of age at size within a population.

1.2 Fishery Management

As the longest-living bivalve on Earth, *A. islandica* can achieve lifespans longer than 200 y in the US Mid-Atlantic; however, age determinations are difficult to estimate and age variability at size is extreme (Pace et al. 2017a, 2017b). *Arctica islandica* is a

commercially important bivalve in the eastern United States (US) but very little is known about the recruitment frequency and rebuilding capacity of this species due to deficient age composition data applicable at a fishery scale. Therefore, assessment models for *A. islandica* rely solely on length-based metrics (NEFSC 2017, 2020) because of the substantial sample size required to develop adequate population age distributions for such a long-lived species (Pace et al. 2017a), the unknown error associated with age estimates, and the extensive time and financial investment required to create production-scale age datasets.

1.3 Project Objectives

This dissertation will expand on previous research completed by Pace et al. (2017a, 2017b, 2018) to develop more robust, and data-rich, age-length keys and corresponding population dynamics data for the Georges Bank and Long Island *A. islandica* populations. Analyses will create the two largest ocean quahog age databases in the world for a single population, while also analyzing sex differentials in growth rates, identifying changing growth rates over time, and providing inferential population dynamics from age-frequency distributions.

Specifically, objectives for this study include the creation of an extremely large, error-validated, age-composition dataset for *A. islandica* to constrain age-at-length variability, develop reliable age-length keys, and describe sex-based population dynamics for the quasi-virgin population at Georges Bank (GB) and the Long Island (LI) population that over the last two decades has provided the greatest commercial landing of *A. islandica* within the US Mid-Atlantic stock. This study will also assess how growth

rates have changed spatially and temporally to inform future growth dynamics of the fishery when a changing climate is considered.

1.4 Figures

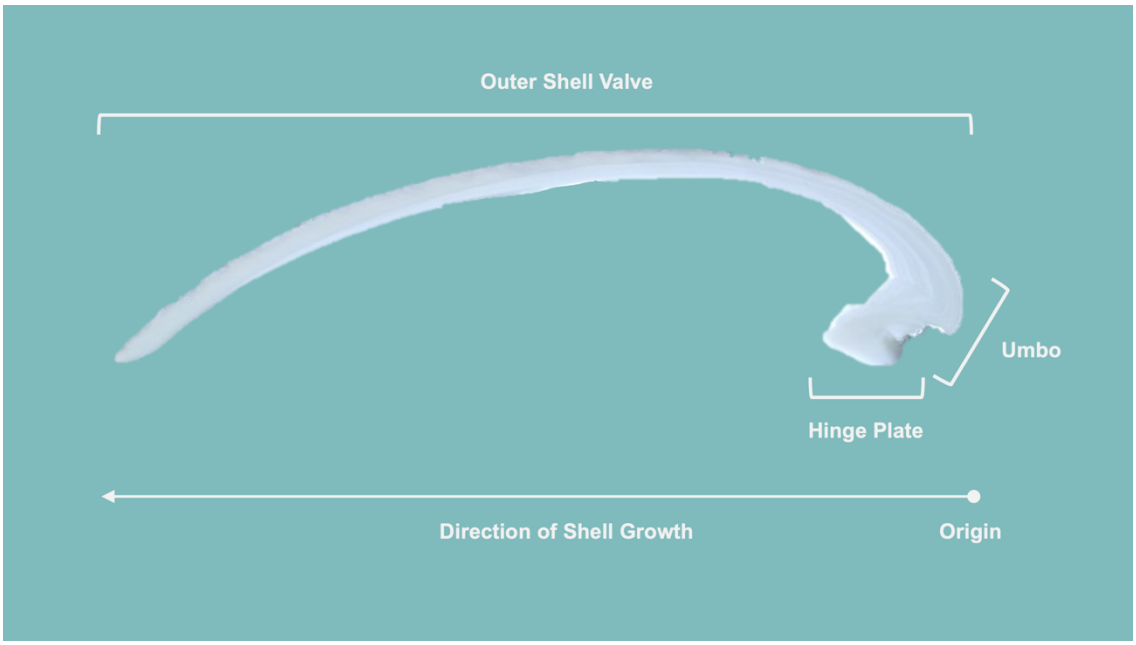

Figure 1.1 Image of shell cross section. Shell valve cut along shell height to expose the concentric and continuous interior annuli in the shell valve, umbo, and hinge plate regions.

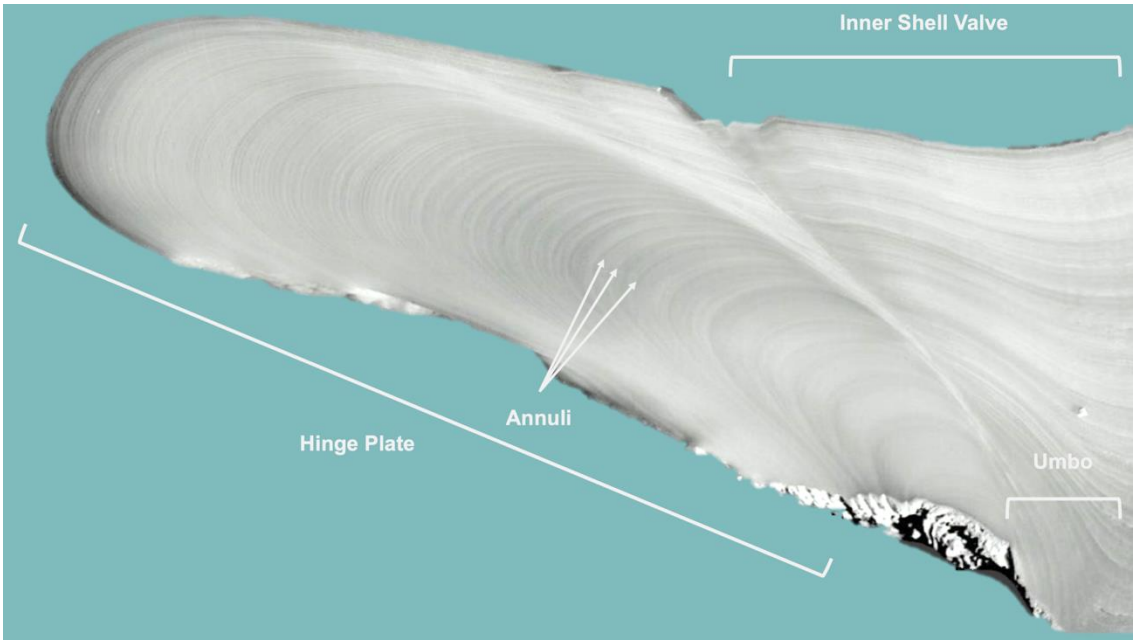

Figure 1.2 Image of shell hinge plate. Magnified image of hinge plate with annuli visible as dark rings.

1.5 References

Abele D, Strahl J, Brey T, Philipp EER (2008) Imperceptible senescence: ageing in the ocean quahog *Arctica islandica*. Free Radic Res 42:474-480

Begum S, Abele D, Brey T (2019) Toward the morphometric calibration of the environmental biorecorders *Arctica islandica*. J Coast Res 35:369-375

Butler PG, Richardson CA, Scourse JD, Wanamaker AD, Shammon TM, Bennell JD (2010) Marine climate in the Irish Sea: analysis of a 489-year marine master chronology derived from growth increments in the shell of the clam *Arctica islandica*. Quat Sci Rev 29:1614-1632

Butler PG, Wanamaker AD, Scourse JD, Richardson CA, Reynolds DJ (2013) Variability of marine climate on the North Icelandic Shelf in a 1357-year proxy archive based on growth increments in the bivalve *Arctica islandica*. Palaeogeogr Palaeoclimatol Palaeoecol 373:141-151

Dahlgren TG, Weinberg JR, Halanych KM (2000) Phylogeography of the ocean quahog (*Arctica islandica*): influences of paleoclimate on genetic diversity and species range. Mar Biol 137:487-495

Golikov, AN, Scarlato OA (1973) Method for indirectly defining optimum temperatures of inhabitancy for marine cold-blooded animals. Mar Biol 20:1-5

Gruber H, Schaible R, Ridgway ID, Chow TT, Held C, Philipp EER (2014) Telomere-independent ageing in the longest-lived non-colonial animal, *Arctica islandica*. Exp Gerontol 51:38-45

Gruber H, Wessels W, Boynton P, Xu J, Wohlgemuth S, Leeuwenburgh C, Qi W, Austad SN, Schaible R, Philipp EER. 2015. Age-related cellular changes in the long-lived bivalve *A. islandica*. Age 37:90

Jones DS (1980) Annual cycle of shell growth increment formation in two continental shelf bivalves and its paleoecologic significance. Palaios 6:331-340

Jones DS (1981) Reproductive cycles of the Atlantic surf clam *Spisula solidissima*, and the ocean quahog *Arctica islandica* off New Jersey. J of Shellfish Res 1:23-32

MAFMC (2020) Environmental Assessment and Regulatory Flexibility Act analysis: 2021-2026 Atlantic surfclam and ocean quahog specifications. Dover, DE: Mid-Atlantic Fishery Management Council. 119 pp

Marali S, Schöne BR (2015) Oceanographic control on shell growth of *Arctica islandica* (Bivalvia) in surface waters of Northeast Iceland — Implications for paleoclimate reconstructions. Palaeogeogr Palaeoclimatol Palaeoecol 420:138-149

Merrill SA, Chamberlin JL, Ropes JW (1969) Ocean quahog fishery. In F.E. Firth ed. Encyclopedia of marine resources. p. 125-129. Van Nostrand Reinhold Publishing Co, NY

Merrill AS, Posgay JA, Nichy FE (1966) Annual marks on shell and ligament of sea scallop *Placopecten magellanicus*. Fish Bull 65:299-311

Mette MJ, Wanamaker AD, Carroll ML, Ambrose WG, Retelle MJ (2016) Linking large-scale climate variability with *Arctica islandica* shell growth and geochemistry in northern Norway. Limnol Oceanogr 61:748-764

NEFSC (2017) 63rd northeast regional stock assessment workshop (63rd SAW) assessment report. Woods Hole, MA: Northeast Fisheries Science Center. NEFSC Ref. Doc.17-10. 414 pp

Oeschger, R (1990) Long-term anaerobiosis in sublittoral marine invertebrates from the western Baltic Sea: *Halicryptus spinulosus* (Priapulida), *Astarte borealis* and *Arctica islandica* (Bivalvia). Mar Ecol Prog Ser 59:133-143

Pace, S. M., E. N. Powell, Mann R (2018) Two-hundred year record of increasing growth rates for ocean quahogs (*Arctica islandica*) from the northwestern Atlantic Ocean. J Exp Mar Biol Ecol 503:8-22

Pace SM, Powell EN, Mann R, Long MC (2017a) Comparison of age-frequency distributions for ocean quahogs *Arctica islandica* on the western Atlantic US continental shelf. Mar Ecol Prog Ser 585:81-98

Pace SM, Powell EN, Mann R, Long MC, Klinck JM (2017b) Development of an age-frequency distribution for ocean quahogs (*Arctica islandica*) on Georges Bank. J Shellfish Res 36:41-53

Poitevin P, Thébault J, Siebert V, Donnet S, Archambault P, Doré J, Chauvaud L, Lazure P (2019) Growth response of *Arctica islandica* to North Atlantic oceanographic conditions since 1850. Front Mar Sci 6:483

Ragnarsson S and Thorarinsdóttir GG (2020) Burrowing behaviour in ocean quahog (*Arctica islandica*) in situ and in the laboratory. *Marine and Freshwater Research Institute, Reykjavík,* no. 2298-9137, 18 pp

Schöne BR (2013) *Arctica islandica* (Bivalvia): A unique paleoenvironmental archive of the northern North Atlantic Ocean. Glob Planet Change 111:199-225

Schöne BR, Houk SD, Castro ADF, Fiebig J, Oschmann W, Kröncke I, Dreyer W, Gosselck F (2005) Daily growth rates in shells of *Arctica islandica*: assessing sub-seasonal Environmental controls on a long-lived bivalve mollusk. Palaios 20:78-92

Serchuk FM, Murawski SA, Ropes JW (1982) Ocean quahog *Arctica islandica*. In MD Grosslein and TR Azarovitz eds. Fish distribution. p. 144-146

Sosnowska D, Richardson C, Sonntag WE, Csiszar A, Ungvari Z, Ridgway I (2014) A heart that beats for 500 years: age-related changes in cardiac proteasome activity, oxidative protein damage and expression of heat shock proteins, inflammatory factors, and mitochondrial complexes in *Arctica islandica*, the longest-living noncolonial animal. J Gerontol A Biol Sci Med Sci 69:1448-1461

Stevenson JA, Dickie LM (1954) Annual growth rings and rate of growth of the giant scallop, *Placopecten magellanicus* (Gmelin) in the Digby area of the Bay of Fundy. J Fish Res Bd Can 11:660–671

Strahl J, Brey T, Philipp EER, Thorarinsdóttir G, Fischer N, Wessels W, Abele D (2011) Physiological responses to self-induced burrowing and metabolic rate depression in the ocean quahog *Arctica islandica*. J Exp Biol 214:4223-4233

Taylor AC (1976) Burrowing behavior and anaerobiosis in the bivalve *Arctica islandica* (L.). J Mar Biol Assoc UK 56:95-109

Thompson I, Jones DS, Dreibelbis D (1980a) Annual internal growth banding and life history of the ocean quahog *Arctica islandica* (Mollusca: Bivalvia). Mar Biol 57:25-34

Thompson I, Jones DS, Ropes JW (1980b) Advanced age for sexual maturity in the ocean quahog *Arctica islandica* (Mollusca: Bivalvia). Mar Biol 57:35-39

Ungvari Z, Ridgway I, Philipp EER, Campbell CM, McQuary P, Chow T, Coelho M, Didier ES, Gelino S, Holmbeck MA, Kim I, Levy E, Sosnowska D, Sonntag WE, Austad SN, Csiszar A (2011) Extreme longevity is associated with increased resistance to oxidative stress in *Arctica islandica*, the longest-living non-colonial animal. J Gerontol A Biol Sci Med Sci 66:741-750

CHAPTER II ATTAINABILITY OF ACCURATE AGE FREQUENCIES FOR OCEAN QUAHOGS (*ARCTICA ISLANDICA*) USING LARGE DATASETS: PROTOCOL, READER PRECISION, AND ERROR ASSESSMENT

Modified from:

Hemeon KM, Powell EN, Robillard E, Pace SM, Redmond TE, Mann R. 2021. Attainability of accurate age frequencies for ocean quahogs (Arctica islandica) using large datasets: protocol, reader precision, and error assessment. J Shellfish Res. 40(2): 255-267.

2.1 Introduction

Calcified structures (e.g., fish otoliths, vertebrae, coral skeletons, and bivalve shells) are commonly used to age animals in the marine realm (Hudson 1981, Pentilla & Dery 1988, Richardson 2001). As the animal grows, calcium carbonate is secreted in layers around the calcified structure and concentric growth rings are created. Growth rings reflect the rate of carbonate deposition correlated with seasonal and annual growth patterns and often retain information on environmental conditions such as temperature and available food (Schöne et al. 2011, Swart 2015, Purroy et al. 2018). The age of an individual can be determined by the sum of its annual growth rings and a collection of ages from a population sample can be extrapolated to construct an age distribution for the population. Age data are critical for managing fisheries as they are the cornerstone records used to estimate recruitment, spawning stock biomass (i.e., fecundity), and mortality rates (Brooks et al. 2008, Martell et al. 2008, Lee et al. 2011, Minte-Vera et al. 2019).

Age compositions are often estimated directly or by age-length keys (Mohn 1994, Harding et al. 2008, Stari et al. 2010). In either case, a sample size sufficient to resolve

the age distribution at length in the population is essential (Kimura 1977, MacDonald & Pitcher 1979, Hoenig 2017, Hulson et al. 2017). The amalgamation of many ages within small-length divisions in adult animals (Weinberg 1999, Hofmann et al. 2006) poses a particular challenge. Species that reach extremely old age, such as the ocean quahog *Arctica islandica*, provide an exceptional example (Ridgway et al. 2012, Pace et al. 2017a, 2017b, 2018). For long-lived species such as *A. islandica*, with upward of 200 possible age classes, the total number of aged animals required to provide a defensible age-length key is very large. Techniques used to create chronologies for this species, particularly cross dating and isotope dating (Butler et al. 2009, Schöne et al. 2011, Reynolds et al. 2017), often cannot provide the number of ages necessary for population age compositions at any affordable cost. Accordingly, traditional visual aging methods must be used (Ropes 1988). Given the life spans involved for this species, an inordinately large number of chances for reader error can occur and close attention must be paid to the precision at which ages can be determined under the constraint of high sample number and accurate age estimations where possible.

Error is a valued statistic used to appraise data quality and consistency across datasets, laboratories, researchers, and methodologies and error analysis is routinely used in the development of population age data for fisheries assessment purposes (Pentilla & Dery 1988, CARE 2006). Error is classically defined as the difference between an estimated value and the true, or accurate, value that is often categorized as either sampling error, observational error, or processing error. Sampling error influences data integrity and challenges typically stem from insufficient sample size or measurement bias (Duval & Tweedie 2000, Hjellvik et al. 2002, Pennington et al. 2002, Johnsen 2003,

Jacobson et al. 2010, Costa et al. 2016, Ritter et al. 2016, Powell et al. 2017). Observational error can amass from the human interpretation of sample data, whereas process error reflects variability in biological processes compelled by biotic and abiotic forces. In the case of determining the age of an animal such as the ocean quahog, age data are susceptible to observational error, as annual growth rings (i.e., annuli) need to be interpreted by different readers with varying experience levels, to distinguish annuli from subannual growth patterns where process errors can be substantial dependent on extreme oceanographic conditions (e.g., yearly, seasonally, and monthly) (Jones 1980, Campana et al. 1995). When sampling error is either negligible or inescapable, observational error is an important facet that can be improved and constrained to elevate data quality with high-precision and low-systematic bias. Reduction of observational error may not always drive the data toward the true value as that value is not known for many species; however, low observational error can improve precision and allow reproducible age data in future studies, which is a noteworthy alternative (Kimura & Lyons 1991).

Observational error is best evaluated by precision and bias metrics using paired blind age comparisons between two age readers. Precision is the scale of reproducibility, or agreement between readers, over time and is conventionally reported as average percent agreement (Beamish & Fournier 1981), average percent error (Beamish & Fournier 1981), and/or average coefficient of variation (ACV) (Chang 1982). Age bias is the systematic difference between paired age estimates and is the product of individual reader interpretation, aging methodology, age class of the animal, and the individual animal itself (processing error) (Kimura & Lyons 1991, Hoenig et al. 1995). Age-reader bias occurs when one set of age determinations is consistently higher or lower than a

comparative set of age determinations for identical samples. Bias may be present even when precision is high, therefore, simple precision statistics alone are not sufficient to describe the quality of an age dataset (Campana et al. 1995, Hoenig et al. 1995, Kimura & Anderl 2005).

The evaluation of observational error is well described in fisheries literature by means of precision metrics (Campana et al. 1995, Campana 2001) and, more recently, tests of symmetry (McBride 2015). Many state and federally managed fisheries are aged at a production scale to inform population models used to set harvest limits, and precision in aging is a critical metric in establishing the degree of uncertainty present in age-composition data used in these population models. The bivalve *A. islandica* is an exceptionally valuable clam commercially harvested and managed at the federal level, but age-based models do not exist for this species (NEFSC 2017) because of its long lifespan (greater than 200 y in the Mid-Atlantic, United States) and the difficult interpretation of growth patterns for consistent aging. As a result, *A. islandica* is not aged at production scale because of the aforementioned constraints and eliminates any opportunity for managers to use quality-controlled age data. To produce age-composition data at production scale for potentially forthcoming *A. islandica* population age models, the same level of quality control must exist for this exceptionally long-lived species as it does for other commercially managed fisheries.

The objective of this paper was to assess three methods of observational error analysis, namely, age bias, age precision, and error frequency, for a large *A. islandica* age dataset (n = 610) created from a proxy age-validation study. Error thresholds for the

sample population and both sexes were established and tested for each of the three error methods.

2.2 Materials and Methods

2.2.1 Sample

In 2017, 706 live *A. islandica* clams were collected from Georges Bank (40.72767° N, 67.79850° W) at a depth of approximately 72 m by the ESS F/V Pursuit using a Dameron-Kubiak dredge that offered variable bar spacing to collect animals smaller than market size (i.e., less than 80 mm in shell length). Clams greater than 70 mm in shell length were retained for this study. Clams were measured for shell length, sex was identified by smear slide, and shell valves were cleaned by immersing in a bleach solution and stored dry for aging. A random subset of valves was chosen for age estimations and included as close to 100 animals per 5-mm size class as possible (n = 645) and equal numbers of males and females per size bin when possible. If 100 shells were not available per size class such as for rare size classes (<80 mm or >100 mm), all available shells were aged. Sizes ranged from 72.6 mm to 119.8 mm and resulted in 10 size-class groups based on the 5-mm delineations.

A single valve from each selected animal was sliced along the axis of greatest growth (largest height dimension) as close to the shell origin as possible using a Kobalt wet tile saw and the sectioned valve was progressively exfoliated with silicone carbide abrasive paper at 240, 320, 400, and 600 grit sizes (Pace et al. 2017a). Exfoliation removed excess shell to bring the cut edge as close to the shell origin as possible while also removing coarse shell texture. Shells were then polished to a reflective finish with a polycrystalline diamond suspension fluid (6 μm and 1 μm diamond sizes) to clearly

display the annual growth lines. After processing, shells were imaged using a high-definition Olympus DP73 digital microscope camera. Segmented images of the hinge and umbo region were stitched together using Olympus CellSens microscopic imaging software. Stitched images created a single, comprehensive image of the entire hinge. Additional details on cleaning, processing, imaging, and aging *A. islandica* shells can be found at: https://www.vims.edu/research/units/labgroups/molluscan_ecology/publications/topic/ocean_quahog_arctica/index.php.

2.2.2 Age Validation Proxy

Of the 645 clams that were processed for aging, 610 clams were used for final error analysis. The excluded were specimens with images that did not display consistently clear growth lines (Ropes et al. 1984a) or those aged by consensus for training using two age readers and consequently pairwise data did not exist. ImageJ software (ObjectJ plugin) was used to annotate annual growth lines on each comprehensive hinge image for aging. Annuli determination was vetted through a comparative aging-technique analysis using two strategies (Figure 2.1). The first strategy applied a grouped hypothesis, where lighter gray lines or repeating patterns (e.g., doublets) were posited to represent periods of reduced growth within season and not terminal annual growth lines. Noticeably, repetitive patterns of lighter gray lines were more commonly observed when the animal was “young” and experiencing periods of rapid growth, but doublets and triplets were routinely observed through much of the growth history. The necessary ignorance of light gray lines in early years of life is a common occurrence in aging bivalves as these are routinely produced during periods of

rapid juvenile growth (Jacobson et al. 2006, Harding et al. 2008, Shirai et al. 2018, Huyghe et al. 2019), but such ignorance may be incorrect in later years. Hence, the second strategy applied a singular hypothesis, where observed repetitive growth patterns such as doublets were judged not to be seasonal, but a manifestation of annual periodicity. The singular hypothesis posits that growth lines, particularly those observed in the middle and later years of life, are true annuli.

Both hypotheses can be supported biologically, yet an arbitrary choice cannot be made because of the extreme differentiation in age estimates between the two aging strategies. To resolve this fundamental problem, shells from 20 of the oldest animals collected from both Georges Bank and Long Island were carbon-14 dated, in addition to two age readers (readers A and B) visually aging the samples using the grouped and singular strategies. The mean age was used for each sample for both visual aging strategies to compare with the carbon-14 results as it was not known which aging protocol was correct.

A Dremel tool removed between 0.018 g and 0.044 g of carbonate dust from the cut shell surface as close to the shell origin as possible (earliest carbonate deposited) without carbon contamination from the shell exterior. Samples were sent to the Keck Carbon Cycle AMS Facility at University of California Irvine for dating. Birth years were estimated by isotope analysis using “prebomb” carbon-dating techniques. Additional details on carbon-14 sampling can be found at: https://www.vims.edu/research/units/labgroups/molluscan_ecology/_docs/lab_manuals/2020-4-carbon-14-quahog-protocol.pdf.

Carbon-14 ages were corrected for the marine reservoir effect using a 400-y correction factor. Animals used for carbon-14 dating were collected in the cold pool, south of Long Island and off Georges Bank (for cold pool, see Sha et al. 2015, Lentz 2017, Chen et al. 2018). This region of the continental shelf has been the site of relatively few reservoir age evaluations (Weidman & Jones 1993, Sherwood et al. 2008) in comparison with extensive work in the northeastern Atlantic (Tisnérat-Laborde et al. 2010, Heaton et al. 2020). The few values available approximate the average marine value; thus, the average marine value was used (Stuiver & Polach 1977, Heaton et al. 2020).

2.2.3 Age Bias

Observational error was redefined for each of the three subsequent error methods. Error, in the context of bias, is defined as the difference between age estimates of two age readers. A test of symmetry can identify systemic bias in ages between age readers when comparing aging methodologies (e.g., scales versus otoliths), or testing for age-reader drift over time (e.g., age reader A versus age reader B, age reader A versus reference dataset, and age reader A at start versus age reader A at end). The detection of age bias should be completed before precision estimates are made, as a bias will confound precision interpretations through artificial inflation of values (Campana & Jones 1992, Campana et al. 1995, Hoenig et al. 1995). Significant difference (asymmetry) is determined using the chi-square statistic for observations falling off the matrix diagonal (diagonal values represent 100% agreement between the two groups being tested) (Bowker 1948). The McNemar test maximally pools data on each side of the diagonal to create one group for chi-square analysis above and below the diagonal for a single

comparison. In contrast, the Bowker test is an unpooled test that treats each pairwise comparison off the diagonal as an independent group, thereby using numerous comparisons. The Evans–Hoenig test pools (semipools) pairwise data immediately off the diagonal and compares these data with pooled groups at incremental levels off the diagonal (± 2 y, ± 3 y, etc.).

The AgeBias function from the "FSA" package (Ogle et al. 2021) in R (R Core Team 2018) was used to calculate tests of symmetry for the McNemar (Eq. 1) (McNemar 1947), Bowker (Eq. 2) (Bowker 1948), and Evans–Hoenig (Eq. 3) (Evans & Hoenig 1998) equations (equation formatting taken from McBride 2015):

$$(1)\ X^2{}_{McNemar} = \frac{\left(\sum_{i=1}^{m-1}\sum_{j=i+1}^{m}(n_{ij}-n_{ji})\right)^2}{\sum_{i=1}^{m-1}\sum_{j=i+1}^{m}(n_{ij}+n_{ji})},$$

$$(2)\ X^2{}_{Bowker} = \sum_{i=1}^{m-1}\sum_{j=i+1}^{m}\frac{(n_{ij}-n_{ji})^2}{n_{ij}+n_{ji}},$$

$$(3)\ X^2{}_{Evans-Hoenig} = \sum_{p=1}^{m-1}\frac{\left(\sum_{j=1}^{m-p}\left(n_{p+j,j}-n_{j,p+j}\right)\right)^2}{\sum_{j=1}^{m-p}\left(n_{p+j,j}+n_{j,p+j}\right)},$$

where X^2 is the chi-square statistic, i is the reader A age (row), j is the reader B age (column), n is the frequency of age estimates at row i and column j, m is the number of readings, and p is $j - i$.

To better understand where a potential bias may exist, an age-bias plot was used to compare reader A ages as the reference ages to reader B. The designation of the reference reader is arbitrary when an age-validated reference collection is not being used, and age readers have similar experience levels (as is the case with readers A and B in this study), because the true ages are not known. If experience levels had differed, the expert reader would have been designated as the reference.

Raw absolute error would be expected to increase with age as error should accumulate with each additional annulus over the lifespan of an animal. If the absolute error is standardized by age to create an error rate (a similar statistic to CV), the slope of these data should be near 0 if no aging bias of this type exists (Kimura & Lyons 1991). Accordingly, the absolute value of the error, or the absolute difference between the age estimates between readers (presented in the age-bias plot on the Y axis), was standardized by age to understand how this type of error changed with age and thus create an error rate (specified as errors per year) (Eq. 4):

$$(4)\ \ Error\ Rate = \frac{|age\ difference|}{Age_{Reference\ Reader}} = \frac{|error|}{Age_{Reference\ Reader}}\ .$$

As the number of animals aged per birth year was often sparse, once the error rate was determined for each reference age, the data were ordered by birth year and smoothed in 10 sample increments to refine any underlying pattern in error rate. The median for each 10-sample increment (i.e., rolling median) of error rate and reference age was used for error rate analysis and fitted to a trendline to elucidate any patterns of underlying bias.

2.2.4 Age Precision

Precision is an error metric represented by several statistics including the coefficient of variation (CV). Coefficient of variation is the more rigorous precision measurement when compared with the more traditional percent agreement and was thus chosen as the best statistic to validate age precision in this study (Beamish & Fournier 1981, Campana et al. 1995, Campana 2001, Kimura & Anderl 2005). In the context of this project, precision error occurred when the ACV is greater than an accepted threshold for pairwise age comparisons (Eq. 5):

$$(5)\ ACV(\%) = \frac{\Sigma\left(\frac{s}{\bar{x}} * 100\%\right)}{n},$$

where s is the standard deviation, $\bar{x}$ is the mean for each set of pairwise ages, and n is the total number of samples. Coefficient of variation standardizes precision across size classes, which is valuable for a long-lived species such as *A. islandica*. Age analyses in marine fisheries often use age estimates that meet a precision error threshold of less than 7.6% ACV (Campana 2001). A 7% or less ACV threshold was chosen for *A. islandica* to mirror methods used by federal and state resource managers.

2.2.5 Error Frequency

Error, in the context of error frequency as used in this study, is any sample with a dual-reader CV greater than 10%. Age estimates are deemed acceptable if the error frequency (i.e., number of samples with CV greater than 10%) is less than 10% of the total dataset (expected probability of error = 0.1) using a binomial test. A significant binomial test, or elevated frequency of samples with CVs greater than 10%, is an indication that at least one age reader is aging differently than another age reader and too many large errors are present in the age data. If the error frequency threshold is exceeded, samples with the highest CV can be aged by consensus (i.e., the sample can be aged jointly by at least two age readers) until the error frequency is less than 10%, but this approach is only useful if all specimens are aged by both readers.

2.3 Results

2.3.1 Age Validation Proxy

Carbon-14 dating is a useful approach to validate aging techniques in animals of lifespans too long to easily follow the time course of growth from birth to death

(Witbaard et al. 1994, Wanamaker et al. 2009, Shirai et al. 2018). A total of 20 shells were sampled for carbon-14 aging, but samples 4, 5, and 13 were contaminated with modern carbon and therefore not used in this analysis. Compared age estimates from the grouped and singular aging options, with the minimum and maximum error bounds for carbon-14 results (Figure 2.2), indicated that the singular hypothesis better captured the validated results from the carbon-14 isotope analysis. Singular age estimates fall within the error bounds of carbon-14 ages more frequently (n = 12) than those of the grouped age estimates (n = 3). A one-way, repeated analysis of variance test coupled with pairwise comparison t-tests (Bonferroni correction), demonstrated that the grouped hypothesis was significantly different from both the singular (P = 1.69e-9) and carbon-14 age estimates (P = 2.37e-5). The singular and carbon-14 age estimates were not significantly different (P > 0.05) (Figure 2.3).

Although isotope dating can be used for age validation for select samples, the carbon-14 data presented herein only apply to a small number of individuals of a similar age caste. Furthermore, the error bounds on the prebomb carbon-14 ages are too large to be used as definitive reference ages. Despite these shortcomings, these carbon-14 results are currently the best validation tool for this set of *A. islandica* samples and serve as a proxy age validation to support aging-technique selection. As a result, the singular aging technique was applied for all age estimates listed herein. This approach is consistent with conclusions of Butler et al. (2009, 2013) and Pace et al. (2017a) for *A. islandica* (Schöne et al. 2005, Harding et al. 2008) and for other long-lived species (Shirai et al. 2018) but diverges from other species frequently showing within-season growth checks of similar

appearance to annuli (e.g., summer breaks and spawning breaks; Goodwin et al. 2001, Fan et al. 2011, Kubota et al. 2017).

2.3.2 Age Bias

Each of the three tests of symmetry pool age frequencies differently, resulting in varying degrees of freedom and significance levels (Table 1). The McNemar test produced the most significant results across all three sample types (Population P = 1.37e-06, Female P = 0.03, and Male P = 3.27e-06), followed by the Evans–Hoenig test (Population P = 0.02, Female P = 0.18, and Male P = 0.02) and finally the Bowker test that detected no significant bias (Population P = 0.28, Female P = 0.47, and Male P = 0.45). The gradient of significant test results suggested a slight bias that is not detected uniformly across pooling methods or sample type. The female age estimates were only significantly different with the McNemar test, whereas the male age estimates were significant for both the Evans–Hoenig and the McNemar tests and likely influenced the significant bias in the population sample results for the same two tests.

To better understand what differences are driving significant asymmetry, the age-bias plots were reviewed for error trends (Figure 2.4). The X axis values at y = 0 represents 100% agreement between readers and a nonbiased dataset would demonstrate errors randomly distributed around the X axis. Between the ages of 60 and 100 y, errors are disproportionately distributed above or below the X axis on the Population and Male age-bias plots, indicating the likely age range driving significant test results. The mean error (difference) for the Population is +1.54 y, Female is +0.40 y, and Male is +2.6 y using a standard deviation of 1.96. In other words, reader B, on average, ages 1.54 y higher than reader A on an animal that can live up to 261 y of age when the entire

population sample is analyzed, but reader B ages, on average, 2.6 y higher than reader A when the male sample is analyzed. The higher mean error in the male data signified that young male samples may drive the bias results detected in the tests of symmetry, whereas error in the female dataset is evenly distributed around the agreement line (X axis, y = 0). Extreme errors (outside the 95% agreement bounds using a 1.96 standard deviation) occurred across the entirety of the reference age range, and the absence of a trend indicated that these errors are the result of particularly challenging samples to age and not an underlying bias (i.e., processing error).

The age-bias plot indicated that a bias may be present in the younger animals of this study and the error rate was examined for similar trends in errors at age (Figure 2.5). A negative logarithmic model best fit the data (Population: R2 = 0.33, P = 2.2e-16; Female: R2 = 0.16, P = 8.423e-13; Male: R2 = 0.34, P = 2.2e-16) and the level of significance indicated a decline in error rate with increasing age. A type III one-way analysis of variance was performed to test the significant effect of specimen age at death on the error rate and all three sample types had a significant effect (Population: P = 3.0e-44, Female: P = 6.48e-12, and Male: P = 1.79e-23). The highest rate of error occurred at approximately 60 y of age and declined steadily with age and was highest for the male and population datasets. The error rate of a 60-y-old animal (0.12 errors/year) was 3.5 times higher than the error rate of a 220-y-old animal (0.034 errors/year). A significant relationship existed between female age at death and error rate, but both linear and negative logarithmic models fit the data similarly (linear: R2 = 0.15, P = 6.48e-12) with a linear slope of nearly 0 (−1.96e-04). The combined data from the age-bias plots and the smoothed error rate plots revealed that the underlying bias is likely manifested in the

youngest animals and males produced higher error rates in these young animals. Bias results indicated that age estimates can be accepted conditionally, where the greatest error rate and bias error occurred for the youngest, male animals in the population.

2.3.3 Age Precision

The Georges Bank samples had a population and sex-based ACV of 5% (Figure 2.6); therefore, Georges Bank precision was high and met ACV precision thresholds. Linear regression depicts a declining CV with the mean age for each set of pairwise ages (Figure 2.7). The R2 values are low (0.05–0.07) indicating that mean age may not be the primary source of variability in the data. Conversely, the relationship between mean age and CV is significant (Population: P = 2.09e-10, Female: P = 4.45e-05, and Male: P = 9.03e-07) where for every year increase in mean age, on average, CV declines by 0.03%.

2.3.4 Error Frequency

Samples aged from Georges Bank met the conditions of a 10% error frequency; 54 samples had CVs greater than 10%, a number fewer than expected by chance (binomial test, P = 0.19). The female dataset (n = 298) contained 24 errors and the male dataset (n = 312) contained 30 errors, both sexes fell within the 10% error frequency. When binomial tests were calculated using a range of expected probabilities (expected error frequency) between 0.01 and 0.2, the 53 population errors are significant with an error frequency set at less than or equal to 7%, the 24 female errors with an error frequency at less than or equal to 6%, and the 30 male errors with an error frequency at less than or equal to 8%.

2.4 Discussion

The development of *A. islandica* age compositions for applications in standard fisheries assessment models requires solutions for the challenging nature of this species age-at-length data including the necessity for large sample sizes, constraining age precision and accuracy for an animal with greater than 200 age classes, and the time commitment and cost of aging such substantial sample sizes. Pace et al. (2017b) identified that number of cohorts in an *A. islandica* population, and the number of cohorts within a narrow length class, required aging more than 20 animals per size class (i.e., greater than 200 animals) to construct robust population age compositions. Given the sample numbers needed and the time and cost commitment (Ropes 1984), maximizing precision in age determination is essential, as the employment of multiple readers to continuously age by consensus is infeasible.

Age determinations require levels of interpretation that inherently introduce error into the data. Historically, precision statistics including percent agreement, percent error, and CV were the only methods to assess error in fisheries age data (Campana et al. 1995, Campana 2001, McBride 2015). Precision statistics do not account for age effects and therefore can change based on the age of the animal (Hoenig et al. 1995). Early analyses regarding age precision in fisheries assumed that variability in age determinations was homogenous across a sample and consequently could be averaged across all age classes (Beamish & Fournier 1981, Chang 1982), yet it is now apparent that the precision of age determinations varies with the age of an animal and that age effect is an important variable to consider. Species as taxonomically divergent as *A. islandica* (Figure 2.7) and the lemon shark (Negaprion brevirostris) (Brown & Gruber 1988) both demonstrate high

CV and percent error (i.e., low precision) at young ages, whereas species such as walleye pollack often show low precision in the older individuals (Kimura & Lyons 1991, Hoenig et al. 1995). Precision variability within a species proves that precision is highly dependent on the species themselves and the age distribution of the sample. In other words, a sample dominated with young *A. islandica* will likely have lower precision than a sample primarily composed of older clams.

For many species without validated reference age collections, constraining precision and bias of age estimates is the best strategy to improve the quality of the ages when accuracy is unknown, and a single test of error (e.g., CV) is not sufficient to accept age data (Beamish & McFarlane 1983, Campana et al. 1995). Error frequency was introduced in this paper as an additional method for evaluating error, but it is not a protocol used in many evaluations of aging precision. Because of the longevity of *A. islandica*, and the tendency of CV to obscure large differences in age estimates between readers for old animals because of age standardization, an option to evaluate exceptionally large CVs was desirable. The imposed error frequency threshold of 10% defined a limit on how many exceptionally large precision errors could arise in a dataset before the dataset is deemed to be unacceptable. A binomial test can then be applied to investigate alternative aging scenarios and determine the maximum number of errors a dataset can incur before it significantly exceeds a 10% error frequency. One such scenario is to identify how many errors would create an error frequency larger than 10%. For a 610-sample dataset, 74 population errors (or 40 female errors and 41 male errors) or more would exceed the designated acceptable error frequency. An alternative scenario is to test a more typical aging strategy where a second age reader only aged a random 20%

subset of the sample (Kimura & Anderl 2005). In such a case, only 18 errors or fewer can be made within the 122-sample subset to maintain a 10% error frequency (or fewer than 10 errors in each of the female and male datasets). This approach to error also allows flexibility in implementation, either by changing the definition of an error to be more conservative, such as to match our acceptable ACV cutoff of 7%, or to allow more errors to occur so that the probability of error frequency surpasses 10%.

Accepting that a designated number of large precision errors can exist in a dataset, the identification of systematic patterns of error across age classes is critical to account for age effects. In the age-bias plot (Figure 2.4), the 95% agreement bounds are seemingly large (± 19 y from the mean), yet when compared with the data on spiny dogfish (Squalus acanthias) provided by Beamish and Fournier (1981) for which 95% agreement was within 8.3% of the total lifespan of the species (± 5 y for 95% agreement; 60-y lifespan), the 95% agreement for *A. islandica* appears reasonable. For *A. islandica*, the 95% agreement was within 7.3% of the total lifespan of the oldest individual from Georges Bank (± 19 y for 95% agreement; 261-y lifespan) or within 3.8% of the lifespan of the species (approximately 500 y).

Tests of symmetry to identify age bias have only recently been adopted in fisheries science and are often not reported alongside precision results (McBride 2015). Three tests of symmetry are easily calculated in contemporary age analyses, yet test selection and interpretation are easily confounded as evidenced by Table 1 where results are vastly different. The McNemar test was designed to perform a single paired test for the entire dataset, and in the case of age contingency tables, age is never accounted for. Regardless of whether the species has five age classes or 500 age classes, only one degree

of freedom exists. The Bowker test is a pairwise comparison, where every cell is compared with its mirror image across the diagonal and no pooling occurs. When the Bowker test is used to analyze a species with many age classes, the degrees of freedom (or number of paired comparisons) will be high, as evidenced by *A. islandica*, whereas when a species with few age classes is analyzed, the degrees of freedom will be low and potentially similar to that of the Evans–Hoenig test. The Evans–Hoenig test pools comparisons based on the degree of difference from the diagonal (or 100% agreement). The Evans–Hoenig test is the only test of symmetry specifically designed for fisheries science to evaluate how age differences are dispersed around the agreement age (i.e., the diagonal) (Evans & Hoenig 1998).

For *A. islandica*, age-bias plots (Figure 2.4) and error rate (Figure 2.5) demonstrated that deviations in age estimates occurred more frequently in the youngest animals and particularly in young male animals and that a bias may be present in those samples. The bias is not necessarily large, but an underlying trend is observed across all three error methods. The McNemar test is the most sensitive and always detected a bias in this dataset. Conversely, the Bowker test was the least sensitive. Arguably, the Evans–Hoenig test was the most reliable test for bias detection as female data were not significantly biased in this test of symmetry, which is supported by error rate, error frequency, and age-bias plot results. Interpretation of these three tests would be extremely difficult if multiple representations of error were not available. Diverse methods to describe error are critical to identify the origin of uncertainty, and to implement procedures to target the most significant sources.

In the case of *A. islandica*, uncertainty in age estimates appears to originate primarily during the first decades of life as clearly shown by the ascending error rate (Figure 2.5) and CV (Figure 2.7) with younger and younger ages. The CV was developed to standardize error by age and error rate was also calculated on a per year basis, whereby an older animal will need larger errors [standard deviation (CV), age differences (error rate)] than a young animal to manifest the same magnitude of standardized error. Furthermore, as is common across many sclerochronological datasets from otoliths to bivalves, as growth rates decline with age, the ability to observe intraannual (subannual) growth lines is diminished. As a result, age readers tend to agree more in the latter years when every line is viewed as a clear annulus, whereas early growth increments are large enough to display subannual changes in growth rates that manifest as repetitive growth lines that are not true annuli (Pannella 1971). The presence of intraannual growth lines in rapidly growing bivalves is well known and their discrimination is normally a challenge (Jacobson et al. 2006). Reducing this source of uncertainty is clearly the primary challenge in aging *A. islandica* (Harding et al. 2008).

Growth lines are created when shell carbonate production slows, and more protein is secreted into the shell matrix. These dark, protein-dense growth lines reflect seasonal depressions in carbonate production because of reduced food supply, spawning events, or unfavorable stratification/mixing that result in suppressed metabolic functions required for growth. Normally, the winter cessation of growth generates the strongest growth line (annulus) in most bivalve species because of cold water temperatures that mark the end of the annual growth period (Jones & Quitmyer 1996, Fan et al. 2011, Chute et al. 2016). A high temperature-induced growth line may produce the primary annulus in some species,

however (Peterson et al. 1985, Goodwin et al. 2001). The transition zone from fast juvenile growth to slower adult growth is the most challenging section of the hinge to age when a reader must decide when each growth line is a true annulus. For this reason, the expectation, clearly demonstrated by this *A. islandica* dataset, is that precision will be low (i.e., high CV) for young animals where many of the annuli are intermixed with subannual growth lines and in which increased scope for growth permits growth over a longer season than observed in the adult animal (Hofmann et al. 2006, Munroe et al. 2013).

Bias error was higher for male clams (Table 1, Figs. 4 and 5) despite an identical ACV between sexes and for the entire population sample (4.6%) (Figs. 6 and 7); clear evidence that precision alone is not a sufficient metric to describe the quality of age estimates. Ropes et al. (1984a) noted that gametogenesis was initiated in males at a smaller size and younger age than females. Possibly, the earlier onset of maturity might increase the number of subannual growth lines in young males, though the physiological mechanism is unclear. The expression of additional subannual growth lines in males relative to females is thus unexplained, but clearly present and results in an increase in contrasting interpretations of true annuli between age readers and an increased occurrence of aging error in males.

The carbon-14 dating used a selective sample of old animals to illuminate what an accurate age for an old *A. islandica* may be. A critical realization is that high precision does not necessarily mean high accuracy. Independent validations of accuracy are important. For *A. islandica* and other bivalves, age validations have generally been provided by carbon-14 dating, amino acid racemization dating, cross dating (as used in

dendrochronology), or oxygen isotopes (Weidman et al. 1994, Machitto et al. 2000, Schöne et al. 2011, Wanamaker et al. 2011, Mette et al. 2016, Reynolds et al. 2016). None of these methods can provide an adequate sample size for fisheries assessment purposes; hence, continued focus on reader precision in determining age, whereas accuracy validation from small subsamples will remain essential (Beamish & McFarlane 1983). As growth rates continue to accelerate over time in portions of the *A. islandica* range (Pace et al. 2018), younger and younger animals will be available to the fishery and these young animals will bring higher rates of error. Thus, both precision and accuracy can be best improved by focusing on the shell growth dynamics of young (but sexually determined) male and female animals, thereby improving the discrimination of subannual increments from annuli.

2.4.1 Summary

Quantification of age-reader error allowed calibration in aging methodologies between age readers, and the development of error thresholds to maintain high precision and low bias of age estimates. Young animals accrued the greatest error standardized by age (CV), and males were consistently age with higher error than females. Future research is needed to resolve accurate aging techniques of young animals (early annuli) and biological growth discrepancies between males and females that resulted in the poor interpretation of male growth patterns across age readers.

2.5 Tables

Table 2.1 Bias analysis. Test of symmetry results for pairwise age comparisons to identify bias.

Test of Symmetry	Sample	Degrees of Freedom	Chi-Square Statistic	*P* Value
Evans-Hoenig	Population	30	48.90	0.02*
	Female	29	35.80	0.18
	Male	26	42.10	0.02*
Bowker	Population	494	512	0.28
	Female	263	264	0.47
	Male	275	277	0.45
McNemar	Population	1	23.32	1.37e-06*
	Female	1	5.01	0.03*
	Male	1	21.65	3.27e-06*

Three tests were applied to an identical dataset. Significant P values (*) indicated a bias between the two age readers.

2.6 Figures

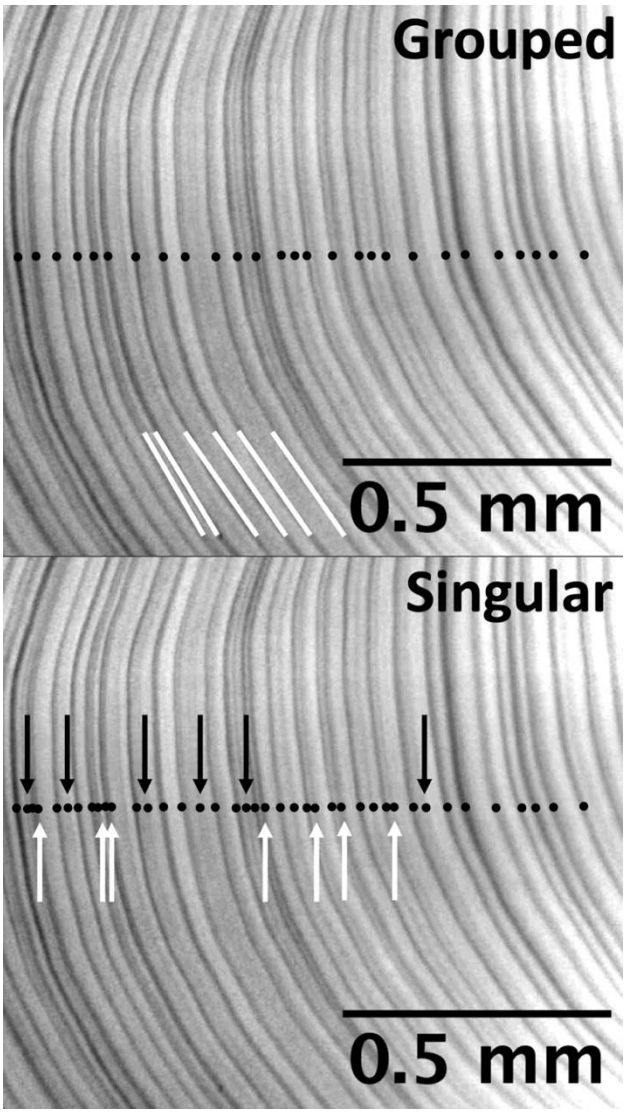

Figure 2.1 Comparative aging techniques. The grouped hypothesis assumed seasonal growth patterns, whereas the singular hypothesis assumed that growth lines are annual. Black circles indicate where an annulus is counted for each strategy. White vertical lines at the bottom of the grouped image (top) highlight dominant growth lines used to distinguish annuli due to their dark/bold appearance. The grouped aging strategy assumes pale growth lines are subannual as they often disappear at the lateral edges of the hinge plate (out of range of these images). Arrows in the singular image (bottom) designate additional annuli added when the singular aging strategy is used including doublets (white arrows below annuli) and weak annuli that appear fainter than surrounding annuli (black arrows above annuli). The singular strategy added 13 annuli.

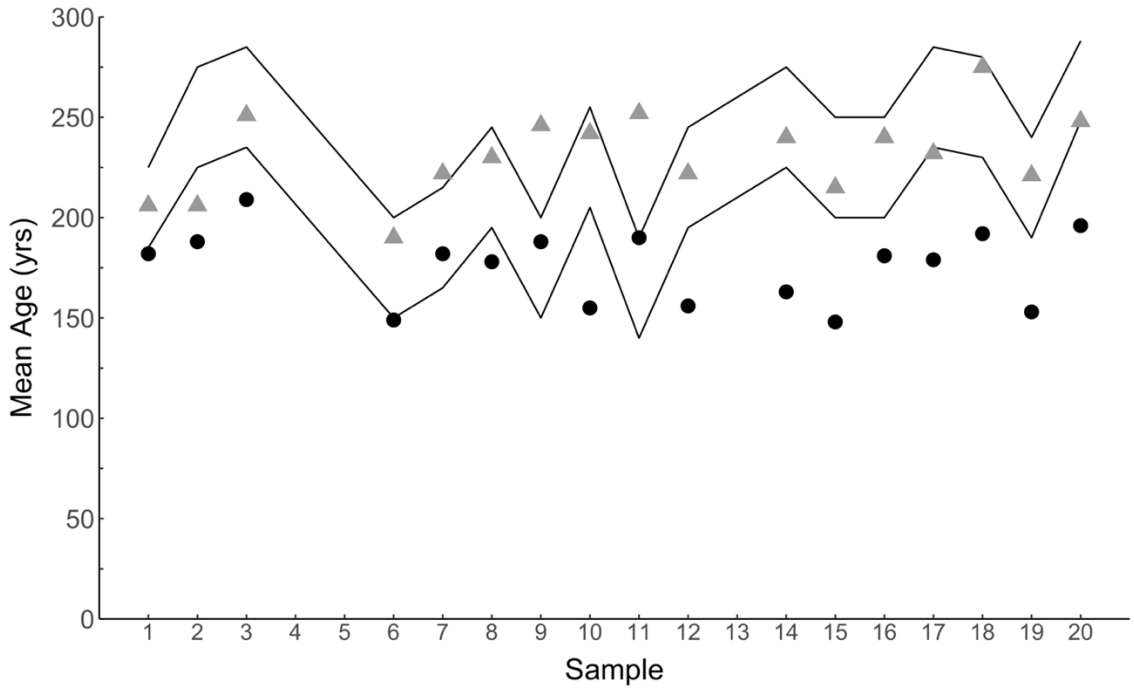

Figure 2.2 Age estimates using each of the two aging techniques. Solid black lines indicate the upper and lower error bounds inherent in carbon-14 ages. Age estimates from the grouped technique (dark, circle symbol) are consistently lower than estimates from the singular technique (medium grey, triangle symbol). The singular age estimates fell within carbon-14 error (black lines) more frequently than the grouped age estimates (12 and 3, respectively).

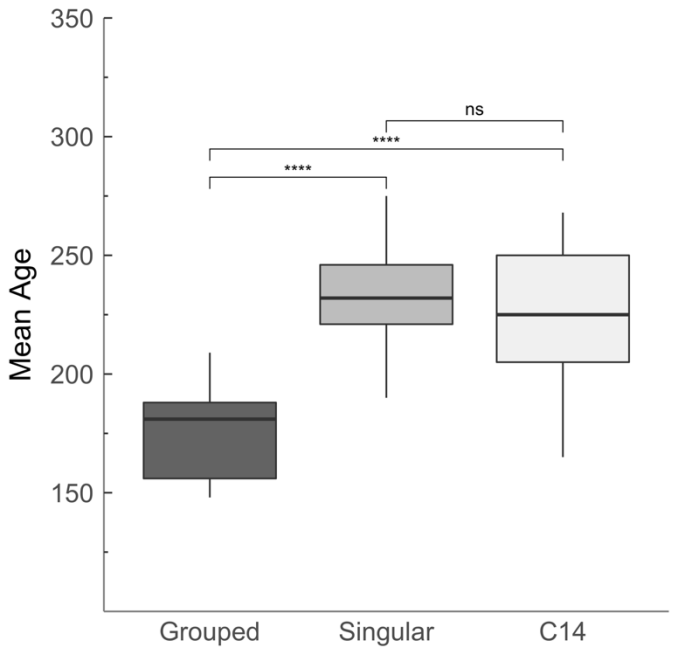

Figure 2.3 Comparison of aging strategies relative to carbon-14 estimated ages. A type III repeated ANOVA identified significant difference in ages between hypotheses (p=5.16e-9). Ages estimated using the grouped and singular strategies (see Figure 2.1) are significantly different (****), whereas no significant difference is observed between ages using the singular protocol and carbon-14 ages (ns) (posteriori pairwise comparison T test). A Bonferroni correction was used to adjust for multiple comparisons.

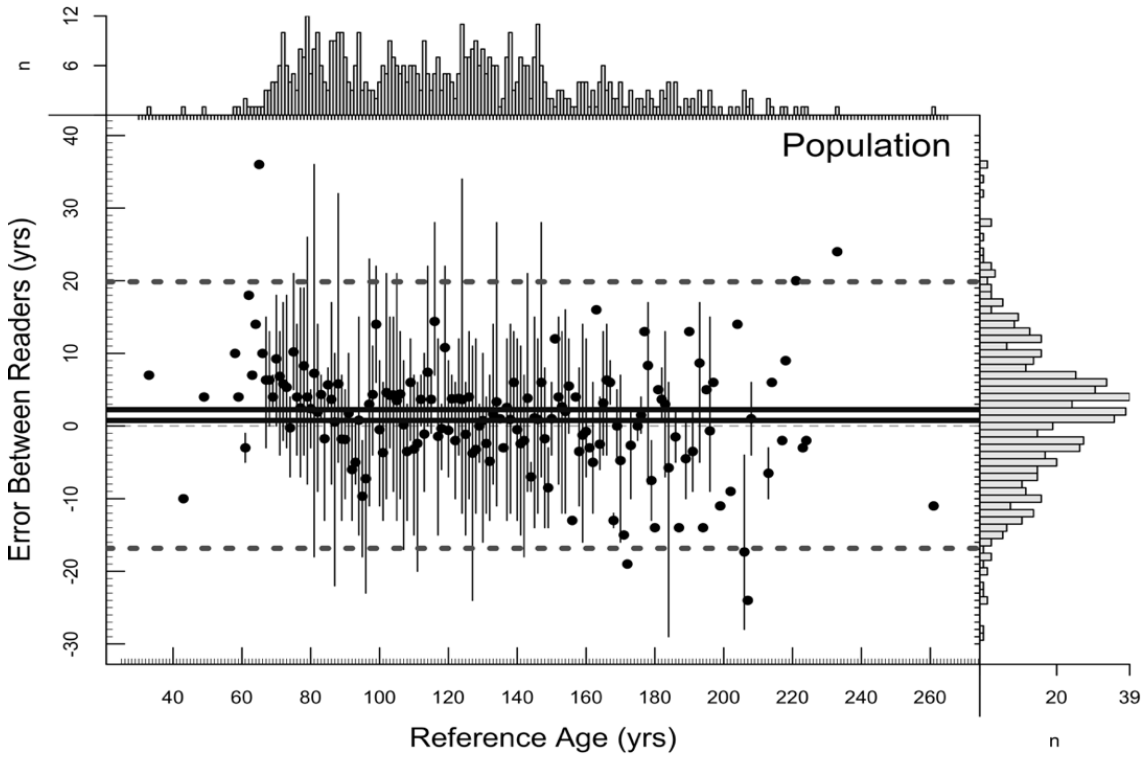
Population
Error Between Readers (yrs)
Reference Age (yrs)
n

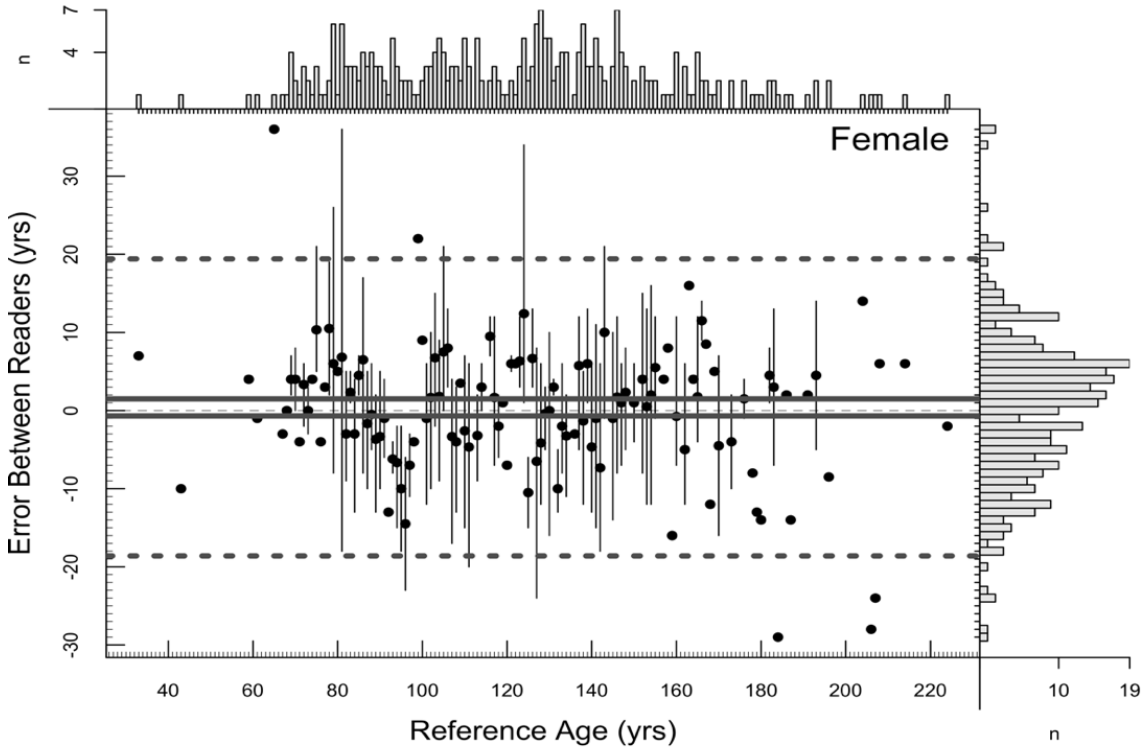
Female
Error Between Readers (yrs)
Reference Age (yrs)
n

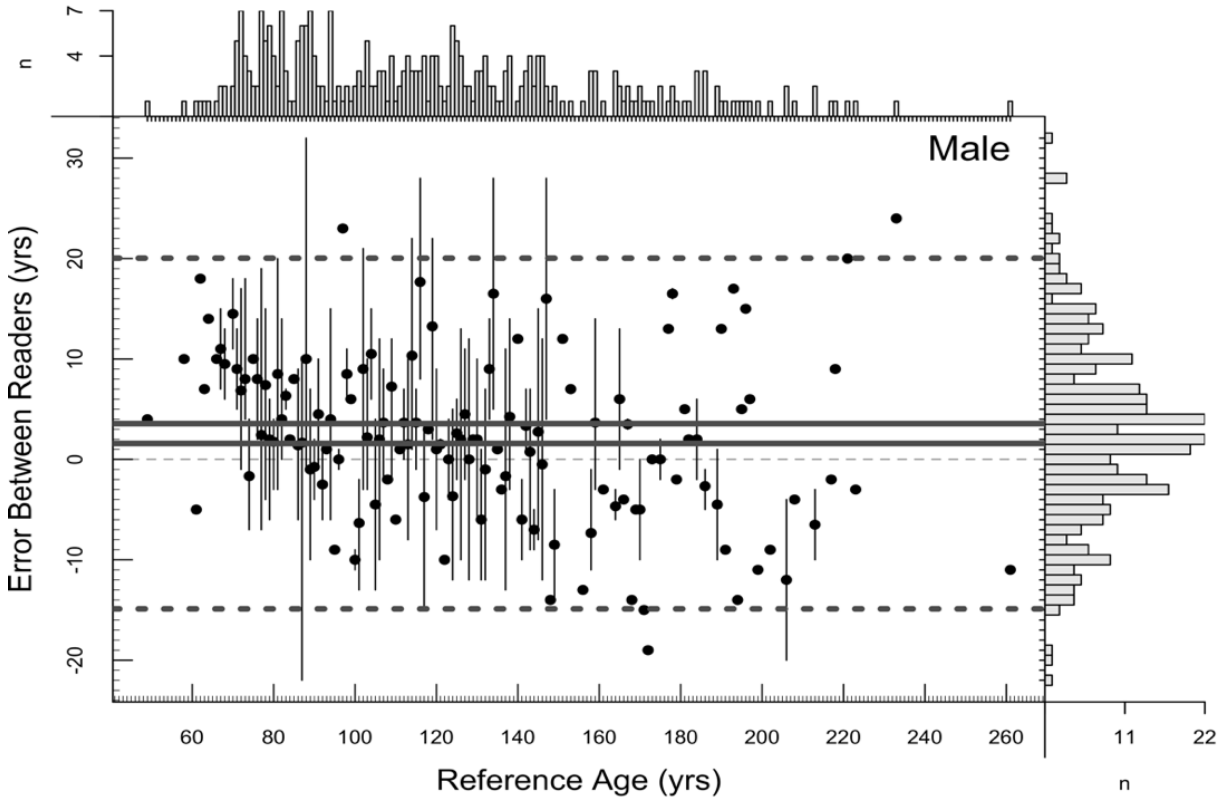

Figure 2.4 Error bias. Difference in age estimates between a second reader (reader B) and a reference reader (i.e., Reference Age). Black points represent the mean difference in age between the two readers at a reference age, and the vertical black lines represent the range of values if more than one error exists for that age (i.e., multiple samples). The two horizontal solid lines represent the 95% confidence intervals of the mean difference using a 1.96 standard deviation. The two horizontal dashed lines represent the 95% agreement bounds using a 1.96 standard deviation. Reader agreement is 100% at y=0. The histogram on the y axis denotes the frequency of difference values and the histogram on the x axis denotes the number of reader B ages at a given reference age. Mean Population error is +1.5 years (n=610), mean Female error is +0.40 years (n=298), and mean Male error is +2.6 years (n=312).

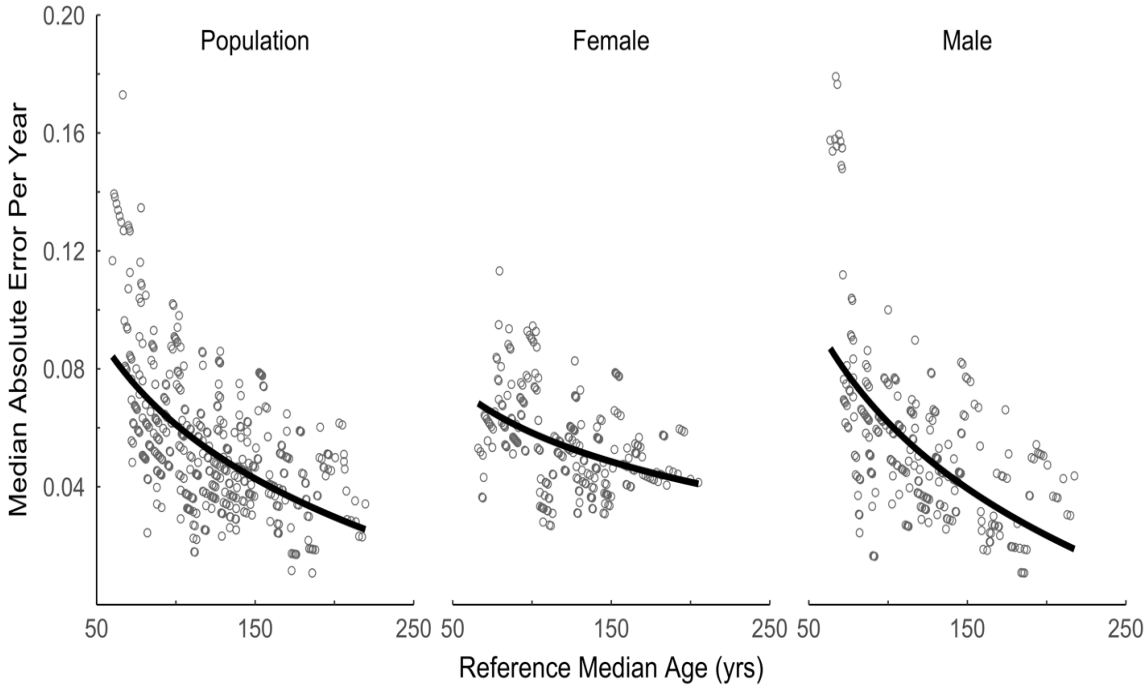

Figure 2.5 Error rate. Rolling median absolute error per year smoothed over 10-sample increments (y axis) versus the rolling median age of reference ages smoothed over the same 10-sample increments (x axis). A type III ANOVA indicated a significant difference between median error rate (median absolute error per year) and median age (Population: p=3.0e-44, Female: p=6.48e-12, Male: p=1.79e-23). A logarithmic relationship provided the best fit for all sample groups. Population f(x)=(-0.0452)ln(x)+0.27 (R2=0.33, p=2.2e-16), Female f(x)=(-0.0241)ln(x)+0.17 (R2=0.16, p=8.423e-13), and Male f(x)=(-0.0553)ln(x)+0.32 (R2=0.34, p=2.2e-16).

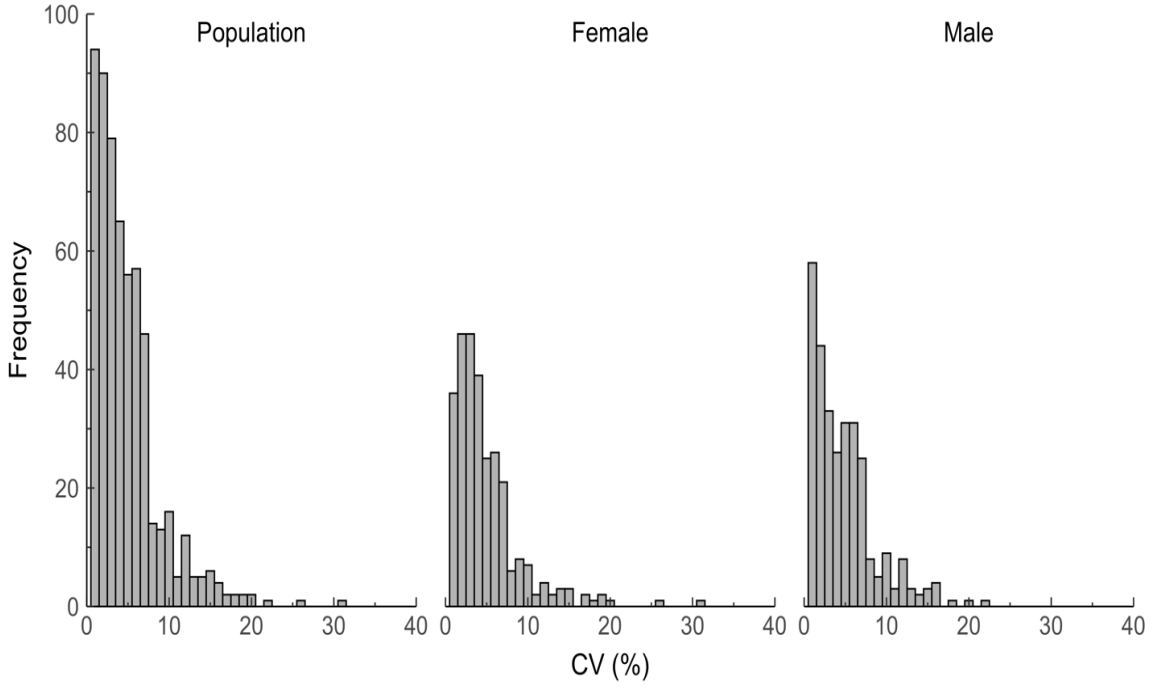

Figure 2.6 Error precision. Frequency of coefficient of variation (CV) results. Average coefficient of variation (ACV) is 4.6% for the entire population and both the female and male subsets.

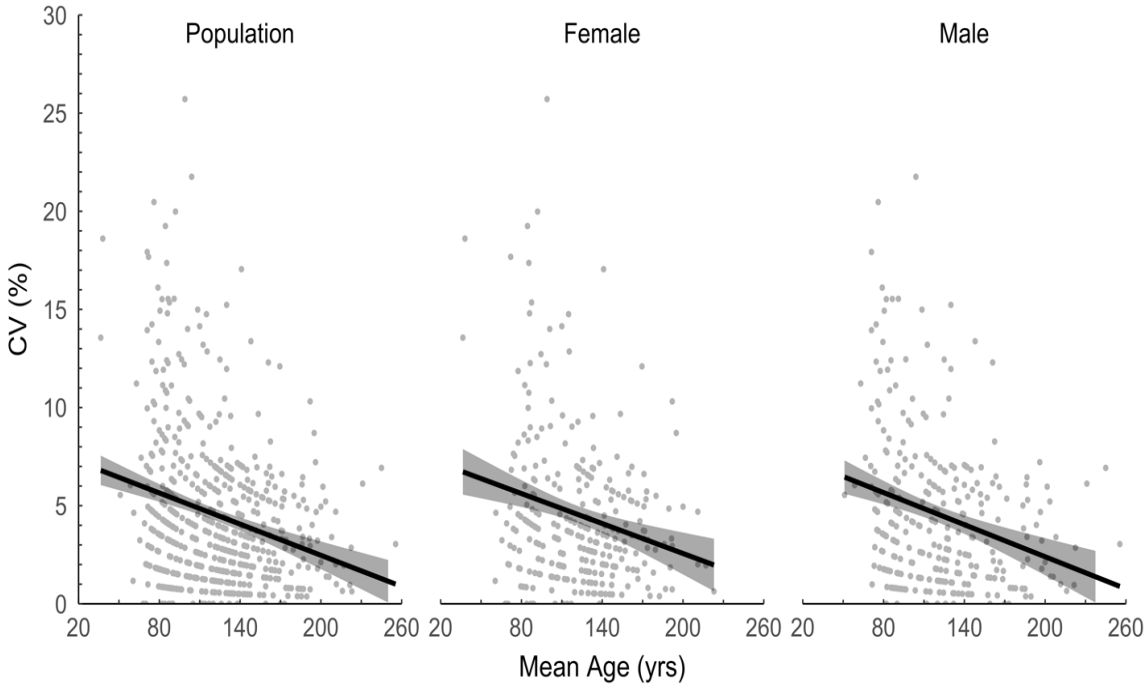

Figure 2.7 Precision by age class. Relationship of coefficient of variation (CV) versus mean age of two age-reader age estimates. Linear regressions of the three samples have identical slopes (-0.03), and significant regressions: Population y=-0.03x+7.95 (R2=0.06, p= 2.09e-10), Female y=-0.03x+8.08 (R2=0.05, p= 4.45e-05), Male y=-0.03x+7.85 (R2=0.07, p= 9.03e-07). R2 values are low, an indication of a significant but poorly defined relationship between CV and mean age.

2.7 Literature Cited

Beamish, R. J. & D. A. Fournier. 1981. A method for comparing the precision of a set of age determinations. *Can. J. Fish. Aquat. Sci*. 38:982–983.

Beamish, R. J. & G. A. McFarlane. 1983. The forgotten requirement for age validation in fisheries biology. *Trans. Am. Fish. Soc*. 112:735–743.

Bowker, A. H. 1948. A test for symmetry in contingency tables. *J. Am. Stat. Assoc*. 43:572–574.

Brooks, E. N., K. W. Shertzer, T. Gedanke & D. S. Vaughan. 2008. Stock assessment of protogynous fish: evaluating measures of spawning biomass used to estimate biological reference points. *Fish. Bull*. 106:12–23.

Brown, C. & S. Gruber. 1988. Age assessment of the lemon shark, *Negaprion brevirostris*, using tetracycline validated vertebral centra. *Copeia* 3:747-753

Butler, P. G., C. A. Richardson, J. D. Scourse, R. Witbaard, B. R. Schöne, N. M. Fraser, A. D. Wanamaker, Jr., C. L. Bryant, I. Harris & I. Robertson. 2009. Accurate increments identification and the spatial extent of the common signal in five *Arctica islandica* chronologies from the Fladen Ground, northern Baltic Sea. *Paleoceanography* 24:1–18.

Butler, P. G., A. D. Wanamaker, Jr., J. D. Scourse, C. A. Richardson & D. J. Reynolds. 2013. Variability in marine climate on the North Icelandic Shelf in a 1357-year proxy archive based on growth increments in the bivalve *Arctica islandica*. *Palaeogeogr. Palaeoclimatol. Palaeoecol*. 373:141–151.

Campana, S. E. 2001. Accuracy, precision and quality control in age determination, including a review of the use and abuse of age validation methods. *J. Fish Biol.* 59: 197-242

Campana, S. E., M. C. Annand & J. K. McMillan. 1995. Graphical and statistical methods for determining the consistency of age determinations. *Trans. Am. Fish. Soc.* 124:131–138.

Campana, S. E. & C. M. Jones. 1992. Analysis of otolith microstructure data. In: Stevenson, D. K. & S. E. Campana, editors. Otolith microstructure examination and analysis. *Can. Spec. Publ. Fish. Aquat. Sci.* 117:73–100.

CARE. 2006. Committee of age reading experts manual on generalized age determination procedures for groundfish. Seattle, WA: The Canada/U.S. Groundfish Committee. 52 pp.

Chang, W. Y. B. 1982. A statistical method for evaluating the reproducibility of age determination. *Can. J. Fish. Aquat. Sci.* 39:1208-1210.

Chen, Z., E. Curchitser, R. Chant & D. Kang. 2018. Seasonal variability of the cold pool over the Mid-Atlantic Bight continental shelf. *J. Geophys. Res. Oceans* 123:8203–8226.

Chute, A. S., R. S. McBride, S. J. Emery & E. Robillard. 2016. Annulus formation and growth of Atlantic surfclam (*Spisula solidissima*) along a latitudinal gradient in the western North Atlantic Ocean. *J. Shellfish Res.* 35:729–737.

Costa, E. G., R. M. Lopes & J. M. Singer. 2016. Sample size for estimating the mean concentration of organisms in ballast water. *J. Environ. Manage.* 180:433–438.

Duval, S. & R. Tweedie. 2000. Trim and fill: a simple funnel-plot-based method of testing and adjusting for publication bias in meta-analysis. *Biometrics* 56:455–463.

Evans, G. T. & J. M. Hoenig. 1998. Testing and viewing symmetry in contingency tables, with application to readers of fish ages. *Biometrics* 54:620.

Fan, C., P. Koeniger, H. Wang & M. Frechen. 2011. Ligamental increments of the mid-Holocene Pacific oyster *Crassostrea gigas* are reliable independent proxies for seasonality in the western Bohai Sea, China. *Palaeogeogr. Palaeoclimatol. Palaeoecol.* 299:437–448.

Goodwin, D. H., K. W. Flessa, B. R. Schöne & D. L. Dettman. 2001. Cross-calibration of daily growth increments, stable isotope variation, and temperature in the Gulf of California bivalve mollusk *Chione cortezii*: implications for paleoenvironmental analysis. *Palaios* 16:387–398.

Harding, J. M., S. E. King, E. N. Powell & R. Mann. 2008. Decadal trends in age structure and recruitment patterns of ocean quahogs *Artica iclandica* from the Mid-Atlantic Bight in relation to water temperatures. *J. Shellfish Res.* 27:667-690.

Heaton, T. J., P. Köhler, M. Butzin, E. Bard, R. W. Reimer, W. E. N. Austin, C. B. Ramsey, P. M. Grootes, K. A. Hughen, B. Kromer, P. J. Reimer, J. Adkins, A. Burke, M. S. Cooke, J. Olsen & L. C. Skinner. 2020. Marine20-the marine radiocarbon age calibration curve (0—55 000 Cal BP). *Radiocarbon* 62:779-820.

Hjellvik, V., O. R. Godø & D. Tjøstheim. 2002. The measurement error in marine survey catches: the bottom trawl case. *Fish. Bull.* 100:720–726.

Hoenig, J. M. 2017. Should natural mortality estimators based on maximum age also consider sample size. *Trans. Am. Fish. Soc.* 146:136–146.

Hoenig, J. M., M. J. Morgan & C. A. Brown. 1995. Analysing differences between two age determination methods by tests of symmetry. *Can. J. Fish. Aquat. Sci.* 52:364–368.

Hofmann, E. E., J. M. Klinck, J. N. Kraeuter, E. N. Powell, R. E. Grizzle, S. C. Buckner & V. M. Bricelj. 2006. A population dynamics model of the hard clam, *Mercenaria*: development of the age- and length-frequency structure of the population. *J. Shellfish Res.* 25:417–444.

Hudson, J. H. 1981. Growth rates in *Montastrea annularis*: a record of environmental change in Key Largo Coral Reef Marine Sanctuary, Florida. *Bull. Mar. Sci.* 31:444–459.

Hulson, P. J. F., D. H. Hanseltnan & S. K. Shotwell. 2017. Investigations into the distribution of sample sizes for determining age composition of multiple species. *Fish. Bull.* 115:326–342.

Huyghe, D., M. de Rafelis, M. Ropert, V. Mouchi, L. Emmanuel, M. Renard & F. Lartaud. 2019. New insights into oyster high-resolution hinge growth patterns. *Mar. Biol.* 166:48.

Jacobson, L. D., D. Hart, K. D. E. Stokesbury, T. Jaffarian, M. A. Allard, M. C. Marino, II, A. Chute, J. I. Nogueira, B. P. Harris & P. Rago. 2010. Measurement errors in body size of sea scallops (*Placopecten magellanicus*) and their effect on stock assessment models. *Fish. Bull.* 108:233–247.

Jacobson, L., S. Sutherland, J. Burnett, M. Davidson, J. Harding, J. Normant, A. Picariello & E. Powell. 2006. Report from the Atlantic surfclam (*Spisula solidissima*) aging workshop. Woods Hole, MA: Northeast Fisheries Science Center. NEFSC Ref. Doc. 06-12. 24 pp.

Johnsen, E. 2003. Improving the precision of length frequency distribution estimates from trawl surveys by including spatial covariance—using Namibian *Merluccius capensis* as an example. *Fish. Res.* 62:7–20.

Jones, D. S. 1980. Annual cycle of shell growth increment formation in two continental shelf bivalves and its paleoecologic significance. *Palaios* 6:331–340.

Jones, D. S. & I. R. Quitmyer. 1996. Marking time with bivalve shells: oxygen isotopes and season of annual increment formation. *Palaios* 11:340–346.

Kimura, D. K. 1977. Statistical assessment of the age-length key. *J. Fish. Res. Board Can.* 34:317–324.

Kimura, D. K. & D. M. Anderl. 2005. Quality control of age data at the Alaska Fisheries Science Center. *Mar. Freshw. Res*. 56:783–789.

Kimura, D. K. & J. J. Lyons. 1991. Between-reader bias and variability in the age-determination process. *Fish. Bull*. 89:53–60.

Kubota, K., K. Shirai, N. Muralcami-Sugihara, K. Seike, M. Hori & K. Tanabe. 2017. Annual shell growth pattern of the Stimpson's hard clam *Mercenaria stimpsoni* as revealed by schlerochronological and oxygen stable isotope measurements. *Palaeogeogr. Palaeoclimatol. Palaeoecol*. 465:307–315.

Lee, H.-H., M. N. Maunder, K. R. Piner & R. D. Methot. 2011. Estimating natural mortality within a fisheries stock assessment model: an evaluation using simulation analysis based on twelve stock assessments. *Fish. Res*. 109:89–94.

Lentz, S. J. 2017. Seasonal warming of the Middle Atlantic Bight cold pool. *J. Geophys. Res. Oceans* 122:941–954.

Lewis, C. V. W., J. R. Weinberg & C. S. Davis. 2001. Population structure and recruitment of the bivalve *Arctica islandica* (Linnaeus, 1767) on Georges Bank from 1980–1999. *J. Shellfish Res.* 20:1135–1144.

MacDonald, P. D. M. & T. J. Pitcher. 1979. Age-groups from size-frequency data: a versatile and efficient method of analyzing distribution mixtures. *J. Fish. Res. Board Can*. 36:987-1001.

Machitto, T. M., Jr., G. A. Jones, G. A. Goodfriend & C. R. Weidman. 2000. Precise temporal correlation of Holocene mollusk shells using sclerochronology. *Quat. Res.* 53:236–246.

Martell, S. J. D., W. E. Pine, III & C. J. Walters. 2008. Parameterizing age-structured models from a fisheries management perspective. *Can. J. Fish. Aquat. Sci.* 65:1586–1600.

McBride, R. S. 2015. Diagnosis of paired age agreement: a simulation of accuracy and precision effects. *ICES J. Mar. Sci.* 72:2149–2167.

McNemar, Q. 1947. Note on the sampling error of the difference between correlated proportions or percentages. *Psychometrika* 12:153-157.

Mette, M. J., A. D. Wanamaker, Jr., M. L. Carroll, W. G. Ambrose, Jr. & M. J. Retella. 2016. Linking large-scale climate variability with *Arctica islandica* shell growth and geochemistry in northern Norway. *Limnol. Oceanogr*. 61:748–764.

Minte-Vera, C. V., M. N. Maunder, K. M. Schaefer & A. M. Aires-da-Silva. 2019. The influence of metrics for spawning output on stock assessment results and evaluation of reference points: an illustration with yellowfin tuna in the eastern Pacific Ocean. *Fish. Res.* 217:35–45.

Mohn, R. 1994. A comparison of three methods to convert catch at length data into catch at age. Int. Comm. Conserv. Atl. Tuna 42:110–119.

Munroe, D.M., E.N. Powell, R. Mann, J.M. Klinck & E.E. Hofmann. 2013. Underestimation of primary productivity on continental shelves: evidence from maximum size of extant surfclam (*Spisula solidissima*) populations. *Fish. Oceanogr*. 22:220–233.

Murawski, S., J. W. Ropes & F. M. Serchuk. 1982. Growth of the ocean quahog, *Arctica islandica*, in the Middle Atlantic Bight. *Fish. Bull.* 80:21–34.

NEFSC. 2017. 63rd northeast regional stock assessment workshop (63rd SAW) assessment report. Woods Hole, MA: Northeast Fisheries Science Center. NEFSC Ref. Doc.17-10. 414 pp.

Ogle, D. H., P. Wheeler & A. Dinno. 2021. FSA: fisheries stock analysis. R package version 0.8.23. Vienna, Austria: R Foundation for Statistical Computing. Available at: https://github.com/droglenc/FSA.

Okamura, H., M. K. McAllister, M. Ichinokawa, L. Yamanoka & K. Holt. 2014. Evaluation of the sensitivity of biological reference points to the spatio-temporal

distribution of fishing effort when seasonal migrations are sex-specific. *Fish. Res.* 158:116–123.

Pace, S. M., E. N. Powell & R. Mann. 2018. Two-hundred year record of increasing growth rates for ocean quahogs (*Arctica islandica*) from the northwestern Atlantic Ocean. *J. Exp. Mar. Biol. Ecol.* 503:8-22.

Pace, S. M., E. N. Powell, R. Mann & M. C. Long. 2017a. Comparison of age-frequency distributions for ocean quahogs *Arctica islandica* on the western Atlantic US continental shelf. *Mar. Ecol. Prog. Ser.* 585:81–98.

Pace, S. M., E. N. Powell, R. Mann, M. C. Long & J. M. Klinck. 2017b. Development of an age-frequency distribution for ocean quahogs (*Arctica islandica*) on Georges Bank. *J. Shellfish Res.* 36:41–53.

Pannella, G. 1971. Fish otoliths: daily growth layers and periodical patterns. *Science* 173(4002):1124–1127.

Pennington, M., L.-M. Burmeister & V. Hjellvik. 2002. Assessing the precision of frequency distributions estimated from trawl-survey samples. *Fish. Bull.* 100:74–80.

Pentilla, J. & L. M. Dery, editors. 1988. Age determination methods for Northwest Atlantic species. Woods Hole, MA: National Marine Fisheries Service. NMFS Report No. 72. 135 pp.

Peterson, C. H., P. B. Duncan, H. C. Summerson & B. F. Beal. 1985. Annual band deposition within shells of the hard clam, *Mercenaria*: consistency across habitat near Cape Lookout, North Carolina. *Fish. Bull.* 88:671–677.

Powell, E. N., R. Mann, K. A. Ashton-Alcox, K. M. Kuykendall & M. C. Long. 2017. Can we estimate molluscan abundance and biomass on the continental shelf? *Estuar. Coast. Shelf Sci.* 198:213-224.

Powell, E. N., J. M. Morson, K. A. Ashton-Alcox & Y. Kim. 2013. Accommodation of the sex-ratio in eastern oysters *Crassostrea virginica* to variation in growth and mortality across the estuarine salinity gradient. *J. Mar. Biol. Ass. U.K.* 93:533–555.

Purroy, A., S. Milano, B. R. Schöne, J. Thébault & M. Peharda. 2018. Drivers of shell growth of the bivalve, *Callista chione* (L. 1758)—combined environmental and biological factors. *Mar. Environ. Res.* 134:138–149.

R Core Team. 2018. R: a language and environment for statistical computing. Vienna, Austria: R Foundation for Statistical Computing. Available at: http://www.R-project.org.

Reynolds, D. J., C. A. Richardson, J. D. Scourse, P. E. Butler, P. Hollyman, A. Pomán-González & I. R. Hall. 2017. Reconstructing North Atlantic marine climate variability using an absolutely-dated sclerochronological network. *Palaeogeogr. Palaeoclimatol. Palaeoecol.* 465:333-346.

Reynolds, D. J., J. D. Scourse, P. R. Halloran, A. J. Niederbragt, A. D. Wanamaker, P. G. Butler, C. A. Richardson, J. Heinemeier, J. Eiriksson, K. Knudsen & I. R. Hall. 2016. Annually resolved North Atlantic marine climate over the last millennium. *Nat. Commun.* 7:13502.

Richardson, C. A. 2001. Molluscs as archives of environmental change. *Oceanogr. Mar. Biol. Annu. Rev*. 39:103–164.

Ridgway, I. D., C. A. Richardson, J. D. Scourse, P. G. Butler & D. J. Reynolds. 2012. The population structure and biology of the ocean quahog, *Arctica islandica*, in Belfast Lough, Northern Ireland. *J. Mar. Biol. Ass. U.K.* 92:539–546.

Ritter, M. N., H. Francischini, L. A. Kuhn, N. C. da Luz, F. H. Michels, A. L. M. de Morais, P. A. V. Paim & P. L. A. Xavier. 2016. El sesgo del operador en la replicabilidad de los estudios tafonómicos comparativos. *Rev. Bras. Paleontol.* 19:449–464.

Ropes, J. W. 1984. Procedures for preparing acetate peels and evidence validating the annual periodicity of growth lines formed in the shells of ocean quahogs, *Arctica islandica*. *Mar. Fish. Rev.* 46:27–35.

Ropes, J. W. 1988. Ocean quahog, *Arctica islandica*. In: Pentilla J. & L. M. Dery, editors. Age determination methods for Northwest Atlantic species. Woods Hole, MA:

Ropes, J. W., D. S. Jones, S. A. Murawski, F. M. Serchuk & A. Jearld, Jr. 1984a. Documentation of annual growth lines in ocean quahogs, *Arctica islandica* Linné. *Fish. Bull.* 82:1–19.

Ropes, J. W., S. A. Murawski & F. M. Serchuk. 1984b. Size, age, sexual maturity, and sex ratio in ocean quahog, *Arctica islandica* Linné, off Long Island, New York. *Fish. Bull.* 82:253–266.

Ropes, J. W. & D. Pyoas. 1982. Preliminary age and growth observations of ocean quahogs, *Arctica islandica* Linné, from Georges Bank. San Diego, CA: ICES C.M. Report No. 1982/K:15. 6 pp.

Schöne, B. R., J. Fiebig, M. Pfeiffer, R. Gleß, J. Hickson, A. L. A. Johnson, W. Dreyer & W. Oschmann. 2005. Climate records from bivalved Methuselah (*Arctica*

islandica, Mollusca; Iceland). *Palaeogeogr. Palaeoclimatol. Palaeoecol*. 228:130–148.

Schöne, B. R., A. D. Wanamaker, Jr., J. Fiebig, J. Thébault & K. Krentz. 2011. Annually resolved δ13Cshell chronologies of long-lived bivalve mollusks (*Arctica islandica*) reveal oceanic carbon dynamics in the temperate North Atlantic during recent centuries. *Palaeogeogr. Palaeoclimatol. Palaeoecol.* 302:31–42.

Sha, J., Y.-H. Jo, X.-H. Yan & W. T. Liu. 2015. The modulation of the seasonal cross-shelf sea level variation by the cold pool in the Middle Atlantic Bight. *J. Geophys. Res. Oceans* 120:7182–7194.

Sherwood, O. A., E. N. Edinger, T. P. Guilderson, B. Ghaleb, M. J. Risk & D. B. Scott. 2008. Late Holocene radiocarbon variability in Northwest Atlantic slope waters. Earth Planet. *Sci. Lett.* 275:146–153.

Shirai, K., K. Kubota, N. Murakami-Sugihara, R. Seike, M. Hakozaki & K. Tanabe. 2018. Stimpson's hard clam *Mercenaria stimpsoni*: a multi-decadal climate recorder for the northwest Pacific coast. *Mar. Environ. Res*. 133:49–56.

Stari, T., K. F. Preedy, E. McKenzie, W. S. C. Gurney, M. R. Heuth, P. A. Kunzlik & D. C. Speirs. 2010. Smooth age length keys: observations and implications for data collection on North Sea haddock. *Fish. Res.* 105:2–12.

Stuiver, M. & H. A. Polach. 1977. Discussion reporting of 14C data. *Radiocarbon* 19:355–363.

Swart, P. K. 2015. The geochemistry of carbonate diagenesis: the past, present and future. *Sedimentology* 62:1233–1304.

Thórarinsdóttir, G. G. & S. A. Steingrímsson. 2000. Size and age at sexual maturity and sex ratio in ocean quahog, *Arctica islandica* (Linnaeus, 1767), off northwest Iceland. *J. Shellfish Res.* 19:943-947.

Tisnérat-Laborde, N., M. Paterne, B. Bétivier, M. Arnold, P. Yiou, D. Blamart & S. Raynaud. 2010. Variability of the Northeast Atlantic sea surface Δ14C and marine reservoir age and the North Atlantic Oscillation (NAO). *Quat. Sci. Rev.* 29:2633–2646.

Wanamaker, A. D., Jr., K. J. Kreutz, B. R. Schöne & D. S. Introne. 2011. Gulf of Maine shells reveal changes in seawater temperature seasonality during the medieval climate anomaly and the Little Ice Age. *Palaeogeogr. Palaeoclimatol. Palaeoecol.* 302:47–51.

Wanamaker, A. D., Jr., K. J. Kreutz, B. R. Schöne, K. A. Maasch, A. J. Pershing, H. W. Burns, D. S. Introne & S. Feindel. 2009. A Late Holocene paleo-productivity record in the western Gulf of Maine, USA, inferred from growth histories of the long-lived ocean quahog (*Arctica islandica*). *Int. J. Earth Sci.* 98:19–29.

Weidman, C. R. & G. A. Jones. 1993. A shell-derived time history of bomb 14C on Georges Bank and its Labrador Sea implications. *J. Geophys. Res. Oceans* 98:14577–14588.

Weidman, C. R., G. A. Jones & K. C. Lohmann. 1994. The long-lived mollusc *Arctica islandica*: a new paleoceanographic tool for the reconstruction of bottom temperatures for the continental shelves of the northern North Atlantic Ocean. *J. Geophys. Res. Oceans* 99:18305–18314.

Weinberg, J. R. 1999. Age-structure, recruitment, and adult mortality in populations of the Atlantic surfclam, *Spisula solidissima*, from 1978–1997. *Mar. Biol.* 134:113–125.

Wilderbuer, T. K. & B. J. Turnock. 2009. Sex-specific natural mortality of arrowtooth flounder in Alaska: implications of a skewed sex ratio on exploitation and management. *N. Am. J. Fish. Manage*. 29:306–322.

Witbaard, R., M. I. Jenness, K. van der Borg & G. Gaussen. 1994. Verification of annual growth increments in *Arctica islandica* L. from the North Sea by means of oxygen and carbon isotopes. *Neth. J. Sea Res.* 33:91–101.

CHAPTER III POPULATION DYNAMICS OF *ARCTICA ISLANDICA* AT GEORGES BANK (USA): AN ANALYSIS OF SEX-BASED DEMOGRAPHICS

Modified from:

Hemeon KM, Powell EN, Pace SM, Redmond TE, Mann R (Accepted) Population dynamics of Arctica islandica at Georges Bank (US): an analysis of sex-based demographics. J Mar Biol Assoc UK.

3.1 Introduction

Arctica islandica (Linnaeus, 1767) is a boreal bivalve with an expansive range in the northern hemisphere that also has the unique capacity for individuals to survive for centuries. The last extant species of the family Arcticidae, *A. islandica* (*i.e.*, ocean quahog) is endemic to the Arctic and Atlantic oceans and currently inhabits shelf waters from Norway to the British Isles and Iceland, the Baltic and White Seas, and from Newfoundland to Cape Hatteras (Cargnelli *et al*., 1999; Dahlgren *et al.*, 2000; Butler *et al*., 2009; Gerasimova & Maximovich, 2013). This species is found at depths between 25-61 m and occurs at an average depth of 42 m in the western Mid-Atlantic (Merrill & Ropes, 1969), but depth and distance offshore are regional responses to bottom water temperatures (Franz & Merrill, 1980; Dahlgren *et al.*, 2000).

In addition to the fascinating longevity exhibited by *A. islandica*, this species represents an important fishery in the western Atlantic. Fishery landings in the United States (US) are divided into a Gulf of Maine fishery that targets younger and smaller clams (*i.e.*, mahogany clams), and the southern fishery that targets larger clams (>80 mm shell length) that spans Cape Hatteras in the south to Georges Bank in the northeast (Merrill & Ropes, 1969, Franz & Merrill, 1980; Dahlgren *et al.*, 2000). Georges Bank is considered a separate management area within the southern fishery due to the extreme

distance offshore and separation from the contiguous southern fishery by the Great South Channel (NEFSC, 2017). Paralytic shellfish poisoning closed Georges Bank for surfclam and ocean quahog commercial harvests in 1989 and this area remained closed until recently reopened to these fisheries in 2013 (DeGrasse *et al.*, 2014; NEFSC, 2017). Accordingly, the Georges Bank population can be considered quasi-virgin (*i.e.*, unfished) due to restricted commercial accessibility and minimal annual ocean quahog landings (less than 0.5% of total stock landings between 2000-2016, with no reported landings prior to 2000) (NEFSC, 2017).

Arctica islandica is managed in the US by means of length-based population models, a stark contrast to the age-based models applied to many other fisheries. The extreme variability in age-at-size (Pace *et al.*, 2017a, 2017b) makes producing reliable age estimations from size difficult when using age-length keys (ALK) or growth curves, thereby limiting the use of age-based models. In addition, the longevity of this species poses particular management challenges because a recruitment index is unavailable over a time frame consistent with the longevity of the animal, thereby creating uncertainty as to sustainable yield and the time frame required for rebuilding should the stock be overfished. Historic presumptions for *A. islandica* include prolonged lapses in recruitment to sustain such longevity (Powell & Mann, 2005), but this conclusion was based on recent recruitment data from the southernmost portion of the Western Atlantic range; a longer-term recruitment time series cannot be predicted without age-frequency data. Pace *et al.* (2017a) identified that extremely large sample sizes are likely required to provide adequate resolution in the *A. islandica* ALK to develop a suitable, population-scale age frequency.

A further impediment to understanding *A. islandica* population dynamics is the differential growth rates of male and female *A. islandica* (Ropes *et al*., 1984; Fritz, 1991; Thorarinsdóttir & Steingrímsson, 2000). Sexual dimorphism is rare in bivalves, excepting the protandrous taxa. The degree of sexual dimorphism in *A. islandica* may require sex-specific ALKs. Sexual dimorphism often co-occurs with sex-dependent mortality rates, whereby distinct age frequencies may also exist and might influence both length- and age-based models (Wilderbuer & Turnock, 2009; Maunder & Wong, 2011).

The objectives of this study are to address gaps in the current fishery assessment models by examining the ability to produce age-based model parameters including a reliable ALK to estimate ages, estimates of mortality and longevity, evaluating proxies for recruitment indices such as age-frequency distributions, and determining whether sex-specific considerations need to be made. Georges Bank was chosen for this analysis as it represents a nearly virgin stock, thus providing proxy baseline data on the population dynamics of this species and potential recruitment trends over time in the western Mid-Atlantic region.

3.2 Materials and Methods

3.2.1 Sample Collection

Two field samples were collected for this project: a length sample and a shucked sample. Each sample was obtained from approximately the same site (40.72767°N, 67.79850°W) at a depth of approximately 72 m (Figure 3.1). This site falls within the new federal survey stratum 9Q (Jacobson & Hennen, 2019). Both samples are unbiased representations of the population in that no subsampling occurred. The length sample was collected in 2015 for a previous *Arctica islandica* age study (see Pace *et al.*, 2017a,b) by

a hydraulic clam dredge employed by both the fishery and federal survey (Hennen *et al.*, 2016). Commercial fishing gear, including the survey gear used for this collection, targets, and is therefore highly selective for, animals greater than ~75 mm (Hennen *et al.*, 2016; NEFSC, 2017); selectivity falls rapidly for sizes < 60 mm. To limit uncertainty imposed by a correction for selectivity, this study focused on the highly selected size classes ≥75 mm. Analysis, thusly, focuses on the length classes pertinent to fishery stock demographics and to the federal stock assessment program. The 2015 length sample included shell lengths for 2,778 *Arctica islandica* that were used to construct the length frequency.

In 2017, a more intensive age analysis was conducted to age more *A. islandica* per size class than the Pace *et al*. studies (2017a,b). A differential sampling protocol was used so that sufficient animals of a range of size classes could be obtained for aging. The 2017 shucked sample was collected from the same location as the 2015 length sample which permitted reutilization of the 2015 length sample. The 2017 shucked sample was collected with a Dameron-Kubiak (DK) dredge that allowed variable bar spacing to collect animals less than 80 mm and increase sample sizes for smaller animals available to the fishery (Hennen *et al.*, 2016). Although animals between 70-74 mm in shell length were not included in the 2015 length sample, these animals were retained by the DK dredge and included in the shucked sample so no age data would be omitted for such a data-poor species. Multiple 5-min tows from the same site were required to obtain sufficient numbers of animals for the large, rare size classes. Clam sexes were determined using gonadal tissue samples that were examined microscopically for the presence of sperm or eggs. The 2017 shucked sample included a total of 706 clams measured for shell

length, sexed, shucked to remove all tissue, and the shell valves retained in dry storage for subsequent aging.

3.2.2 Length Frequency

To obtain an accurate representation of Georges Bank population demographics, the 2015 length sample was adjusted using a dredge selectivity coefficient (see Table 15 in NEFSC, 2017). This selectivity coefficient was derived by federal assessment biologists across 20 sites within the US Mid-Atlantic *A. islandica* stock management area for the survey dredge employed by this study to collect the length sample.

Sex data were not collected for the 2015 length sample; therefore, the length sample was divided into male and female length frequencies by use of sex proportion at size from the 2017 shucked sample (n=706) for each 1-mm size class. The population length frequency is the unsexed 2015 selectivity-adjusted length sample and included 3,159 animals, that was subsequently divided to produce the female (n=1,470) and male (n=1,689) length frequencies.

3.2.3 Age Frequency

The 2017 shucked sample was divided into 5-mm size classes and 100 animals per size class were chosen for aging to create the age sample. These 100 animals consisted of approximately 50% randomly selected males and 50% randomly selected females (if available) to prevent a sex bias in numbers of aged animals per size class. All animals were aged for rare size classes that contained less than 100 animals. Sample processing methods were consistent with Pace *et al.* (2017b) and aging techniques were consistent with Pace *et al.* (2017b) and Hemeon *et al.* (2021). Animals selected for aging

constituted the age sample and included true age and length data. This dataset was quality controlled using a second age reader for precision, bias, and error frequency error analyses (Hemeon *et al.*, 2021). A total of 615 animals were aged, including 306 females and 309 males.

Age-length keys (ALK) are probability arrays that describe the probability of different animal ages at a given length and are created by amassing many samples with associated age and length data (Mohn 1994; Harding *et al*., 2008; Stari *et al*., 2010). Unique ALKs were created in this study for the population, female, and male groups using the age sample binned into 5-mm length size classes. Following ALK construction using the 2017 age sample, the corresponding 2015 length frequency (population, male, female) was applied to the analogous ALK to produce 2015 population, female, and male estimated age frequencies. Resulting fractions in the age frequency were rounded up to whole individuals to prevent the elimination of a fraction of an animal due to rounding which would remove data for rare age classes. Consequently, male and female age frequencies do not sum to the number of animals in the population age frequency because each age frequency was created independently from unique ALKs and unique length frequencies. The population age frequency included 3,248 animals, female age frequency 1,525 animals, and male age frequency 1,742 animals.

3.2.4 Longevity and Mortality

Georges Bank is a site with no historic, and limited contemporary, commercial harvest of *Arctica islandica*. Consequently, total mortality is assumed to be equivalent to natural mortality (ocean quahog bycatch from the Atlantic surfclam fishery is also considered negligible at Georges Bank; see NEFSC, 2017). The descending right tails of

the age frequencies were used to estimate mortality and longevity by linear regression of the natural log of the age frequencies (*e.g.*, Ricker, 1975; Kilada *et al*., 2007; Ridgway *et al*., 2012; Hoenig, 2005). Data were collapsed into 10-y age classes for this analysis to remove extreme noise in the data. The descending left tail of the age frequency is likely a product of low selectivity to the commercial dredge rather than low abundance and was not used to estimate mortality. Therefore, linear regression was evaluated for age frequencies greater than 100 y and represented 49% of the population and male age frequency data, and 48% of the female age frequency data. The x-intercept denoted the longevity estimate and slope represented the mortality rate.

3.2.5 Statistics

3.2.5.1 Frequency Distributions

Tests to analyze significant differences between male and female length- and age-frequency distributions included the Kolmogorov-Smirnov (KS) (Conover, 1980), Wald-Wolfowitz Runs (Conover, 1980), and Anderson-Darling (AD) (Pettitt, 1976; Engmann & Cousineau, 2011) tests at both 0.05 and 0.01 significance levels. The Runs test identifies systematic shifts in the distribution and, as used here, is designed to identify limited crossings of frequency distributions as might occur if male and female growth rates differed. The KS test and AD test compare the deviation between two frequency distributions, with the KS test being more sensitive to deviations in the central portion of the distribution and the AD test to deviations at the tails of the distribution. The AD test was included due to the rarity of old animals in the age-frequency distributions (distribution tails) and the KS test was included to identify episodic recruitment and mortality events (distribution central tendencies). Critical values were obtained from

Conover (1980) for the KS and Runs tests and from Rahman *et al*. (2006) for the AD test. The KS test and the AD test were operated as two-sample, two-tailed tests, and rows without data outside the range of frequency data (leading and trailing double zeros) were deleted. For the KS and AD tests, the number of observations (n) was defined as the number of classes instead of the sum of the data supporting the classes, as doubling or halving the number collected and measured would not have materially changed the cumulative frequency distribution. The Runs test was operated as a one-sided test to evaluate only the "low" condition, by which the distributions failed to cross each other at a minimal frequency expected by chance. In many cases, the total number of males and females of a length frequency differed due to sex ratios at size. To exclude a sex-ratio bias for the Runs test, the number of males and females was represented proportionately by length or age class.

In addition to the standard KS, Runs, and AD tests listed above, a separate round of distribution test statistics were applied to modified versions of the distribution data used in the previous analysis. These modifications address the heavily right-skewed age frequencies that contain many instances of low to zero numbers of individuals in the tails of the distribution which can overly influence statistical evaluation of the distribution as a whole. Accordingly, in the spirit of the same approach used commonly in chi-square, the age and length classes with small numbers were also compressed by amalgamating adjacent classes. Unlike chi-square (*e.g.*, Conover, 1980), no standard rule is available to amalgamate class groups. In the present case, the median number in all classes was used and adjacent classes amalgamated until the number of individuals reached or exceeded this value. One of the two datasets (*i.e.*, male or female) is required to designate the

median to be applied to both datasets. That dataset herein is referred to as the reference dataset and the analysis is completed twice with each dataset assigned as the reference dataset. Once data were grouped into new frequency bins using the median, the KS, Runs, and AD analyses were again performed, and this new type of analysis is herein referred to as median bin modification.

3.2.5.2 Age-Length Keys

To test the reliability of the male and female age-lengths keys (ALKs), 50 Monte-Carlo simulations were performed for each sex by randomly sampling with replacement from the true age-length data and new ALKs were created for each simulation. Random samples included the same number of animals aged per 5-mm size class as the true dataset in order to represent the real aging intensity, thereby preventing oversampling of rare size classes. The corresponding sex-specific length frequency was applied to the new ALK produced by each of the 50 simulations (herein referred to as the base simulations), and the resulting female and male age frequencies were tested for significant differences from the true age frequency by the KS, AD, and Runs statistical tests.

A second set of 50 Monte Carlo simulations was completed in the same manner listed above, but new simulated ALKs were applied to the opposite sex length frequency and produced an additional 50 age frequencies per sex. These new age frequency distributions (herein referred to as the substituted simulations) were tested against the true age frequency using the KS, AD and Runs tests. If no significant difference exists between ALKs when the same length frequency is applied, the proportion of significant differences across 50 simulations would be the same for both the base and substituted simulated age frequencies. The proportion of base simulations with significant test results

from the true age frequency was deemed the expected proportion of differences from a sampled population. A one-sample approximate binomial test for large samples [*i.e.*, proportions test (R Core Team, 2018)] was used to compare the proportion of significantly different substituted simulations from the expected proportion of significantly different base simulations (*e.g.*, if the base simulations were statistically different from the true age frequency $\frac{x}{50}$ times, this would be the expected proportion; the proportion of significantly different substituted simulations would be compared to the expected proportion using a binomial test). If the ALKs were similar between sexes, substitution of the ALK applied to the same length frequency would create similar age frequencies to those of the true age frequencies and base simulations; whereas, if the ALKs were significantly different between sexes, the substituted ALKs would create different age frequencies when compared to the true age frequencies and the base simulations.

3.2.5.3 Sex Ratios

Sex ratios were expected to be at one-to-one proportions across size classes. A one-sample binomial test [approximate binomial test for large samples (total n>30), and one-sample exact binomial test for small samples (total n<30) (Conover, 1980)] (R Core Team, 2018) was used to evaluate a proportional sex ratio hypothesis for sex differentiated animals in the shucked sample (n=706). A two-tailed analysis was performed to identify if the ratio is significantly different than what would be expected by chance (expected proportion of 0.5) and, if significant, a one-tailed test was used to identify if the ratio of females is less than or greater than what would be expected by chance.

3.2.5.4 Comparison of the Means

Distribution statistics were applied to test differences in the shapes and spread of the length- and age-frequency data, likewise, mean statistics were applied as a secondary analysis to test whether male and female datasets represent the same population. Male and female length frequency data were tested for significant difference with a Mann-Whitney U test using R base statistics functions (population data omitted from this analysis as it is not an independent or paired dataset) (R Core Team, 2018).

Age data are positively skewed and therefore ranked (use of mean ties) before use in ANOVAs with alpha=0.05 [it should be noted that that an independent analysis that compared both parametric (raw ages) and non-parametric (ranked ages) tests produced similar results]. Age composition between size classes were evaluated by type III one-way ANOVA and Tukey post-hoc tests, and age composition by sex between size classes were evaluated with a type III one-way multiplicative ANOVA model (R Core Team, 2018). Age compositions between population, female, and male frequencies were assessed by type III ranked one-way ANOVA (R Core Team, 2018).

3.3 Results

3.3.1 Length Frequency

The 2015 length frequency was divided into male and female length datasets by applying a sex proportion at size (1 mm) to the original dataset (Table 3.1-3.2). The Georges Bank population length frequency had a mean length of 93 mm (*SD*=7) and ranged from 76-116 mm (Figure 3.3). The central tendencies for the female length frequency (*M*=96 mm, *SD*=6; median=95 mm) were larger than central tendencies for the male length frequency (*M*=91 mm, *SD*=6; median=90 mm) (Figures 3.4-3.5). The

cumulative length frequency plot (Figure 3.5) shows that the female length frequency is of similar shape to the male length frequency but, on average, females are offset to larger shell lengths. A Mann-Whitney U-test substantiates these findings that the females are larger than the males in the Georges Bank population (p=2.2E-16), and distribution statistics are significantly different for the KS, Runs, and AD tests at an $\alpha = 0.05$ significance level (Table 3.4). Therefore, the female and male length-frequency distributions are unique. When size classes with low frequency were amalgamated using the median of the reference dataset, the distribution statistics were only significant for the Runs test at the $\alpha = 0.01$ and 0.05 significance levels (Table 3.4), indicating the strong influence of the tails of the distribution on the KS and AD comparisons.

3.3.2 Shucked Sample

All 706 *A. islandica* that were sexed from the shucked sample were grouped into 5-mm size classes and the sex ratio at size was compared. Each size-class name refers to the lower boundary of the data bin (*e.g.*, 80-84 mm are assigned to the 80-mm size class). Males dominated size classes less than 95 mm and females dominated size classes 95 mm and larger (Figure 3.6). At the transitional 95-mm boundary between sex dominant size classes, the magnitude of proportional difference lessens, likely representing a near 1:1 sex ratio between 90-100 mm shell lengths (Figure 3.6). A 1:1 sex ratio between 90-100 mm is supported by the non-significant binomial sex-ratio results for these size classes (Table 3.3). Size classes 70, 115, and 120 mm similarly did not have significant binomial tests, but these size classes also had the smallest sample sizes ($n<10$).

3.3.3 Age-Length Data

In the following, age-length data refer to animals in the age sample (a subset of the 2017 shucked sample) and have true age, sex, and length metrics. From the 2017 shucked sample (n=706), 615 animals that fit size class requirements (~100 animals per 5-mm size class) constituted the age sample and were of sufficient quality to age and be included in the age-length dataset. These 615 samples were also quality controlled using an age-reader error assessment protocol (Hemeon *et al.*, 2021). The median female length (101 mm) and age (123 y) were greater than the male median length (91 mm) and age (113 y) (Figure 3.7). Median length discrepancies are the result of sampling rare size classes dominated by one sex over the other. Females tend to be larger than males at comparable ages indicating that females grow faster than males, and females tend to be older than males in this sample (Figure 3.7), assuming that *A. islandica* is not protandrous [see *e.g.*, Powell *et al*., (2013) and Harding *et al*., (2013) for an example of size- and age-dependent protandry]. The oldest animal was a 261-y-old male that recruited to the population in 1756. Old age is not indicative of size for ocean quahogs, however, and the oldest animal was only 107 mm whereas the largest animal was a 120-mm female of 166 y. A commercial dredge targets large ocean quahogs greater than 80 mm, but smaller animals can still be retained by the dredge; therefore, for reference, the smallest and youngest animals retained for the age sample were females of 73 mm shell length (43 y) and 33 y old (85 mm), respectively.

One-way ranked ANOVA detected significant differences between 5-mm size classes in age composition ($p<2.2E-16$) (Figure 3.8). Tukey post-hoc tests indicated that size classes between 75-90 mm were statistically different than size classes greater than

95 mm ($p<0.05$), and the 95-mm size class was different than size classes greater than or equal to 100 mm. These results suggest that the age compositions in the 95-mm size class is different than all other size classes. A two-way ranked ANOVA with a sex and size class interaction revealed no significant difference between the ages of males and females within size classes (Figure 3.9).

The reliability of the constructed ALKs (Figure 3.10) from the age-length data was analyzed using 50 simulated age frequencies sampled from the same age-length data and the sex-appropriate length frequency (*i.e.*, base simulations). At $\alpha = 0.05$, the male and female base simulations are significantly different from corresponding true age frequencies 2% [*i.e.*, in reference to table 3.5 (1-0.98*100)] of the time for the KS test, approximately 25% of the time for the Runs test, and 96% of the time for female and 100% of the time for male AD tests (Table 3.5). For $\alpha = 0.01$, the KS and Runs tests are significantly different less than 10% of the time for both male and female base simulations, but the AD tests are often significantly different for both sexes. Few cases of significantly different KS base simulations for both sexes indicate that ALKs produced from these age-length data are reliable for the central tendency of the age-frequency distributions. Conversely, high proportions of significant differences of AD results from base simulations denoted that the tails of the age-frequencies are poorly specified, likely due to the rarity of samples from these age classes. When the distribution was modified using median values to amalgamate adjacent classes with small numbers, the median results were comparable to the null results, but the female ALK was better at predicting the true age-frequency distribution when analyzed by the median Runs test.

The substituted simulations were created to examine how the ALKs performed with opposite-sex length frequencies. If the ALKs are not different, the same length frequency should produce similar results between the base and substituted simulations regardless of ALK used. For both $\alpha = 0.05$ and 0.01 levels, the KS test had the greatest change between base and substituted simulation types (Table 3.5). The AD test results had a high proportion of significant differences for both the base and substituted simulations, presumably because rare age classes are difficult to predict regardless of ALK, but the frequency of significant differences rose in the substituted simulation set. Runs test results varied only modestly. After implementing the "median" data modification to reduce the influence of age classes with low numbers, the probability of significant differences increased between substituted and true age frequencies, except for the median KS test results that slightly decreased by 2-10%.

For tests with a $\alpha = 0.05$ significance level, an approximate binomial test identified that the male substituted ALK failed the female KS test, and the female ALK failed the male KS and AD test (Table 3.5). At a $\alpha = 0.01$ significance level, the substituted male ALK failed both the female KS and AD tests, and the female substituted ALK failed all three male distribution tests. The "median" data modification further magnified the differences between the male and female ALKs, and at $\alpha = 0.01$ significance level, both male and female substituted ALKs failed to recreate the base simulations for all three tests and only the AD test at 0.05 significance level was similar to the base simulations (Table 3.5).

3.3.4 Age Frequency

Estimations of age frequency by sex are derived from the 2015 length frequencies specified by sex-proportion at size (see shucked sample) that were applied to the sex-differentiated 2017 ALKs. The 2015 age frequencies represent *Arctica islandica* available to the commercial fishery and support the primary dataset used for stock management. These frequencies are predominantly composed of animals estimated between 70-140 y of age (Figure 3.11). The mean estimated age of the population is 104 y (*SD*=30), the mean estimated age of females is 102 y (*SD*=29), and the mean estimated age of males is 104 y (*SD*=29) (Figures 3.11-3.13). The youngest animal was estimated as a 33-y female, the oldest animal was estimated as a 261-y male. A type III ranked one-way ANOVA detected no significant difference of age composition between the population, female, or male groups (Figure 3.13). A low frequency of females estimated between 110-125 y of age occurred near the center of the distribution and also the region of the distribution where the KS test is most sensitive. Female, male, and population age-frequency distributions are depressed between the estimated ages of 90-100 y that correspond to birth years 1917-1927 (Figures 3.11-3.12). However, only the female distribution demonstrates a second profound depression in animals born approximately 110-125 y ago (Figure 3.12A). Across all three groups, a rapid increase in *A. islandica* frequency occurred approximately 150-y ago prior to sampling (1867) and periodic recruitment ebbs and flows occurred approximately every 5-10 y between 1867-1984 (*i.e.*, to the end of dataset) (Figures 3.11-3.12).

3.3.5 Longevity and Mortality

Estimated natural mortality rate for the population was 0.04, females 0.05, and males 0.04 (Figure 3.15). Population longevity was 257 y, females 219 y, and males 244 y (Figure 3.15). Mortality and longevity estimates were approximated by linear regression models with high coefficients of determination (population, female, male: R^2=0.96).

3.4 Discussion

3.4.1 Validity of Age-Length Keys

Ropes *et al.* (1984) and Thorarinsdóttir & Steingrímsson (2000) documented that sex ratios at size varied for *Arctica islandica*, evidence that sex should be considered when evaluating length relationships of this species. Sex proportions at size were unequal in the Georges Bank (GB) population, where males and females dominated different portions of the population length frequency (Figure 3.3, Table 3.4). Therefore, a grouped age-length key (ALK) may not adequately predict the true age frequency of the population if size dimorphism is not considered, and particularly if the number of males and females differs. It is consequently important to determine when different ALKs need to be used over time, between regions, specific to survey gear (*e.g.*, research, commercial, survey), and for different sexes.

Base simulations tested the reliability of male and female ALKs and determined that the generated age frequencies are reproducible and the ALKs are sufficient at predicting the central tendency of the sex-specific age distributions given the number of animals aged from each sex (Table 3.5). Both the male and female ALKs failed to predict the tails (or rare age classes) of the distributions reliably. The female base simulations

were significantly different from the true age frequency 96% of the time and the male base simulations were significantly different 100% of the time using the AD test (null, $\alpha = 0.05$). This is not surprising since the right-hand tail of both the male and female age frequencies is populated with extremely few animals and random sampling may not select these animals in random draws; that is, the age distribution at old age is poorly determined even with several hundreds of animals aged from a population. For instance, the oldest animals in the age-length dataset are in the 105-mm length class which is the second largest length class (*i.e.*, frequency) and ages within that length class span 120 y, but the older animals represent less than 10% of the 105-mm length class (Figure 3.10A, but also observe same trends in Figure 3.10B-C). Given hundreds of aged animals, consistently predicting all sections of the age-frequency distribution using an ALK for *A. islandica* remains uncertain, yet these ALKs do predict the central tendency of the distributions 98% of the time for both sexes (see KS results in Table 3.5). Accurately predicting the age-frequency tails may become important, however, if suitable habitat contracts and biases the surveyed GB site to older individuals, recruitment declines, or biomass-standardized fecundity is found to vary with age. One option is aging ever more animals to increase the number of extremely old *A. islandica* (>200 y) aged, thereby adding data to the tail of the age frequency. A second option might be to identify attributes of the shell, such as periostracum coverage, that may indicate age and permit a more efficient search. Results from Butler *et al*. (2020) do not provide much hope for this outcome, however.

Simulations designed to test the differences between sex-specific ALKs revealed that the male ALK cannot accurately predict the female age frequency and the female

ALK cannot accurately predict the male age frequency (Table 3.5). If the ALKs are not significantly different from one another, the same length frequency should produce similar age frequencies regardless of which ALK is applied. When the male ALK was substituted for the female ALK, the female length frequency produced age frequencies that were significantly different from the true age frequency 100% of the time for both the KS test and the AD test. When the female ALK was substituted for the male ALK, the male length frequency produced age frequencies that were significantly different from the true age frequency 100% of the time for the KS test and 82% of the time for the AD test. Thus, for portions of the male and female age-frequency distributions with the most animals (*i.e.*, ages with highest probability of being fished), the male and female ALKs differ. The male and female ALKs can predict the true age frequencies 98% of the time but, when ALKs are swapped, the true age frequencies cannot be predicted by the opposing ALK. Therefore, male and female ALKs reliably produce the true sex-specific age frequencies but are not interchangeable. Male and female age frequencies are relatively similar and the primary cause producing the differential ALKs is age at length; females tend to be larger at a given age.

3.4.2 Dimorphism

Female *Arctica islandica* clearly reach larger sizes at younger ages than males, yet the age structure is comparable between sexes. Divergent length-frequency distributions combined with similar age-frequency distributions are indications of dimorphic growth (Figure 3.5, Figure 3.14) (Thorarinsdóttir & Steingrímsson, 2000), a phenomenon common throughout the animal kingdom, but rare in bivalve molluscs. The dominant sex proportion at size changes at approximately 95 mm and this is reliably

determined based on the copious sample size at 95 mm and neighboring size classes (Figure 3.6, Table 3.3- 3.3). Consequently, the switch in dominance of the sex ratio at approximately 95 mm is well supported by this study. Ropes *et al.* (1984) also identified a transition from predominantly male *A. islandica* to predominantly female between 70-99 mm, and in animals larger than 100 mm the percent males plummeted to approximately 8% whereas animals smaller than 30 mm were 100% male in their study. On average, in the present study, males comprised only 14% of animals larger than 100 mm and ranged between 0-35% male composition with the lowest male sex compositions at the largest sizes. Also similar to Ropes *et al.* (1984), average male sex composition was 89% for animals less than 85 mm. Thorarinsdóttir & Steingrímsson (2000) likewise observed a transition from male to female sex-ratio dominance with increasing shell length, but for their Icelandic population the transition occurred at much smaller sizes (40 mm) and could be attributed to the slower growth rates observed at northern latitudes (Thorarinsdóttir & Jacobson, 2005).

Although the female and male age frequencies clearly differed in some details (Figure 3.12), the female to male population sex ratio obtained from the length frequency dataset was 1:1.1 (Table 3.2). Jones (1981) found more males than females in a sample of 352 individuals collected from New Jersey greater than 75 mm (1:1.4), and Mann (1982) also observed more males than females with a sample size of 354 specimens collected from southern New England (1:1.1). Therefore, the population sex ratio obtained by this study is comparable to the sex ratios identified from other regions and sample sizes.

Sexual dimorphism in *A. islandica* might be the result of suppressed early growth rates during initial maturation and development. Coe (1932) hypothesized that

dimorphism could be the result of three life-history strategies: high mortality/short longevity of males, environmentally determined sex, or protandry. Protandry, the transition from male to female reproductive structures at later life stages, is common in many bivalve groups [*e.g.*, pteriids (Chávez-Villalba *et al*., 2011; Serna-Gallo *et. al*., 2014), pinnids (Camacho-Mondragón *et al*., 2015), crassostreid oysters (Powell *et al*., 2013; Yasuoka & Yusa, 2016), cardiids (Yau *et al*., 2014)], but unreported to our knowledge in the Venerida. Apropos of this case, Ropes *et al.* (1984) identified that maturation data do not support a protandric life history in *A. islandica*. Age-frequency results described here (Figure 3.11-3.13, Table 3.4) agree with the interpretation of Ropes *et al.* (1984), in that the size differential is primarily a function of distinctive growth rates between the sexes as the age frequencies are very similar. The age-frequency results also do not support an abnormally high male mortality rate and shorter longevity; in fact, mortality and longevity estimates demonstrate the opposite. Data do not currently exist to support the hypothesis that *A. islandica* sexes are environmentally determined, and divergent growth may instead be a manifestation of deviating energy allotment. The extreme case in molluscs is the rare phenomenon of small males with early-onset maturity exemplified by dwarf males such as in a number of gastropod taxa (Elder, 1979; González-Vallejo, 2008) and the bivalve *Zachsia zenkewitschi* where the male delegates its life as a pseudo parasite within the mantle pouches of the female (Turner & Yakovlev, 1983). In *A. islandica*, where males are free-living, male germinal cells are documented at younger ages and smaller sizes than females (Ropes *et al.*, 1984; Rowell *et al*., 1990; Thorarinsdóttir & Steingrímsson, 2000) which could result in reduced energy devoted to somatic growth in early years for the males. Earlier maturity in males would offer

females a “head start” in their growth trajectory while relegating males to a smaller size-at-age, resulting in the observed length-frequency distributions that are similar in shape but simply offset with age (Figure 3.5, Table 3.4).

Observed sex ratios of ocean quahog size classes available to the fishery may result in harvests biased in favor of male *A. islandica* if sex-ratio relationships are stable across regions and landing size frequencies are dominated by 80-100 mm animals, which is the case in most years (NEFSC, 2017). To what extent and at what fishing mortality rate the preferential loss of males might influence population fecundity is as yet unknown. This study evaluated the population dynamics available to the commercial fishery, but it is yet undetermined if these trends apply to animals younger than 40 years of age and consequently born since 1977, or animals smaller than 75 mm.

3.4.3 Recruitment Frequency

Recruitment inferred from the age frequency, assuming that the decline in abundance at older age is primarily due to natural mortality, appears to be relatively consistent between the years of 1767-1957 as *Arctica islandica* births are recorded for each year of this time range in the age-frequency data. These results support findings by Pace *et al.* (2017b). Effective recruitment, as evidenced by *A. islandica* that survive to market size and therefore become available to the fishery, is present for most yearly cohorts and, because ocean quahogs exhibit annual spawning (Loosanoff, 1953; von Oertzen, 1972; Jones, 1981; Mann, 1982), periodic reductions in recruitment observed throughout the age frequency can likely be attributed to unfavorable environmental conditions. Conversely, pulses in recruitment appear to occur in 8-y intervals beginning post 1900 (Figure 3.11). The apparent 8-year signal in recruitment is reminiscent of a

well-described ~8-y cyclicity in the North Atlantic Oscillation (NAO) (Soniat *et al.*, 2006, 2009), however no direct lead-lag relationships have yet been investigated between recruitment pulses in this study and NAO indices. Recruitment pulses occurring on 8-y cycles may also represent additive signals from strong year classes that begin spawning at approximately 6-13 y of age in the Mid-Atlantic (Ropes *et al.*, 1984) and subsequent cohorts preserve the ~8-y strong year class cycle in younger, but mature, generations. The NAO indices are important effectors of sea temperatures and mixed-layer depths in the Northwest Atlantic (Bojariu & Gimeno, 2003; Hurrell & Deser, 2009) and might influence larval dispersion and recruitment in *A. islandica*. Lutz *et al.* (1982) described the tightly coupled response of larval settlement to temperature, whereby faster settlement occurred at warmer temperatures (13ºC), and colder temperatures (8.5-10ºC) prolonged the planktonic larval phase by nearly 23 days. The energy investment for annual spawning by a long-lived species may be an evolutionary advantage when larval and juvenile survivorship is unstable and tightly connected to fluctuating environmental conditions (Krebs, 1972; Stearns, 1976), such as the NAO.

Several birth year time sequences have depressed frequencies (*i.e.*, apparently lower recruitment) in relation to neighboring birth years as inferred from periodic declines in the age-frequency distributions (Figures 3.11-3.12). Both male and female age frequencies decrease between 1917-1927. Harding *et al.* (2008) identified a direct relationship between bottom water temperature and *A. islandica* recruitment events along the Mid-Atlantic Bight (U.S.). This time frame (1917-1927) overlaps with an extreme cold period of the Atlantic Multidecadal Oscillation (AMO) that persisted from 1905-1920 (see Figure 1 in Knudsen *et al.*, 2011; and Figure 1 in Alexander *et al.*, 2014; see

also Bellucci *et al*., 2017) and an unusually cold period in the southern New England region (Nixon *et al.*, 2004). An extreme excursion of the NAO is also documented (Joyce, 2002) and this interruption in recruitment is also evident in the Belfast Lough population (see Figure 5 in Ridgway *et al.*, 2012). The latter similarity suggests a potentially widespread event during which time ocean quahog recruitment was poor.

An increase in numbers at age in the age-frequency distributions began 150 y before sampling (circa 1867) and coincides with the termination of the Little Ice Age and subsequent warming period of the late Holocene (Mann *et al.*, 2009; Cronin *et al*., 2010; Wanner *et al.*, 2011; Oliva *et al.*, 2018). Interestingly, these paleo-climate events also co-occur with the observed increase in ocean quahog settlement in Belfast Lough, Northern Ireland in the northeast Atlantic (Ridgway *et al.*, 2012). Pace *et al.* (2017a) also observed a population expansion from GB south to New Jersey (US) between 1855-1900. What might have precipitated a population expansion throughout large portions of the North Atlantic is unclear, though climate forcing would seem a likely precursor. The AMO positive and negative phases develop in both the eastern and western Atlantic dependent on complex atmospheric and oceanographic forces, whereby water temperature is a dominant defining characteristic of each phase (Nye *et al.*, 2014). Positive AMO phases are characterized by warmer sea-surface temperatures, a northward migration of the inter-tropical convergence zone (ITCZ), higher precipitation in northern latitudes resulting from a northernly ITCZ, weak NE trade winds, and shallow mixed layer depths (Nye *et al.*, 2014). A majority of the GB animals surveyed in this study (1867-1980s), and presumably populations west and south throughout the Mid-Atlantic Bight, experienced positive (warm anomalous SST) AMO indices (Nye *et al.*, 2014) and warming water

temperatures of the late Holocene (Mann *et al.*, 2009) that may have assisted in the population expansion observed 150 y before sampling (*i.e.*, 2017). Recent research into the formation of the Cold Pool, the body of water that permits *A. islandica* to live at unusually low latitudes in the western Atlantic, show that formation water is derived in varying proportions from Arctic and North Atlantic sources depending on the year (Wang *et al.*, 2019; Chen & Curchitser, 2020; Chen *et al.*, 2021; Miles *et al.*, 2021). Currents flow around Georges Bank from the Scotian Shelf, through the Great South Channel, and subsequently west and south with variations driven by the proportion of Labrador Sea water entrained in the downcoast current. The cold, northern waters that accumulate in the Mid-Atlantic Bight form the Cold Pool feature. This basic current flow would provide a hydrodynamic mechanism supporting a basin-wide population expansion once initiated by climatic changes after the ending of the Little Ice Age.

No significant AMO cold or warm periods occurred between 1892-1907 when the females exhibited an extreme drop in the age-frequency distribution (Knudsen *et al.*, 2011; Alexander *et al.*, 2014; Nye *et al.*, 2014), nor did Nixon *et al.* (2004) observe any unusual temperature excursions during this interval in southern New England. The unique recession in only one sex age-frequency distribution suggests a mortality event or recruitment failure specific to female ocean quahogs. The latter would seem implausible. Ridgway *et al.* (2012) observed a break in recruitment, but it occurred just prior to the GB population expansion event (1860-1870). Perhaps the GB females were more sensitive to the warm-cold AMO transition when it initiated around 1895 CE. Gribben & Wright (2006) document sex-specific developmental responses as a result of adverse habitat conditions (*e.g.*, invasive species, nutrient supply, unfavorable temperatures). The

AMO transition between 1892-1907 may have led to greater female mortality because female energetic requirements were not met during this new temperature regime and potentially altered food supply, as a result of higher energetic costs associated with female gamete production. However, differing energy requirements for male and female gamete production is not well described in the literature for bivalves, and it is unknown if this hypothesis applies to *A. islandica*. Regardless, the 1892-1907 frequency depression demonstrates that *A. islandica* is vulnerable to events that differentially affect recruitment and survival of the two sexes over significant multi-year periods of time and again emphasizes the necessity of evaluating size and age relationships within a sex-specific framework.

Regular recruitment and the presumed absence of reproductive senility (Thompson *et al.*, 1980) would indicate that the GB population is relatively stable under current environmental conditions. Thompson *et al.* (1980) posits that reproductive success does not diminish with age, whereas Thorarinsdóttir & Steingrímsson (2000) observed smaller follicles in older versus younger ocean quahogs and potentially reduced reproductive output. Understanding fecundity at age is critical for a species such as *A. islandica* with upwards of 250 age classes in order to use age frequencies and allometric models to estimate the extent of local larval production. This study targeted animals available to the fishery and it is unknown if recent cohorts continue this trend of consistent recruitment to present time, but Powell & Mann (2005) and Harding *et al.* (2008) suggest more sporadic recruitment recently at the southern end of the range, consistent with the rapidly warming temperatures in the northwestern Atlantic (Alexander *et al*., 2020). Nevertheless, the consistency of recruitment over a 150+ year time span is

remarkable given the more intermittent recruitment dynamics of other long-lived species (*e.g.*, Davis & VanBlaricom, 1978; Morsán & Orensanz, 2004; Zhang & Campbell, 2004; Gerasimova & Maximovich, 2013) and reminiscent of another relatively long-lived bivalve in the Mid-Atlantic, *Spisula solidissima* (Weinberg, 1999).

3.4.4 Longevity and Mortality

Georges Bank maximum age and longevity estimates in the current study are higher than the Georges Bank maximum age published by Pace *et al.* (2017b) and the longevity estimate from Northern Ireland (Ridgway *et al.*, 2012), a population that generally mirrored Georges Bank in regard to settlement chronology. Male longevity was estimated to be 244 y while female longevity was estimated at 219 y. It is expected that the oldest *A. islandica* collected from Iceland (507 y) is an extremely rare occurrence (Butler *et al.*, 2013), but it is curious why the oldest animals from GB are not closer to the maximum age observed for this species. Four hypotheses could be possible: 1) *Arctica islandica* expanded its southern range during the latter half of the Holocene and the 261-y-old clam aged from the 2017 age sample represents a recent (re)colonizing generation as Mid-Atlantic shelf waters cooled to optimal temperatures (Dahlgren *et al.*, 2000; Sachs, 2007); 2) the southern extent of the range experiences environmental conditions that are met with higher mortality rates (*e.g.*, longer periods of seasonal thermal stress and high metabolism) or reduced effective recruitment whereby maximum longevity is not obtained outside of the core, boreal range (Merrill & Ropes, 1969; Franz & Merrill, 1980; Mann & Wolf, 1983; Cargnelli *et al.*, 1999); 3) *A. islandica* populations are in a state of migration or submergence across the US continental shelf as they follow optimal isotherms, resulting in the oldest individuals of the population inshore from the

current core population and the 2017 dataset represented a sampling bias for younger animals moving across the continental shelf (Franz & Merrill, 1980; Powell *et al.*, 2020); or 4) the population expansion on Georges Bank and throughout the Mid-Atlantic (Pace *et al*., 2017a) marks a regime shift in the northwestern Atlantic at the beginning of the period of warming temperatures at the end of the Little Ice Age, a climate shift well documented in meteorological time series (Auger *et al*., 2019). If a regime shift occurred in response to subsequent warming after the Little Ice Age (approximately 1860 CE), many more centuries of inhabitation would be necessary to reach the maximum species' longevity of 500 y.

The NEFSC (2017) currently adopts a constant 0.02 natural mortality rate for ocean quahog length-based assessment models (NEFSC, 1995) and 0.02 is also the natural mortality rate estimated for Belfast Lough, Northern Ireland (Ridgway *et al.*, 2012), whereas Kilada *et al.* (2007) estimated an offshore natural mortality rate of 0.03 in Canadian waters. This study estimated a constant natural mortality rate for GB males to be 0.04, but female natural mortality is estimated at 0.05, higher than both the population and male mortality rates. It should be noted, however, that while fishing is extremely limited at Georges Bank and we assume mortality represents natural mortality, the Atlantic surfclam fishery may introduce an additive fishing mortality to *A. islandica* at Georges Bank in the form of Surfclam bycatch. It is unclear at what magnitude bycatch rates may affect our estimates of natural mortality and if natural mortality is in fact a representation of total mortality.

As an increase in recruitment during the post-1860 period may also have occurred and, to the extent that it did, would produce an overestimate of the natural mortality, the estimated values may be an upper bound for the analytical period. Notwithstanding that uncertainty, the females of the GB population not only exhibited a unique recruitment hiatus between 1892-1907, but mortality affects the females at a 1% higher rate than males. Females are younger and larger than the smaller but older males at Georges Bank which could indicate that sexes exhibit different behavioral responses to escape unfavorable environmental conditions (*e.g.*, burrowing timing, burrowing depth) possibly due to shell size, or it is evolutionarily advantageous for females to grow large and fecund at risk of greater rates of associated mortality. This latter option, wherein females have an increased cost of reproduction, is well described across a range of species (*e.g.*, Bell, 1980; Gribben & Wright, 2006), but a female bias, anticipated from the differential energy investment into reproduction between females and males, is not commonly reported for bivalve molluscs, though reproductive cost has received some study (*e.g.*, Thompson, 1984; Royer *et al.*, 2008). Regardless of the source, the differing mortality rates, though seemingly of small difference, result in a distinctive male bias in the older age classes (Figure 3.15) and the presence of apparent gaps in recruitment biased toward females indicates a possible increased sensitivity of females to environmental conditions (Figure 3.12A).

3.4.5 Summary

Arctica islandica at GB are sexually dimorphic. Females are larger and have higher growth rates than males, where females are younger at size than males. Females also have a higher mortality rate and lower longevity than males. Divergences in female

and male age-length data resulted in distinct, but reliable ALKs for each sex. It is unclear if these trends are consistent through time, or these trends are recent adaptations to changing oceanographic conditions at GB.

3.5 Tables

Table 3.1 Georges Bank sex proportions at size.

Length (mm)	Female	Male
78	0.17	0.83
79	0.00	1.00
80	0.17	0.83
81	0.60	0.40
82	0.20	0.80
83	0.13	0.87
84	0.07	0.93
85	0.26	0.74
86	0.25	0.75
87	0.23	0.77
88	0.27	0.73
89	0.43	0.57
90	0.19	0.81
91	0.31	0.69
92	0.64	0.36
93	0.50	0.50
94	0.57	0.43
95	0.50	0.50
96	0.72	0.28
97	0.48	0.52
98	0.53	0.47
99	0.59	0.41
100	0.65	0.35
101	0.84	0.16
102	0.68	0.32
103	0.89	0.11
104	0.79	0.21
105	0.86	0.14
106	0.72	0.28
107	0.86	0.14
108	0.80	0.20
109	0.86	0.14
110	0.83	0.17
111	0.89	0.11
112	1.00	0.00
113	1.00	0.00

114	1.00	0.00
115	1.00	0.00
116	1.00	0.00
117	0.50	0.50
119	1.00	0.00
120	1.00	0.00

Table 3.2 Georges Bank dataset summary. Table includes the number aged at length (age-length), length-frequency, and age-frequency datasets. Population age-frequency was created with a unique age-length key, so population sample number is not the sum of male and female sample numbers. Each age-frequency sample (male, female, population) is subject to individual rounding procedures.

Dataset	Class	Number of Samples		
		Population	Female	Male
Age	70 mm	5	1	4
	75 mm	26	2	24
	80 mm	67	14	53
	85 mm	94	31	63
	90 mm	97	39	58
	95 mm	94	61	33
	100 mm	95	54	41
	105 mm	96	67	29
	110 mm	33	30	3
	115 mm	8	7	1
	Total	615	306	309
Length Frequency	75 mm	54	3	51
	80 mm	244	51	193
	85 mm	621	177	444
	90 mm	928	392	536
	95 mm	765	427	338
	100 mm	385	284	101
	105 mm	129	106	23
	110 mm	30	27	3
	115 mm	3	3	0
	Total	3,159	1,470	1,689
Age Frequency	30 y	10	11	0
	40 y	17	3	6
	50 y	18	11	9
	60 y	185	119	73
	70 y	547	226	301
	80 y	579	253	324
	90 y	317	187	174
	100 y	395	239	197
	110 y	315	89	197
	120 y	273	117	157
	130 y	219	141	96
	140 y	160	53	95
	150 y	60	29	32
	160 y	50	17	19
	170 y	29	13	21

180 y	37	9	21
190 y	19	3	7
>200 y	24	5	13
Total	3,248	1,525	1,742

Table 3.3 Georges Bank sex ratios. Population sex ratio derived from the length sample (corrected for dredge selectivity). Sex ratio by size derived from the shucked sample. One-sample binomial test applied to shucked sample (n=706) to analyze observed female proportion versus expected female proportion (H_0=0.5 expected probability of female occurrence) using a 0.05 significance level.

Dataset	**Sex Ratio**	**N_F**	**N_M**	**%F**	**P Value**	
					Two-Tailed	**True Prop F**
Length Sample	Population	1,470	1,689	47	1.04E-04	Less
	70-mm	0	3	0	ns	
	75-mm	1	14	7	9.78E-04	Less
	80-mm	8	37	18	2.99E-05	Less
	85-mm	17	45	27	6.06E-04	Less
	90-mm	30	40	43	ns	
Shucked Sample	95-mm	68	54	56	ns	
	100-mm	155	48	76	1.01E-13	Greater
	105-mm	114	25	82	8.39E-14	Greater
	110-mm	34	3	92	8.14E-07	Greater
	115-mm	7	1	88	ns	
	120-mm	2	0	100	ns	

N_F, number of females; N_M, number of males; %F, percent females; ns, non-significant.
All animals from the shucked sample were analyzed. Numbers of female (N_F) and male (N_M) *A. islandica* are listed with the percent of females per 5-mm size class (%F).True Prop F indicates if the proportion of females is greater or less than the expected probability of 0.5 if the two-tailed test is significant. Non-significant two-tailed tests (ns) indicates that female proportion is approximately 0.5.

Table 3.4 Georges Bank distribution statistics. Length- and age-frequency distribution results between sexes. Results for the unmodified age- and length-frequency datasets were listed under the "Null" bin modification column, and results for data that were collapsed into bins modified by median values were listed under the "Median" bin modification column (see Materials and Methods: Statistics-Frequency Distributions). Data modified using the median, were modified using a reference dataset that provided the median values for bin construction and these datasets are listed under the "Reference" column. Three tests were evaluated: Kolmogorov-Smirnov (KS), Wald-Wolfowitz Runs, and the Anderson-Darling (AD) tests. Statistical significance was determined using α = 0.05 and 0.01. Significant results are indicated by "*", non-significant results were indicated by "ns". Blank cells in the "Null" column do not contain results because no data modification occurred; therefore, results are identical for male and female "Reference" datasets.

Sample	Reference	Test	Alpha	Bin Modification	
				Null	Median
Length Frequency	Male	KS	0.01	*	ns
			0.05	*	ns
		Runs	0.01	*	*
			0.05	*	*
		AD	0.01	ns	ns
			0.05	*	ns
	Female	KS	0.01		ns
			0.05		ns
		Runs	0.01		*
			0.05		*
		AD	0.01		ns
			0.05		ns
Age Frequency	Male	KS	0.01	ns	ns
			0.05	ns	ns
		Runs	0.01	ns	ns
			0.05	ns	ns
		AD	0.01	ns	ns
			0.05	ns	*
	Female	KS	0.01		ns
			0.05		ns
		Runs	0.01		ns
			0.05		ns
		AD	0.01		ns
			0.05		*

*, significant; ns, non-significant; KS, Kolmogorov-Smirnov; AD, Anderson-Darling.

Table 3.5 Georges Bank age-length key validation. Values represent the proportion of simulations that are significantly different from the true age frequencies. Shaded boxes represent cases with a significant approximate binomial test, i.e., substituted simulations were significantly different than the base simulations.

Data Modification	Alpha	Test	Female Length Frequency		Male Length Frequency	
			Base	Sub	Base	Sub
Null	0.01	KS	0.00	1.00	0.02	1.00
		Runs	0.08	0.08	0.08	0.14
		AD	0.78	1.00	1.00	0.36
	0.05	KS	0.02	1.00	0.02	1.00
		Runs	0.26	0.26	0.24	0.32
		AD	0.96	1.00	1.00	0.82
Median	0.01	KS	0.00	0.98	0.00	1.00
		Runs	0.02	0.42	0.22	0.70
		AD	0.88	1.00	0.90	1.00
	0.05	KS	0.02	0.90	0.02	0.98
		Runs	0.14	0.66	0.34	0.84
		AD	0.98	1.00	1.00	1.00

Sub, substituted; KS, Kolmogorov-Smirnov; AD, Anderson-Darling.

3.6 Figures

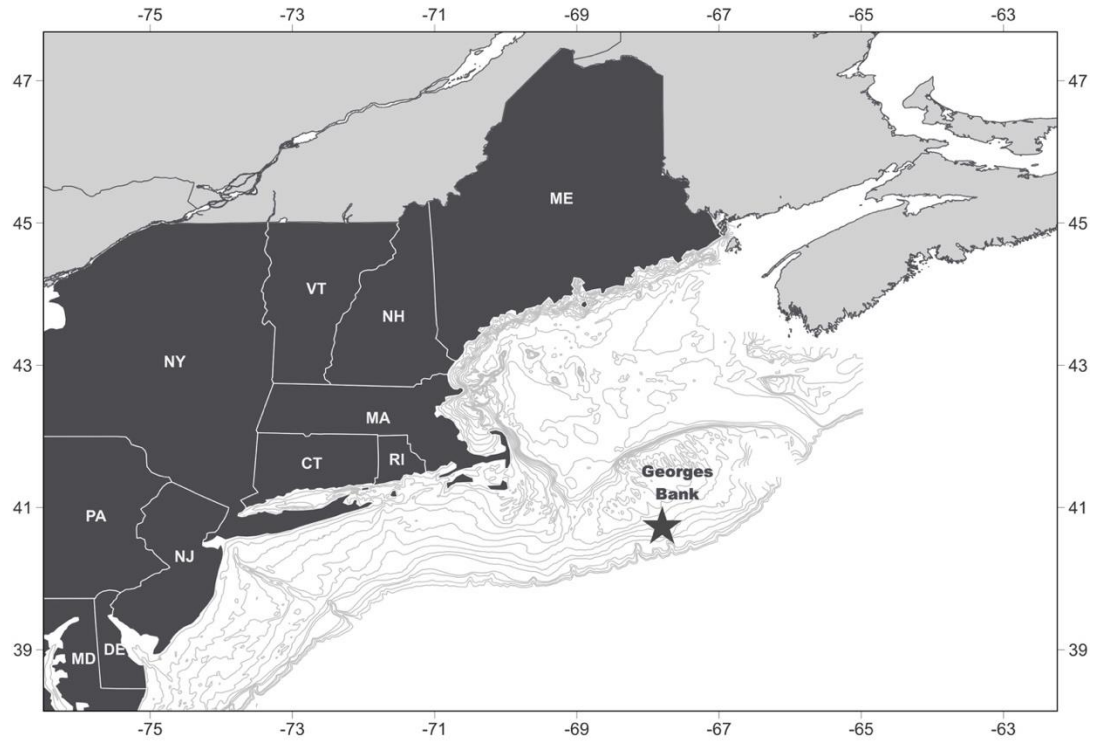

Figure 3.1 Georges Bank sample site. Location of the 2015 length- and 2017 shucked-sample site (star) on Georges Bank.

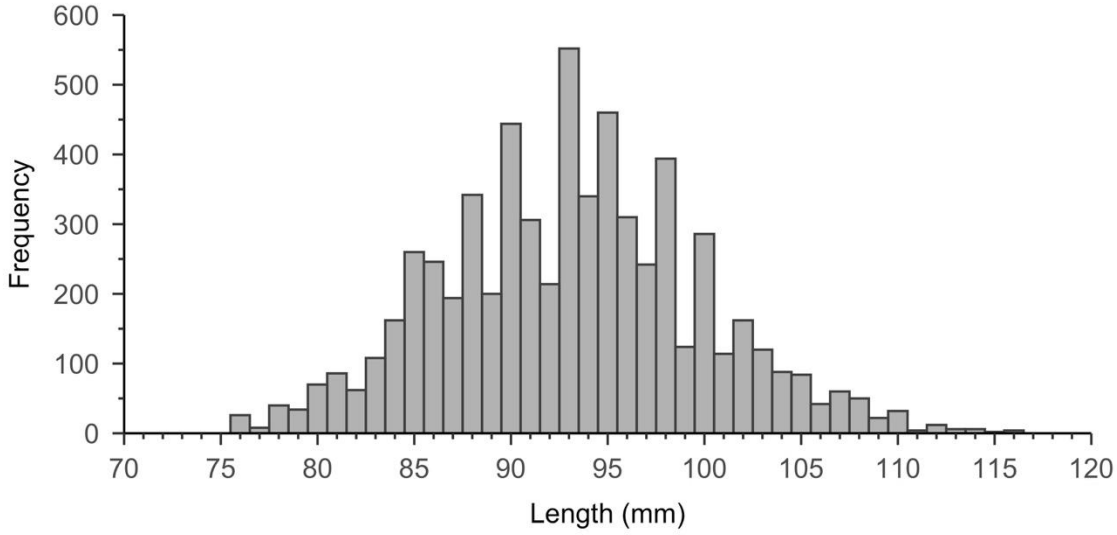

Figure 3.2 Georges Bank population length frequency. Population (n=3,159) mean length is 93 mm (SD=6.7 mm).

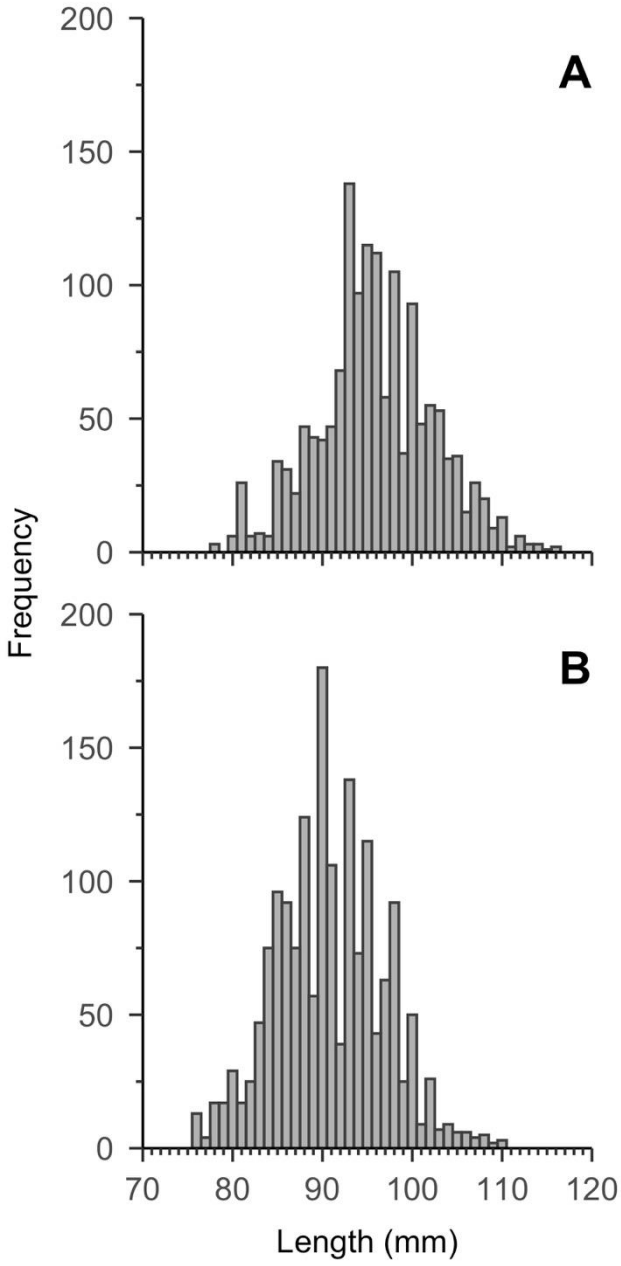

Figure 3.3 Georges Bank sex-specific length frequencies. (A) Female (n= 1,470) mean length is 96 mm (SD=6.4 mm); (B) male (n=1,689) mean length is 91 mm (SD=6.0 mm). Descending left tail for small shell lengths is an artifact of dredge selectivity for smaller clams.

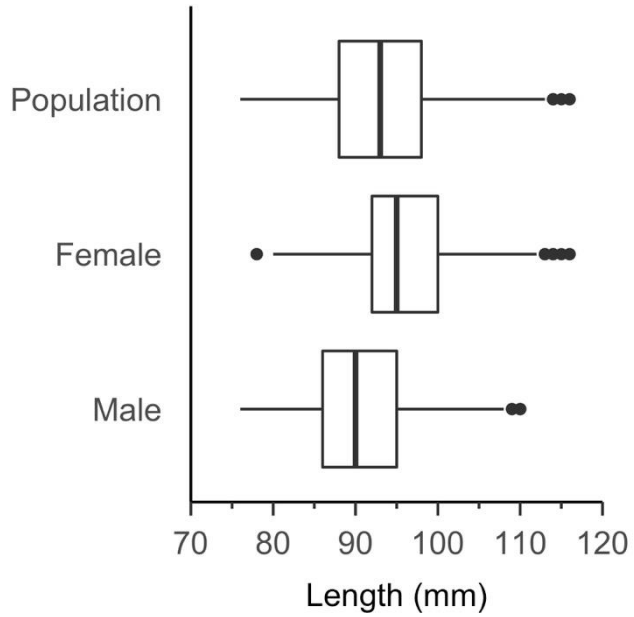

Figure 3.4 Georges Bank length frequencies. Length summaries by population (n=3,159) and sex (female n= 1,470, male n=1,689). Central line indicates median (50th percentile), box represents the 25th and 75th percentiles (interquartile range [IQR]), whiskers represent the minimum and maximum (25th percentile - 1.5*IQR, 75th percentile + 1.5*IQR, respectively), and black circles are outliers.

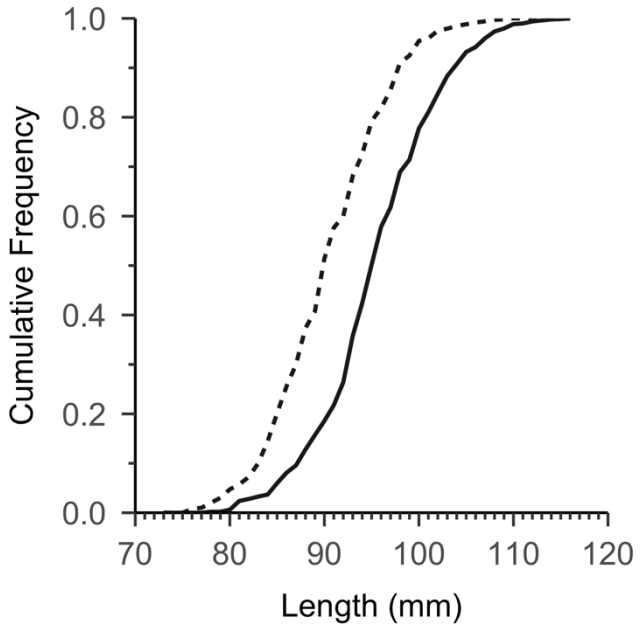

Figure 3.5 Georges Bank cumulative length frequencies. Females (solid line) are shifted to larger size classes compared to males (dashed line) collected from the same length frequency sample.

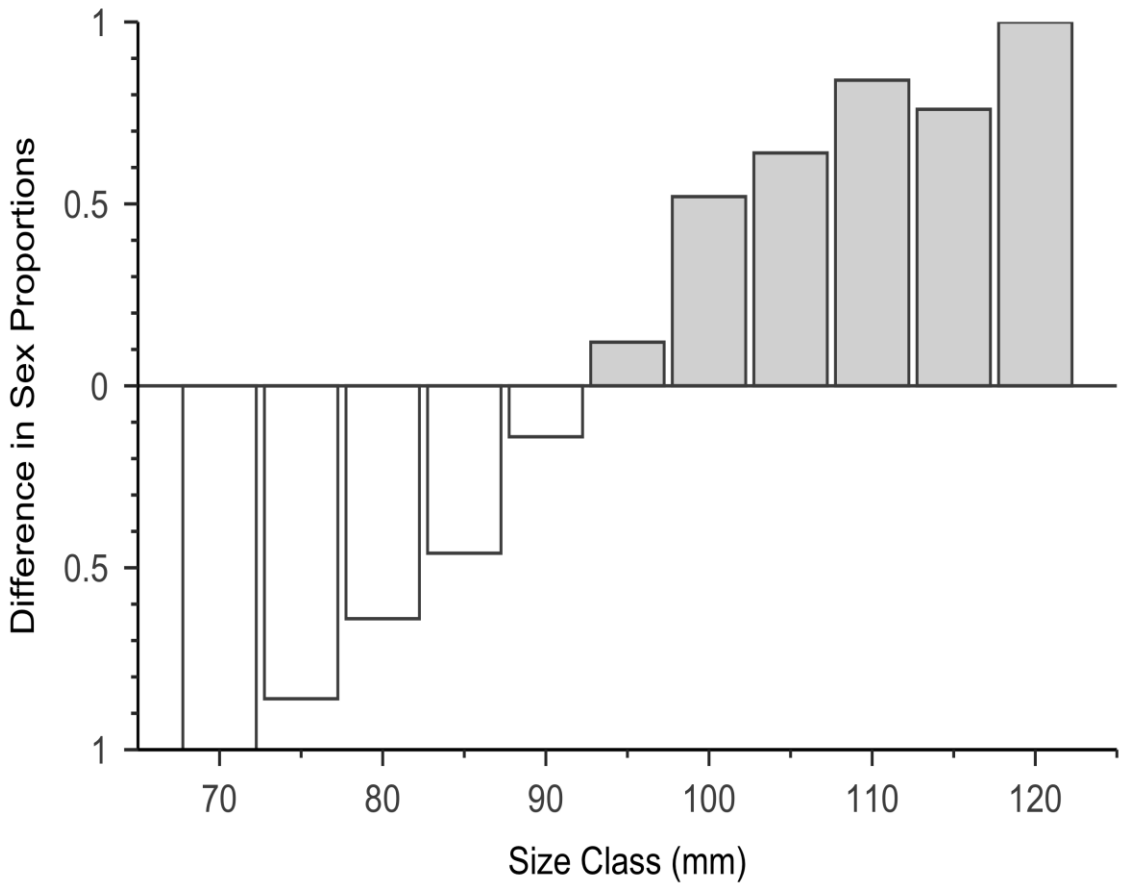

Figure 3.6 Georges Bank sex ratio by size. Sex ratio of each length class (5-mm bins) (n=706) of all sexed differentiated *Arctica islandica* from the 2017 shucked sample. Dark grey bars represent a female dominated size class and white bars represent a male dominated size class. The y axis denotes the proportional difference between sex frequency at size where y=0 is a 1:1 sex ratio, and y=0.5 is a 1:1.5 sex ratio. Between 90 mm and 95 mm, the sex ratio converts from male-dominated small size classes to female-dominated large size classes.

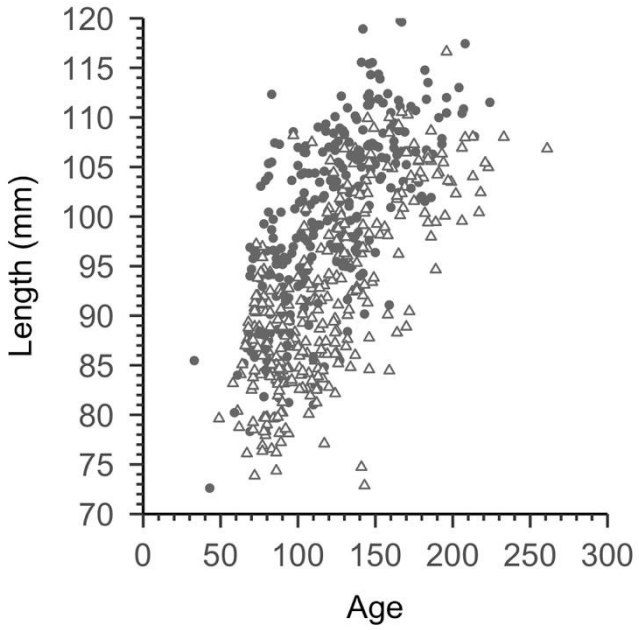

Figure 3.7 Georges Bank age-length data. Age-length data from the age sample (n=615) by sex (female black circles, male white triangles). Time 0, or x=0, represents the sample year 2017. Females tend to be larger than males at comparable ages. The oldest animal was born in approximately 1756 (106.9 mm) and the youngest animal was born in approximately 1984 (85.5 mm); whereas the largest animal (119.8 mm) was 166 y of age, and the smallest animal (72.6 mm) was 43 y of age.

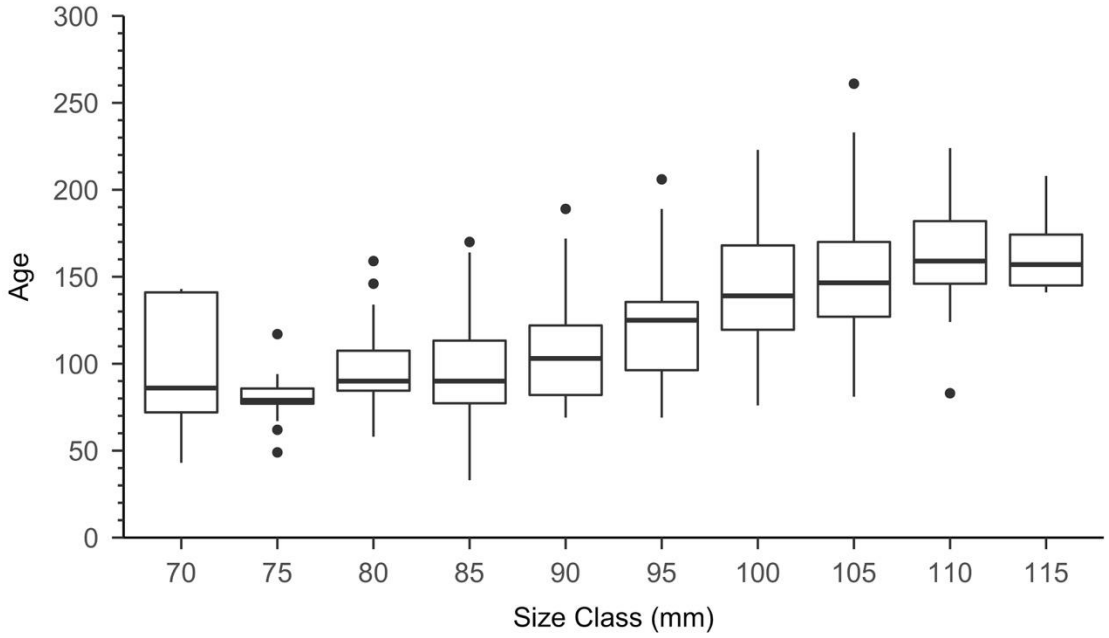

Figure 3.8 Georges Bank age-length data by size class. Age-length data analyzed by 5-mm length classes (n=615). Central line indicates median (50th percentile), box represents the 25th and 75th percentiles (interquartile range [IQR]), whiskers represent the minimum and maximum (25th percentile - 1.5*IQR, 75th percentile + 1.5*IQR, respectively), and black circles are outliers. Type III ranked one-way ANOVA was significant between size classes ($p<2.2E-16$). Tukey post-hoc results identified significant differences in age between large size classes (greater than 95 mm) and comparatively smaller size classes, and size classes less than 95 mm were not statistically different from other size classes less than 95 mm.

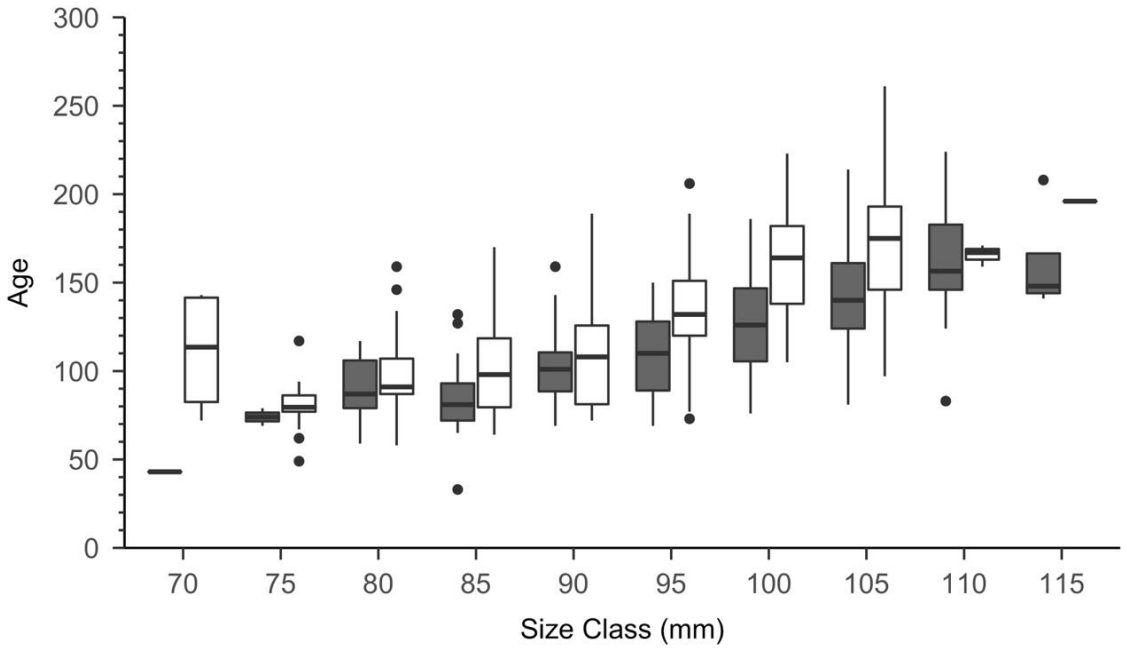

Figure 3.9 Georges Bank age-length data by sex and size class. Age-length composition by sex analyzed in 5-mm length classes. Central line indicates median (50th percentile), box represents the 25th and 75th percentiles (interquartile range [IQR]), whiskers represent the minimum and maximum (25th percentile - 1.5*IQR, 75th percentile + 1.5*IQR, respectively), and black circles are outliers. Female ages (grey) tend to be younger at size than the males (white) within the same size class. Type III ranked two-way ANOVA was not significant between size classes and sex using a multiplicative model.

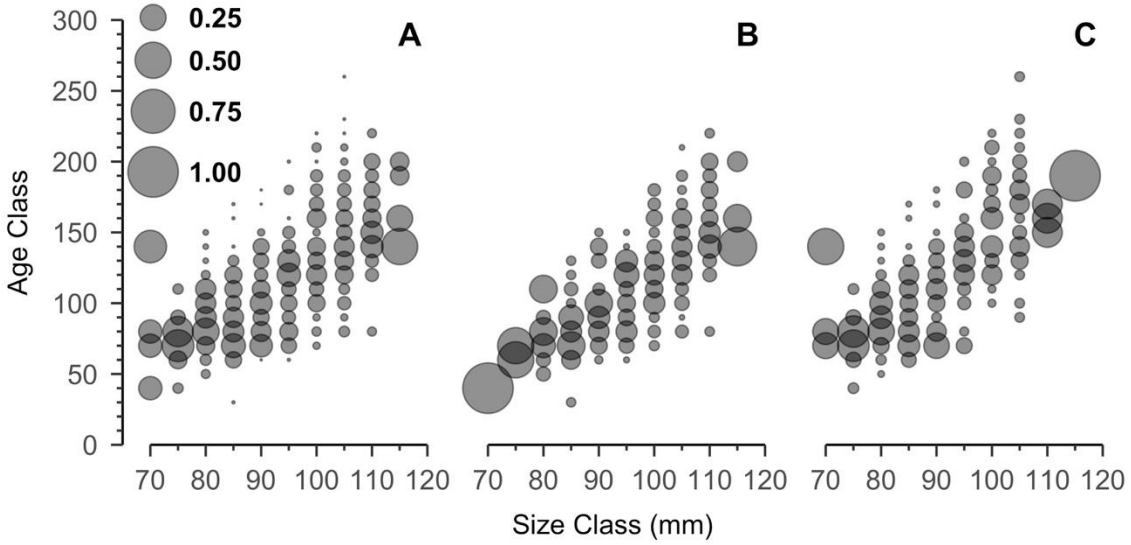

Figure 3.10 Georges Bank age proportions at size. Age proportions at size for (A) population, (B) female, (C) and male age-length data. Size is described in 5-mm shell length classes as used when the age-length key was created, and ages are presented in 10-year age classes. Circle diameter is representative of what proportion of the size class is represented by each age class. The largest diameter circle identified a size class for which all samples were from the same age class.

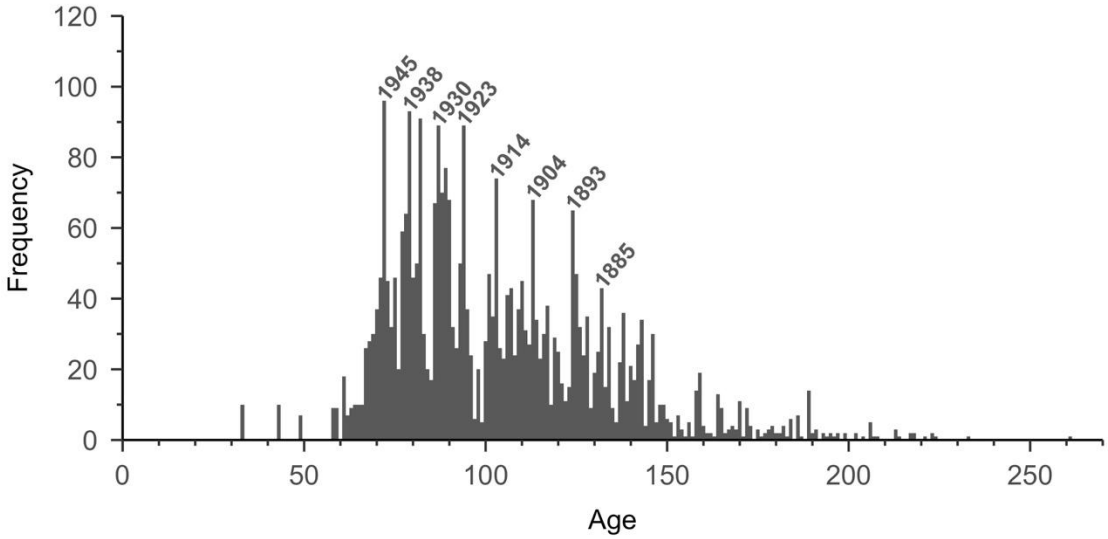

Figure 3.11 Georges Bank population age frequency. Age frequency (n=3,248) created using a 5-mm size class age-length key. Time 0, or x=0, represents the sample year 2017. Population mean age is 104 years (birth year 1913) (SD=30). Peaks in age frequency average an 8-y periodicity. A peak at year 1935 is attached to same frequency pulse as 1938 but may be an independent event. Descending left tail at young age is an artifact of dredge selectivity at smaller shell lengths.

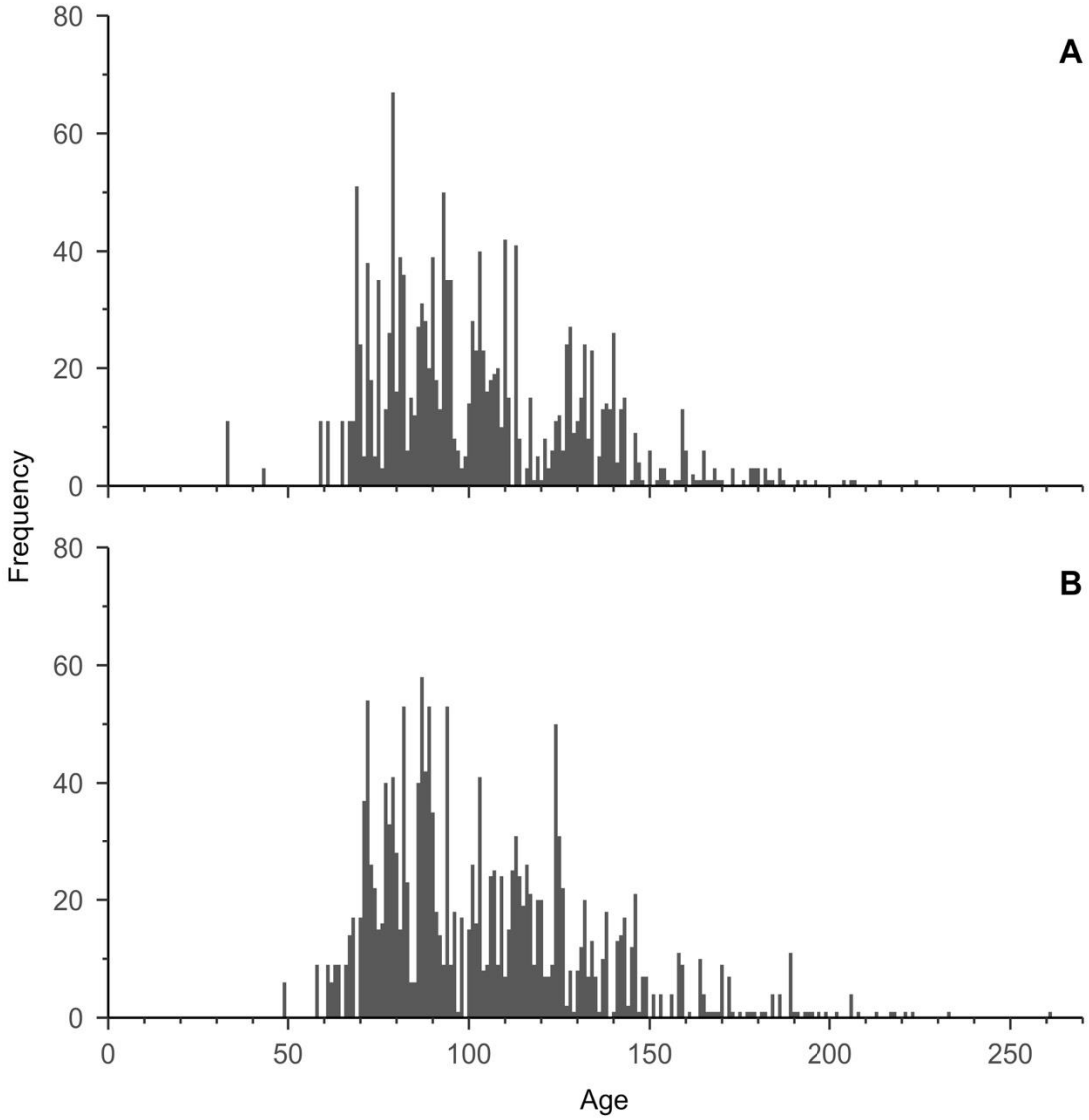

Figure 3.12 Georges Bank age frequency by sex. (A) Female age frequency (n=1,525), mean age is approximately 102 y (birth year 1915) (SD=29); (B) male age frequency (n=1,742), mean age is approximately 104 y (birth year 1913) (SD=29). Descending left tail at young age is an artifact of dredge selectivity at smaller shell lengths.

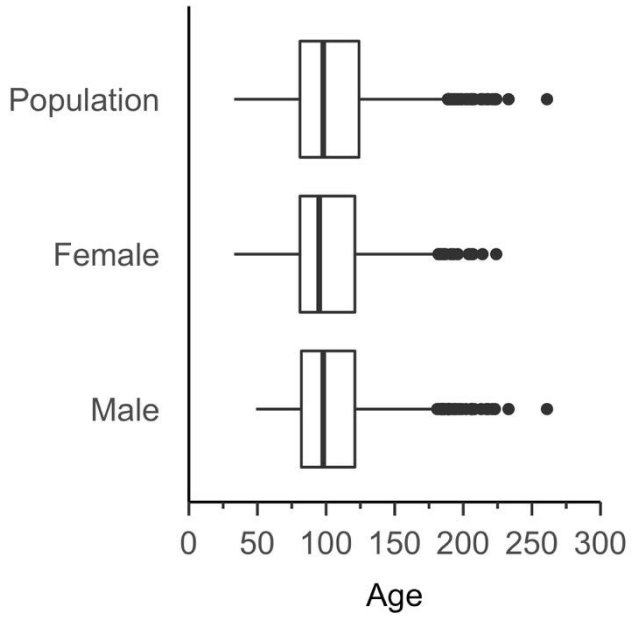

Figure 3.13 Georges Bank comparison of age frequencies. Central line indicates median (50th percentile), box represents the 25th and 75th percentiles (interquartile range [IQR]), whiskers represent the minimum and maximum (25th percentile - 1.5*IQR, 75th percentile + 1.5*IQR, respectively), and black circles are outliers. Median population age is 104 y (range 33-261 y), female median age is 95 y (range 33-224 y), and male median age is 98 y (range 49-261 years). Type III ranked one-way ANOVA was not significant between groups.

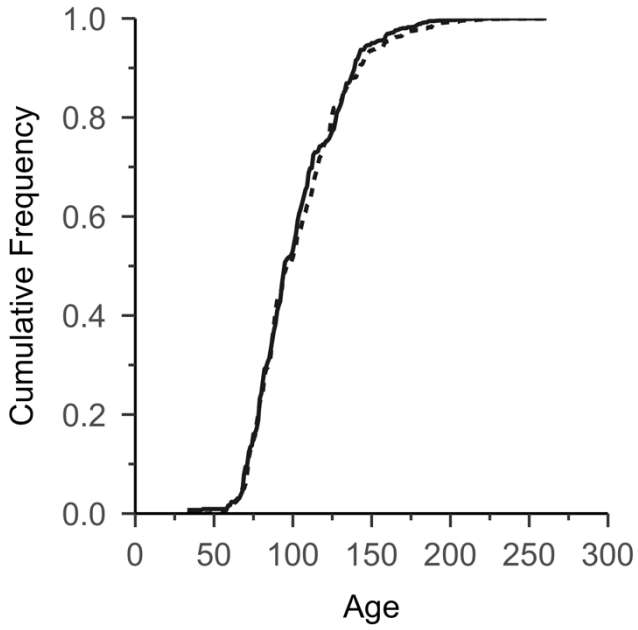

Figure 3.14 Georges Bank cumulative age frequencies by sex. Female (solid line) and male (dashed line) *A. islandica* are equally divided around an identical median age of 94 years.

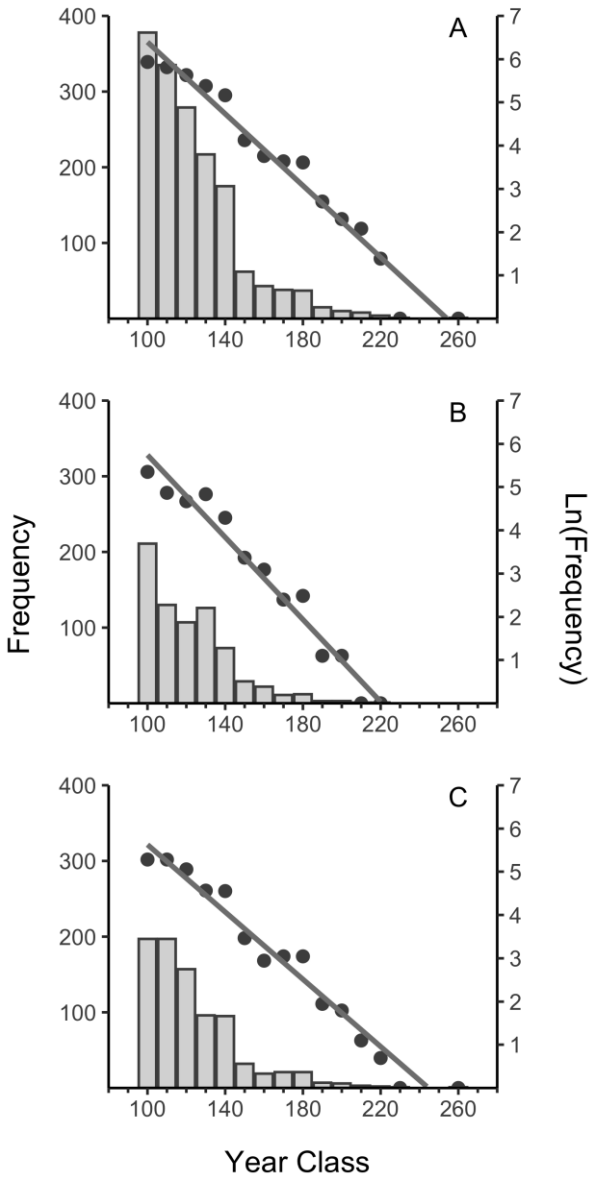

Figure 3.15 Georges Bank longevity and mortality. (A) Population, (B) female, and (C) male age frequencies (histogram, primary y axis); natural log of age frequencies (points, secondary y axis) with linear regression analyses (solid line). Population: slope = - 0.041, x-intercept = 257.13 (R^2 = 0.96); female: slope = - 0.048, x-intercept = 218.68 (R^2 = 0.96); male: slope = - 0.039, x-intercept = 244.04 (R^2 = 0.96).

3.7 References

Alexander MA, Halimeda Kilbourne K and Nye JA (2014) Climate variability during warm and cold phases of the Atlantic Multidecadal Oscillation (AMO) 1871–2008. *Journal of Marine Systems* 133, 14–26.

Alexander MA, Shin S-I, Scott JD, Curchitser E and Stock C (2020) The response of the Northwest Atlantic Ocean to climate change. *Journal of Climate* 33, 405-428.

Auger JD, Mayewski PA, Maasch KA, Schuenemann KC, Carleton AM, Birkel SD and Saros JE (2019) 2000 years of North Atlantic-Arctic climate. *Quaternary Science Reviews* 216, 1-17.

Bellucci A, Mariotti A and Gualdi S (2017) The role of forcings in the twentieth-century North Atlantic multidecadal variability: the 1940-75 North Atlantic cooling case study. *Journal of Climate* 30, 7317-7337.

Bell G (1980) The costs of reproduction and their consequences. *The American Naturalist* 116, 45-76.

Bojariu R and Gimeno L (2003) Predictability and numerical modelling of the North Atlantic Oscillation. *Earth-Science Reviews* 63, 145-168.

Butler PG, Fraser NM, Scourse JD, Richardson CA, Bryant C and Heinemeier J (2020) Is there a reliable taphonomic clock in the temperate North Atlantic? An example from a North Sea population of the mollusc *Arctica islandica*. *Palaeogeography, Palaeoclimatology, Palaeoecology* 560, 109975.

Butler PG, Richardson CA, Scourse JD, Witbaard R, Schöne BR, Fraser NM, Wanamaker Jr AD, Bryant CL, Harris I and Robertson I (2009) Accurate increment identification and the spatial extent of the common signal in five

Arctica islandica chronologies from the Fladen Ground, northern North Sea. *Paleoceanography* 24, 1-18.

Butler PG, Wanamaker AD, Scourse JD, Richardson CA and Reynolds DJ (2013) Variability of marine climate on the North Icelandic Shelf in a 1357-year proxy archive based on growth increments in the bivalve *Arctica islandica*. *Palaeogeography, Palaeoclimatology, Palaeoecology* 373, 141–151.

Camacho-Mondragón MA, Ceballos-Vázquez BP, Rivera-Camacho AR and Arellano-Martinez M (2015) Unnoticed sex change in *Atrina maura* (Bivalvia: Pinnidae): histological and size structure evidence. *American Malacological Bulletin* 33, 43-51.

Cargnelli LM, Griesbach SJ, Packer DB and Weissberger E (1999) *Arctica islandica*: life history and habitat characteristics. *National Oceanic and Atmospheric Administration Technical Memorandum*, NMFS-NE-148, 12 pp.

Chávez-Villalba J, Soyez C, Huvet A, Gueguen Y, Lo C and Moullac G le (2011) Determination of gender in the pearl oyster *Pinctada margaritifera*. *Journal of Shellfish Research* 30, 231-210.

Chen Z and Curchitser EN (2020) Interannual variability of the Mid-Atlantic Cold Pool. *Journal of Geophysical Research: Oceans* 125, 2020JC016445.

Chen Z, Kwon Y-O, Chen K, Fratantoni P, Gawarkiewicz G, Joyce TM, Miller TJ, Nye JA, Saba VS and Stock BC (2021) Seasonal prediction of bottom temperature on the northeast U.S. continental shelf. *Journal of Geophysical Research: Oceans* 126, 2021JC017187.

Coe WR (1932) Development of the gonads and the sequence of the sexual phases in the California oyster (*Ostrea lurida*). *Bulletin of the Scripps Institution of Oceanography Technical Series* 3, 119-144.

Conover WJ (1980) *Practical nonparametric statistics*. New York: John Wiley & Sons. 493 pp.

Cronin TM, Hayo K, Thunell RC, Dwyer GS, Saenger C and Willard DA (2010) The Medieval Climate Anomaly and Little Ice Age in Chesapeake Bay and the North Atlantic Ocean. *Palaeogeography Palaeoclimatology Palaeoecology* 297, 299-310.

Dahlgren TG, Weinberg JR and Halanych KM (2000) Phylogeography of the ocean quahog (*Arctica islandica*): influences of paleoclimate on genetic diversity and species range. *Marine Biology* 137, 487–495.

Davis N and VanBlaricom GR (1978) Spatial and temporal heterogeneity in a sand bottom epifaunal community of invertebrates in shallow water. *Limnology and Oceanography* 23, 417-427.

DeGrasse S, Conrad S, DiStefano P, Vanegas C, Wallace D, Jensen P, Hickey JM, Cenci F, Pitt J, Deardorff D, Rubio F, Easy D, Donovan MA, Laycock M, Rouse D and Mullen J (2014) Onboard screening dockside testing as a new means of managing paralytic shellfish poisoning risks in federally closed waters. *Deep Sea Research Part II: Topical Studies in Oceanography* 103, 288-300.

Elder HY (1979) Studies on the host parasite relationship between the parasitic prosobranch *Thyca crystallina* and the asteroid starfish *Linckia laevigata*. *Journal of Zoology* 187, 369-391.

Engmann S and Cousineau D (2011) Comparing distributions: the two-sample Anderson-Darling test as an alternative to the Kolmogorov-Smirnoff [sic] test. *Journal of Applied Quantitative Methods* 6, 1-17.

Franz DR and Merrill SA (1980) Molluscan distribution patterns on the continental shelf of the Middle-Atlantic Bight (Northwest Atlantic). *Malacologia* 19, 209-225.

Fritz LW (1991) Seasonal condition change, morphometrics, growth and sex ratio of the ocean quahog, *Arctica islandica* (Linnaeus, 1767) off New Jersey, U.S.A. *Journal of Shellfish Research* 10, 79-88.

Gerasimova AV and Maximovich NV (2013) Age-size structure of common bivalve mollusc populations in the White Sea. The causes of instability. *Hydrobiologia* 706, 119-137.

González-Vallejo NE (2008) Paraitism in *Monogamus minibulla* (Olsson and McGinty, 1958) (Gastropoda: Eulimidae) on the Red Sea urchin *Echinometra lucunter* (Linnaeus 1758) (Echinodermata: Echinometridae) on the Caribbean coast of Mexico. *Nautilus* 122, 178-181.

Gribben PE and Wright JT (2006) Sublethal effects on reproduction in native fauna: are females more vulnerable to biological invasions? *Oecologia* 149, 352-361.

Harding JM, King SE, Powell EN and Mann R (2008) Decadal trends in age structure and recruitment patterns of ocean quahogs *Arctica islandica* from the Mid-Atlantic Bight in relation to water temperatures. *Journal of Shellfish Research* 27, 667-690.

Harding JM, Powell EN, Mann R and Southworth MJ (2013). Variations in eastern oyster (*Crassostrea virginica*) sex-ratios from three Virginia estuaries: protandry,

growth and demographics. *Journal of the Marine Biological Association of the United Kingdom* 93, 519-531.

Hemeon KH, Powell EN, Robillard E, Pace SM, Redmond TE and Mann RL (2021) Attainability of accurate age frequencies for ocean quahogs (*Arctica islandica*) using large datasets: protocol, reader precision, and error assessment. *Journal of Shellfish Research* 40, 255-267.

Hennen DR, Mann R, Charriere N and Nordahl VA (2016) Testing the performance of a hydraulic clam dredge modified to capture small animals. *National Oceanic and Atmospheric Administration Technical Memorandum* NMFS-NE-237, 15 pp.

Hoenig JM (2005) Empirical use of longevity data to estimate mortality rates. *SEDAR*, 33-RD17, 8 pp.

Hurrell JW and Deser C (2009) North Atlantic climate variability: the role of the North Atlantic Oscillation. *Journal of Marine Systems* 78, 28-41.

Jacobson L and Hennen D (2019) Improving the NEFSC clam survey for Atlantic surfclams and ocean quahogs. *Northeast Fisheries Science Center Reference Document* 19-06, 89 pp.

Jones DS (1981) Reproductive cycles of the Atlantic surf clam *Spisula solidissima*, and the ocean quahog *Arctica islandica* off New Jersey. *Journal of Shellfish Research* 1, 23–32.

Joyce TM (2002) One hundred plus years of wintertime climate variability in the Eastern United States. *Journal of Climate* 15,1076-1086.

Kilada RW, Campana SE and Roddick D (2007) Validated age, growth, and mortality estimates of the ocean quahog (*Arctica islandica*) in the western Atlantic. *ICES Journal of Marine Science*. 64, 31–38.

Knudsen MF, Seidenkrantz M-S, Jacobsen BH and Kuijpers A (2011) Tracking the Atlantic Multidecadal Oscillation through the last 8,000 years. *Nature Communications* 2, 1-8.

Krebs CJ (1972) *Ecology: the experimental analysis of distribution and abundance*. New York: Harper and Row Publishers.

Loosanoff VL (1953) Reproductive cycle in *Cyprina islandica*. *Biological Bulletin* 104, 146–155.

Lutz RA, Mann R, Goodsell JG and Castagna M (1982) Larval and Early Post-Larval Development of *Arctica Islandica*. *Journal of the Marine Biological Association of the United Kingdom* 62,745–769.

Mann ME, Zhang Z, Rutherford S, Bradley RS, Hughes MK, Shindell D, Ammann C, Faluvegi G and Ni F (2009) Global signatures and dynamical origins of the Little Ice Age and Medieval Climate Anomaly. *Science* 326, 1256–1260.

Mann R (1982) The seasonal cycle of gonadal development in *Arctica islandica* from the southern New England shelf. *Fishery Bulletin* 80, 315-326.

Mann R and Wolf CC (1983) Swimming behaviour of larvae of the ocean quahog *Arctica islandica* in response to pressure and temperature. *Marine Ecological Progress Series* 13, 211–218.

Maunder MN and Wong RA (2011) Approaches for estimating natural mortality: applications to summer flounder (*Paralichthys dentatus*) in the U.S. Mid-Atlantic. *Fisheries Science* 111, 92-99.

Merrill AS and Ropes JW (1969) The general distribution of the surf clam and ocean quahog. *Proceedings of the National Shellfisheries Association* 59, 40–45.

Miles T, Murphy S, Kohut J, Borsetti S and Munroe D (2021) Offshore wind energy and the Mid-Atlantic Cold Pool: a review of potential interactions. *Marine Technology Society Journal* 55, 72-87.

Mohn R (1994) A comparison of three methods to convert catch at length data into catch at age. *Collective Volumes of Scientific Papers-International Commission for the Conservation of Atlantic Tunas* 42, 110-119.

Morsán EM and Orensanz JM (2004) Age structure and growth in a unusual population of purple clam Amiantis. *Journal of Shellfish Research* 23, 73–80.

NEFSC (1995) Report of the 19th Northeast Regional Stock Assessment Workshop (19th SAW). *Northeast Fisheries Science Center Reference Document* 95-08, 221 pp.

NEFSC (2017) Report of the 63rd Northeast Regional Stock Assessment Workshop (63rd SAW). *Northeast Fisheries Science Center Reference Document* 17-10, 414 pp.

Nixon SW, Granger S, Buckley BA, Lamont M and Rowell B (2004) A one hundred and seventeen year coastal water temperature record from Woods Hole, Massachusetts. *Estuaries* 27, 397-404.

Nye JA, Baker MR, Bell R, Kenny A, Kilbourne KH, Friedland KD, Martino E, Stachura MM, Van Houtan KS and Wood R (2014) Ecosystem effects of the Atlantic Multidecadal Oscillation. *Journal of Marine Systems* 133, 103–116.

Oliva M, Ruiz-Fernández J, Barriendos M, Benito G, Cuadrat JM, Domínguez-Castro F, García-Ruiz JM, Giralt S, Gómez-Ortiz A, Hernández A, López-Costas G, López-Moreno JI, López-Sáez JA, Martínez-Cortizas A, Moreno A, Prohom M, Saz MA, Serrano E, Tejedor E, Trigo R, Valero-Garcés B and Vicente-Serrano SM (2018) The Little Ice Age in Iberian mountains. *Earth-Science Reviews* 177, 175-208.

Pace SM, Powell EN, Mann R and Long MC (2017a) Comparison of age-frequency distributions for ocean quahogs *Arctica islandica* on the western Atlantic US continental shelf. *Marine Ecological Progress Series* 585, 81–98.

Pace SM, Powell EN, Mann R, Long MC and Klinck JM (2017b) Development of an age—frequency distribution for ocean quahogs (*Arctica islandica*) on Georges Bank. *Journal of Shellfish Research* 36, 41–53.

Pettitt AN (1976) A two-sample Anderson-Darling rank statistic. *Biometrika* 63, 161-168.

Powell EN, Ewing AM and Kuykendall KM (2020) Ocean quahogs (*Arctica islandica*) and Atlantic surfclams (*Spisula solidissima*) on the Mid-Atlantic Bight continental shelf and Georges Bank: the death assemblage as a recorder of climate change and the reorganization of the continental shelf benthos. *Palaeogeography, Palaeoclimatology, Palaeoecology* 537, 109205.

Powell EN and Mann RL (2005) Evidence of recent recruitment in the ocean quahog, *Arctica islandica* in the Western Atlantic Ocean. *Journal of Shellfish Research* 24, 517–530.

Powell EN, Morson JM, Ashton-Alcox KA and Kim Y (2013) Accommodation of the sex-ratio in eastern oysters *Crassostrea virginica* to variation in growth and

mortality across the estuarine salinity gradient. *Journal of the Marine Biological Association of the United Kingdom* 93, 533-555.

R Core Team (2018) R: A language and environment for statistical computing. Vienna, Austria: R Foundation for Statistical Computing. Available at: http://www.R-project.org.

Ragnarsson S and Thorarinsdóttir GG (2020) Burrowing behaviour in ocean quahog (*Arctica islandica*) in situ and in the laboratory. *Marine and Freshwater Research Institute*, *Reykjavík*, no. 2298-9137, 18 pp.

Rahman M, Pearson LM and Heien HC (2006) A modified Anderson-Darling test for uniformity. *Bulletin of the Malaysian Mathematical Science Society* 29, 11-16.

Ricker, WE (1975) Computation and interpretation of biological statistics of fish populations. *Bulletin of the Fisheries Research Board of Canada* 191, 1-382.

Ridgway ID, Richardson CA, Scourse JD, Butler PG and Reynolds DJ (2012) The population structure and biology of the ocean quahog, *Arctica islandica*, in Belfast Lough, Northern Ireland. *Journal of the Marine Biological Association of the United Kingdom* 92, 539–546.

Ropes JW, Murawski SA and Serchuk FM (1984) Size, age, sexual maturity and sex ratio in ocean quahogs, *Arctica islandica* Linné, off Long Island, New York. *Fishery Bulletin* 82, 253–267.

Rowell TW, Chaisson DR and Mclane JT (1990) Size and age of sexual maturity and annual gametogenic cycle in the ocean quahog, *Arctica islandica* (Linnaeus, 1767), from coastal waters in Nova Scotia, Canada. *Journal of Shellfish Research* 9, 195-20.

Royer J, Seguineau C, Park K-I, Pouvreau S, Choi K-S and Costil K (2008) Gametogenic cycle and reproductive effort assessed by two methods in 3 age classes of Pacific oysters, *Crassostrea gigas*, reared in Normandy. *Aquaculture* 277, 313-320.

Sachs JP (2007) Cooling of Northwest Atlantic slope waters during the Holocene. *Geophysical Research Letters* 34, L03609.

Serna-Gallo I, Ruíz-Velazco JMJ, Acosta-Salmón H, Peña-Messina E, Torres-Zepeda G and Saucedo PE (2014) Growth and reproduction patterns of the winged pearl oyster, *Pteria sterna*, cultivated in tropical environments of Mexico: implications for pearl farming. *Ciencias Marinas* 40, 75-88.

Soniat TM, Hofmann EE, Klinck JM and Powell EN (2009) Differential modulation of eastern oyster (*Crassostrea virginica*) disease parasites by the El Niño-Southern Oscillation and the North Atlantic Oscillation. *International Journal of Earth Science* 98, 99-114.

Soniat TM, Klinck JM, Powell EN and Hofmann EE (2006) Understanding the success and failure of oyster populations: climatic cycles and *Perkinsus marinus*. *Journal of Shellfish Research* 25, 83-93.

Stari T, Preedy KF, McKenzie E, Gurney WS, Heath MR, Kunzlik PA and Speirs DC (2010) Smooth age length keys: observations and implications for data collection on North Sea haddock. *Fisheries Research* 105, 2-12.

Stearns S. (1976) Life-history tactics: a review of the ideas. *The Quarterly Review of Biology* 51, 3-47.

Thompson I, Jones DS and Dreibelbis D (1980) Annual internal growth banding and life history of the ocean quahog *Arctica islandica*. *Marine Biology* 57, 25–34.

Thompson RJ (1984) Production, reproductive effort, reproductive value and reproductive cost in a population of the blue mussel *Mytilus edulis* from a subarctic environment. *Marine Ecology Progress Series* 16, 249-257.

Thorarinsdóttir GG and Jacobson LD (2005) Fishery biology and biological reference points for management of ocean quahogs (*Arctica islandica*) off Iceland. *Fisheries Research* 75, 97–106.

Thorarinsdóttir G and Steingrímsson S (2000) Size and age at sexual maturity and sex ratio in the ocean quahog, *Arctica islandica* (Linnaeus, 1767), off Northwest Iceland. *Journal of Shellfish Research* 19, 943–947.

Turner RD and Yakovlev Y (1983) Dwarf males in the Teredinidae (Bivalvia, Pholadacea). *Science* 219, 1077-1078.

von Oertzen JA Von (1972) Cycles and rates of reproduction of six Baltic Sea bivalves of different zoogeographical origin. *Marine Biology* 14, 143–149.

Yasuoka N and Yusa Y (2016) Effects of size and gregariousness on individual sex in a natural population of the Pacific oyster *Crassostrea gigas*. *Journal of Molluscan Studies* 82, 485-491.

Yau AJ, Lenihan HS and Kendall BE (2014) Fishery management priorities vary with self-recruitment in sedentary marine populations. *Ecological Applications* 24, 1490-1504.

Wang Z, Brickman D and Greenan BJW (2019) Characteristic evolution of the Atlantic Meridional Overturning Circulation from 1990 to 2015: an eddy-resolving ocean model study. *Deep-Sea Research Part I: Oceanographic Research Papers* 149, 103056.

Wanner H, Solomina O, Grosjean M, Ritz S and Jetel M (2011) Structure and origin of Holocene cold events. *Quaternary Science Reviews* 30, 3109-3123.

Weinberg JR (1999) Age-structure, recruitment, and adult mortality in populations of the Atlantic surfclam, *Spisula solidissima*, from 1978-1997. *Marine Biology* 134, 113-125.

Wilderbuer TK and Turnock BJ (2009) Sex-specific natural mortality of arrowtooth flounder in Alaska: implications of a skewed sex ratio on exploitation and management. *North American Journal of Fisheries Management* 29, 306-322.

Zhang Z and Campbell A (2004) Natural mortality and recruitment rates of the Pacific geoduck clam (*Panope abrupta*) in experimental plots. *Journal of Shellfish Research* 23, 675-682.

CHAPTER IV POPULATION DYNAMICS OF *ARCTICA ISLANDICA* OFF LONG ISLAND (US): AN ANALYSIS OF SEX-BASED DEMOGRAPHICS AND REGIONAL COMPARISONS

Formatted for the Journal of Marine Ecology Progress Series

4.1 Introduction

The ocean quahog (*Arctica islandica*; Linnaeus, 1767) is a commercially harvested clam in the US Mid-Atlantic. A federally managed species, *A. islandica* is managed as a single unit that combines two area-specific assessment models to create a single harvest quota (excluding the limited Gulf of Maine fishery). One assessment model analyzes the northern portion of the stock at Georges Bank (federally referenced as GBK-North) and the second model analyzes the southern portion of the stock from Virginia in the south to the western edge of the Great South Channel to the northeast (federally referenced as SVA/SNE-South) (Figure 4.1). Georges Bank is modeled as a separate area due to its distinctive oceanographic setting, limited contemporary harvests, and more restricted survey data (NEFSC 2020). Unlike many other federally managed species, the *A. islandica* fishery quota is derived using only length-based assessments since age compositions are notoriously difficult to assemble for this species (NEFSC 2020). Even the traditional use of growth curves or age-length keys (ALK) to estimate age at size are currently not employed due to the extreme variability of age at size (Pace et al. 2017a,b, Hemeon et al. accepted), although Hemeon et al. (accepted) have developed defensible ALKs for Georges Bank using large age-length datasets.

Studies spanning the north and mid-Atlantic demonstrate distinct regional and sex-specific growth dynamics for this species (Ropes et al. 1984, Thorarinsdóttir &

Steingrímsson 2000, Ridgway et al. 2012, Pace et al. 2018, Poitevin et al. 2019, Hemeon et al. accepted), results that suggest ALKs used to estimate age and time to maturity are also regionally and sexually explicit. Moreover, it is unclear at what spatial scale ALKs might diverge. A detailed age-length analysis was conducted for a site on Georges Bank (US) to decipher population dynamics specific to the Mid-Atlantic using a quasi-virgin *A. islandica* population (Hemeon et al. accepted). Hemeon et al. (accepted) found that longevity and mortality estimates were higher than previously documented for the US stock, that sex-ratios at size were statistically different, and that male and female *A. islandica* growth dynamics were dimorphic, warranting separate sex-based analyses (e.g., ALKs, mortality, longevity). Georges Bank is a relatively unfished population and is located a considerable distance offshore compared to other management areas to the west. The fishery off Long Island produces the largest fraction of total US landings, but a comprehensive population dynamics study has not been conducted for the Long Island population.

The objectives of this study are to describe sex-specific population dynamics of *A. islandica* collected from the Long Island portion of the stock (management area SVA/SNE-South) and to perform a comparative analysis with the population dynamics derived from Georges Bank (GBK-North, Hemeon et al. accepted). The population dynamics analyzed include length frequencies, ALKs, age frequencies, sex ratios at size, mortality, and longevity. As the dominant harvest region, this study addresses the imperative that Long Island population dynamics be available to fishery managers, and that differences between intra-stock populations be identified.

4.2 Materials and Methods

4.2.1 Sample Collection

Two types of field samples were collected from Long Island (LI): a sample to estimate length frequency (sampled in 2015) and a shucked sample to obtain sex ratios and animals for subsequent aging (sampled in 2017). Both samples were collected from approximately 40.09658°N 73.01057°W at a depth of 48 m. This study was designed to evaluate the demographics of *A. islandica* available to the fishery; therefore, only animals selective to commercial gear were retained for analysis and at LI this included clams greater than 60 mm in shell length. The length sample was collected in 2015 with a commercial hydraulic clam dredge used by both the fishery and federal surveys (Hennen et al. 2016), and only shell lengths were measured. Formerly, this length sample was used alongside a 2015 age analysis by Pace et al. (2017a,b), and the length data were reutilized for the present study.

Results from Pace et al. (2017a, 2017b) suggested that a more intensive age-at-length analysis using a larger age dataset was necessary for this site to fully explain LI population dynamics. Therefore, in 2017, the second sample from this same location was collected with different sampling gear to collect a larger sample to be used for a new age analysis. The 2017 sample, hereafter termed the shucked sample, was collected using a Dameron-Kubiak (DK) dredge that can target smaller *A. islandica* and allowed more animals to be retained from the smaller size classes of the fishery (60-80 mm) (Hennen et al. 2016). To meet desired age sample-size specifications (~100 animals per 5-mm size class), multiple 5-min tows were required. The shucked sample included all animals collected in the DK dredge. To assure an unbiased sample of the population for further

analysis, all animals were measured for shell length, tissue shucked from the shell, sex determined by gonadal smear slide, and shell valves retained in dry storage for future analysis (Pace et al. 2017a, Hemeon et al. accepted).

4.2.2 Sample Preparation

The 2017 shucked sample was subsampled and approximately 100 animals per 5-mm size class were visually aged (herein referred to as the age sample). If available, each size class included 50% randomly selected females and 50% randomly selected males. All samples were aged for rare size classes with less than 100 animals. Shells to be aged were cross sectioned using a tile saw, ground and polished to a reflective finish, and the hinge plate imaged by cellSens software and a high-resolution Olympus microscope (see Pace et al. 2017a, Hemeon et al. 2021). ImageJ software (ObjectJ plugin) was used for image annotation to allow precise aging.

4.2.3 Error Assessment

A primary and secondary age reader each aged a random 20% subsample of the 2017 age sample and error metrics were evaluated using a three-fold error analysis of precision, bias, and extreme error frequency (Hemeon et al. 2021). This error protocol ensured precision between two age readers were within acceptable thresholds, determined that no aging bias occurred, and permitted the assessment of the frequency of extreme deviations of precision (i.e., extreme errors) (Hemeon et al. 2021). Once error was constrained, the primary age reader aged the entire age sample.

4.2.4 Length Frequency

The 2015 length sample was adjusted for dredge selectivity to increase numbers at size to better reflect the true length frequency of the population (Table 15, NEFSC 2017).

The population length frequency was then divided into male and female length frequencies by use of sex-proportion at size derived from the shucked sample.

Male and female length frequencies were compared using the Kolmogorov-Smirnov (KS) (Conover 1980), Wald-Wolfowitz Runs (Runs) (Conover 1980), and Anderson-Darling (AD) (Pettitt 1976, Engmann & Cousineau 2011) statistical tests with *A. islandica*-specific modifications listed in Hemeon et al. (accepted). Means were also compared using the Mann-Whitney U test in the R base statistics function (R Core Team 2020) between males and females, as the population length frequency was not independent from the sex-specific data as they were simply split from the population length frequency.

4.2.5 Age Frequency

The original age sample was expanded to include more shells than required (~100 per size class), as additional shells were imaged to replace those omitted due to poor image quality and all available ages were retained for such a data-poor species. Therefore, 904 ages were available to create the 2017 ALK binned into 5-mm size classes. Separate ALKs were created for the population, male, and female groups. Corresponding 2015 length frequencies were applied to the 2017 ALKs to create 2015 age frequencies for all three groups. Ceiling rounds were applied to the age frequency results to prevent the elimination of ages represented by fractional animals at rare ages.

Population, male, and female age frequencies were compared using the KS, Runs, and AD tests using an $\alpha = 0.05$ significance level and test modifications identical to Hemeon et al. (accepted). Means of population, male, and female age frequencies were

also compared using a Type III ranked one-way ANOVA (R Core Team 2020) with Tukey post-hoc analyses.

4.2.6 Age-Length Key Validation

For each sex, ALK reliability was analyzed using 50 Monte-Carlo simulations (herein referred to as base simulations) to re-select age data and create 50 new ALKs and 50 new age frequencies (Figure 4.2). Age frequencies were then compared with the original group-specific (e.g., population, male, female) age frequency using the KS, AD, and Runs tests. The probability of a significantly different test across simulations was reported. Sex-specific ALK reliability was performed by Hemeon et al. (accepted), but the GB population ALK was analyzed in this study for population-scale ALK verification.

To test whether the population, male, and female ALKs were in fact unique, an additional 50 simulations (herein referred to as "substituted-group simulations") were completed to develop 50 new ALKs, but the substituted-group length frequency was applied to the ALKs to create substituted-group age frequencies (Figure 4.2). Simulated datasets were obtained by choosing with replacement the same number of animals as in each original 5-mm size class using Knuth's Ran1 and Ran3 random number generators alternately, with the generator reinitialized by a new seed number for each simulation (Press et al. 1989). The probability of a significantly different test from the original group-specific age frequency across simulations was reported. If the ALKs are effectively the same and group-specific ALKs are not required, the probability of a significant test across all 50 substituted simulations would be similar to the probability of significant tests for the base simulations using binomial analysis (Hemeon et al. accepted).

To determine if LI and Georges Bank (GB) require different ALKs, group-specific simulations were completed in a similar fashion as the substituted simulations, where 50 simulations (herein referred to as "substituted-site simulations") were completed to develop 50 new site-specific ALKs, but the substituted-site, group-specific length frequency was applied to the ALKs to create substituted-site, group-specific age frequencies. The probability of significantly different tests across simulations was reported. If the ALKs are effectively the same and site-specific ALKs are not required, the probability of a significant test across all 50 substituted simulations would be similar to the probability of significant tests for the base simulations for each site using binomial analysis (Table 6, Hemeon et al. accepted).

4.2.7 Mortality and Longevity

Due to the extremely rich age composition dataset, and the use of age-frequency derived *A. islandica* mortality estimates from other regions (e.g., Ridgeway et al. 2012), mortality was first estimated by linear regression of the age frequency (Ricker 1975). Age frequency data were only used in this analysis for the peak and right-hand portions of the frequency distribution after grouping into 10-y age classes to minimize year-to-year variability. This technique prevents smaller animals not fully selected by the dredge from affecting the mortality estimate.

For comparison, an alternative estimate that does not demand expansive age compositions was used, namely the $\text{Hoenig}_{\text{nls}}$ function that only requires the maximum age of the population (Eq 4.1) (see Table 3, Then et al. 2015).

$$\text{(Eq. 4.1)}\quad M_{est} = 4.899 t_{max}^{-0.916}.$$

Where M_{est} represents natural mortality and t_{max} represents maximum age.

4.2.8 Sex Ratios

Sex ratios of the shucked sample were evaluated by 5-mm size classes using an exact binomial test for size classes where n<30, and an approximate binomial test for size classes where n>30 (R Core Team 2018). A population sex ratio was calculated from the length frequency after the length frequency was adjusted for selectivity and divided by sex. Sex ratios were also compared between regions using a two-sample binomial test under the same test conditions listed previously.

4.3 Results

4.3.1 Error Assessment

A total of 158 samples were randomly selected from the LI dataset for an age-reader error assessment between two experienced *A. islandica* agers. This exercise ensured the primary age reader was aging consistently and to acceptable standards. Three rounds of error analysis (whereby a new 20% random subset was selected for each round) were required to meet species-specific error thresholds for precision and bias set forth in Hemeon et al. (2021). Precision, as measured by median coefficient of variation (CV), was 6% for the total population, 5% for females, and 6% for males. Median CV was used instead of the mean due to the extreme number of age classes (greater than 300 y) and high skewness of both age and error data. Evans-Hoenig bias results were non-significant (P>0.05) for all groups.

Error frequency (i.e., frequency of extreme error) was also evaluated for samples with CV greater than 10% and error frequency was greater than for GB as described in Hemeon et al. (2021) and was 20% for the population, 13% for females, and 30% for males. The target error frequency is set at 10% of the sample. Samples collected from LI

are more challenging to age due to the higher occurrence of suspected intra-annual growth lines that need to be interpreted by age readers, and thus resulted in more extreme cases of error between samples (particularly male samples). Due to high precision and no age-reader bias, error was deemed acceptable with the caveat that LI has higher error for less than 30% of the sample when compared to GB, and that males are aged with higher error than females at both sites.

4.3.2 Length Frequency

The LI length frequency sample was adjusted for dredge selectivity and divided into male and female datasets by sex proportion at size from the shucked sample (Table 4.1) to better reflect the true population. The adjusted length frequency included 1,205 female and 1,700 male shell lengths for clams available to the commercial (and federal survey) dredge (Table 4.2, Table 4.3). Female median shell length was 89 mm (61-111 mm) with a mean length also of 89 mm (SD = 8 mm). Male median shell length was 83 mm (61-107 mm) with a mean length also of 83 mm (SD = 8 mm) (Figure 4.3A). A Mann-Whitney-Wilcoxon test determined a significant difference between the mean female and male lengths ($p < 2.2e-16$) (Figure 4.3A), where female lengths are offset to larger sizes than males (Figure 4.3B). The distribution statistics (Table 4.4) comparing LI male and female length frequencies were significant for the KS and Runs tests ($p < 0.01$), but non-significant for the AD test. Results indicated that the tails of the distributions were similar, but the modal sections diverged and were offset (see conditions of the Runs test) (Figure 4.3B).

Length frequencies at GB were consistently offset to larger sizes when compared to LI (Figure 4.4). This trend was most apparent in the sex-specific length frequencies,

where LI females were offset to smaller sizes than GB females and the respective means were significantly different (Mann-Whitney-Wilcoxon test, $p < 2.2e-16$) (Figure 4.4B). Long Island males were also offset to smaller sizes than GB males (Mann-Whitney-Wilcoxon test, $p < 2.2e-16$) (Figure 4.4C) (see Hemeon et al. accepted for GB data). Regional length distributions were also evaluated, and tails were similar between sexes at the two sites, but the modal section of the distributions was different and both GB female and male length frequencies were offset to larger sizes (Table 4.4, Figure 4.4).

4.3.3 Age-Length Data

The age sample included ages and lengths for 904 samples, including 448 female samples and 456 male samples. A target of 100 animals aged per 5-mm size class was exceeded for size classes 80-95 mm due to the availability of images (Table 4.5). The mean female age was 119 y (SD = 58 y), and the mean male age was 107 y (SD = 58 y). Size class 105 mm had the largest range of ages that spanned 249 y (n=86) with a mean age of 181 y (SD = 46 y) (Table 4.5) and the dataset ranged in ages from 17-310 y (median = 96 y) and lengths from 51-114 mm (median = 90 mm) (Figure 4.5A). Only 0.1% of the aged sample was born in the past 20 y, and only 3% of the age sample was born in the past 30 y. Limited numbers at young age is an artifact of the restriction of aging to individuals from larger size classes; younger ages and smaller sizes were collected and will be reported elsewhere (Mann, unpubl. data).

Age compositions described by sex and size class at LI were significantly different only for the 90-mm ($p = 6.70E-10$) size class using Tukey post-hoc analysis, where females are younger than males within that size class (type III ranked two-way ANOVA: $p = 0.01$, $df = 10$) (Figure 4.5). When aged data are compared between LI and

GB, females are statistically different regionally in the 95-mm (p = 0.0003) and 105-mm (p = 0.0002) size classes. Georges Bank females are younger than LI females within those size classes (type III ranked two-way ANOVA: p = 6.68E-06, df = 8) (Figure 4.5C). Males are statistically different regionally in the 70-mm (p = 4.45E-05), 75-mm (p = 0.04), 80-mm (p = 0.002), and 90-mm (p = 6.28E-08) size classes in that GB males are younger than LI males within the 90-mm size class but older in the 70-mm, 75-mm, and 80-mm size classes (type III ranked two-way ANOVA: p = 2.20E-16, df = 8) (Figure 4.5D). The significantly older GB males in the 70-mm size class compared to the LI males is likely not reliable due to the extremely small sample size of aged GB males in that size class (n = 4) (Hemeon et al. accepted).

4.3.4 Age Frequency

Age frequencies for population, female, and male groups were created independently with unique ALKs derived from the age sample. The population age frequency data ranged in age between 17-310 y (median = 84 y), female age frequency data ranged between 17-272 y (median = 87 y), and male age frequency data ranged between 21-310 y (median = 81 y) (Figure 4.3). Type III ranked one-way ANOVA resulted in significant differences between population, female, and male groups (p = 6.32E-06, df = 2). Tukey post-hoc analysis was significant between male and female (p = 3.02E-06), male and population (p = 0.05), and female and population (p = 0.003). Cumulative age frequencies of male and female data do appear offset between 40-130-y, but otherwise track the other age frequency very closely (Figure 4.3D).

Age-frequency distribution statistics (Table 4.4) identified a significant difference between LI male and female age frequencies only for the KS test, an indication that the

frequencies are different in the modal portion of the distribution (Figure 4.5) and likely near the median birth years of the two groups (~1927-1937) (Figure 4.6). The population, female, and male age frequencies all present a large depression in the abundance of animals born during that time frame, but the male frequency is particularly deficient in animals born during 1920-1930. Notable reductions in effective recruitment (i.e., animals that survive to reach the fishery) also occurred between 1935-1945, and again in the 1970s. Younger animals (recent birth years) tend to be smaller and less available to the commercial dredge due to dredge size selectivity. An artificial drop in the frequency distribution of animals born in recent years is a consequence; however, isolated patterns can still be evaluated for the right-hand tail of the age-frequency distribution as long as the numbers are not compared to those on the left-hand tail due to gear selectivity effects. The population age frequency appeared to capture the modal section of both males and females since only the AD test is significantly different between the population age frequency and the two sex-specific age frequencies (Table 4.4).

Regional age frequencies are statistically different for all distribution tests for all groups (i.e., population, male, female), despite similar periods of depressed effective recruitment (i.e., animals born that recruit to the fishery) ~1920-1930 in both the LI and GB age frequencies (Figure 4.6, Table 4.4; see also Hemeon et al. accepted, Figure 11-12). Female age frequencies between LI and GB, and male age frequencies between LI and GB, were statistically significantly different for all three tests (Table 4.4). Therefore, differences in sex-specific age frequencies exist within and between populations of the Mid-Atlantic stock.

4.3.5 Age-Length Key Validation

Simulations were used to evaluate ALKs for reliability, and versatility, across groups (e.g., group, site) (Table 4.6). The LI population ALK was reliable at replicating the modal section of the population age frequency (Figure 4.6, Table 4.6), only producing an age-frequency distribution shift 16% of the time (see Runs results). Female and male LI ALKs were also reliable at the replication of the true sex-specific age frequency modes but resulted in distribution shifts 26-28% of the time. The reliability of ALKs at both GB and LI are very similar, in that the modal section of the age-frequency distributions are reproducible greater than 98% of the time, the replicated age-frequency distributions may be offset in age between 16-28% of the time (although GB population ALK produced offsets 40% of the time), and the age-frequency distribution tails are generally not reproducible (GB population ALK is better than others at predicting the distribution tails) (Table 4.6). Thus, the long tail of old animals is least defined and remains poorly defined even with the large dataset used in this analysis to describe population age frequency.

Sex-specific ALKs are reliable, but not interchangeable within a region. In other words, a male or female ALK alone cannot replicate a true population age frequency. Likewise, ALKs are reliable at reproducing age-frequency distributions within a local population, but a single ALK from one location cannot be substituted for the other to represent a region (i.e., LI and GB combined).

4.3.6 Mortality and Longevity

The age frequency for each LI group was evaluated for longevity using the Ricker method (Ricker 1975). Longevity was greatest for the population at 347 y, followed by

females at 324 y, and finally males at 316 y (Figure 4.7), despite a male with the maximum observed LI age. Longevity was greater than maximum observed age for all three groups, with female longevity being 19%, population 12%, and males 2% greater than the maximum observed age.

Estimates of total mortality were calculated using linear regression and the $Hoenig_{nls}$ formulations. Linear regression estimates were similar between population, females, and males at 0.022, 0.021, and 0.023 y^{-1}, respectively (multiple R^2 of 0.92, 0.91, and 0.89 respectively) (Figure 4.7). Natural mortality estimates from the $Hoenig_{nls}$ formulation were 0.029 y^{-1} for females and 0.026 y^{-1} for males.

Females at GB exhibited a higher total mortality (i.e., all natural due to the unexploited nature of the stock) (0.048 y^{-1}) than males (0.039 y^{-1}) and the population (0.041 y^{-1}) using the linear regression method (Hemeon et al. accepted). The $Hoenig_{nls}$ method also supported a slightly higher female natural mortality than males, but at lower rates than did the linear regression method (0.034 y^{-1} and 0.030 y^{-1}, respectively; this study). Estimates of total mortality rates were consistently higher at GB than at LI. As the fishery catch is fully selected for the size classes used for these analyses, the influence of fishing is unlikely to have biased the LI estimates, despite the importance of the region to total landings.

4.3.7 Sex Ratios

A significant sex ratio pattern across 5-mm size classes was identified: males dominated size classes 65 mm-84 mm, and females dominated size classes 95 mm-114 mm (Table 4.2). Between 85 mm-94 mm, dominance transitioned from males to females and the two sexes were at an approximately 1:1 ratio. In other words, the sex ratios of the

85-mm and 95-mm size classes were not significantly different than a 0.5 expected ratio using the binomial test (Table 4.2, Figure 4.8). The population sex ratio available to the fishery is 1:1.4 (F:M) and is significantly dominated by males despite similar mortality rates between sexes for fully-selected age classes (Table 4.2). A two-sample approximate binomial test identified that sex ratios were significantly different between LI and GB at the 80-, 85-, 95-, and 105-mm size classes.

4.4 Discussion

4.4.1 Reliability of Age-Length Keys

This study aims to compare the population dynamics of *A. islandica* from two distinct management areas of the US Mid-Atlantic fishery. The two management areas are contiguous but delineated by the Great South Channel. If stock assessments move forward with integrating age data into the assessment models, one critical element is the application of an ALK to estimate ages from a length sample, as the majority of the survey and landings data are solely represented by lengths. Determining whether a single ALK is sufficient to represent the entire stock or if multiple ALKs are required is crucial. If the latter, ascertaining at what geographic scale age-length dynamics vary and therefore necessitate different ALKs becomes an imperative.

This study found that population ALKs created for LI and GB were sufficient to produce site-specific population age frequencies. A population age frequency would be a time- and cost-effective alternative to sex-specific age frequencies, since additional laboratory equipment and slide preparation would not be necessary to distinguish samples by sex. However, ALKs are distinct by sex and site and a single ALK cannot be used interchangeably between LI and GB without generating increased uncertainty in the

population age frequency. Also, organizing age-length data by sex provides extensive information on local population dynamics and illuminates an unusual life-history not common in marine bivalves.

4.4.2 Dimorphism

Female length distributions are consistently offset to larger sizes in comparison to males from the same population at both GB and LI. Mann-Whitney-Wilcoxon tests identified that the mean female lengths are significantly larger than the males at LI, and KS and Runs tests identified that the length distribution modes are significantly different and length distributions are offset between males and females. Age compositions are not significantly different between males and females at GB by mean age or age-frequency distribution (Hemeon et al. accepted). A large difference in size but not age between sexes of a species is a strong indicator of sexual dimorphism, as demonstrated at GB by Hemeon et al. (accepted). LI age compositions were significantly different between sexes by both mean age and age-frequency distribution. No evidence exists, however, for protandry. Since very old and small males exist at LI, and male and female length distributions are significantly offset, our findings support those of Hemeon et al. (accepted) that *A. islandica* are sexually dimorphic and agree with Ropes et al. (1984) that this dimorphism arises from differential growth and not protandry.

Observation of sexual dimorphism is reinforced when sex ratios at size are considered. A significant difference in sex ratio exists for *A. islandica* at GB, and for animals less then 85 mm and greater than 95 mm at LI. Males at both sites dominated small size classes, and females dominated large size classes. A knife-edge transition in dominance occurred at 95 mm for GB, whereas LI demonstrated a gradual transition in

dominance between 85-95 mm. Ropes et al. (1984) collected samples in 1978 and 1980 at the onset of an *A. islandica* fishery in Long Island, New York (43,400 lbs harvested between 1979-1980, NOAA 2021), and also recorded a gradual transition of male and female dominance between 70-90 mm. A study by Thorarinsdóttir & Steingrímsson (2000) in northwest Iceland, where growth rates and maximum size are lower than those reported from the US continental shelf, identified the transition from male to female sex-ratio dominance at a smaller size of 40 mm. Maximum length and modal length distributions at LI are smaller than those at GB; it is unclear if the size discrepancy between sites is the result of reduced growth rates at LI or a size bias due to an active fishery, but a sex-ratio transition at a smaller size than observed at GB could indicate lower growth rates at LI as observed at northern latitudes (e.g., northwest Iceland). In other words, female *A. islandica* growth rates eclipse male growth rates at smaller sizes in colder/slower growing environments.

4.4.3 Fishery Effects

The two *A. islandica* populations analyzed in this study were chosen to compare a relatively virgin population with a population supplying the greatest fishery landings in the Mid-Atlantic. The substantial, observed differences between the two populations may accrue as a consequence of the fishery and/or local oceanographic conditions.

Long Island had a greater maximum observed age but smaller maximum and median lengths than observed at GB. The fishery at LI may bias the length distribution to smaller sizes but interestingly, no age bias (age truncation) attributable to the fishery appears to be present. Mortality rate estimates are lower at LI, a result unexpected if age truncation was present. However, the stock may be resistant to age truncation. Pace et al.

(2018) observed increased growth rates over time in the Mid-Atlantic, in that recent cohorts reached large sizes faster than earlier cohorts. Thus, a fishery that targets large animals will increasingly harvest younger animals, thus limiting age truncation as an outcome.

A second distinction between GB and LI are the population sex ratios for animals >70 mm. Hemeon et al. (accepted) discovered a 1:1.1 (F : M) sex ratio of the "unfished" GB population where male *A. islandica* were more available than females. A 1:1.4 population sex ratio was observed at LI, a fished population with an even more dramatic bias towards male *A. islandica*. Hemeon et al. (accepted) hypothesized that a future GB fishery would be comprised predominantly of male clams, since males constituted 57% of the most common size classes available to fishery gear (see Hemeon et al. accepted, Table 1). This study does not support this anticipation, though possibly the fishing mortality rate may be too low to obtain the expected outcome as males continue to dominate the fishery at LI (Table 4.2). Studies by Thorarinsdóttir & Steingrímsson (2000) in northwest Iceland and Rowell et al. (1990) in southwest Nova Scotia of unfished *A. islandica* populations, determined that the sex ratios were male dominated and aligned with results from Hemeon et al. (accepted); even fished populations tended to be dominated by males (Jones 1981, Mann 1982). In fact, Ropes et al. (1984) is one of very few studies to find a population sex ratio biased towards females, but this study occurred at the onset of the Long Island *A. islandica* fishery. Possibly, the decades-old fishery at LI may have fished down the largest *A. islandica* resulting in smaller maximum observed size and a length frequency shift to smaller size classes. The length compositions reported in NEFSC (2020) do not support this expectation, but these do not overlap the Ropes

(1984) timeframe; thus a fishery that potentially targeted the large females of the population when the fishery first began could have resulted in the reduced overall size and female abundance at LI.

Georges Bank exhibited a sex-specific mortality rate in that females had a higher total mortality rate than males. At LI, mortality rates are both equal between sexes and lower overall when compared to GB. An important distinction between the two populations, aside from the fishery, is the relationship of LI *A. islandica* with the seasonal Cold Pool. The Cold Pool is an extremely important feature along the Mid-Atlantic Bight (MAB) that provides cold, low-salinity water to the MAB benthos as the spring/summer thermocline prevent mixing with the warmer surface waters (Bigelow 1933, Brown et al. 2012). Cold water advances from the Gulf of Maine, around Georges Bank, and extends southward towards Cape Hatteras (Xu et al. 2015). Chen et al. (2018) hypothesize that the cold water is composed of residual winter water and northernly-sourced water from latitudes as distant as the Labrador Sea. The Cold Pool persists through the summer until advection begins to warm the northern edges of the feature, and September storms mix the warm surface water with the cold bottom water. Chen et al. (2018) also report that the northern boundary of the Cold Pool degrades faster than that further south. Consequently, *A. islandica* located closer to the northern boundary of the Cold Pool (e.g., Long Island), may be subject to higher variability and warmer temperatures than at GB as the the Cold Pool footprint degrades in the fall. Sufficiently warmer temperatures in the fall may negatively influence growth. One outcome from this Cold Pool seasonality as manifested in *A. islandica* population dynamics may be subannual growth signatures giving rise to higher aging errors at LI.

Seasonal Cold Pool variability also may trigger burrowing behavior in *A. islandica*. These animals burrow into the sediment periodically and drastically lower metabolic functions; a process thought to promote longevity for this species (e.g., Strahl et al. 2011, Ballesta-Artero et al. 2019). Both extensive anaerobiotic capability and sulfide tolerance (Oeschger & Storey 1993) support an evolutionary adaptation for prolonged burial. When LI aging error, smaller size, and longevity are considered, perhaps Cold Pool dynamics induce burrowing to escape Fall warm termpaturea. The effect of the Cold Pool on total mortality may only be resolved with the addition of multiple Cold Pool sites and the comparison of mortality rates throughout the Southern Management Area, and a more thorough understanding of burrowing response to adverse environmental changes (see Ragnarsson & Thorarinsdóttir 2020).

4.4.4 Regional Recruitment Trends

The most apparent distinction between GB and LI, is the lack of young animals in the observed length classes at GB and the extreme longevity at LI. Age-length data indicated that *A. islandica* at GB, regardless of sex, are younger at size than LI suggesting that GB growth rates are faster than growth rates at LI. If so, animals should reach the dredge selectivity minimum size at younger ages at GB than LI but contrary to expectation, very few young animals were aged at GB. Inconsistency between expected growth rates and observed ages may be the result of recent post-settlement mortality of animals within the past three decades, reduced recruitment over the past three decades, or patchy demographics at GB where smaller and potentially younger animals were not fully intermixed at the GB sample site.

At the older spectrum of the age-frequency distribution, extremely old animals were absent at GB compared to LI and could be the result of higher estimated natural mortality at GB. Mortality is estimated from age frequencies assuming mortality is constant across time and age classes (Ricker 1975). Natural mortality estimates from GB age frequencies are higher than total mortality estimates at LI due to the extremely old ages discovered at LI that reduced mortality rates derived from a shallower regression model slope. If mortality is assumed to be stable over time and across ages, a higher mortality rate at GB could account for the lower representation of old animals.

The age frequency can also be viewed as a proxy for recruitment. Recruitment was consistent at LI between 1890 and 1970, in that animals effectively recruited to the fishable size classes for each birth year during this time frame. Prior to 1890, animals were still born in most birth years but at lower frequency and with a few missing cohorts (Figure 4.6). Proceeding from 1890, the age frequency began to steadily increase until its peak in 1955. The observed decline in the age frequency between 1955-2017 is likely a sampling artifact of younger animals not being fully available to the survey dredge. Harding (2008) attributed bottom water temperature as a primary driver for divergent growth trends for this species, but local food availability is also considered an important factor. Mann et al. (2009) demonstrated a consistent warming trend that initiated in the early to mid 1800s at the conclusion of the Little Ice Age (1400-1700 CE), a warming temperature trend could have driven the late 1800 increase in effective recruitment at both LI and GB (see Hemeon et al. accepted).

In the 1970s, the LI population and sex-specific age frequencies declined dramatically and was followed by increased effective recruitment between 1980-1990

(see Figure 4.6). Since many animals were born after the 1970s decline in the age frequency, the reduced number of animals surviving to the fishery from the 1970s is likely a true recruitment effect and not solely a result of low gear selectivity for these age classes. All age frequencies from LI also presented large decreases in effective recruitment during the mid-1920s. The Atlantic Multidecadal Oscillation (AMO) is an oceanographic cycle with recurring 20-80 y periodicity in the northern Atlantic Ocean and is predominantly characterized by positive (warm) and negative (cold) temperature indices (Alexander et al. 2014). The AMO had an observed negative index (negative temperature anomaly) in the mid 1970s that was comparable to the AMO negative index in the 1910-1920s (Nye et al. 2014), followed by a positive AMO index immediately following in the 1990-2000s. The entire 40-60 y period of an AMO cycle is not easily observed in an age frequency from either GB or LI, but extreme temperature anomalies do correspond with dramatic *A. islandica* effective recruitment events (e.g., lows 1920s, 1970s). Hemeon et al. (accepted) also observed substantial declines in the GB age frequencies during the 1920s, but very few young animals were sampled from GB to illuminate the presence of a 1970s recruitment decline during the sample time series. If the 1970s were a truly poor decade for *A. islandica* recruitment in the Mid-Atlantic, it may explain why very few young animals were observed at GB or even suggest a stronger 1970s negative-recruitment effect at GB compared to LI. Temporal coherence between AMO indices and effective recruitment trends of *A. islandica* support findings that extreme negative AMO indices (extreme cold temperature anomalies) produce years of reduced population recruitment at GB and LI. It is well known that climatic cycles with strong bottom-water temperature variability affect *A. islandica* growth rates

(Harding et al. 2008, Poitevin et al. 2019), and it would not be surprising if the same positive and negative thermal growth trends apply to positive and negative recruitment trends.

Hemeon et al. (accepted) identified 8-y recruitment signals in the GB age frequencies and theorized that apparently stronger year classes could be the product of the North Atlantic Oscillation (NAO) cycles (Visbeck et al. 2001, Soniat et al. 2006, 2009). High recruitment years at LI occurred in approximately 1953, 1945, 1942, 1932, 1927, 1922, 1915, 1905, and 1889 (Figure 4.6), with a mean peak recruitment cycle of also 8 y. Along with 8-y periods of high recruitment, there are also 8-y periods of low, to very-low recruitment, resulting in decades with extremely high recruitment followed quickly by extremely low recruitment within only a 3-5 y time span (Figure 4.6). The peak recruitment years at GB and LI are often only different by a year or two between the two sites, with LI lagging behind the GB pulses. Despite localized differences in benthic conditions on either side of the Great South Channel separating Georges Bank from the Long Island/southern New England continental shelf, recruitment timing appears to be consistent in this Mid-Atlantic region and could be the result of underlying oceanographic cycles such as the NAO. These two sites are also tightly linked by the Labrador Current that carries Arctic water from the Labrador Sea through the Great South Channel and around the southern flank of Georges Bank past the Nantucket Shoals to the Mid-Atlantic Cold Pool (Chen et al. 2018, Chen & Curchitser 2020). The movement of Arctic water to Georges Bank and the Mid-Atlantic strongly influences bottom-water temperatures and the lead/lag in recruitment cycles of GB and LI are potentially a reflection of the lead/lag relationship between water movement throughout

this region. Lagged recruitment pulses at LI from GB would be appropriate considering the water mass movement from the Labrador Sea arrives at GB first, before moving southward and contributing to the formation of the Cold Pool off LI (Xu et al. 2015). Understanding the stable periodicity and drivers of successful recruitment can substantiate stock projections when other parameters are difficult to predict.

4.4.5 Summary

It is clear that *A. islandica* are sexually dimorphic in the US Mid-Atlantic. Mortality rates are lower at LI than GB and resulted in older observed maximum age and longevity at LI compared to GB. Age-length keys are also distinct between the Northern- and Southern-management areas, and ALKs cannot be interchanged. However, population-scale ALKs are reliable and can reproduce population age frequencies with high reliability. Such findings may eliminate the costly need to develop sex-based ALKs if not required for other analyses. *Arctica islandica* populations comprise a large number of cohorts at both GB and LI. Recruitment into the populations occurs routinely with substantive hiatuses being rare and substantive year classes occurring at least decadally with lesser, but contributing, recruitment in most years in between. Routine recruitment may insolate this species from risks posed by overfishing to an extent not typical for other long-lived species.

4.5 Tables

Table 4.1 Long Island sex proportions at size.

Length (mm)	Female	Male
61	0.50	0.50
65	0.00	1.00
66	0.00	1.00
67	0.00	1.00
68	0.25	0.75
69	0.20	0.80
70	0.19	0.81
71	0.07	0.93
72	0.18	0.82
73	0.32	0.68
74	0.12	0.88
75	0.10	0.90
76	0.24	0.76
77	0.21	0.79
78	0.29	0.71
79	0.24	0.76
80	0.38	0.63
81	0.26	0.74
82	0.42	0.58
83	0.36	0.64
84	0.36	0.64
85	0.33	0.67
86	0.30	0.70
87	0.34	0.66
88	0.56	0.44
89	0.61	0.39
90	0.51	0.49
91	0.53	0.47
92	0.57	0.43
93	0.56	0.44
94	0.58	0.42
95	0.57	0.43
96	0.58	0.42
97	0.67	0.33
98	0.75	0.25
99	0.81	0.19
100	0.78	0.22
101	0.76	0.24
102	0.90	0.10
103	0.82	0.18
104	0.86	0.14
105	0.81	0.19
106	1.00	0.00
107	0.88	0.12
108	1.00	0.00
109	0.92	0.08
110	0.88	0.13
111	1.00	0.00

112	1.00	0.00
113	1.00	0.00
114	1.00	0.00
115	1.00	0.00
116	1.00	0.00

Table 4.2 Long Island sex ratios. Population sex ratio determined from the length sample (after selectivity adjustment). Sex ratios by size class determined from the shucked sample. Sex ratios were evaluated using exact and approximate binomial tests, a significant result ($p < 0.05$) indicated that the sex ratio was not 1:1 and significant ratios are in bold font.

Dataset	Sex Ratio	Numbers			F : M
		N_T	N_F	N_M	
Length Sample	LI Population	2,905	1,205	1,700	**1 : 1.4**
Shucked Sample	60-mm	2	1	1	1 : 1.00
	65-mm	26	4	22	**1 : 5.50**
	70-mm	84	16	68	**1 : 4.25**
	75-mm	116	27	89	**1 : 3.30**
	80-mm	193	69	124	**1 : 1.80**
	85-mm	219	96	123	1 : 1.28
	90-mm	318	176	142	1 : 0.81
	95-mm	397	267	130	**1 : 0.49**
	100-mm	303	249	54	**1 : 0.22**
	105-mm	107	98	9	**1 : 0.09**
	110-mm	21	20	1	**1 : 0.05**
	115-mm	2	2	0	-

N_T, total number of samples; N_F, number of females; N_M, number of males; LI, Long Island; GB, Georges Bank (Hemeon et al. accepted).

Table 4.3 Long Island length frequency.

Size Class (mm)	Population	Female	Male
60	14	7	7
65	52	6	46
70	219	40	179
75	408	86	322
80	661	234	427
85	570	232	338
90	570	310	260
95	282	182	100
100	100	82	18
105	28	25	3
110	1	1	0
Total	2905	1205	1700

Table 4.4 Regional distribution statistics. Statistics for length- and age-frequency distributions between males and females, between population and sex-specific age-frequency distributions, and between sites (Region) for Long Island and Georges Bank of the same sex and between population age-frequency distributions. Tests include the AD, Runs, and KS tests and significance at an alpha of 0.05.

Site	Dataset	Comparison	AD	Runs	KS
Long Island	Length	M-F	ns	p<0.01	p<0.01
	Age	M-F	ns	ns	p<0.01
		P-F	p<0.01	ns	ns
		P-M	p<0.01	ns	ns
Region	Length	M-M	ns	p<0.01	p<0.01
		F-F	ns	p<0.01	p<0.01
	Age	M-M	p<0.01	p<0.01	p<0.01
		F-F	p<0.01	p<0.01	p<0.01
		P-P	p<0.01	p<0.01	p<0.01

AD, Anderson-Darling; Runs, Wald-Wolfowitz Runs; KS, Kolmogorov-Smirnov; Georges Bank values compiled from Hemeon et al. (accepted); Region compares sex-specific distributions between Georges Bank and Long Island; ns, non-significant p value; M, Male; F, Female; P, Population.

Table 4.5 Long Island age sample.

Size Class (mm)	Total	Female	Male	Mean Age (y)	SD (y)	Range (y)
60	3	1	2	54	32	63
65	30	4	26	43	15	49
70	78	15	63	48	21	141
75	97	32	65	63	17	96
80	125	63	62	77	23	163
85	126	63	63	98	33	169
90	120	59	61	123	43	201
95	125	62	63	151	43	179
100	96	52	44	169	47	209
105	86	80	6	181	46	249
110	18	17	1	188	44	141
Mean	82	41	41	109	33	151

SD, Standard Deviation.

Table 4.6 Age-length key validation. Reliability and redundancy verification for site, sex, and regional age-length keys (ALK). A "True" designation indicates the length frequency data applied to base and substituted ALKs, and the age frequency tested against simulation results in the KS, Runs, and AD tests. Grey highlighted cells signified when a substituted (italicized text) ALK produces simulations that were significantly different from the base simulations (plain text, bold) using a one-sample binomial test ($p<0.05$). Expected proportions are those of the base simulations. Georges Bank analysis results taken from Hemeon et al. (accepted). Regional analysis compares female to female, and male to male ALKs when the opposite-site same-sex ALK is substituted.

Analysis	True	ALK	KS	Runs	AD
Long Island	Female	**Female**	**0.00**	**0.28**	**1.00**
		Male	*1.00*	*0.50*	*1.00*
	Male	**Male**	**0.00**	**0.26**	**1.00**
		Female	*1.00*	*0.62*	*1.00*
	Population	**Population**	**0.00**	**0.16**	**0.96**
		Female	*0.84*	*0.68*	*1.00*
		Male	*1.00*	*1.00*	*1.00*
Georges Bank	Female[1]	**Female**	**0.02**	**0.26**	**0.96**
		Male	*1.00*	*0.26*	*1.00*
	Male[1]	**Male**	**0.02**	**0.24**	**1.00**
		Female	*1.00*	*0.32*	*0.82*
	Population[2]	**Population**	**0.00**	**0.40**	**0.78**
		Female	*0.98*	*0.12*	*1.00*
		Male	*0.58*	*0.20*	*1.00*
Region	LI Population	*GB Population*	*1.00*	*1.00*	*1.00*
	LI Female	*GB Female*	*1.00*	*1.00*	*1.00*
	LI Male	*GB Male*	*1.00*	*1.00*	*1.00*
	GB Population[2]	*LI Population*	*1.00*	*1.00*	*1.00*
	GB Female[2]	*LI Female*	*1.00*	*1.00*	*0.92*
	GB Male[2]	*LI Male*	*1.00*	*0.94*	*0.38*

ALK, Age-Length Key; KS, Kolmogorov-Smirnov; AD, Anderson-Darling; LI, Long Island; GB, Georges Bank; [1], data from Hemeon et al. (accepted); [2], new Georges Bank analysis for current study.

4.6 Figures

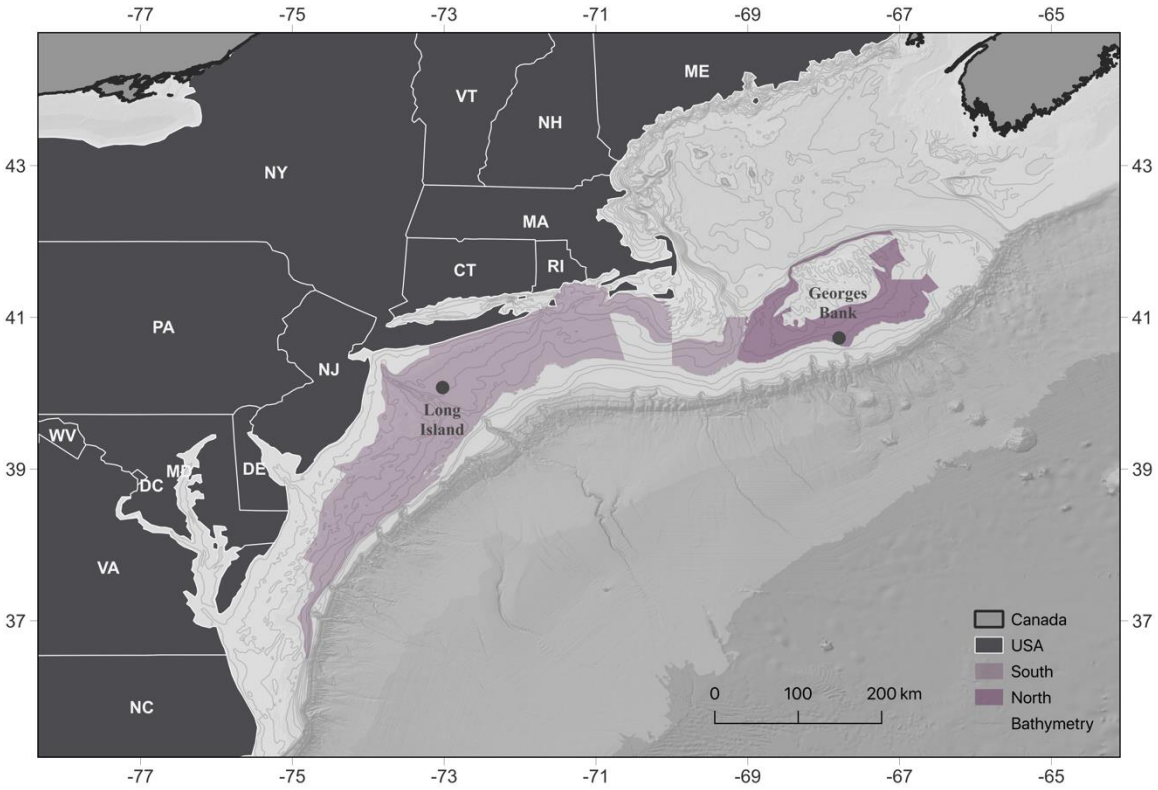

Figure 4.1 Regional map. Blue polygons represent federal management areas. Southern Management Area (South, SCA-SNE) separated from the Northern Management Area (North, GBK), by black line. The Long Island site is located in management strata 4Q, and the Georges Bank site is located in management strata 9Q.

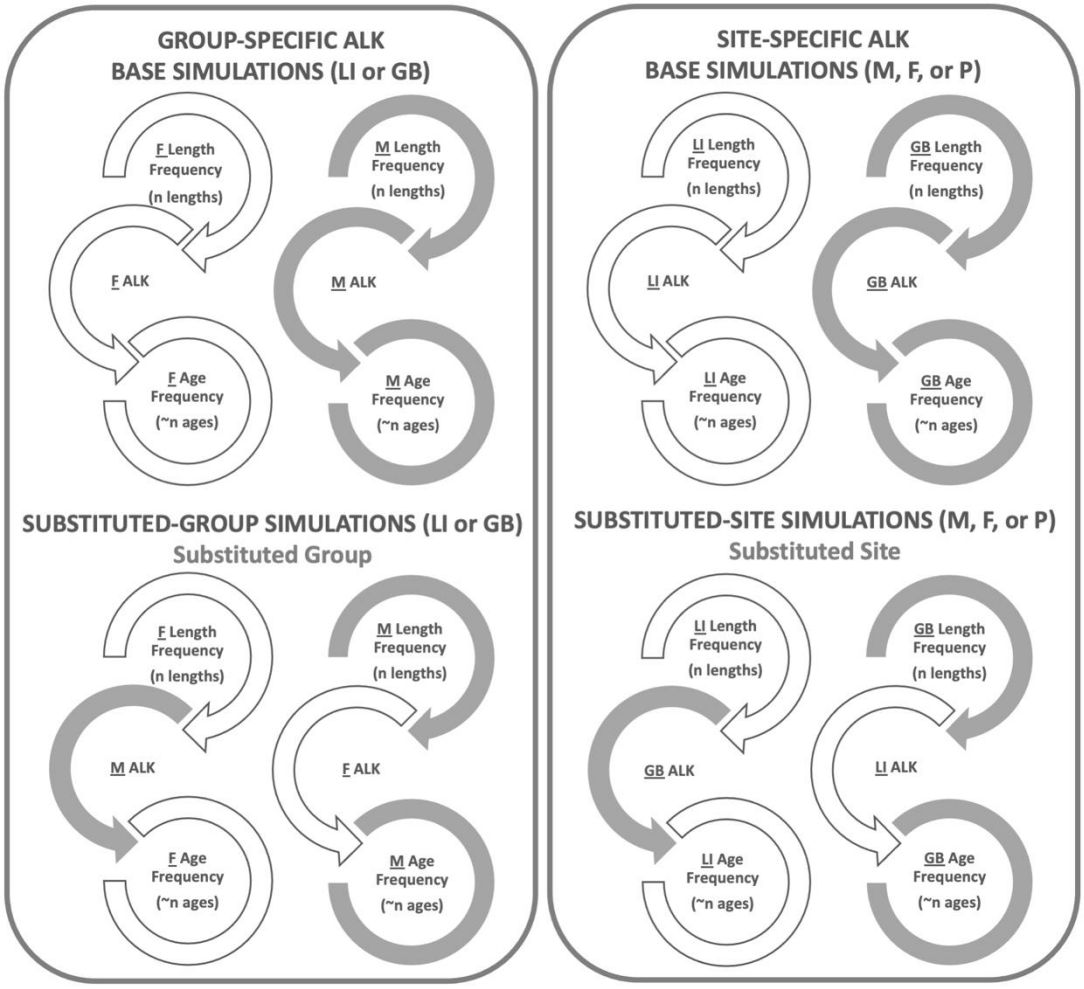

Figure 4.2 Age-length key schematic. Age-length keys (ALK) were validated with base simulations for group-specific (population, female, male) and site-specific (Long Island [LI], Georges Bank [GB]) ALKs. Substituted simulations used a substituted-group or substituted-site ALK to test differences in simulated age frequencies from true age frequencies.

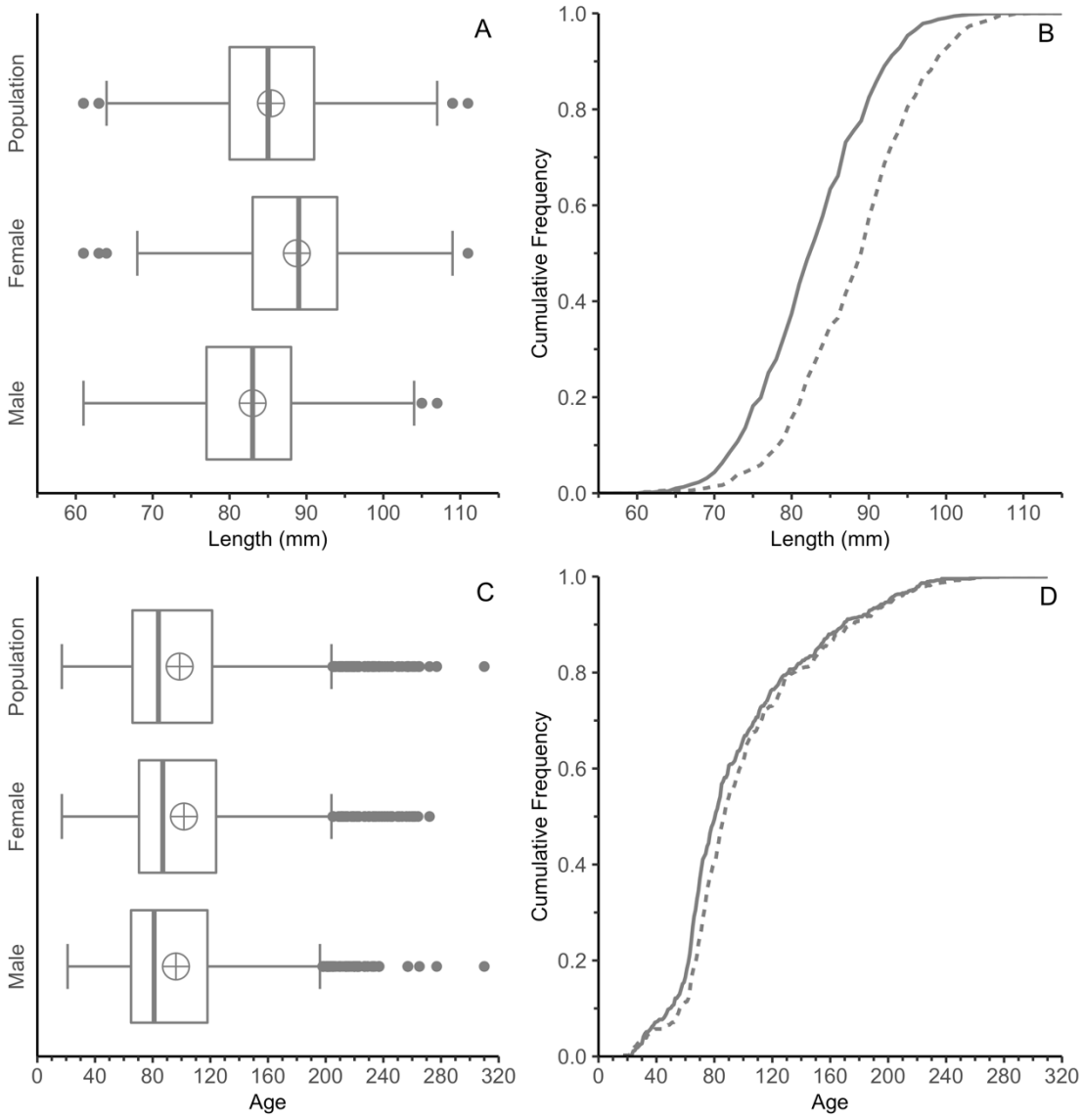

Figure 4.3 Long Island length- and age-frequency data summaries. (A) length-frequency data; (B) cumulative-length frequencies of female (dashed) and male (solid) length data; (C) age frequency data; (D) cumulative age frequencies of female (dashed) and male (solid) data. For boxplots, target represents mean, box represents the interquartile range (IQR) with 50th percentile bar (median), whiskers represent 15*IQR, and points are outliers.

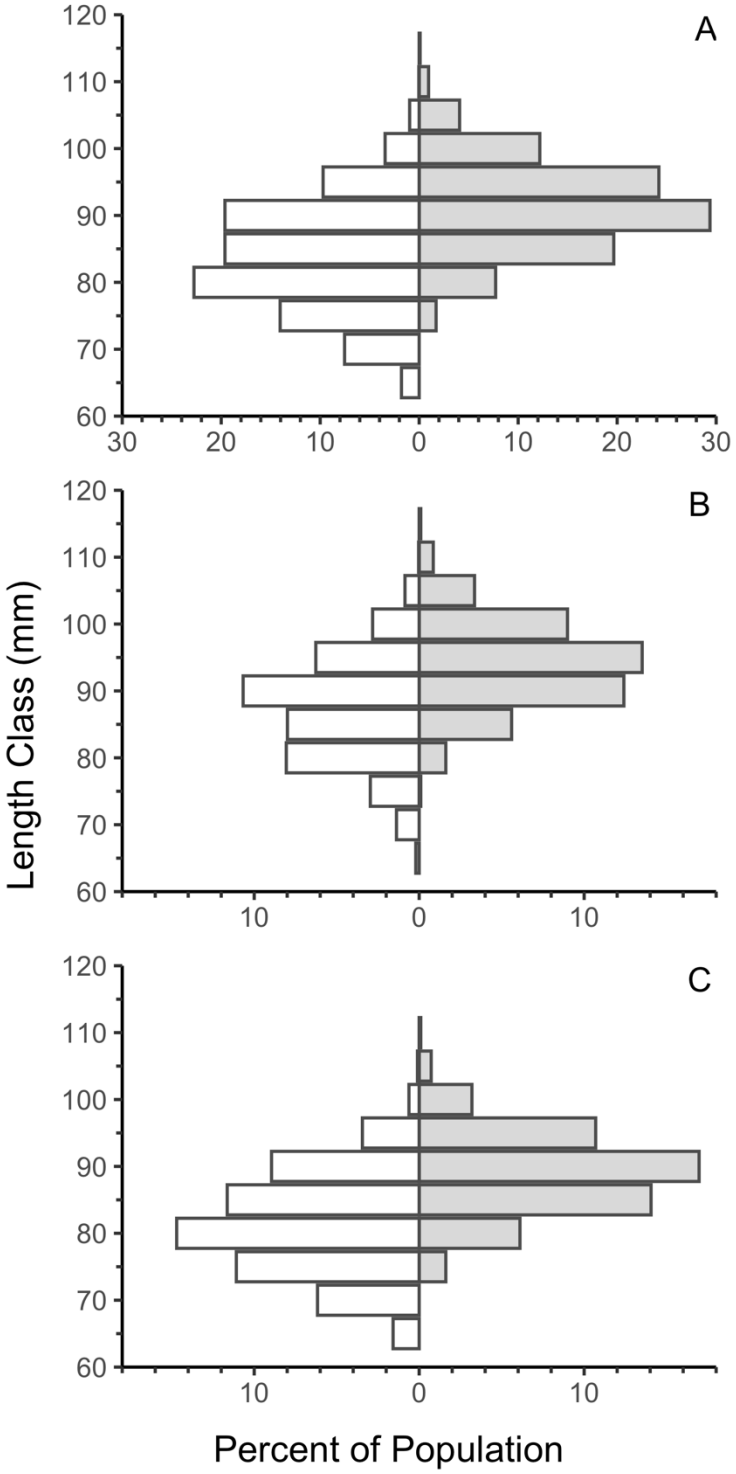

Figure 4.4 Regional length-frequency data. Long Island (white) vs Georges Bank (grey) length frequencies as a percent of the total site-specific population by 5-mm size class of the (A) population, (B) female, and (C) male groups.

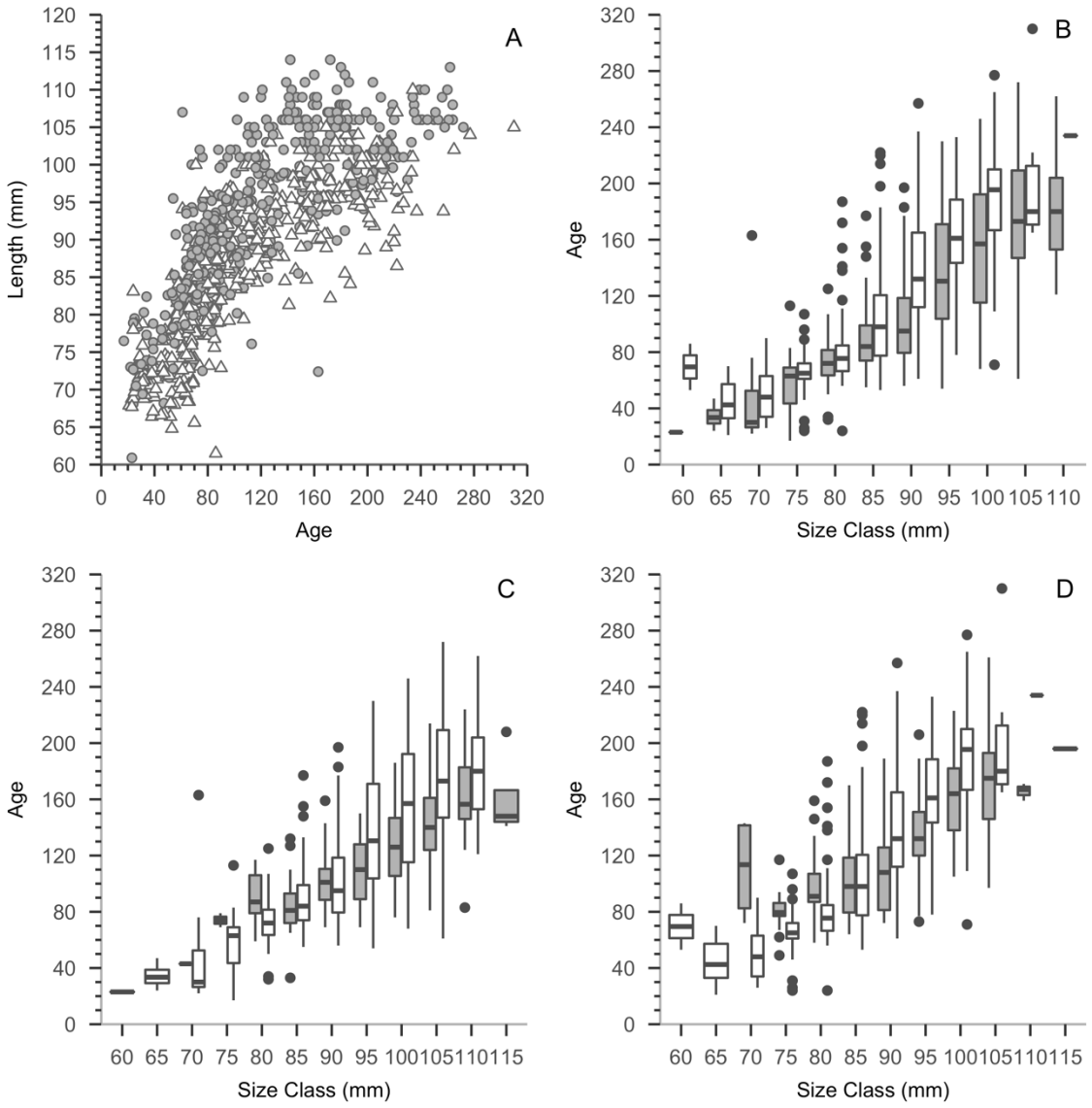

Figure 4.5 Regional age-length data. Long Island aged data and comparisons with Georges Bank aged data. (A) Age at length data for Long Island female (grey) and male (white); (B) Long Island age compositions by 5-mm size classes between females (grey) and males (white); (C) female age compositions between Long Island (white) and Georges Bank (grey); (D) male age compositions between Long Island (white) and Georges Bank (grey). For boxplots, box represents the interquartile range (IQR) with 50th percentile bar (median), whiskers represent 15*IQR, and points are outliers.

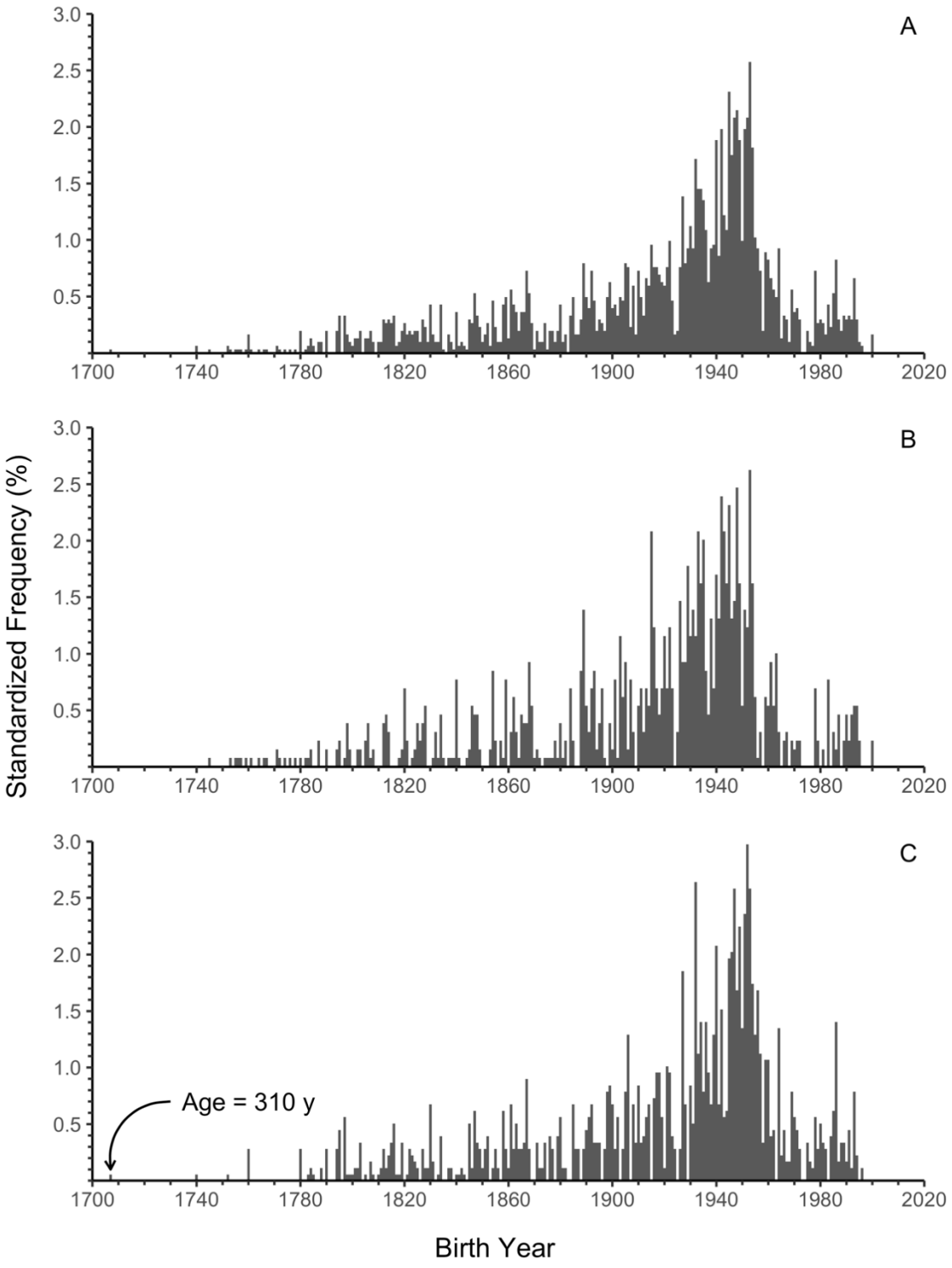

Figure 4.6 Long Island age frequencies by birth year. Age frequencies as a percent of the total frequency for the (A) population, (B) female, and (C) male datasets by birth year. Decrease in age frequency for recent years (~1960-2017) represents animals not fully recruited to the fishery and fishery gear (gear highly selective for animals >80 mm).

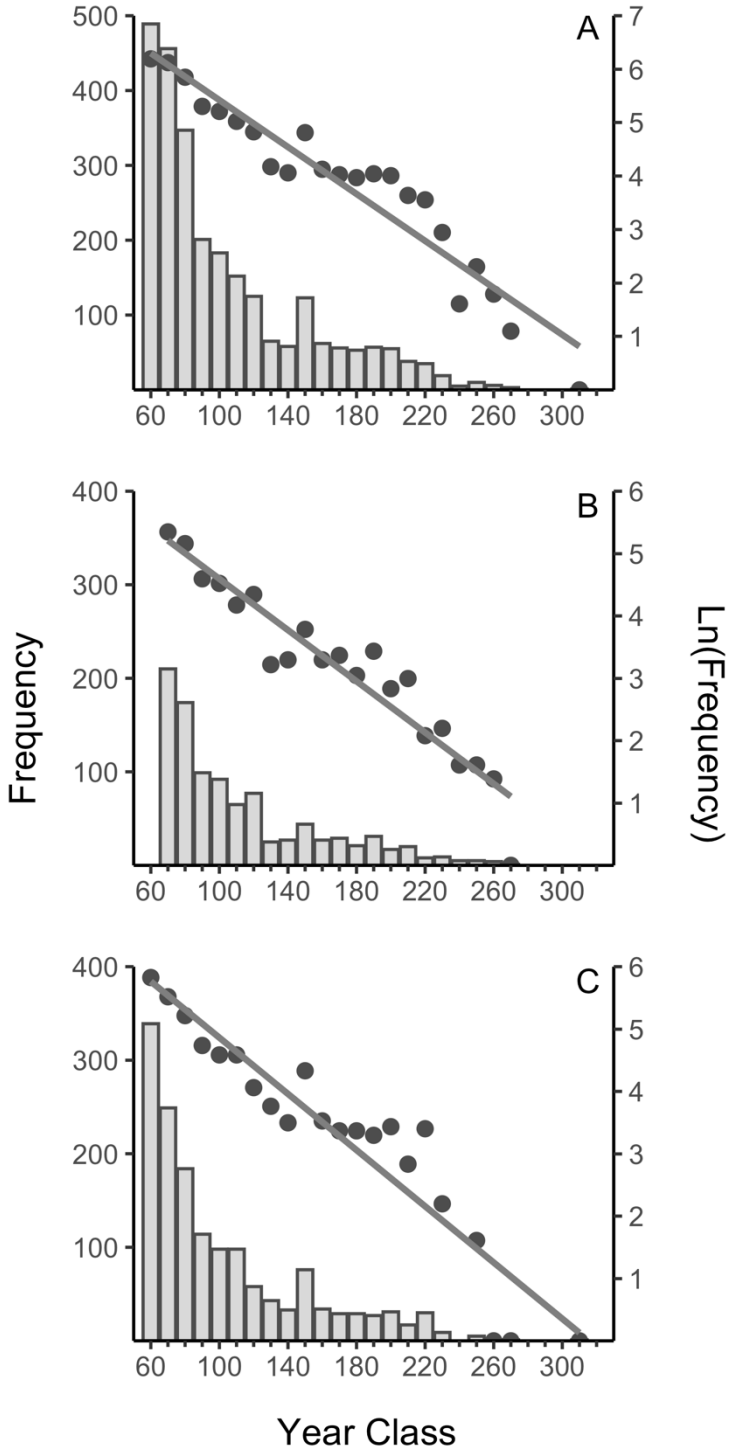

Figure 4.7 Long Island mortality and longevity. Total estimated mortality and longevity for Long Island (A) population, (B) female, and (C) male age-frequency data. Population longevity is 347 y, mortality is 0.02 (R^2 = 0.91); female longevity is 324 y, mortality is 0.02 (R^2 = 0.90); male longevity is 316 y, mortality is 0.02 (R^2 = 0.88).

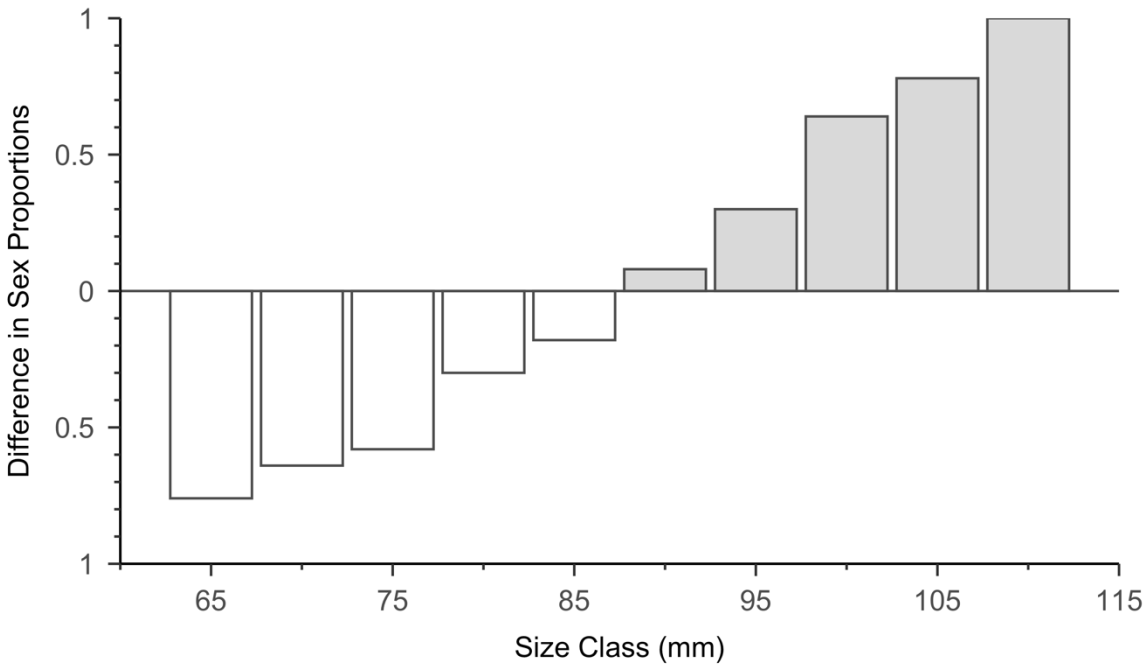

Figure 4.8 Long Island sex ratios by size. Proportions by 5-mm size class of the shucked sample. The x axis (y = 0) indicates a 1:1 sex ratio, white bars indicate a male dominated class, and grey bars indicate a female dominated class. The y axis denotes the proportional difference of the sex ratio, where 0.5 indicates a 1.5 to 1 sex ratio.

4.7 Literature Cited

Alexander MA, Halimeda Kilbourne K, Nye JA (2014) Climate variability during warm and cold phases of the Atlantic Multidecadal Oscillation (AMO) 1871–2008. J of Mar Syst 133:14-26

Ballesta-Artero I, Augustine S, Witbaard R, Carroll ML, Mette MJ, Wanamaker Alan D, van der Meer J (2019) Energetics of the extremely long-living bivalve *Arctica islandica* based on a Dynamic Energy Budget model. J Sea Res 143:173-182

Bigelow HB (1933) Studies of the waters on the continental shelf, Cape Cod to Chesapeake Bay. Pap Phys Oceanogr Meteorol 2:94 p

Brown W, Boicourt W, Flagg C, Gangopadhyay A, Schofield O, Glenn S, Kohut J (2012) Mapping the Mid-Atlantic Cold Pool evolution and variability with ocean gliders and numerical models. In: 2012 Oceans. IEEE:1–6 p

Chen Z, Curchitser EN. 2020. Interannual variability of the mid-atlantic bight cold pool. J Geophys Res Oceans 125

Chen Z, Curchitser E, Chant R, Kang D (2018) Seasonal Variability of the Cold Pool Over the Mid-Atlantic Bight Continental Shelf. J Geophys Res, C, Oceans 123:8203–8226

Conover WJ (1980) Practical nonparametric statistics. New York: John Wiley & Sons. 493 pp

Engmann S, Cousineau D (2011) Comparing distributions: the two-sample Anderson-Darling test as an alternative to the Kolmogorov-Smirnoff [sic] test. J Appl Quant Methods 6:1-17

Fritz LW (1991) Seasonal condition change, morphometrics, growth and sex ratio of the ocean quahog, *Arctica islandica* (Linnaeus, 1767) off New Jersey, U.S.A. J Shellfish Res 10:79-88

Harding JM, King SE, Powell EN and Mann R (2008) Decadal trends in age structure and recruitment patterns of ocean quahogs *Arctica islandica* from the Mid-Atlantic Bight in relation to water temperatures. J Shellfish Res 27:667-690

Hemeon KH, Powell EN, Robillard E, Pace SM, Redmond TE, Mann RL (2021) Attainability of accurate age frequencies for ocean quahogs (*Arctica islandica*) using large datasets: protocol, reader precision, and error assessment. J Shellfish Res 40:255-267

Hemeon KM, Powell EN, Pace SM, Redmond TE, Mann R (Accepted) Population dynamics of *Arctica islandica* at Georges Bank (US): an analysis of sex-based demographics. J Mar Biol Assoc UK

Jones DS (1981) Reproductive cycles of the Atlantic surf clam *Spisula solidissima*, and the ocean quahog *Arctica islandica* off New Jersey. J Shellfish Res 1:23-32

Mann R (1982) The seasonal cycle of gonadal development in *Arctica islandica* from the southern New England shelf. Fish B-NOAA 80:315-326

Mann ME, Zhang Z, Rutherford S, Bradley RS, Hughes MK, Shindell D, Ammann C, Faluvegi G, Ni F (2009) Global signatures and dynamical origins of the Little Ice Age and Medieval Climate Anomaly. Science 326:1256-1260

NEFSC. 2020. Stock assessment of the ocean quahog for 2020. Woods Hole, MA: Northeast Fisheries Science Center. NEFSC Ref. Doc.20-XXXX. 210 pp

NOAA (2021) Annual Commercial Landing Statistics. www.fisheries.noaa.gov/national/sustainable-fisheries/commercial-fisheries-landings (accessed 18 Feb 2022)

Nye JA, Baker MR, Bell R, Kenny A, Kilbourne KH, Friedland KD, Martino E, Stachura MM, Van Houtan KS, Wood R (2014) Ecosystem effects of the Atlantic Multidecadal Oscillation. J Marine Syst 133:103-116

Oeschger R, Storey KB (1993) Impact of anoxia and hydrogen sulphide on the metabolism of *Arctica islandica* L. (Bivalvia). J Exp Mar Biol Ecol 170:213-226

Pace SM, Powell EN, Mann R (2018) Two-hundred year record of increasing growth rates for ocean quahogs (*Arctica islandica*) from the northwestern Atlantic Ocean. J Exp Mar Biol Ecol 503:8-22

Pace SM, Powell EN, Mann R, Long MC (2017a) Comparison of age-frequency distributions for ocean quahogs *Arctica islandica* on the western Atlantic US continental shelf. Mar Ecol Prog Ser 585:81-98

Pace SM, Powell EN, Mann R, Long MC, Klinck JM (2017b) Development of an age—frequency distribution for ocean quahogs (*Arctica islandica*) on Georges Bank. J Shellfish Res 36:41-53

Pace SM, Powell EN, Mann R (2018) Two-hundred year record of increasing growth rates for ocean quahogs (*Arctica islandica*) from the northwestern Atlantic Ocean. J Exp Mar Biol Ecol 503:8-22

Pettitt AN (1976) A two-sample Anderson-Darling rank statistic. Biometrika 63:161-168

Press WH, Flannery BP, Teukolsky SA, Vetterling WT (1989) Numerical recipes. Cambridge: Cambridge University Press. 702 pp

Poitevin P, Thébault J, Siebert V, Donnet S, Archambault P, Doré J, Chauvaud L, Lazure P (2019) Growth response of *Arctica islandica* to north Atlantic oceanographic conditions since 1850. Front Mar Sci 6:483

Ragnarsson S, Thorarinsdóttir GG (2020) Burrowing behaviour in ocean quahog (*Arctica islandica*) in situ and in the laboratory. Marine and Freshwater Research Institute: ISSN 2298-9137

Ricker WE (1975) Computation and interpretation of biological statistics of fish populations. Bulletin of the Fisheries Research Board of Canada, Ottawa:382 p

Ridgway ID, Richardson CA, Scourse JD, Butler PG, Reynolds DJ (2012) The population structure and biology of the ocean quahog, *Arctica islandica*, in Belfast Lough, Northern Ireland. J Mar Biol Assoc UK 92:539-546

Ropes JW, Murawski SA, Serchuk FM (1984) Size, age, sexual maturity and sex ratio in ocean quahogs, *Arctica islandica* Linné, off Long Island, New York. Fish B-NOAA 82:253-267

Rowell TW, Chaisson DR, McLane JT (1990) Size and age of sexual maturity and annual gametogenic cycle in the ocean quahog, *Arctica islandica* (Linnaeus, 1767), from coastal waters in Nova Scotia, Canada. J Shellfish Res 99:195-203

Soniat TM, Hofmann EE, Klinck JM, Powell EN (2009) Differential modulation of eastern oyster (*Crassostrea virginica*) disease parasites by the El Niño-Southern Oscillation and the North Atlantic Oscillation. Int J Earth Sci 98:99-114

Soniat TM, Klinck JM, Powell EN, Hofmann EE (2006) Understanding the success and failure of oyster populations: climatic cycles and *Perkinsus marinus*. J Shellfish Res 25:83-93

Strahl J, Brey T, Philipp EER, Thorarinsdóttir G, Fischer N, Wessels W, Abele D. 2011. Physiological responses to self-induced burrowing and metabolic rate depression in the ocean quahog *Arctica islandica*. J Exp Biol 214:4223-4233.

Then AY, Hoenig JM, Hall NG, Hewitt DA (2015) Evaluating the predictive performance of empirical estimators of natural mortality rate using information on over 200 fish species. J Mar Sci 72:82–92

Thorarinsdóttir G, Steingrímsson S (2000) Size and age at sexual maturity and sex ratio in the ocean quahog, *Arctica islandica* (Linnaeus, 1767), off Northwest Iceland. J Shellfish Res 19:943–947

Visbeck MH, Hurrell JW, Polvani L, Cullen HM (2001) The North Atlantic Oscillation: past, present, and future. Proc Natl Acad Sci USA 98:12876-12877

Xu H, Kim H-M, Nye JA, Hameed S (2015) Impacts of the North Atlantic Oscillation on sea surface temperature on the Northeast US Continental Shelf. Cont Shelf Res 105:60-66

CHAPTER V *ARCTICA ISLANDICA* REGIONAL GROWTH RATE AND SYNCHRONICITY ANALYSES BETWEEN TWO POPULATIONS IN THE WESTERN MID-ATLANTIC (US)

5.1 Introduction

5.1.1 Background

Fishery growth models are essential functions integrated into assessment models for the estimation of ages from subsampled length frequencies of a stock. Similar to age-length keys, growth models provide an expected relationship of length over time dependent on age and are essential in stock management to construct age-frequency distributions (e.g., catch curves). Age-frequency distributions allow the estimation of important life-history characteristics necessary to describe a stock such as recruitment indices, mortality rates, and growth rates.

The choice of a best-fit growth model to real data does not always translate to model selection in assessment models (Flinn & Midway 2021). The von Bertalanffy growth function (VB) is the most common growth model used in US fisheries management, and despite better fit growth models to select species, the benefit of replacing the VB in an assessment model with an alternative growth relationship must be weighed against new uncertainty incorporated into the assessment model and new uncertainty associated with estimated parameters derived from the alternative growth function (Flinn & Midway 2021, Neves et al. 2022). The VB is an easily described model, in that model parameters have clear biological meaning in terms of age and growth (von Bertalanffy 1938). Other models such as the Tanaka growth model (i.e., power growth functions) are models well-fit to animals with indeterminate growth and

have gained favor to describe marine invertebrate age-growth relationships (e.g., McShane & Anderson 1997, Velázquez-Abunader et al. 2016, Pace et al. 2017b). However, power models with attenuated growth produce ambiguous model parameters with limited biological definitions (Tanaka 1982, Sebens 1987, Tanaka 1988), a stark contrast to the k (growth rate) and L_{inf} (maximum body size) parameters derived from the VB (von Bertalanffy 1938). Despite cautionary measures required to update assessment models with new and complex growth functions, the reward includes more accurate and precise estimates of age, maximum size, growth rates, mortality, and age frequencies.

Growth is predominantly controlled by ontogeny, genetics, and the environment (Sebens 1987). Growth data associated with a time-series can be detrended to remove ontogenetic growth effects and isolate environmentally driven growth over time to create growth indices (Grissino-Mayer 2001, Black et al. 2008, Peharda et al. 2018). Correlation of temporally associated growth indices to known environmental indices can uncover time periods and ecological conditions that were beneficial, neutral, or detrimental to growth. Identification of strong ecological controls on growth can improve growth projections for future climate scenarios. Wavelet analysis is a mathematical tool that can isolate periods of similar frequencies between two time series indexed to a zero-mean, even when the frequency is variable through time (Torrence & Compo 1998). When growth indices are considered, wavelets can identify common frequency power and frequency coherence between a temporal growth index and oceanographic indices derived from data such as temperature, salinity, and chlorophyll abundance (Machu et al. 1999, Kirby 2005, Soniat et al. 2006).

5.1.2 Objectives

Arctica islandica is an extremely long-lived boreal bivalve that can live in excess of 300 y in US waters and supports an important commercial fishery in the US Mid-Atlantic (NEFSC 2017, 2020). The US *A. islandica* fishery is managed by length-based assessment models that contain no age data and apply a VB growth function (NEFSC 2017, 2020). Until recently, reliable age-length keys (ALK) were not available for this species due to extreme variability in age at size data (Pace et al. 2017a, 2017b) and ages could not be dependably estimated for the stock.

The objectives of this study are to evaluate best-fit growth models for two mid-Atlantic *A. islandica* populations, use these models to detrend yearly growth data to create growth indices, and evaluate growth indices between site and sex using wavelet analysis. The analyses illuminate the scale to which growth rates change over time, between populations, and between sexes; trends that may be important to inform assessment models.

5.2 Materials and Methods

5.2.1 Growth Data

Arctica islandica clams were collected from Georges Bank (GB) (40.72767°N, 67.79850°W) and the Long Island (LI) (40.09658°N 73.01057°W) continental shelf in 2017 with a Dameron-Kubiak dredge outfitted to collect fishery-sized *A. islandica* (Figure 5.1). Clam meat was removed from each sample and used for sex-determination by gonadal smear slide. Shells were measured for length, immersed in a bleach solution, and stored dry for later aging.

Prior to aging, each site underwent an independent age-reader error analysis that compared visual ages by two expert age readers of a random 20% subsample from each site. This analysis increased precision between readers (<7.6% average or median coefficient of variation [CV]) and ensured that no aging bias occurred (see Evans-Hoenig test of symmetry in Hemeon et al. 2021). Once error was minimized, the primary age reader aged samples from both sites using methods by Pace et al. (2017a) and Hemeon et al. (2021) using ImageJ annotation software to estimate age from the shell hinge plate. Annual growth increments were measured in pixels by the ObjectJ plugin for ImageJ and data were exported in annual hinge plate growth increments in pixels. Annuli observed on the shell hinge plate are proportional to the outer shell valve (Thompson et al. 1980a); therefore, annual growth increments on the hinge plate were extrapolated to annual growth increments of the total shell length. First, growth in pixels on the hinge plate per year were converted to proportions of total hinge plate growth to eliminate pixel units. Next, proportions of growth per year on the hinge plate were multiplied by the total length of the shell to obtain annual shell growth increments in mm.

5.2.2 Growth Models: Group

Growth increments for each sample were cumulatively summed to produce a shell length at age array, by individual sample, for each site. For each site, von Bertalanffy (VB), Tanaka, and modified Tanaka (MT) growth models were fit to the population, female, and male group growth data. The VB model was chosen as it is the standard growth function currently applied in the federal *A. islandica* fishery assessment model (von Bertalanffy 1938, NEFSC 2017, NEFSC 2020) (Eq 1), and the Tanaka model was also selected as it successfully fits species with indeterminate, attenuated growth at old

age (Tanaka 1982, Sebens 1987, Tanaka 1988, McShane & Anderson 1997, Pace et al. 2017b) (Eq 2). The third model, the MT, contained a fifth parameter "*g*" added to the traditional Tanaka model that forced a better model fit at older age classes (Powell & Klinck pers comm) (Eq 3).

Eq (1) $$L_t = L_\infty\left(1 - e^{-k(t-t_0)}\right),$$

Eq (2) $$L_t = d + \frac{1}{\sqrt{f}}\, log\left(2f(t-c) + 2\sqrt{f^2(t-c)^2 + fa}\right),$$

Eq (3) $$L_t = d + \frac{1}{\sqrt{f}}\, log\left(2f(t-c) + 2\sqrt{f^2(t-c)^2 + fa}\right) + gt^{2.5}.$$

Where L_t is length in mm at time t. All Tanaka and Modified Tanaka model parameters except for *d*, were forced to be greater than or equal to 0 during model convergence to prevent the estimation of negative square roots. A growth model was chosen by the Akaike information criterion (AIC).

5.2.3 Growth Models: Cohort

As a benthic invertebrate with limited horizontal mobility, *A. islandica* adaptively grow in relative synchrony with the local environment (e.g., temperature, food availability) (Schöne et al. 2005, Harding et al. 2008, Marali & Schöne 2015, Ballesta-Artero et al. 2018). The *A. islandica* fishery comprises animals born centuries apart (Hemeon et al. accepted, Chapter 4), and thus growth curves are expected to vary between animals depending on the environment into which they were born and in which they predominantly lived. To understand these temporal changes in growth, samples from each site were divided into birth-year cohorts and the chosen growth model from the previous section (5.2.1) was fit to each cohort.

5.2.4 Growth Rates

Growth rates were evaluated by the time needed to reach important fishery or biological milestones (i.e., age to milestone size). For this species, it was important to understand how fast animals recruit into the fishery, how fast animals reach a size at 50% maturity representative of recruits in recent decades, and how many years *A. islandica* are reproductive before entering the fishery using the aforementioned size at 50% maturity. The size milestone selected for time to the fishery was set at 80 mm as this is the size that commercial fishery dredge selectivity stabilizes, and the minimum size at which fishery dredges are highly selective (see Figure 5.12, and NEFSC 2017, Table 15).

The size milestone at which 50% of the population was mature was derived from maturity data obtained from animals that recruited over the last few decades collected in 2017 from GB and LI (Mann unpublished). This sample included 103 immature, and 227 mature *A. islandica* between 16-91 mm. A binomial logistic regression identified the mean size at 50% population maturity as 52-mm with a 95% confidence interval of 50.4-53.0 (Mann unpublished) (Figure 5.13). These results are comparable to those by Thompson et al. (1980b) and Thorarinsdóttir & Steingrímsson (2000), who observed maximum immature sizes of 47 mm and 60 mm (respectively) and a mature minimum size between 36-44 mm (Thorarinsdóttir & Steingrímsson 2000). The degree to which the 52-mm milestone is representative for recruits over the last several centuries is unknown, but 52 mm is consistent with the estimate of average maturity size for bivalves of 44% of maximum size (Powell and Stanton, 1985), as the estimated maximum size of 118 mm from this relationship is consistent with the maximum sizes observed at GB and LI. Thus, an assumption of maturity at this size being a stable property of ontogeny in *A. islandica*

is consistent with the known ontogenetics of bivalves. Years of reproduction before recruitment to the fishery were approximated as the number of years needed for each animal to grow from size at 50% maturity (52 mm) to size to fishery recruitment (80 mm).

Each individual sample from GB and LI was plotted by birth year and the time to each of the three milestones, and regression analyses were fit to these data by site and sex. In addition, population MT models for birth-year cohorts were also used to estimate time to milestone size, and subsequent growth rates were also recorded. Time to size and growth rates derived from the regression and Tanaka models were compared.

5.2.5 Growth Periodicity

Growth synchrony and periodicity were evaluated by Morlet wavelet analyses with Bartlett window transformations (Torrence & Compo 1998, Kirby 2005, Soniat et al. 2006) processed from the R package WaveletComp (Roesch & Schmidbauer 2018). Prior to wavelet analysis, growth data were detrended and standardized. Ontogenetic growth was removed from each individual sample by subtracting cohort-specific growth curves from each sample that resulted in a residual for each individual sample for each calendar year of life (see 5.2.3). Mean and unit variance were calculated for each calendar year to standardize growth over time for each site as a total population, and each sex within each site.

Cross wavelet analyses compared paired data series for significant power relationships at alpha = 0.10. A 10% significance level was chosen, as multiple phases of data reduction likely resulted in accumulated error. Within-region analyses compared GB and LI population growth data, and a parallel analysis applied a 15-y loess smoother to

test smoothing on frequency resolution. Within-sex analyses compared GB females with LI females, and GB males with LI males. Finally, within-site analyses compared GB males to females, and LI males to females. A lead/lag evaluation of period phase shifts identified which data series led the other over time within a known, significant-power period.

5.3 Results

5.3.1 Growth Models: Group

The Modified Tanaka (MT) model was the best fit model to all groups (population, female, male) at both LI and GB (Tables 5.1-5.2, Figures 5.1-5.2) using AIC model selection criteria. Von Bertalanffy (VB) models consistently overfit early ages near the origin, and drastically underfit mid to late ages when the true growth curve began to arch, as it forced an asymptote when one did not exist. The Tanaka and MT models fit similarly until approximately 160 y, after which the two models begin to diverge and the Tanaka model underestimated size at old age. Attenuated, or indeterminate, growth at mid to old age (greater than approximately 160 y) was best captured by the MT.

Tanaka (1988) described the Tanaka model parameters as such: "*a*" influences maximum growth rate, and a larger *a* lessens the maximum growth rate; "*c*" represents age at maximum growth rate; "*f*" is the rate of change in growth rate; and "*d*" is a scaler of body size. When GB and LI were compared by group, GB had a larger maximum growth rate than LI, i.e., smaller *a* (Table 5.3). Age at maximum growth rate, *c*, was younger at GB than LI. A scale of body size, *d*, was larger at GB than LI across all groups. The *f* parameter is a more cryptic model coefficient, and a clear ecological

comparison between sites cannot be made at this time. The MT model had an additional term "*g"* that increased length at larger *t*, i.e., at older ages, and resulted in larger length estimates at older ages.

5.3.2 Growth Models: Cohort

Modified Tanaka models were fit to 20-y birth-year cohorts for LI and GB by group using a Levenberg-Marquardt algorithm (Tables 5.4-5.5, Figures 5.3-5.8). Tanaka and VB models were also fit to each cohort to present model comparisons that included time-varying k and t_0 values for future comparisons with existing VB growth models in *A. islandica* assessment models (Tables 5.6-5.9), but it is highly advised that L_{inf} parameters not be used in analyses due to obvious inaccuracies (Figures 5.1-5.2).

When evaluated by 20-y cohorts, the cohort model fits are similar to those of the group model fits, as the VB model overfit young ages and underfit mid to old ages, and the Tanaka and MT were similar until the end of the data series where the Tanaka model tended to underfit and the MT to overfit at extrapolated ages where no length data existed (Figures 5.3-5.8). Quite obviously, length at age by cohort using any of the models presented here cannot be extrapolated beyond the observed lengths and ages (e.g., projections of length data at ages older than 117 y for the 1900 cohort).

Figures 5.9-5.11 displayed temporal trends of MT growth parameters over time. After plots were divided into median delineated quadrats (Rothschild & Mullen 1985), parameter value distribution probabilities were evaluated using chi-square goodness of fit with expected probabilities for each of the four quadrats set to 0.25. Only the *c* parameter for population and female growth models at GB and LI, and the LI population *d* parameter were significantly different than a 0.25 probability occurrence over time (Table

5.10). The age at maximum growth rate at GB and LI (population and female) has changed over time, as did the body size scaler at LI which is an indication that body size has likely increased for males at LI since approximately 1880 (Figure 5.11B). The dashed horizontal lines in Figures 5.9-5.11 represented the MT model parameters of the group growth models (i.e., not separated by 20-y cohorts, see Table 5.3) and revealed that the group model parameters rarely reflected modern cohorts, and that model parameters fluctuated over time in less than predictable trends.

5.3.3 Growth Rates

Growth rates can be conveyed as the time it takes an *A. islandica* clam to reach a milestone size, in other words, the age at a size of interest. The age (i.e., number of years elapsed) when the animal reached fishable size as estimated by the size that is approximately 100% selected by the gear (80 mm, NEFSC 2017), the age of an animal when the population was at the modern (born post 1987) length for 50% maturity (52 mm, Mann et al. unpublished), and the years of reproduction were approximated as the time from maturation to recruitment to the fishery (52 mm-80 mm) are important metrics for the fishery.

When GB and LI were evaluated by group regardless of birth year, GB reached size at 50% maturity (median = 13 y, range = 7-55 y) slightly faster ($p = 2.27E-16$) than LI (median = 16 y, range = 6-70 y), GB recruited to the fishery (median = 53 y, range = 16-127 y) faster ($p < 2.2E-16$) than LI (median = 66 y, range = 17-178 y), and as a result of faster fishery recruitment, GB had fewer reproductive years (median = 45 y, range = 14-99 y) than LI (median = 56 y, range = 17-129 y) ($p < 2.2E-16$) (Figure 5.14). At GB, time needed to reach each size milestone was less for female *A. islandica* than males

(maturity: p = 5.77E-03; fishery: p < 2.2E-16; years of reproduction: p < 2.2E-16). Likewise, LI females also reached the fishery at a younger age (p = 4.47E-12) and had fewer years of reproduction (p = 4.62E-11) than males, but LI males and females matured at similar ages.

Regression models were fit to the age at milestone size, by birth year, and were expressed for GB (Eq 1-9) (Figures 5.15-5.17, Figure 5.21A-C) and LI (Eq 10-18) (Figures 5.18-5.21A-C) as follows:

Eq (1) $GB\ Fishery_P = 279 - 0.12B,$

Eq (2) $GB\ Fishery_F = 258 - 0.11B\ ,$

Eq (3) $GB\ Fishery_M = 302 - 0.13B,$

Eq (4) $GB\ 50\%\ Maturity_P = (1.28 \cdot 10^4)(9.96 \cdot 10^{-1})^B,$

Eq (5) $GB\ 50\%\ Maturity_F = (2.39 \cdot 10^4)(9.96 \cdot 10^{-1})^B,$

Eq (6) $GB\ 50\%\ Maturity_M = (1.05 \cdot 10^4)(9.97 \cdot 10^{-1})^B,$

Eq (7) $GB\ Reproductive\ Time_P = (2.29 \cdot 10^2)(9.99 \cdot 10^{-1})^B,$

Eq (8) $GB\ Reproductive\ Time_F = (3.70 \cdot 10^2)(9.99 \cdot 10^{-1})^B,$

Eq (9) $GB\ Reproductive\ Time_M = (2.05 \cdot 10^2)(9.99 \cdot 10^{-1})^B,$

Eq (10) $LI\ Fishery_P = 834 - 0.40B,$

Eq (11) $LI\ Fishery_F = 730 - 0.35B\ ,$

Eq (12) $LI\ Fishery_M = 939 - 0.46B,$

Eq (13) $LI\ 50\%\ Maturity_P = (4.32 \cdot 10^5)(9.95 \cdot 10^{-1})^B,$

Eq (14) $LI\ 50\%\ Maturity_F = (1.10 \cdot 10^6)(9.94 \cdot 10^{-1})^B,$

Eq (15) $LI\ 50\%\ Maturity_M = (2.57 \cdot 10^5)(9.95 \cdot 10^{-1})^B,$

Eq (16) $LI\ Reproductive\ Time_P = (2.31 \cdot 10^5)(9.96 \cdot 10^{-1})^B,$

Eq (17) $$LI\ Reproductive\ Time_F = (1.02 \cdot 10^5)(9.96 \cdot 10^{-1})^B,$$

Eq (18) $$LI\ Reproductive\ Time_M = (3.71 \cdot 10^5)(9.95 \cdot 10^{-1})^B,$$

where B was the birth year; F, female; M, male; and P, population. Regressions for GB were significant for maturity and fishery milestones for all groups (time to maturity: population $p < 2.0E\text{-}16$, female $p = 2.58E\text{-}09$, male $p = 3.88E\text{-}11$; fishery: population $p = 1.11E\text{-}08$, female $p = 1.62E\text{-}05$, male $p = 5.53E\text{-}06$), but birth year accounted for less than 20% of the variation in growth rates (time to maturity: population adjusted $R^2 = 0.19$, female adjusted $R^2 = 0.19$, male adjusted $R^2 = 0.20$; fishery: population adjusted $R^2 = 0.06$, female adjusted $R^2 = 0.06$, male adjusted $R^2 = 0.07$). Birth year explained more variation in small animal growth rates (up to 52 mm) than large animal growth rates (up to 80 mm) at GB; however, regression of reproductive years by birth year was not significant ($p > 0.05$). Regression models for LI were significant for all milestones and all groups ($p < 2.0E\text{-}16$), and birth year accounted for greater than 43% of the growth rate variance (time to maturity: population adjusted $R^2 = 0.48$, female adjusted $R^2 = 0.56$, male adjusted $R^2 = 0.43$; fishery: population adjusted $R^2 = 0.63$, female adjusted $R^2 = 0.61$, male adjusted $R^2 = 0.70$; reproductive years: population adjusted $R^2 = 0.52$, female adjusted $R^2 = 0.48$, male adjusted $R^2 = 0.63$). At LI, growth rate was strongly related to birth year at larger size such as when animals recruited to the fishery, and the weakest relationship between birth year and growth rate occurred prior to assumed maturation (assumed since it is not known if maturity consistently occurred at 52 mm in previous centuries). Factors that may covary with calendar year that also affect growth, such as bottom water temperatures, appear to have a stronger effect on LI *A. islandica* growth rates than those at GB, particularly for larger animals with sizes greater than 52 mm.

To compare sites, population regression models listed above were plotted for each milestone (Figure 5.21A-C) by growth rate (mm y^{-1}) to compare changes over time by birth year between sites. Birth year was a poor predicter of growth rate at GB (adjusted $R^2 < 21\%$), while birth year was a strong predictor of growth rate for LI *A. islandica*. Growth rates not only increased with increasing birth year at LI, but growth rates have been accelerating over time. When age at length data were grouped by site and sex, GB clearly had faster growth rates than LI (Figure 5.14), but when birth year and cohorts are considered, recent LI cohorts have matched growth rates at GB and have even exceeded GB growth rates since the 1950s (Figure 5.21A-C). To validate that the MT growth curves captured changing growth rates over time by birth year, the 20-y birth-year cohort MT models were used to estimate growth rates at these identical milestones (Figure 5.21D-F). The MT models are not only within the same scale as the true age-length data, but also captured the accelerating growth rate trend at LI (see Figure 5.21A-C) and the exceedance of LI growth rates in the 1980 cohorts.

Modified Tanaka growth rate estimates using population 20-y cohort models were also compared to the population regression models for all three milestones to better compare these two model interpretations of growth rate using specific birth years as examples (Table 5.11). Across the data time series (1740-1980), regression models estimated that the time to maturity at GB and LI increased by 140% and 233%, respectively. The MT models were more conservative and estimated an increased time to maturity at GB and LI as 100% and 167%, respectively. In fact, the MT estimates were often more conservative at estimating increased growth rates over time except for the time of reproduction at LI, yet the regression and MT models had very similar results of

percent change for time of reproduction compared to time to maturity and time to the fishery. Overall, however, the regression and MT models appeared to both be adequate representations of changing growth rates over time; this further supports the use of MT models to describe *A. islandica* growth.

5.3.4 Growth Periodicity

With confidence in the MT cohort growth models, cohort growth curves were used to detrend biological growth from each corresponding individual sample by birth year. Mean residuals per calendar year were calculated and a unit variance retained as a growth index for each group for cross-wavelet analyses. Growth indices were compared within region to identify common growth signatures between two populations in separate geospatial areas of a stock. Within-sex analyses (i.e., GB female to LI female, GB male to LI male) were used to identify if the sexes were growing in synchrony despite geospatial differences. Finally, within-site analyses identified if female and male *A. islandica* were growing similarly within populations in response to common environmental conditions.

Within-region cross wavelets of GB and LI population growth indices (Figure 5.22) revealed significant power period of 31 y (Figure 5.23A). Within-sex cross-wavelet analyses demonstrated that female growth indices between sites (Figure 5.24) had significant power frequencies at approximately 24- and 42-y periods (Figure 5.25), while male growth indices (Figure 5.26) have significant frequency powers at approximately 23- and 39-y periods (Figure 5.235B). The similar power frequency periods between sexes, indicated that the two sexes are growing in tandem to similar growth cycles.Within-site cross wavelets compared male and female growth indices at GB and

male and female growth indices at LI. Both sites presented power frequencies at approximately 22-y periods, but LI had an additional power frequency at a 39-y period while GB had additional power frequencies at 12-, 32-, and 62-y periods (Figure 5.28).

Significant high-power periods were analyzed for phase shifts by the same set of paired data series discussed previously. A phase shift represented a lead or lag of one time series (i.e., growth index) in relation to the other for a specific frequency period. When GB and LI were evaluated, GB lagged LI for the 31-y period frequency until the early 1940s, but once the lag was too large the relationship overturned, and GB led LI until the end of the time series when the animals were collected in 2017 (Figure 5.28A). Between 1760-1840, and again between 1970-2017, GB and LI were in phase meaning the two sites were growing in relative synchrony (phase shift less than $\frac{\pi}{2}$). Within-sex comparisons of GB and LI females indicated that GB females led the LI females during the 42-y period between 1800-1980s, when GB then lagged LI (Figure 5.28B). The 24-y period frequencies were led by LI for nearly the entire time period except for a brief time between 1970-1990, but the two sites were often out of phase indicating that the growth responses were nearly opposite during the 24-y period frequencies. The within-sex male 23-y period was erratic in regard to one site leading or lagging the other, whereas the 39-y periods was often led by LI until the 1960s (Figure 5.28C). Interestingly, the common 40-y period between males and females were led by opposite sites between sexes, but the periods were often in phase after the 1900s. Within site comparisons of males and females at GB showed that males led females in phase for 62-y periods, while females generally led males in the 32-y periods from 1820-1970 (Figure 5.28D). Georges Banks also had 12- and 22-y periods in common between males and females, but the lead lag

relationship is unclear. Conversely, LI only had two common periods within site between males and females at 22- and 39-y periods, and males predominantly led both periods (Figure 5.28E).

5.4 Discussion

5.4.1 Fishery Growth Rates

Studies by Ropes et al. (1984), Thorarinsdóttir & Steingrímsson (2000), Fritz (1991), and Hemeon et al. (accepted) have posited that *A. islandica* are sexually dimorphic. Clearly, from this study, growth rates differ between sexes and between populations in the Mid-Atlantic Bight. Females grow faster than males as indicated by growth years to life-history and fishery milestones sizes, and also by the Modified Tanaka (MT) *a*, and von Bertalanffy (VB) *k* estimated parameters. Faster growing female *A. islandica* support findings by Hemeon et al. (accepted) and Chapter 4 of this document. Despite the rapid march of female *A. islandica* into the fishery compared to males, the fishery demographics of LI are highly male biased (Chapter 4.3.7). At LI, males dominated small size classes up to 85 mm within a length frequency collected by fishery equipment (60 mm – 120 mm) but the length-frequency sex-ratio was 1:1.4 (F:M). As females grow to larger sizes faster than males, a fishery that targeted large animals would be expected to be composed predominantly of females, leading to size and age truncation. No evidence exists for this outcome, possibly due to the low fishing mortality rate under current management restrictions (NEFSC 2020). For example, LI does not have a higher female total mortality rate that might reduce the number of females in a population and create a skewed sex ratio.

One explanation for a limited impact on females is better dredge evasion by large *A. islandica*. If large *A. islandica* are, in fact, deeper or more frequent burrowers than smaller animals, and large *A. islandica* are predominantly female, an under-sampling of large females would result. Positive correlations between shell length and burrowing depth of clams support this hypothesis (e.g., Zaklan & Ydenberg 1997, Ragnarsson & Thorarinsdóttir 2020). This explanation would be plausible if it was also true that *A. islandica* at LI also have higher burrowing rates than GB due to local environmental variability that is not observed at GB since GB does not show a deficit in fishery-sized females.

Additionally, a length truncation is not observed at LI once again suggesting that a fishery bias towards large females is not predominant. One cannot exclude, however, the simpler explanation that a skewed sex ratio originates from the sampling of a patchy population, where a larger tow-area would be required to sample a more complete demographic distribution. This study sampled a coverage area greater than 1.764 km^2 and samples collected in this spatial extent was assumed to be representative of the population. If patchy demographics exist, the scale would be larger than approximately 2 km^2.

The MT growth curve proved to be the best fit model for *A. islandica*, as the VB growth curve drastically overestimated size at young age and rarely approached the origin, and underestimated size at old age and large size. The MT growth models also change with birth year. As birth-year cohorts advanced through time, the model parameters also changed through time. Georges Bank *A. islandica* exhibited faster growth rates than those at LI based on the MT and VB parameters listed previously, as well as

growth rates to milestones sizes when age-length data were aggregated by group. Findings that *A. islandica* grow faster at GB than at LI confirm age at size relationships identified in Chapter 4, but also previous findings by Pace et al. (2018) that GB growth rates were higher than other locations in the Mid-Atlantic Bight. In this study, growth rates of immature animals at LI increased by 167% over 240 y and by 100% at GB using MT models. Growth rates were the fastest for animals up to 52 mm and predictably declined after maturation as energy allotment was diverted to reproduction (Ballesta-Artero et al. 2018). Increased growth rates over time, as observed in the regression and cohort MT models, not only reduced the amount of time needed to reach fishable size, but also the number of reproductive years prior to potential fishery harvest. For instance, GB lost between 19-20% of reproductive years over the time period, while LI lost between 62-66% of reproductive years. Interestingly, however, the regression models predict LI has 2.6 times more reproductive years for animals born in 1980 compared to at GB, but the MT models predict a nearly equal number of reproductive years between sites. Additional reproductive years per animal at LI compared to GB, would indicate that LI may be resilient to a commercial fishery if the time to maturity was low and fecundity constant.

Long Island displayed a clear relationship between birth year and growth rates, whereas GB showed more subtle birth-year dependent change in growth rates. For instance, the time to recruit to the fishery at GB decreased from 70 y to 41 y by regression model predictions, while LI time to recruit to the fishery dropped from 138 y to 42 y by regression model predictions (results comparable to MT estimates). A 70% decrease in years to fishable size at LI compared to only a 41% decrease in time to

fishable size at GB over the temporal extent of this study. This study also provides strong evidence that growth rates have been accelerating at LI and LI growth rates have recently matched those at the more growth-stable GB population, data that support previous findings by Pace et al. (2018).

5.4.2 Growth Indices Over Time

Regional similarities in growth anomalies existed between GB and LI. An anomaly in this case refers to a positive or negative growth index that deviates from the zero-mean. A frequency periods of 31 y has significant power in the GB and LI population time series. Generally, GB lagged behind LI in timing. In the case of the 31-y period, GB lagged behind LI by less than 15 y, but has been in phase since the 1970s. The in-phase 31-y periods are an indication that that growth frequencies were in synchrony on either side of the Great South Channel in recent decades. The Atlantic Multidecadal Oscillation (AMO) is a well-described, low-frequency oceanographic cycle with flexible periods ranging between 20-80 y (Knudsen et al. 2014, Moore et al. 2017) but often centered around a 60-y period (Kilbourne et al. 2014). The frequency of the AMO is variable over time, and could drive the repeating approximately 20-, 30-, 40-y power periods observed at GB and LI that are simply harmonics of the larger AMO cycle. It is also possible, that the North Atlantic Oscillation (NAO) plays a role as it cycles between 7, 13, 20, 26, and 34 y (Seip et al. 2019), but the NAO is extremely noisy and would require direct cross wavelet analyses to distinguish positive (negative) NAO phases with positive (negative) *A. islandica* growth.

5.4.3 Summary

This study found that the Modified Tanaka growth model best fit age and growth data of *A. islandica* at GB and LI and strongly suggests that other growth models will seriously underestimate size at old age and growth rate after maturity. Due to assessment model limitations, and the integration of von Bertalanffy parameters to estimate other stock metrics, VB k, t_0, and L_{inf} parameters were listed by cohort to offer time-varying conditions, but clearly the L_{inf} parameter should not be used to estimate maximum body size, as this parameter vastly underestimates the true length at age. Female growth rates exceed those of males, and GB growth rates eclipse growth rates at LI until recent decades. These results support findings by Hemeon et al. (accepted) and Chapter 4, that area-specific ALKs and growth models should be used when estimating age for different management areas in the US Mid-Atlantic. Also of note is the accelerating growth rate of *A. islandica* at LI and the consequent implications for population resilience. Not only are LI animals recruiting into the fishery faster over time, but this fact also implies that fewer reproductive years are available before a higher probability of being harvested. If fecundity does not decrease with age, important spawning stock biomass may be removed from the population faster than replacement in future climate scenarios. An increasing growth rate over time also implies that a single growth curve is not sufficient to represent the LI population. Finally, growth indices at GB and LI varied significantly on 31-y periods, and GB lags behind LI in response to these periods. Additional wavelet analyses between *A. islandica* growth indices and temperature, salinity, chlorophyll-a derived datasets can inform managers of future growth trends in response to projected climate scenarios.

5.5 Tables

Table 5.1 Georges Bank best fit growth models.

Georges Bank	N	Model	ΔAIC
Population	569	von Bertalanffy	20,039
		Tanaka	189
		Modified Tanaka	**0**
Female	284	von Bertalanffy	11,907
		Tanaka	94
		Modified Tanaka	**0**
Male	285	von Bertalanffy	12,634
		Tanaka	517
		Modified Tanaka	**0**

N, sample size; ΔAIC, change in Akaike information criterion (AIC) from best fit AIC

Table 5.2 Long Island best fit growth models.

Long Island	N	Model	ΔAIC
Population	865	von Bertalanffy	12,689
		Tanaka	350
		Modified Tanaka	**0**
Female	426	von Bertalanffy	11,485
		Tanaka	82
		Modified Tanaka	**0**
Male	439	von Bertalanffy	12,045
		Tanaka	335
		Modified Tanaka	**0**

N, sample size; ΔAIC, change in Akaike information criterion (AIC) from best fit AIC

Table 5.3 Regional model parameters.

Model	Group	Parameter	Georges Bank		Long Island	
			Estimate	SE	Estimate	SE
von Bertalanffy	Population	L_{inf}	9.73E+01	7.78E-02	9.17E+01	6.92E-02
		K	2.80E-02	1.16E-04	2.70E-02	1.07E-04
		t_0	-1.12E+01	9.47E-02	-1.15E+01	9.53E-02
	Female	L_{inf}	1.00E+02	9.71E-02	9.48E+01	9.84E-02
		K	2.93E-02	1.48E-04	2.61E-02	1.40E-04
		t_0	-9.91E+00	1.10E-01	-1.18E+01	1.33E-01
	Male	L_{inf}	9.47E+01	1.11E-01	8.80E+01	9.07E-02
		K	2.63E-02	1.57E-04	2.85E-02	1.58E-04
		t_0	-1.31E+01	1.47E-01	-1.10E+01	1.28E-01
Tanaka	Population	a	2.70E-03	7.50E-04	1.11E-02	7.61E-04
		c	1.31E-01	6.92E-02	1.06E+00	6.35E-02
		d	9.03E+01	1.26E-01	7.98E+01	9.69E-02
		f	2.71E-03	1.69E-05	3.44E-03	2.05E-05
	Female	a	4.60E-03	9.24E-04	9.69E-03	1.14E-03
		c	2.54E-01	8.86E-02	7.99E-01	9.44E-02
		d	9.56E+01	1.71E-01	8.38E+01	1.45E-01
		f	2.46E-03	1.90E-05	3.09E-03	2.55E-05
	Male	a	6.08E-04	1.02E-03	1.32E-02	9.16E-04
		c	0.00E+00	9.01E-02	1.47E+00	7.74E-02
		d	8.51E+01	1.53E-01	7.52E+01	1.17E-01
		f	3.00E-03	2.50E-05	3.98E-03	3.18E-05
Modified Tanaka	Population	a	7.36E-03	7.34E-04	1.57E-02	7.29E-04
		c	7.62E-01	7.62E-02	1.77E+00	6.88E-02
		d	8.78E+01	2.03E-01	7.73E+01	1.53E-01
		f	3.00E-03	2.82E-05	3.90E-03	3.48E-05
		g	6.04E-06	4.29E-07	5.07E-06	2.66E-07
	Female	a	8.73E-03	9.27E-04	1.36E-02	1.14E-03
		c	8.50E-01	1.01E-01	1.34E+00	1.06E-01
		d	9.31E+01	2.91E-01	8.19E+01	2.38E-01
		f	2.70E-03	3.28E-05	3.37E-03	4.21E-05
		g	6.37E-06	6.41E-07	3.47E-06	3.74E-07
	Male	a	9.21E-03	8.52E-04	1.77E-02	8.45E-04
		c	1.18E+00	8.84E-02	2.27E+00	8.15E-02
		d	8.06E+01	2.20E-01	7.24E+01	1.77E-01
		f	3.71E-03	4.48E-05	4.68E-03	5.55E-05
		g	1.14E-05	4.87E-07	6.56E-06	3.51E-07

SE, standard error

Table 5.4 Georges Bank 20-y cohort Modified Tanaka model parameters.

Cohort	Parameter	Population		Female		Male	
		Estimate	SE	Estimate	SE	Estimate	SE
	a	6.55E-03	9.64E-03			6.55E-03	9.64E-03
	c	0.00E+00	8.07E-01			0.00E+00	8.07E-01
1740	d	8.10E+01	1.45E+00			8.10E+01	1.45E+00
	f	2.19E-03	1.34E-04			2.19E-03	1.34E-04
	g	9.14E-06	1.01E-06			9.14E-06	1.01E-06
	a	1.14E-02	6.26E-03			1.14E-02	6.26E-03
	c	0.00E+00	4.09E-01			0.00E+00	4.09E-01
1780	d	8.42E+01	6.49E-01			8.42E+01	6.49E-01
	f	2.61E-03	8.21E-05			2.61E-03	8.21E-05
	g	7.67E-06	6.34E-07			7.67E-06	6.34E-07
	a	5.74E-03	6.39E-03	1.22E-02	5.18E-03	8.31E-03	6.74E-03
	c	0.00E+00	5.14E-01	1.32E+00	5.48E-01	0.00E+00	4.95E-01
1800	d	8.78E+01	1.01E+00	9.19E+01	1.28E+00	8.52E+01	9.11E-01
	f	2.53E-03	1.15E-04	2.69E-03	1.56E-04	2.54E-03	1.06E-04
	g	6.91E-06	1.17E-06	7.37E-06	1.59E-06	6.78E-06	1.04E-06
	a	9.56E-03	4.31E-03	1.52E-02	7.51E-03	6.22E-03	4.69E-03
	c	0.00E+00	3.24E-01	0.00E+00	5.46E-01	0.00E+00	3.71E-01
1820	d	8.95E+01	6.58E-01	9.39E+01	1.10E+00	8.71E+01	7.69E-01
	f	2.41E-03	6.72E-05	2.13E-03	9.03E-05	2.59E-03	8.89E-05
	g	9.31E-06	8.87E-07	8.87E-06	1.36E-06	8.22E-06	1.09E-06
	a	9.48E-03	4.35E-03	1.14E-02	4.27E-03	8.38E-03	6.66E-03
	c	2.64E-01	3.63E-01	2.99E-01	3.67E-01	3.52E-01	5.44E-01
1840	d	9.11E+01	8.51E-01	9.65E+01	8.96E-01	8.48E+01	1.22E+00
	f	2.52E-03	8.96E-05	2.26E-03	7.77E-05	2.91E-03	1.66E-04
	g	9.38E-06	1.50E-06	7.56E-06	1.49E-06	1.23E-05	2.32E-06
	a	1.12E-02	2.63E-03	9.82E-03	2.63E-03	1.27E-02	4.55E-03
	c	9.50E-01	2.62E-01	7.21E-01	2.70E-01	1.22E+00	4.31E-01
1860	d	8.82E+01	7.35E-01	9.35E+01	7.90E-01	8.06E+01	1.12E+00
	f	2.91E-03	9.38E-05	2.56E-03	8.04E-05	3.54E-03	2.05E-04
	g	1.91E-05	1.87E-06	1.77E-05	1.87E-06	1.94E-05	3.20E-06
	a	1.01E-02	1.67E-03	6.29E-03	2.33E-03	1.29E-02	2.02E-03
	c	1.08E+00	1.84E-01	4.11E-01	2.49E-01	1.71E+00	2.27E-01
1880	d	8.69E+01	5.93E-01	9.38E+01	8.15E-01	7.94E+01	7.09E-01
	f	3.11E-03	8.17E-05	2.54E-03	7.93E-05	3.97E-03	1.49E-04
	g	1.79E-05	2.04E-06	1.14E-05	2.46E-06	2.10E-05	2.85E-06
	a	1.13E-02	1.71E-03	1.23E-02	2.16E-03	1.10E-02	1.84E-03
	c	1.41E+00	2.07E-01	1.50E+00	2.76E-01	1.48E+00	2.15E-01
1900	d	8.57E+01	7.81E-01	9.22E+01	1.11E+00	7.82E+01	7.58E-01
	f	3.31E-03	1.14E-04	2.90E-03	1.27E-04	3.99E-03	1.54E-04
	g	7.25E-06	3.84E-06	1.02E-05	5.15E-06	1.12E-05	4.08E-06
	a	1.01E-02	8.86E-04	9.83E-03	1.39E-03	1.01E-02	8.75E-04
	c	1.95E+00	1.33E-01	1.78E+00	2.17E-01	2.02E+00	1.27E-01
1920	d	7.94E+01	6.25E-01	8.73E+01	1.08E+00	7.36E+01	5.66E-01
	f	4.57E-03	1.48E-04	3.68E-03	1.74E-04	5.43E-03	1.81E-04
	g	3.71E-05	5.76E-06	2.33E-05	8.74E-06	3.91E-05	5.78E-06
	a	1.06E-02	9.45E-04	1.05E-02	1.25E-03	1.07E-02	1.23E-03
	c	2.21E+00	1.65E-01	2.11E+00	2.23E-01	2.30E+00	2.11E-01
1940	d	8.31E+01	9.85E-01	8.76E+01	1.39E+00	8.01E+01	1.23E+00
	f	4.27E-03	1.93E-04	3.78E-03	2.20E-04	4.68E-03	2.84E-04
	g	7.39E-05	1.30E-05	6.97E-05	1.76E-05	8.40E-05	1.69E-05

	a	8.76E-03	1.52E-03	3.75E-03	5.45E-03	9.07E-03	2.02E-03
	c	3.27E+00	2.82E-01	9.90E-01	1.20E+00	2.07E+00	4.32E-01
1960	d	7.61E+01	2.79E+00	8.91E+01	1.17E+01	8.71E+01	3.83E+00
	f	6.70E-03	1.01E-03	3.17E-03	1.22E-03	4.08E-03	6.25E-04
	g	0.00E+00	1.15E-04	0.00E+00	3.67E-04	0.00E+00	1.08E-04
	a	1.48E-02	1.09E-03	1.48E-02	1.09E-03		
	c	4.21E+00	2.42E-01	4.21E+00	2.42E-01		
1980	d	1.05E+02	4.64E+00	1.05E+02	4.64E+00		
	f	2.97E-03	3.78E-04	2.97E-03	3.78E-04		
	g	3.77E-04	2.57E-04	3.77E-04	2.57E-04		

SE, standard error

Table 5.5 Long Island 20-y cohort Modified Tanaka model parameters.

Cohort	Parameter	Population		Female		Male	
		Estimate	SE	Estimate	SE	Estimate	SE
	a	2.41E-02	2.15E-02			2.41E-02	2.15E-02
	c	0.00E+00	8.08E-01			0.00E+00	8.08E-01
1700	d	6.23E+01	5.97E-01			6.23E+01	5.97E-01
	f	3.84E-03	1.91E-04			3.84E-03	1.91E-04
	g	1.19E-05	3.98E-07			1.19E-05	3.98E-07
	a	9.91E-03	9.63E-03	5.59E-02	2.71E-02	5.71E-03	1.22E-02
	c	0.00E+00	5.85E-01	0.00E+00	1.02E+00	0.00E+00	5.89E-01
1740	d	7.09E+01	7.68E-01	7.32E+01	9.29E-01	5.92E+01	5.54E-01
	f	2.91E-03	1.26E-04	2.73E-03	1.49E-04	4.54E-03	2.22E-04
	g	1.46E-05	5.97E-07	1.51E-05	6.48E-07	1.88E-05	5.39E-07
	a	4.46E-02	2.83E-02	5.24E-02	3.09E-02	7.90E-02	8.87E-03
	c	0.00E+00	1.22E+00	0.00E+00	1.25E+00	2.51E+00	3.53E-01
1760	d	7.36E+01	1.29E+00	7.36E+01	1.26E+00	5.88E+01	2.93E-01
	f	2.56E-03	1.76E-04	2.61E-03	1.79E-04	4.37E-03	1.11E-04
	g	1.58E-05	9.69E-07	1.82E-05	9.48E-07	1.29E-05	2.96E-07
	a	1.46E-02	8.31E-03	6.29E-02	2.21E-02	2.04E-02	1.80E-02
	c	0.00E+00	4.77E-01	0.00E+00	8.44E-01	0.00E+00	8.68E-01
1780	d	6.98E+01	6.71E-01	7.24E+01	8.53E-01	6.56E+01	1.04E+00
	f	2.84E-03	1.01E-04	2.68E-03	1.26E-04	3.15E-03	1.97E-04
	g	2.02E-05	6.73E-07	2.14E-05	7.51E-07	2.03E-05	1.09E-06
	a	1.33E-02	5.85E-03	5.96E-02	2.73E-02	1.56E-02	7.66E-03
	c	0.00E+00	3.52E-01	0.00E+00	1.14E+00	0.00E+00	4.00E-01
1800	d	7.24E+01	5.46E-01	7.63E+01	1.33E+00	6.88E+01	5.42E-01
	f	2.83E-03	7.92E-05	2.51E-03	1.67E-04	3.23E-03	1.02E-04
	g	2.10E-05	6.53E-07	2.45E-05	1.34E-06	2.22E-05	6.87E-07
	a	2.50E-02	9.59E-03	2.29E-02	1.13E-02	1.32E-02	8.49E-03
	c	0.00E+00	4.73E-01	0.00E+00	6.00E-01	0.00E+00	4.93E-01
1820	d	7.54E+01	6.61E-01	7.89E+01	9.05E-01	7.32E+01	7.81E-01
	f	2.99E-03	1.07E-04	2.79E-03	1.27E-04	3.06E-03	1.27E-04
	g	2.49E-05	9.34E-07	2.50E-05	1.24E-06	2.19E-05	1.15E-06
	a	4.37E-03	4.27E-03	8.51E-03	6.96E-03	1.11E-02	3.70E-03
	c	0.00E+00	3.12E-01	0.00E+00	4.94E-01	1.01E+00	3.04E-01
1840	d	7.77E+01	6.29E-01	8.22E+01	1.00E+00	7.18E+01	6.25E-01
	f	3.21E-03	1.04E-04	2.79E-03	1.30E-04	4.13E-03	1.60E-04
	g	2.60E-05	1.24E-06	2.44E-05	1.80E-06	2.86E-05	1.46E-06
	a	4.62E-03	3.72E-03	5.33E-03	5.16E-03	9.82E-03	3.15E-03
	c	1.51E-01	3.05E-01	0.00E+00	4.29E-01	9.29E-01	2.69E-01
1860	d	8.00E+01	7.24E-01	8.66E+01	1.06E+00	7.10E+01	6.10E-01
	f	3.16E-03	1.11E-04	2.69E-03	1.23E-04	4.18E-03	1.54E-04
	g	3.13E-05	1.78E-06	2.81E-05	2.40E-06	3.80E-05	1.77E-06
	a	1.43E-02	3.30E-03	1.54E-02	4.35E-03	1.37E-02	4.20E-03
	c	8.66E-01	2.89E-01	8.82E-01	3.91E-01	9.01E-01	3.59E-01
1880	d	8.33E+01	8.02E-01	8.75E+01	1.12E+00	7.87E+01	9.62E-01
	f	2.99E-03	1.06E-04	2.75E-03	1.27E-04	3.30E-03	1.52E-04
	g	3.01E-05	2.59E-06	2.77E-05	3.44E-06	3.28E-05	3.29E-06
	a	1.97E-02	1.63E-03	1.46E-02	2.59E-03	2.43E-02	1.70E-03
	c	2.28E+00	1.88E-01	1.50E+00	2.92E-01	3.22E+00	2.03E-01
1900	d	8.16E+01	6.72E-01	8.55E+01	1.06E+00	7.69E+01	7.13E-01
	f	3.57E-03	1.12E-04	3.13E-03	1.40E-04	4.25E-03	1.61E-04
	g	3.99E-05	3.42E-06	3.94E-05	5.00E-06	4.16E-05	4.02E-06

	a	1.94E-02	9.52E-04	1.83E-02	1.10E-03	2.11E-02	1.54E-03
	c	3.00E+00	1.31E-01	2.91E+00	1.59E-01	3.09E+00	1.99E-01
1920	d	7.95E+01	5.90E-01	8.24E+01	7.45E-01	7.61E+01	8.49E-01
	f	4.33E-03	1.27E-04	4.04E-03	1.42E-04	4.68E-03	2.11E-04
	g	3.71E-05	5.11E-06	3.55E-05	6.22E-06	3.44E-05	7.65E-06
	a	1.25E-02	5.62E-04	1.31E-02	9.01E-04	1.20E-02	6.79E-04
	c	2.74E+00	9.12E-02	2.53E+00	1.48E-01	2.80E+00	1.08E-01
1940	d	7.39E+01	5.22E-01	7.97E+01	8.56E-01	7.04E+01	6.18E-01
	f	5.60E-03	1.63E-04	4.59E-03	1.90E-04	6.29E-03	2.35E-04
	g	9.39E-05	8.46E-06	6.18E-05	1.20E-05	8.86E-05	1.11E-05
	a	2.09E-02	1.85E-03	1.74E-02	2.30E-03	2.35E-02	2.66E-03
	c	2.75E+00	3.04E-01	2.52E+00	4.18E-01	2.71E+00	4.07E-01
1960	d	8.22E+01	2.17E+00	8.90E+01	3.21E+00	8.05E+01	2.78E+00
	f	3.69E-03	3.11E-04	3.20E-03	3.59E-04	3.70E-03	4.03E-04
	g	1.91E-05	4.73E-05	2.99E-05	6.38E-05	0.00E+00	6.08E-05
	a	1.41E-02	9.61E-04	1.39E-02	1.44E-03	1.56E-02	1.29E-03
	c	3.25E+00	2.18E-01	3.72E+00	2.76E-01	3.40E+00	2.81E-01
1980	d	8.87E+01	3.23E+00	8.90E+01	4.51E+00	8.82E+01	4.08E+00
	f	3.79E-03	4.11E-04	4.21E-03	6.67E-04	3.75E-03	5.10E-04
	g	0.00E+00	2.00E-04	0.00E+00	3.24E-04	0.00E+00	2.42E-04
	a	4.45E-03	6.19E-04	4.45E-03	6.19E-04		
	c	3.05E+00	1.57E-01	3.05E+00	1.57E-01		
2000	d	1.02E+02	7.43E+00	1.02E+02	7.43E+00		
	f	3.91E-03	7.96E-04	3.91E-03	7.96E-04		
	g	0.00E+00	2.09E-03	0.00E+00	2.09E-03		

SE, standard error

Table 5.6 Georges Bank 20-y cohort Tanaka growth models.

Cohort	Parameter	Population		Female		Male	
		Estimate	SE	Estimate	SE	Estimate	SE
1740	*a*	5.54E-02	3.61E-02			5.54E-02	3.61E-02
	c	0.00E+00	1.51E+00			0.00E+00	1.51E+00
	d	8.74E+01	9.89E-01			8.74E+01	9.89E-01
	f	1.88E-03	9.88E-05			1.88E-03	9.88E-05
1780	*a*	1.99E-02	8.34E-03			1.99E-02	8.34E-03
	c	0.00E+00	4.47E-01			0.00E+00	4.47E-01
	d	8.87E+01	3.81E-01			8.87E+01	3.81E-01
	f	2.28E-03	4.93E-05			2.28E-03	4.93E-05
1800	*a*	9.55E-03	6.59E-03	3.84E-03	5.74E-03	7.62E-03	5.07E-03
	c	0.00E+00	4.48E-01	0.00E+00	5.08E-01	0.00E+00	3.77E-01
	d	9.13E+01	4.88E-01	9.74E+01	6.76E-01	8.99E+01	4.45E-01
	f	2.29E-03	5.89E-05	2.18E-03	7.22E-05	2.20E-03	4.92E-05
1820	*a*	1.53E-02	4.49E-03	2.18E-02	7.53E-03	1.06E-02	4.94E-03
	c	0.00E+00	2.83E-01	0.00E+00	4.63E-01	0.00E+00	3.25E-01
	d	9.37E+01	3.20E-01	9.85E+01	5.31E-01	9.05E+01	3.72E-01
	f	2.14E-03	3.36E-05	1.88E-03	4.39E-05	2.35E-03	4.59E-05
1840	*a*	9.83E-03	4.34E-03	1.11E-02	4.14E-03	7.40E-03	6.40E-03
	c	0.00E+00	3.06E-01	0.00E+00	3.03E-01	0.00E+00	4.61E-01
	d	9.46E+01	4.06E-01	9.98E+01	4.23E-01	8.99E+01	6.08E-01
	f	2.27E-03	4.45E-05	2.06E-03	3.85E-05	2.45E-03	7.64E-05
1860	*a*	5.55E-03	2.95E-03	6.28E-03	2.85E-03	4.21E-03	5.33E-03
	c	0.00E+00	2.40E-01	0.00E+00	2.41E-01	0.00E+00	4.10E-01
	d	9.43E+01	3.87E-01	9.90E+01	4.05E-01	8.69E+01	6.10E-01
	f	2.36E-03	4.26E-05	2.16E-03	3.80E-05	2.74E-03	8.90E-05
1880	*a*	2.50E-03	1.84E-03	4.09E-03	2.26E-03	5.97E-03	2.33E-03
	c	0.00E+00	1.67E-01	0.00E+00	2.05E-01	5.81E-01	2.14E-01
	d	9.19E+01	3.09E-01	9.70E+01	3.92E-01	8.45E+01	3.82E-01
	f	2.57E-03	3.77E-05	2.29E-03	3.90E-05	3.15E-03	6.74E-05
1900	*a*	9.97E-03	1.65E-03	1.05E-02	2.11E-03	8.90E-03	1.84E-03
	c	1.16E+00	1.69E-01	1.14E+00	2.26E-01	1.11E+00	1.82E-01
	d	8.71E+01	3.66E-01	9.43E+01	5.25E-01	8.01E+01	3.65E-01
	f	3.13E-03	5.96E-05	2.70E-03	6.48E-05	3.65E-03	7.92E-05
1920	*a*	8.16E-03	9.88E-04	8.44E-03	1.45E-03	8.32E-03	9.93E-04
	c	1.40E+00	1.22E-01	1.41E+00	1.87E-01	1.48E+00	1.18E-01
	d	8.32E+01	3.29E-01	8.99E+01	5.40E-01	7.73E+01	3.01E-01
	f	3.85E-03	7.11E-05	3.31E-03	8.85E-05	4.51E-03	8.69E-05
1940	*a*	8.95E-03	1.11E-03	8.78E-03	1.44E-03	8.95E-03	1.50E-03
	c	1.59E+00	1.54E-01	1.52E+00	2.05E-01	1.60E+00	2.04E-01
	d	8.84E+01	5.33E-01	9.28E+01	7.39E-01	8.60E+01	6.86E-01
	f	3.45E-03	8.79E-05	3.12E-03	1.01E-04	3.64E-03	1.25E-04
1960	*a*	8.59E-03	1.34E-03	6.01E-03	6.12E-04	8.22E-03	8.74E-04
	c	3.32E+00	2.45E-01	4.03E+00	1.02E-01	2.60E+00	1.65E-01
	d	7.55E+01	1.29E+00	6.86E+01	6.02E-01	8.04E+01	8.29E-01
	f	6.94E-03	6.16E-04	1.02E-02	5.48E-04	5.60E-03	2.79E-04
1980	*a*	1.57E-02	9.55E-04	1.57E-02	9.55E-04		
	c	4.00E+00	2.42E-01	4.00E+00	2.42E-01		
	d	1.11E+02	2.31E+00	1.11E+02	2.31E+00		
	f	2.51E-03	1.70E-04	2.51E-03	1.70E-04		

SE, standard error

Table 5.7 Long Island 20-y cohort Tanaka growth models.

Cohort	Parameter	Population		Female		Male	
		Estimate	SE	Estimate	SE	Estimate	SE
1700	*a*	9.24E-02	8.29E-02			9.24E-02	8.29E-02
	c	0.00E+00	2.47E+00			0.00E+00	2.47E+00
	d	7.59E+01	9.96E-01			7.59E+01	9.96E-01
	f	2.27E-03	1.67E-04			2.27E-03	1.67E-04
1740	*a*	1.06E-01	4.00E-02	1.42E-01	4.60E-02	1.00E-01	7.54E-02
	c	0.00E+00	1.28E+00	0.00E+00	1.46E+00	0.00E+00	2.23E+00
	d	8.31E+01	6.50E-01	8.81E+01	7.65E-01	7.57E+01	9.89E-01
	f	1.98E-03	7.71E-05	1.73E-03	7.01E-05	2.30E-03	1.61E-04
1760	*a*	1.37E-01	4.68E-02	1.51E-01	4.89E-02	7.24E-02	4.23E-02
	c	0.00E+00	1.58E+00	0.00E+00	1.64E+00	0.00E+00	1.32E+00
	d	8.88E+01	9.19E-01	9.07E+01	9.50E-01	7.01E+01	6.27E-01
	f	1.64E-03	7.37E-05	1.58E-03	7.17E-05	2.55E-03	1.20E-04
1780	*a*	1.31E-01	2.87E-02	1.34E-01	3.14E-02	1.21E-01	4.47E-02
	c	0.00E+00	9.42E-01	0.00E+00	1.05E+00	0.00E+00	1.44E+00
	d	8.42E+01	5.56E-01	8.74E+01	6.37E-01	8.01E+01	8.23E-01
	f	1.82E-03	5.28E-05	1.74E-03	5.56E-05	1.95E-03	8.92E-05
1800	*a*	1.09E-01	1.91E-02	1.70E-01	4.16E-02	9.20E-02	1.99E-02
	c	0.00E+00	6.52E-01	0.00E+00	1.44E+00	0.00E+00	6.71E-01
	d	8.45E+01	4.20E-01	9.40E+01	9.73E-01	8.07E+01	4.19E-01
	f	1.95E-03	4.34E-05	1.53E-03	6.46E-05	2.17E-03	5.28E-05
1820	*a*	5.72E-02	1.17E-02	7.95E-02	1.91E-02	7.01E-02	1.95E-02
	c	0.00E+00	4.97E-01	0.00E+00	7.57E-01	0.00E+00	7.25E-01
	d	8.80E+01	4.13E-01	9.17E+01	6.00E-01	8.30E+01	5.23E-01
	f	2.02E-03	4.18E-05	1.89E-03	5.50E-05	2.23E-03	6.56E-05
1840	*a*	2.10E-02	6.64E-03	3.08E-02	1.10E-02	1.15E-02	6.54E-03
	c	0.00E+00	3.56E-01	0.00E+00	5.70E-01	0.00E+00	3.79E-01
	d	8.65E+01	3.74E-01	9.13E+01	5.98E-01	8.13E+01	4.08E-01
	f	2.42E-03	4.86E-05	2.13E-03	6.17E-05	2.80E-03	6.84E-05
1860	*a*	1.33E-02	5.11E-03	1.59E-02	6.74E-03	1.05E-02	5.58E-03
	c	0.00E+00	3.21E-01	0.00E+00	4.33E-01	0.00E+00	3.38E-01
	d	8.83E+01	4.14E-01	9.41E+01	5.84E-01	8.11E+01	4.08E-01
	f	2.43E-03	5.08E-05	2.18E-03	5.86E-05	2.81E-03	6.56E-05
1880	*a*	1.09E-02	3.89E-03	1.09E-02	4.84E-03	1.02E-02	5.20E-03
	c	0.00E+00	2.73E-01	0.00E+00	3.54E-01	0.00E+00	3.53E-01
	d	9.04E+01	4.33E-01	9.43E+01	5.86E-01	8.62E+01	5.37E-01
	f	2.36E-03	4.69E-05	2.22E-03	5.65E-05	2.53E-03	6.65E-05
1900	*a*	1.07E-02	2.06E-03	4.80E-03	3.17E-03	1.84E-02	2.25E-03
	c	6.99E-01	1.85E-01	0.00E+00	2.81E-01	1.73E+00	2.07E-01
	d	8.94E+01	3.84E-01	9.34E+01	5.94E-01	8.44E+01	4.16E-01
	f	2.62E-03	4.59E-05	2.36E-03	5.91E-05	3.05E-03	6.55E-05
1920	*a*	1.78E-02	1.09E-03	1.67E-02	1.25E-03	1.95E-02	1.74E-03
	c	2.38E+00	1.21E-01	2.32E+00	1.46E-01	2.51E+00	1.83E-01
	d	8.35E+01	3.07E-01	8.65E+01	3.86E-01	7.97E+01	4.39E-01
	f	3.62E-03	6.01E-05	3.41E-03	6.75E-05	3.95E-03	1.01E-04
1940	*a*	1.17E-02	6.89E-04	1.21E-02	1.04E-03	1.16E-02	8.07E-04
	c	2.09E+00	9.13E-02	2.04E+00	1.37E-01	2.26E+00	1.08E-01
	d	7.95E+01	2.97E-01	8.39E+01	4.52E-01	7.52E+01	3.48E-01

	f	4.29E-03	7.19E-05	3.84E-03	9.01E-05	4.92E-03	1.07E-04
1960	*a*	2.08E-02	1.89E-03	1.72E-02	2.36E-03	2.35E-02	2.34E-03
	c	2.67E+00	2.46E-01	2.40E+00	3.39E-01	3.00E+00	2.91E-01
	d	8.29E+01	1.01E+00	9.03E+01	1.50E+00	7.80E+01	1.14E+00
	f	3.58E-03	1.63E-04	3.06E-03	1.84E-04	4.12E-03	2.35E-04
1980	*a*	1.49E-02	8.98E-04	1.37E-02	1.23E-03	1.58E-02	1.17E-03
	c	4.07E+00	1.52E-01	3.68E+00	2.41E-01	4.23E+00	1.87E-01
	d	8.22E+01	1.23E+00	8.76E+01	2.12E+00	8.03E+01	1.46E+00
	f	5.04E-03	2.95E-04	4.37E-03	3.92E-04	5.23E-03	3.76E-04
2000	*a*	4.42E-03	4.22E-04	4.42E-03	4.22E-04		
	c	2.98E+00	1.41E-01	2.98E+00	1.41E-01		
	d	1.02E+02	3.09E+00	1.02E+02	3.09E+00		
	f	3.86E-03	3.85E-04	3.86E-03	3.85E-04		

SE, standard error

Table 5.8 Georges Bank 20-y cohort von Bertalanffy growth models. The L_{inf} parameter is not reliable for these growth datasets and should not be used to predict maximum length. The k and t_0 parameters may be useful for estimating growth at young age/small size.

Cohort	Parameter	Population		Female		Male	
		Estimate	SE	Estimate	SE	Estimate	SE
1740	L_{inf}	1.13E+02	9.02E-01			1.13E+02	9.02E-01
	k	9.18E-03	2.66E-04			9.18E-03	2.66E-04
	t_0	-3.14E+01	1.40E+00			-3.14E+01	1.40E+00
1780	L_{inf}	1.05E+02	4.55E-01			1.05E+02	4.55E-01
	k	1.46E-02	3.11E-04			1.46E-02	3.11E-04
	t_0	-2.30E+01	8.74E-01			-2.30E+01	8.74E-01
1800	L_{inf}	1.04E+02	3.55E-01	1.08E+02	5.15E-01	1.02E+02	3.59E-01
	k	1.76E-02	3.19E-04	1.92E-02	5.25E-04	1.69E-02	3.03E-04
	t_0	-1.80E+01	6.42E-01	-1.69E+01	9.46E-01	-1.84E+01	6.41E-01
1820	L_{inf}	1.04E+02	2.06E-01	1.06E+02	3.06E-01	1.02E+02	2.66E-01
	k	1.92E-02	1.94E-04	1.92E-02	2.73E-04	1.92E-02	2.62E-04
	t_0	-1.52E+01	3.16E-01	-1.38E+01	4.29E-01	-1.65E+01	4.40E-01
1840	L_{inf}	1.02E+02	2.20E-01	1.05E+02	2.29E-01	9.87E+01	3.58E-01
	k	2.30E-02	2.69E-04	2.35E-02	2.77E-04	2.24E-02	4.37E-04
	t_0	-1.29E+01	3.18E-01	-1.20E+01	3.12E-01	-1.41E+01	5.51E-01
1860	L_{inf}	9.95E+01	2.02E-01	1.03E+02	2.14E-01	9.43E+01	3.40E-01
	k	2.63E-02	2.88E-04	2.62E-02	2.90E-04	2.67E-02	5.34E-04
	t_0	-1.11E+01	2.60E-01	-1.07E+01	2.59E-01	-1.18E+01	4.85E-01
1880	L_{inf}	9.52E+01	1.52E-01	9.85E+01	1.87E-01	9.06E+01	2.11E-01
	k	3.18E-02	2.85E-04	3.11E-02	3.21E-04	3.35E-02	4.59E-04
	t_0	-8.86E+00	1.80E-01	-8.65E+00	2.08E-01	-8.85E+00	2.73E-01
1900	L_{inf}	8.95E+01	1.62E-01	9.41E+01	2.19E-01	8.50E+01	1.87E-01
	k	4.17E-02	4.44E-04	4.11E-02	5.45E-04	4.19E-02	5.55E-04
	t_0	-5.77E+00	1.66E-01	-5.51E+00	2.04E-01	-6.19E+00	2.11E-01
1920	L_{inf}	8.48E+01	1.46E-01	8.92E+01	2.19E-01	8.09E+01	1.54E-01
	k	5.42E-02	5.72E-04	5.36E-02	7.90E-04	5.54E-02	6.69E-04
	t_0	-4.51E+00	1.31E-01	-4.22E+00	1.80E-01	-4.68E+00	1.50E-01
1940	L_{inf}	8.50E+01	2.03E-01	8.73E+01	2.82E-01	8.36E+01	2.68E-01
	k	6.50E-02	8.90E-04	6.48E-02	1.18E-03	6.49E-02	1.20E-03
	t_0	-2.75E+00	1.31E-01	-2.59E+00	1.71E-01	-2.87E+00	1.79E-01
1960	L_{inf}	7.42E+01	5.75E-01	7.01E+01	5.54E-01	7.73E+01	4.99E-01
	k	1.32E-01	6.26E-03	1.56E-01	7.48E-03	1.20E-01	4.87E-03
	t_0	1.38E-02	2.12E-01	6.13E-01	1.71E-01	-5.22E-01	2.12E-01
1980	L_{inf}	8.81E+01	9.88E-01	8.81E+01	9.88E-01		
	k	1.04E-01	4.12E-03	1.04E-01	4.12E-03		
	t_0	7.01E-01	1.41E-01	7.01E-01	1.41E-01		

SE, standard error

Table 5.9 Long Island 20-y cohort von Bertalanffy growth models. The L_{inf} parameter is not reliable for these growth datasets and should not be used to predict maximum length. The k and t_0 parameters may be useful for estimating growth at young age/small size.

Cohort	Parameter	Population		Female		Male	
		Estimate	SE	Estimate	SE	Estimate	SE
	L_{inf}	1.20E+02	1.77E+00			1.20E+02	1.77E+00
1700	k	5.32E-03	2.27E-04			5.32E-03	2.27E-04
	t_0	-6.16E+01	2.76E+00			-6.16E+01	2.76E+00
	L_{inf}	1.17E+02	9.08E-01	1.17E+02	8.41E-01	1.27E+02	2.21E+00
1740	k	7.05E-03	1.67E-04	7.60E-03	1.72E-04	4.76E-03	2.05E-04
	t_0	-4.31E+01	1.23E+00	-3.85E+01	1.14E+00	-6.60E+01	2.44E+00
	L_{inf}	1.13E+02	8.58E-01	1.16E+02	8.98E-01	9.51E+01	1.05E+00
1760	k	8.68E-03	2.15E-04	8.36E-03	2.04E-04	1.01E-02	4.32E-04
	t_0	-3.03E+01	1.11E+00	-3.10E+01	1.08E+00	-2.97E+01	2.04E+00
	L_{inf}	1.11E+02	6.03E-01	1.14E+02	6.46E-01	1.07E+02	9.52E-01
1780	k	8.63E-03	1.42E-04	8.56E-03	1.46E-04	8.72E-03	2.38E-04
	t_0	-3.06E+01	6.83E-01	-3.06E+01	7.03E-01	-3.06E+01	1.13E+00
	L_{inf}	1.06E+02	3.87E-01	1.10E+02	6.50E-01	1.05E+02	4.46E-01
1800	k	1.06E-02	1.29E-04	1.10E-02	2.15E-04	1.03E-02	1.48E-04
	t_0	-2.65E+01	4.68E-01	-2.23E+01	7.04E-01	-2.88E+01	5.67E-01
	L_{inf}	1.03E+02	3.13E-01	1.05E+02	4.00E-01	1.01E+02	4.46E-01
1820	k	1.37E-02	1.61E-04	1.41E-02	2.09E-04	1.31E-02	2.18E-04
	t_0	-2.16E+01	4.07E-01	-2.04E+01	5.05E-01	-2.34E+01	5.94E-01
	L_{inf}	9.98E+01	2.83E-01	1.03E+02	3.98E-01	9.64E+01	3.66E-01
1840	k	1.75E-02	2.19E-04	1.73E-02	2.88E-04	1.78E-02	3.10E-04
	t_0	-1.86E+01	3.93E-01	-1.78E+01	5.12E-01	-1.96E+01	5.60E-01
	L_{inf}	9.85E+01	2.81E-01	1.02E+02	3.59E-01	9.42E+01	3.49E-01
1860	k	2.05E-02	2.66E-04	2.09E-02	3.32E-04	1.97E-02	3.29E-04
	t_0	-1.53E+01	3.52E-01	-1.44E+01	4.22E-01	-1.68E+01	4.71E-01
	L_{inf}	9.41E+01	2.21E-01	9.65E+01	2.88E-01	9.14E+01	3.00E-01
1880	k	2.77E-02	3.15E-04	2.80E-02	4.08E-04	2.73E-02	4.31E-04
	t_0	-9.40E+00	2.35E-01	-9.08E+00	2.97E-01	-9.77E+00	3.30E-01
	L_{inf}	8.98E+01	1.71E-01	9.23E+01	2.55E-01	8.68E+01	2.06E-01
1900	k	3.74E-02	3.71E-04	3.58E-02	5.01E-04	3.97E-02	5.06E-04
	t_0	-5.70E+00	1.56E-01	-6.33E+00	2.28E-01	-4.93E+00	1.92E-01
	L_{inf}	8.38E+01	1.25E-01	8.59E+01	1.58E-01	8.12E+01	1.82E-01
1920	k	5.52E-02	4.72E-04	5.46E-02	5.73E-04	5.65E-02	7.33E-04
	t_0	-2.87E+00	9.47E-02	-2.92E+00	1.17E-01	-2.75E+00	1.41E-01
	L_{inf}	7.86E+01	1.17E-01	8.18E+01	1.71E-01	7.56E+01	1.43E-01
1940	k	7.13E-02	6.15E-04	6.79E-02	8.11E-04	7.64E-02	8.66E-04
	t_0	-2.11E+00	7.48E-02	-2.29E+00	1.07E-01	-1.81E+00	9.28E-02
	L_{inf}	7.48E+01	2.87E-01	7.93E+01	4.24E-01	7.20E+01	3.35E-01
1960	k	8.39E-02	1.47E-03	8.10E-02	1.96E-03	8.72E-02	1.88E-03
	t_0	-4.06E-01	1.03E-01	-4.79E-01	1.47E-01	-3.05E-01	1.22E-01
	L_{inf}	7.27E+01	3.44E-01	7.50E+01	5.53E-01	7.17E+01	4.18E-01
1980	k	1.35E-01	2.59E-03	1.37E-01	4.02E-03	1.33E-01	3.12E-03
	t_0	7.03E-01	5.98E-02	5.81E-01	9.10E-02	7.57E-01	7.41E-02
	L_{inf}	7.88E+01	8.56E-01	7.88E+01	8.56E-01		
2000	k	2.18E-01	8.30E-03	2.18E-01	8.30E-03		
	t_0	9.96E-01	6.05E-02	9.96E-01	6.05E-02		

SE, standard error

Table 5.10 Cohort parameter chi-square goodness of fit analysis. Bold typeface indicated a significant result (alpha=0.05).

Site	Group	P-Value				
		a	***c***	***d***	***f***	***g***
Georges Bank	Population	0.97	**0.003**	0.067	0.067	0.838
	Female	0.463	**0.003**	0.067	0.067	0.557
	Male	1	0.463	0.463	0.973	0.557
Long Island	Population	1	**0.003**	**0.024**	0.094	0.973
	Female	0.463	**0.003**	0.094	0.067	0.463
	Male	1	0.463	0.463	0.973	0.557

Table 5.11 Modeled time to biological and fishery milestones. Regression results were calculated from linear and non-linear data regressions, and Modified Tanaka results were calculated from cohort-specific Modified Tanaka model parameters (Tables 5.4-5.5). Reproductive time regression estimates were calculated from regression equations, while Modified Tanaka reproductive time estimates were calculated by: (Fishable Size Time)-(50% Maturity Time).

Milestone	Model	Birth Year	Georges Bank		Long Island	
			Time (y)	GR (mm/y)	Time (y)	GR (mm/y)
50% Maturity 52 mm (0-52 mm)	Regression	1740	*12*	*4.33*	70	0.74
		1760	*11*	*4.73*	64	0.81
		1780	*10*	*5.20*	58	0.90
		1800	*9*	*5.78*	52	1.00
		1820	*9*	*5.78*	47	1.11
		1840	*8*	*6.50*	43	1.21
		1860	*7*	*7.43*	39	1.33
		1880	*7*	*7.43*	35	1.49
		1900	*6*	*8.67*	32	1.63
		1920	*6*	*8.67*	29	1.79
		1940	*5*	*10.40*	26	2.00
		1960	*5*	*10.40*	23	2.26
		1980	*5*	*10.40*	21	2.48
		% Δ	*-58*	*140*	-70	233
	Modified Tanaka	1740	NA	NA	32	1.63
		1760	NA	NA	34	1.53
		1780	20	2.60	35	1.49
		1800	18	2.89	31	1.68
		1820	18	2.89	25	2.08
		1840	16	3.25	20	2.60
		1860	15	3.47	18	2.89
		1880	14	3.71	17	3.06
		1900	14	3.71	16	3.25
		1920	12	4.33	14	3.71
		1940	11	4.73	13	4.00
		1960	10	5.20	15	3.47
		1980	NA	NA	12	4.33
		% Δ	-50	100	-63	167
Fishable Size 80 mm (0-80 mm)	Regression	1740	*70*	*1.14*	138	0.58
		1760	*68*	*1.18*	130	0.62
		1780	*65*	*1.23*	122	0.66
		1800	*63*	*1.27*	114	0.70
		1820	*61*	*1.31*	106	0.75
		1840	*58*	*1.38*	98	0.82
		1860	*56*	*1.43*	90	0.89
		1880	*53*	*1.51*	82	0.98
		1900	*51*	*1.57*	74	1.08
		1920	*49*	*1.63*	66	1.21
		1940	*46*	*1.74*	58	1.38
		1960	*44*	*1.82*	50	1.60
		1980	*41*	*1.95*	42	1.90
		% Δ	*-41*	*71*	-70	229

	Modified Tanaka	1740	NA	NA	124	0.65
		1760	NA	NA	121	0.66
		1780	77	1.04	127	0.63
		1800	67	1.19	115	0.70
		1820	66	1.21	97	0.82
		1840	58	1.38	83	0.96
		1860	56	1.43	75	1.07
		1880	56	1.43	68	1.18
		1900	57	1.40	63	1.27
		1920	57	1.40	60	1.33
		1940	48	1.67	62	1.29
		1960	56	1.43	62	1.29
		1980	NA	NA	43	1.86
		% Δ	-27	38	-65	188
Reproductive Time 28 mm (52-80 mm)	Regression	1740	*40*	*0.70*	216	0.13
		1760	*39*	*0.72*	200	0.14
		1780	*39*	*0.72*	184	0.15
		1800	*38*	*0.74*	170	0.16
		1820	*37*	*0.76*	157	0.18
		1840	*36*	*0.78*	145	0.19
		1860	*36*	*0.78*	134	0.21
		1880	*35*	*0.80*	123	0.23
		1900	*34*	*0.82*	114	0.25
		1920	*34*	*0.82*	105	0.27
		1940	*33*	*0.85*	97	0.29
		1960	*32*	*0.88*	90	0.31
		1980	*32*	*0.88*	83	0.34
		% Δ	*-20*	*25*	-62	160
	Modified Tanaka	1740	NA	NA	92	0.30
		1760	NA	NA	87	0.32
		1780	57	0.49	92	0.30
		1800	49	0.57	84	0.33
		1820	48	0.58	72	0.39
		1840	42	0.67	63	0.44
		1860	41	0.68	57	0.49
		1880	42	0.67	51	0.55
		1900	43	0.65	47	0.60
		1920	45	0.62	46	0.61
		1940	37	0.76	49	0.57
		1960	46	0.61	47	0.60
		1980	NA	NA	31	0.90
		% Δ	-19	24	-66	197

GR, Growth rate; % Δ, Percent change

5.6 Figures

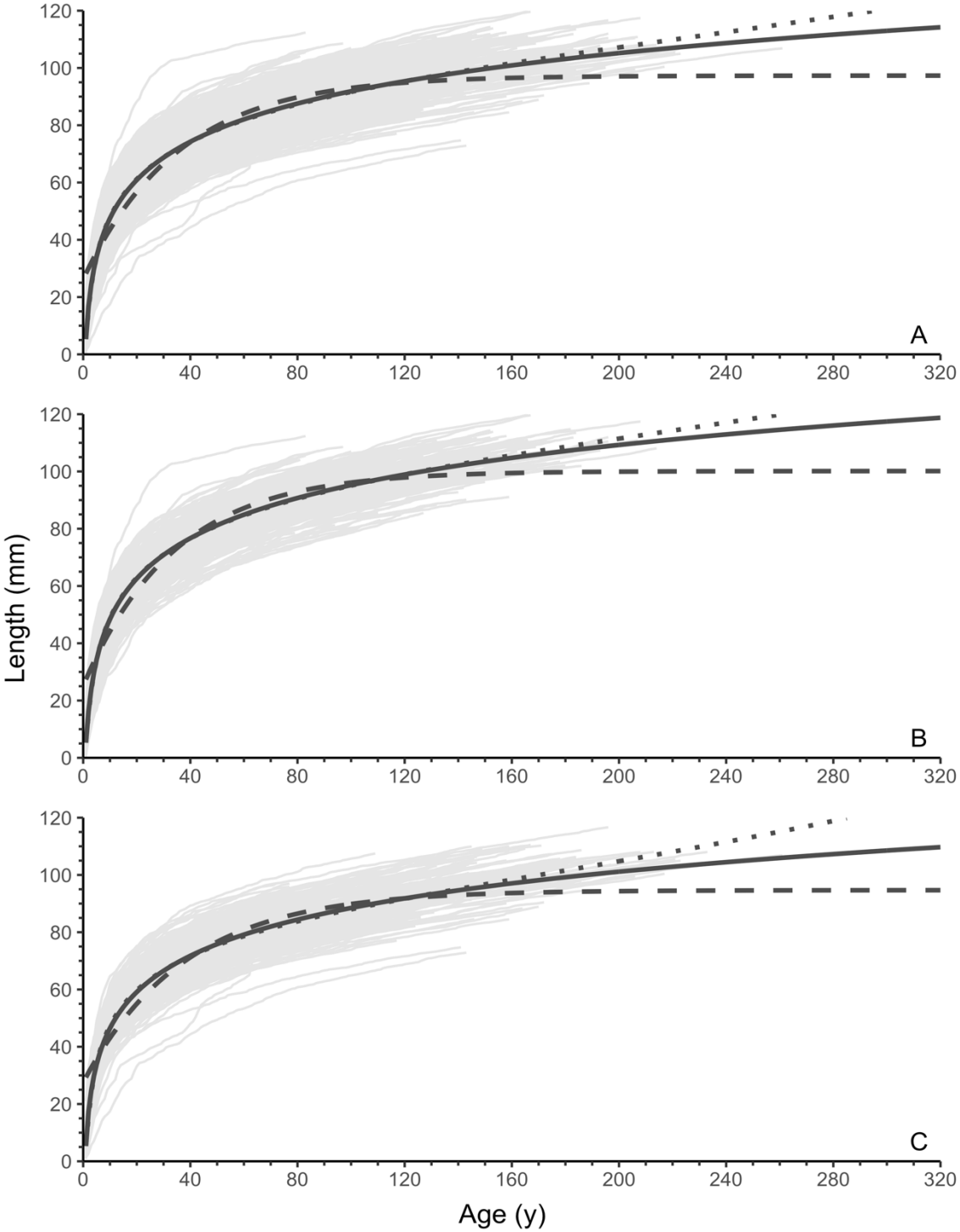

Figure 5.1 Georges Bank growth models. Individual sample age at length growth (grey), von Bertalanffy growth model (dashed line), Tanaka growth model (solid line), and Modified Tanaka growth model (dotted line) for the (A) population, (B) female, and (C) male groups.

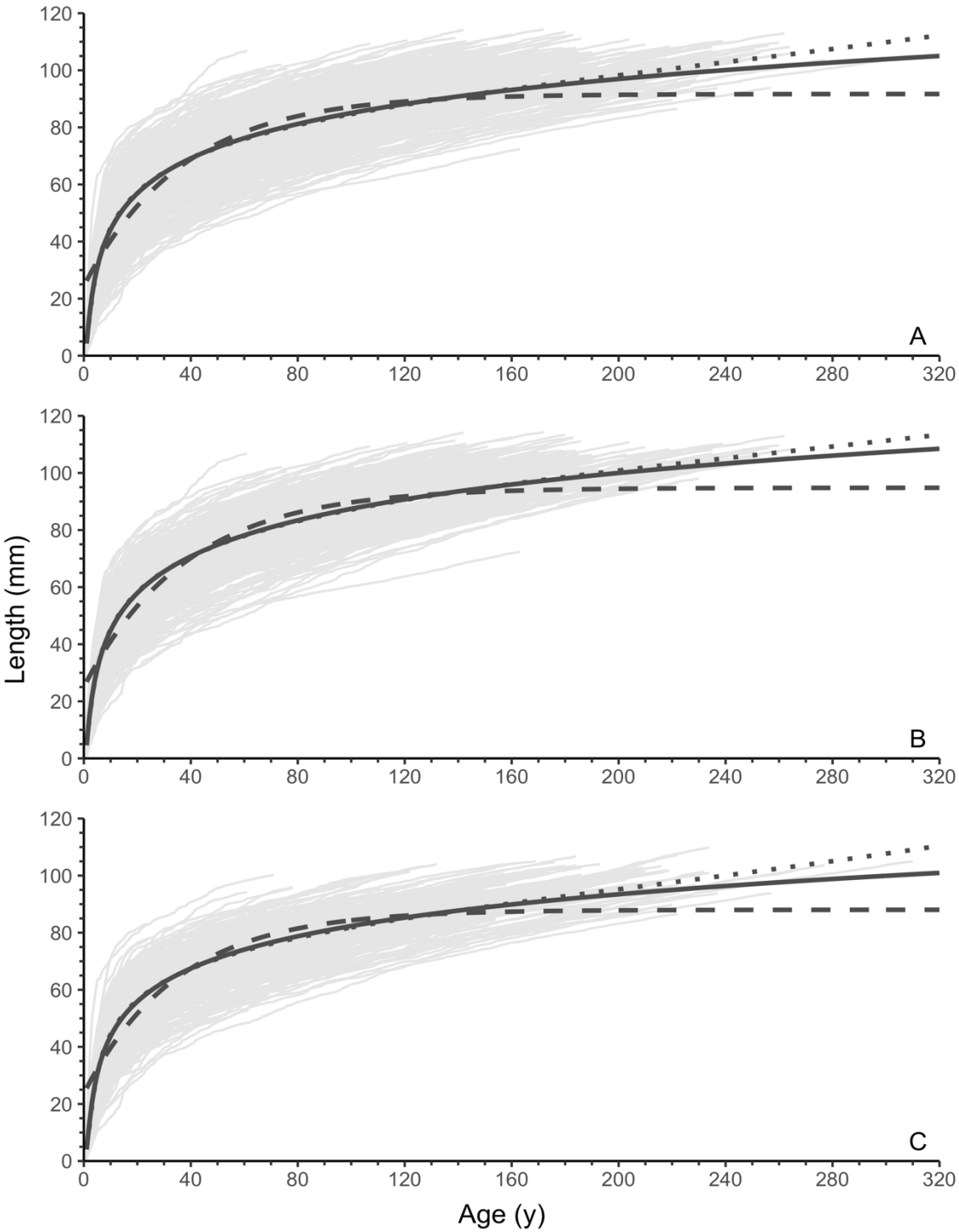

Figure 5.2 Long Island growth models. Individual sample age at length growth (grey), von Bertalanffy growth model (dashed line), Tanaka growth model (solid line), and Modified Tanaka growth model (dotted line) for the (A) population, (B) female, and (C) male groups.

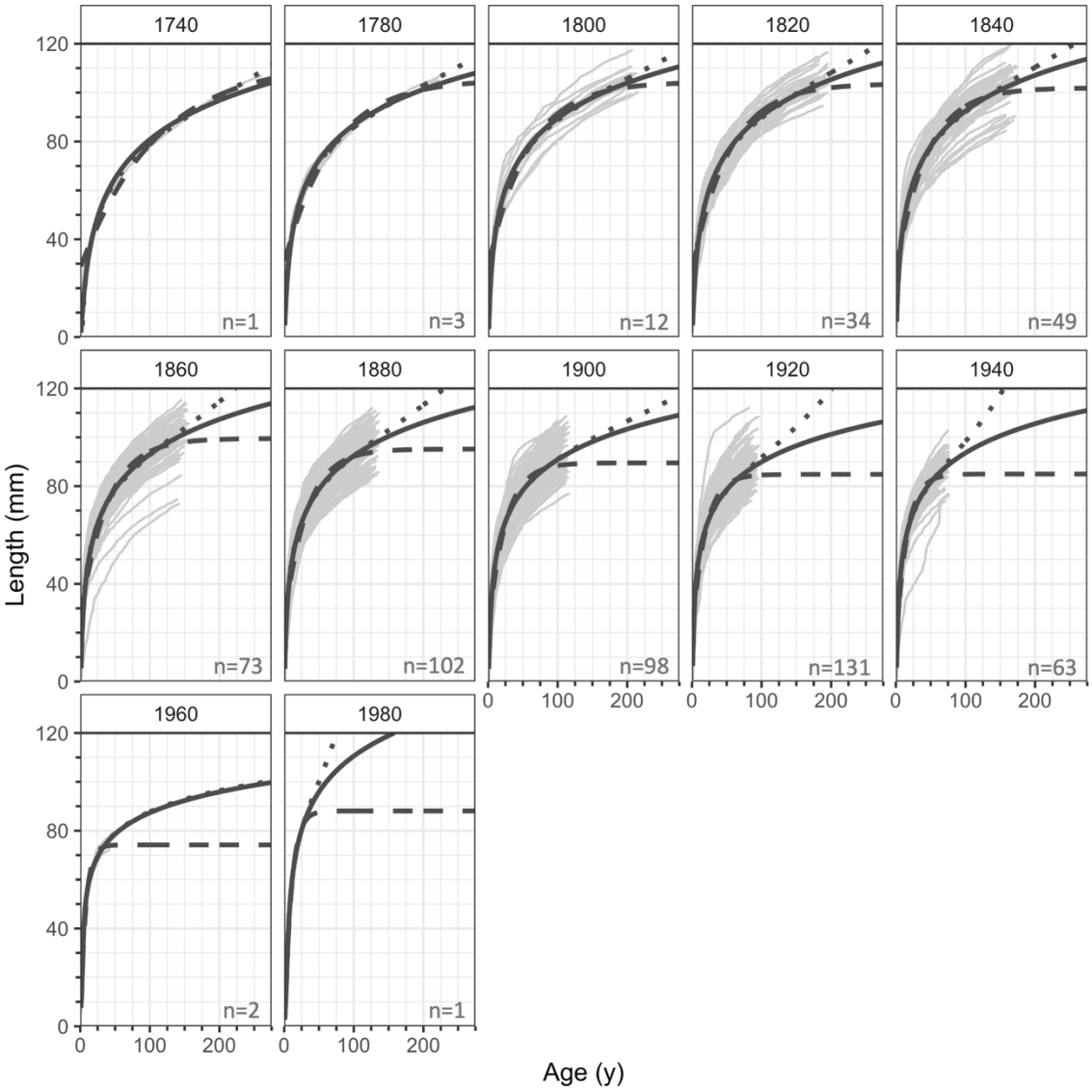

Figure 5.3 Georges Bank population cohort models. Estimated Tanaka (solid line), Modified Tanaka (dotted line), and von Bertalanffy (dashed line) models from individual sample age-length data (light grey) by 20-y birth-year cohorts for *A. islandica*.

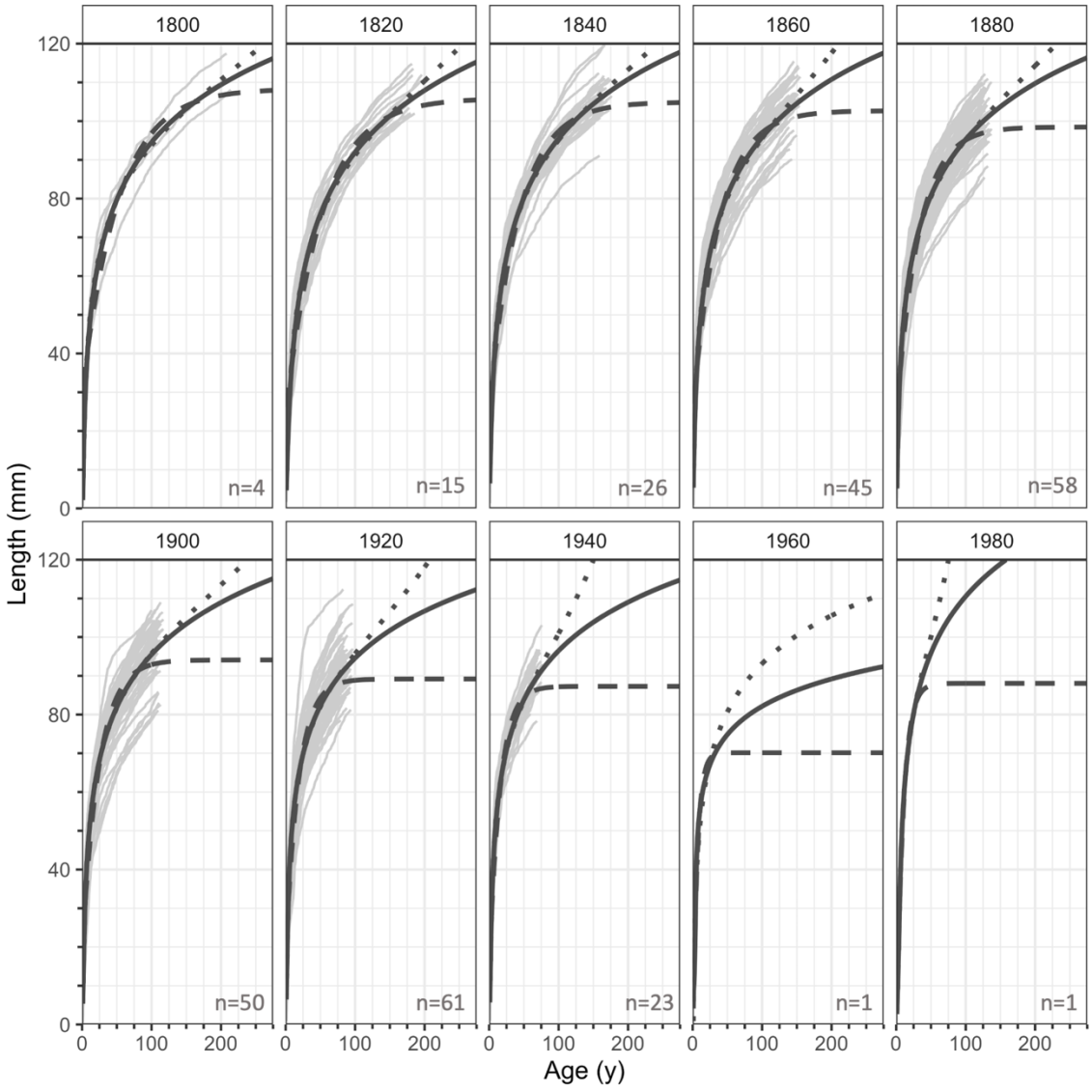

Figure 5.4 Georges Bank female cohort models. Estimated Tanaka (solid line), Modified Tanaka (dotted line), and von Bertalanffy (dashed line) models from individual sample age-length data (light grey) by 20-y birth-year cohorts for *A. islandica*.

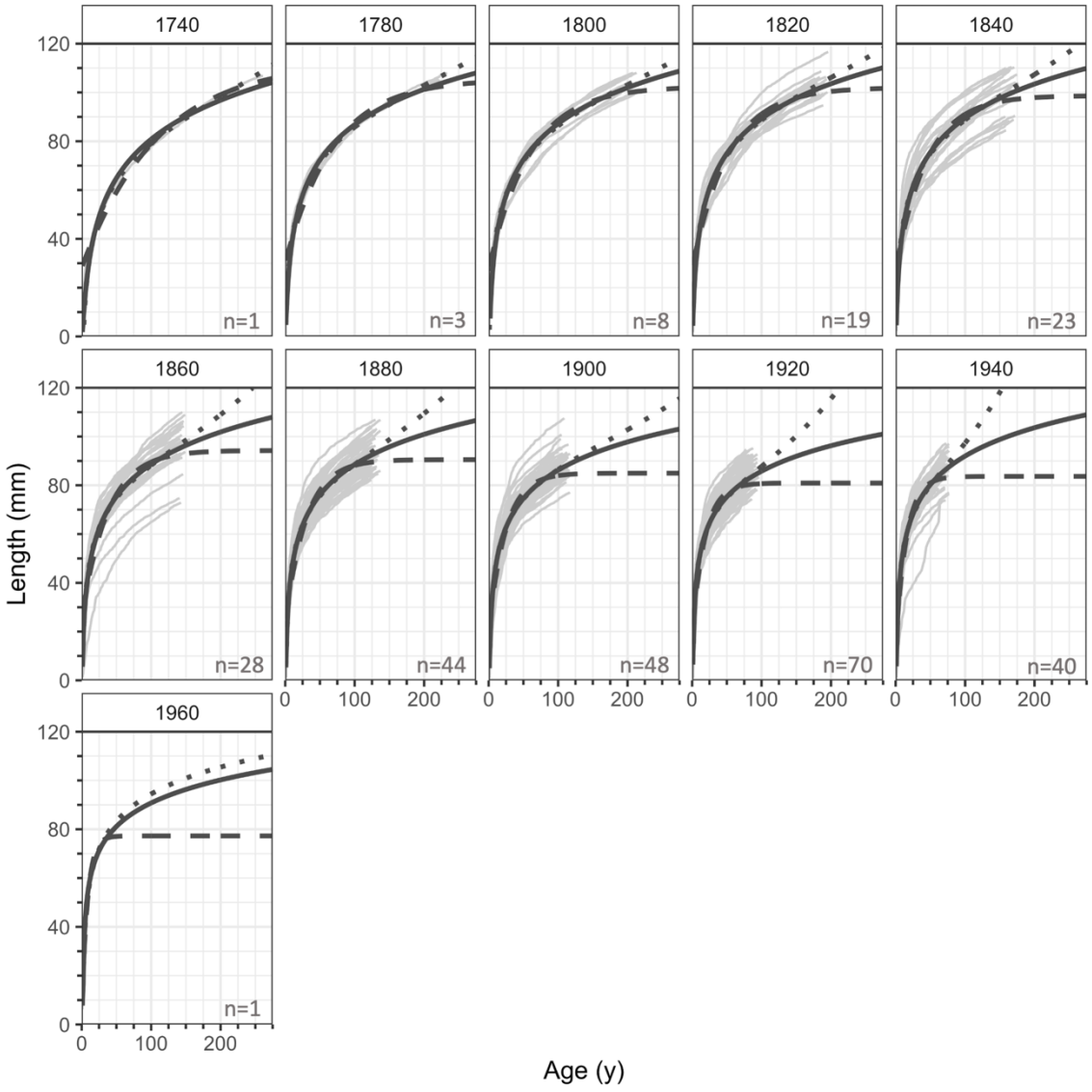

Figure 5.5 Georges Bank male cohort models. Estimated Tanaka (solid line), Modified Tanaka (dotted line), and von Bertalanffy (dashed line) models from individual sample age-length data (light grey) by 20-y birth-year cohorts for *A. islandica*.

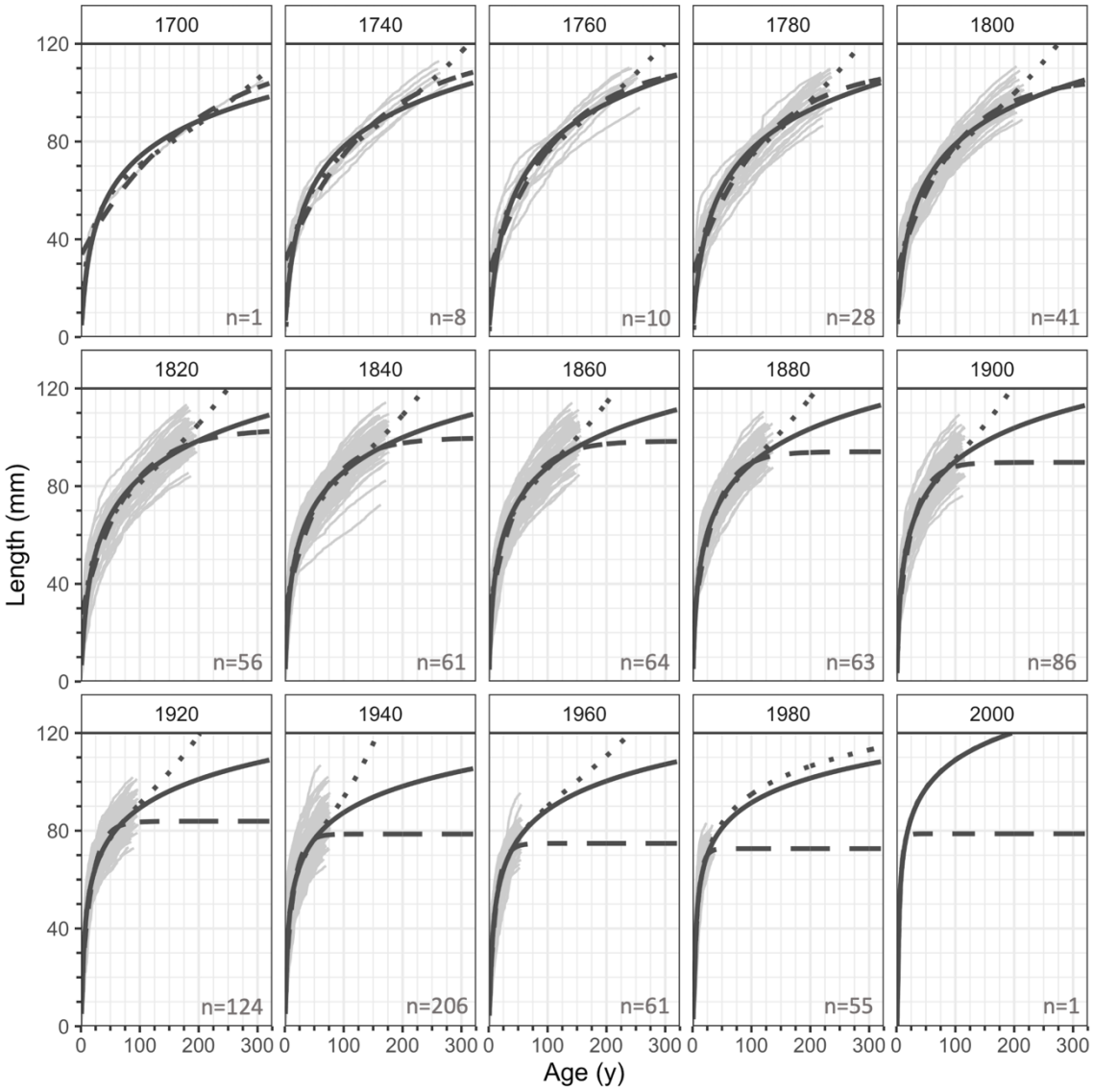

Figure 5.6 Long Island population cohort models. Estimated Tanaka (solid line), Modified Tanaka (dotted line), and von Bertalanffy (dashed line) models from individual sample age-length data (light grey) by 20-y birth-year cohorts for *A. islandica*.

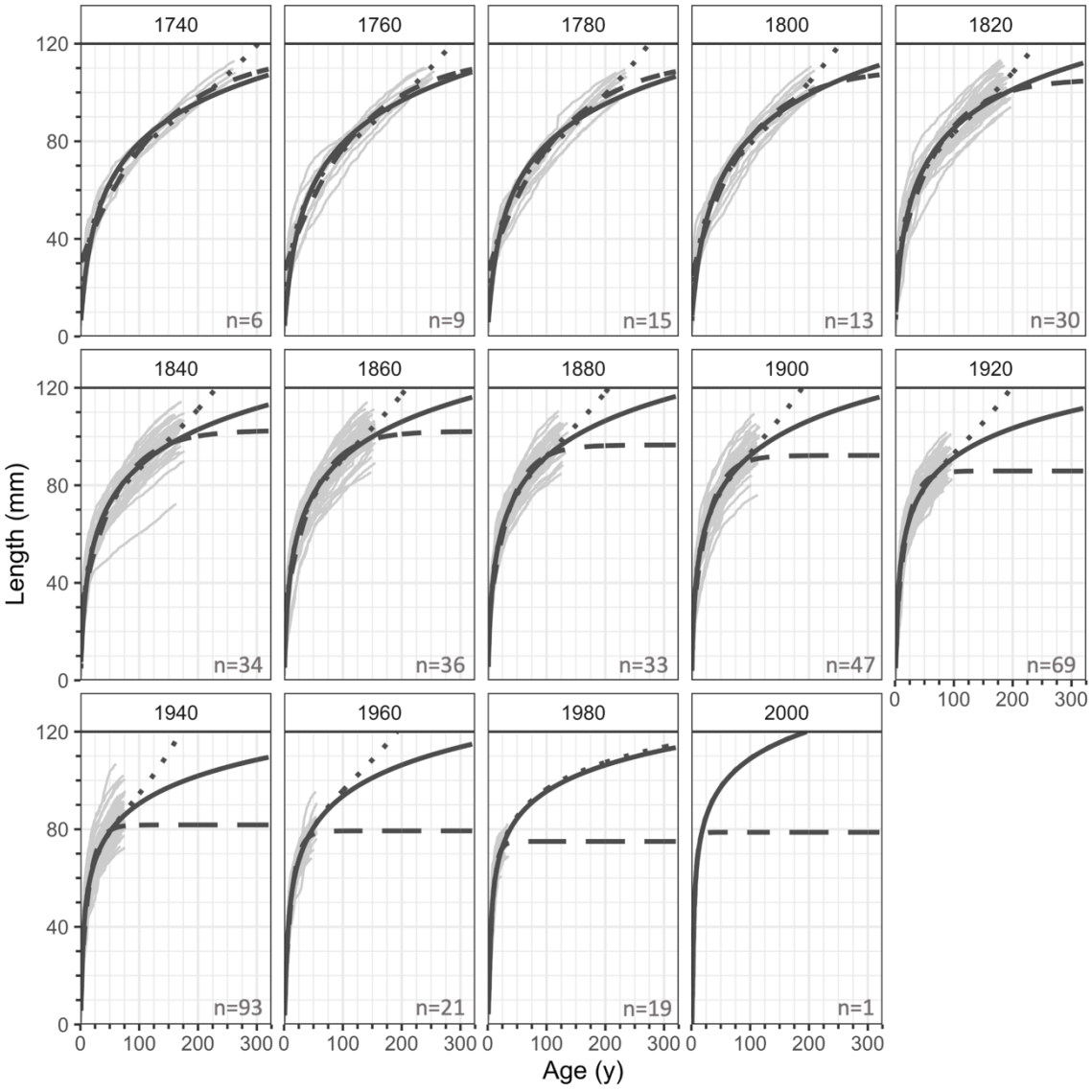

Figure 5.7 Long Island female cohort models. Estimated Tanaka (solid line), Modified Tanaka (dotted line), and von Bertalanffy (dashed line) models from individual sample age-length data (light grey) by 20-y birth-year cohorts for *A. islandica*.

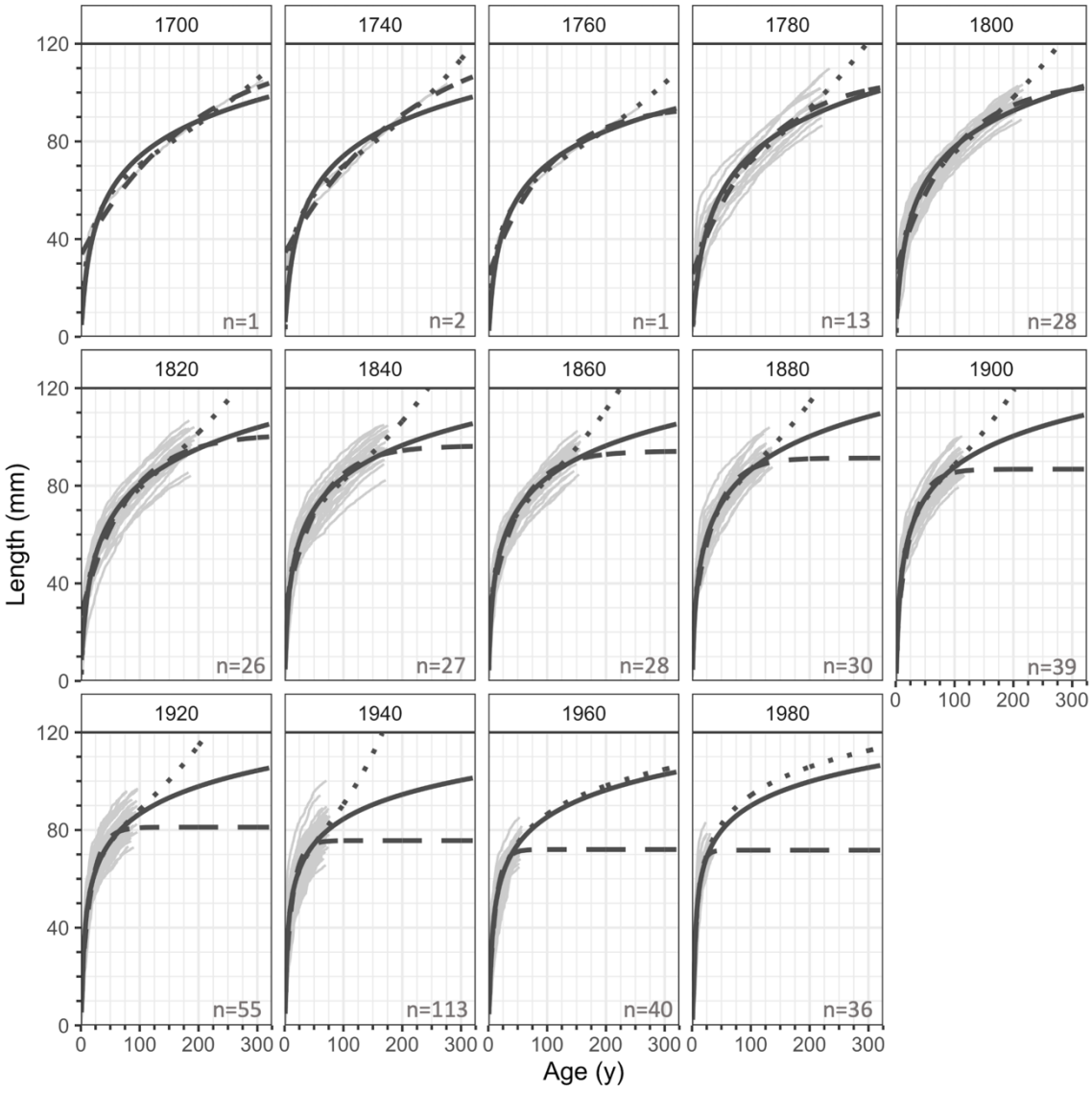

Figure 5.8 Long Island male cohort models. Estimated Tanaka (solid line), Modified Tanaka (dotted line), and von Bertalanffy (dashed line) models from individual sample age-length data (light grey) by 20-y birth-year cohorts for *A. islandica*.

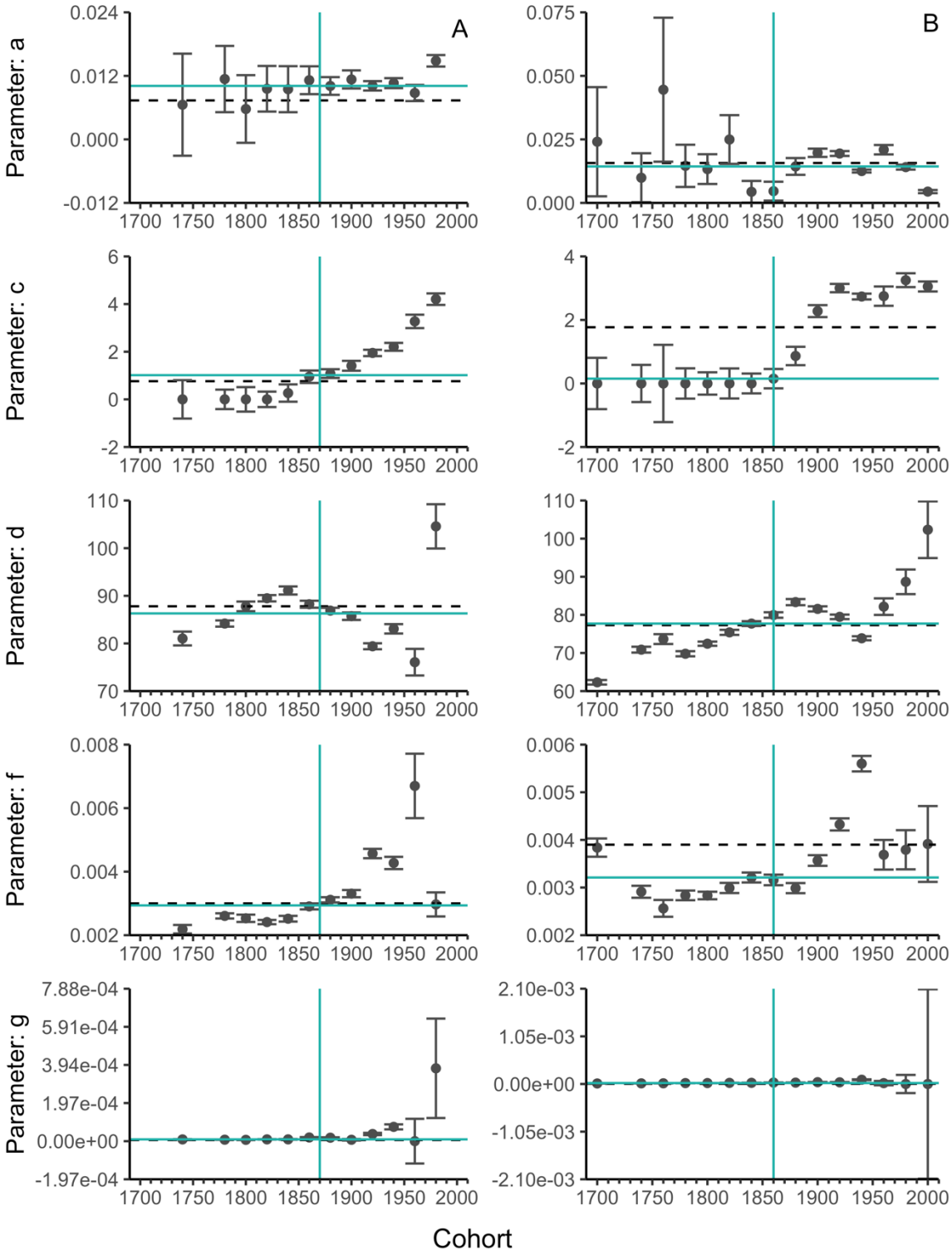

Figure 5.9 Regional population Modified Tanaka parameters. (A) Georges Bank, (B) Long Island. Green quadrants mark the x and y median data values, horizontal dashed line marks the population group parameter.

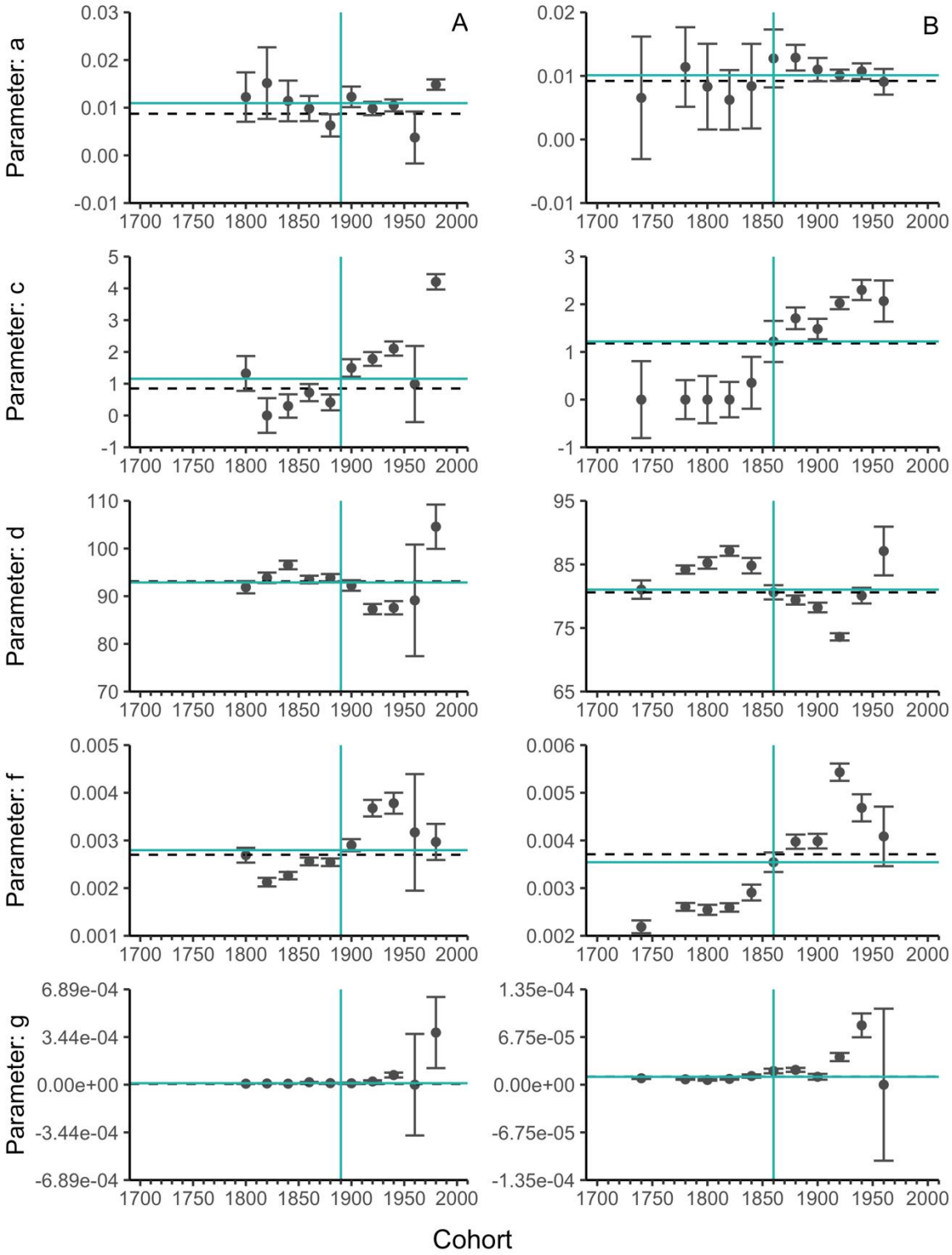

Figure 5.10 Georges Bank Modified Tanaka parameters by sex. (A) Female parameters, (B) male parameters. Green quadrants mark the x and y median data values, horizontal dashed line marks the female group parameter.

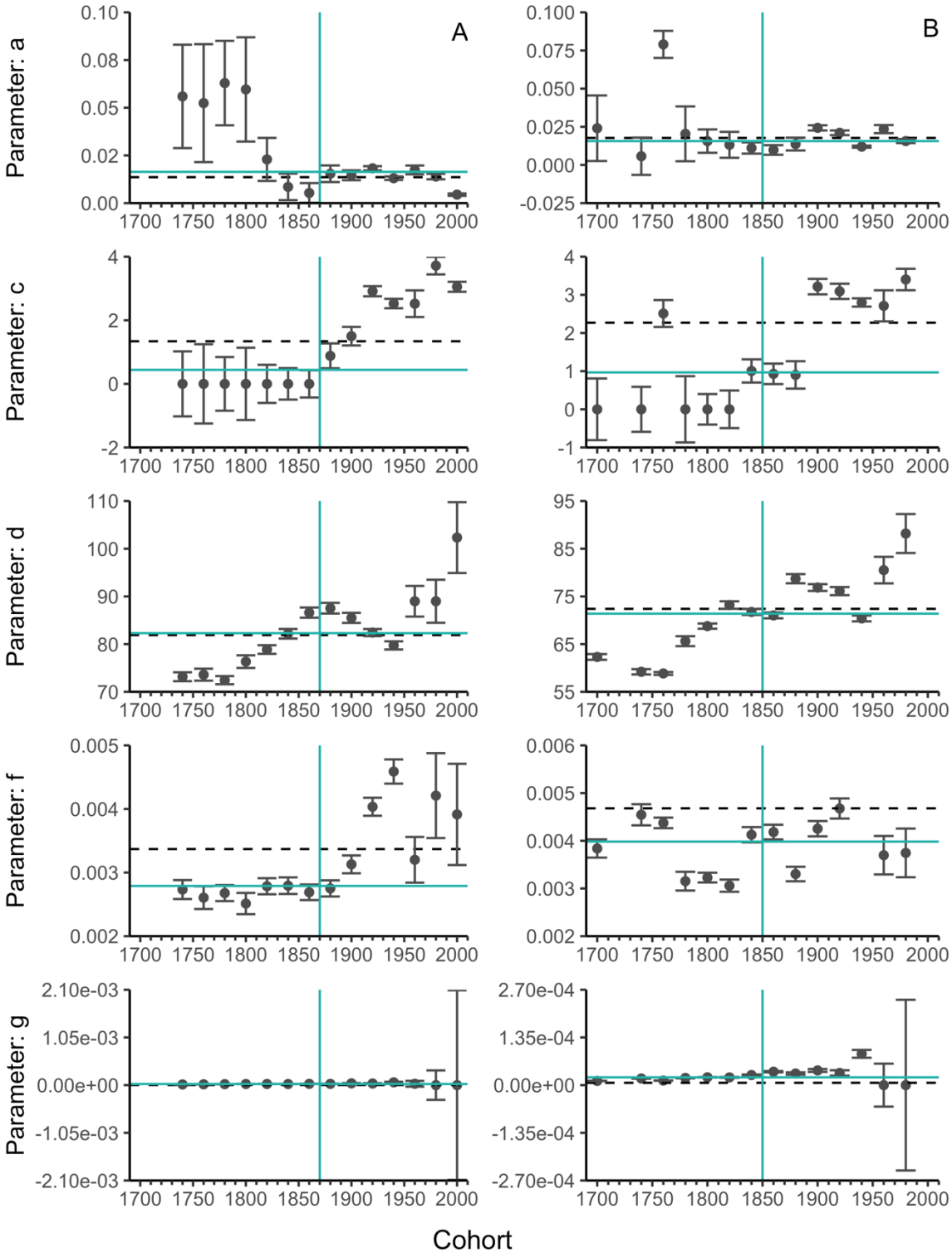

Figure 5.11 Long Island Modified Tanaka parameters by sex. (A) Female parameters, (B) male parameters. Green quadrants mark the x and y median data values, horizontal dashed line marks the female group parameter.

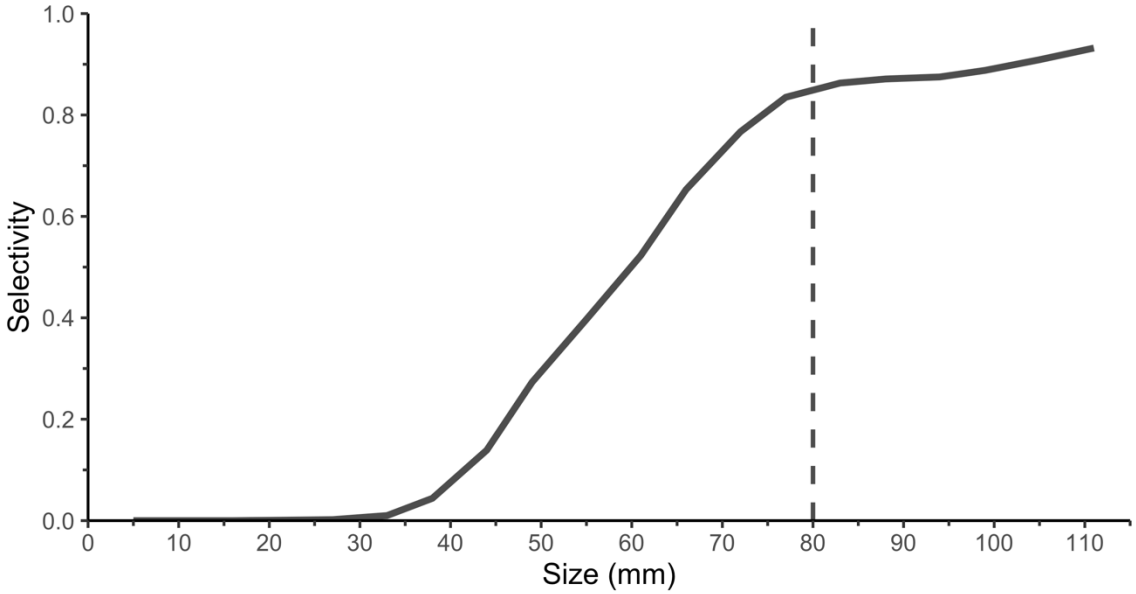

Figure 5.12 Selectivity by size. Selectivity coefficient results from NEFSC (2017, Table 15) that demonstrated dredge selectivity by *A. islandica* shell length. The vertical dashed lines indicated that at 80 mm shell length, selectivity stabilizes for large shell lengths.

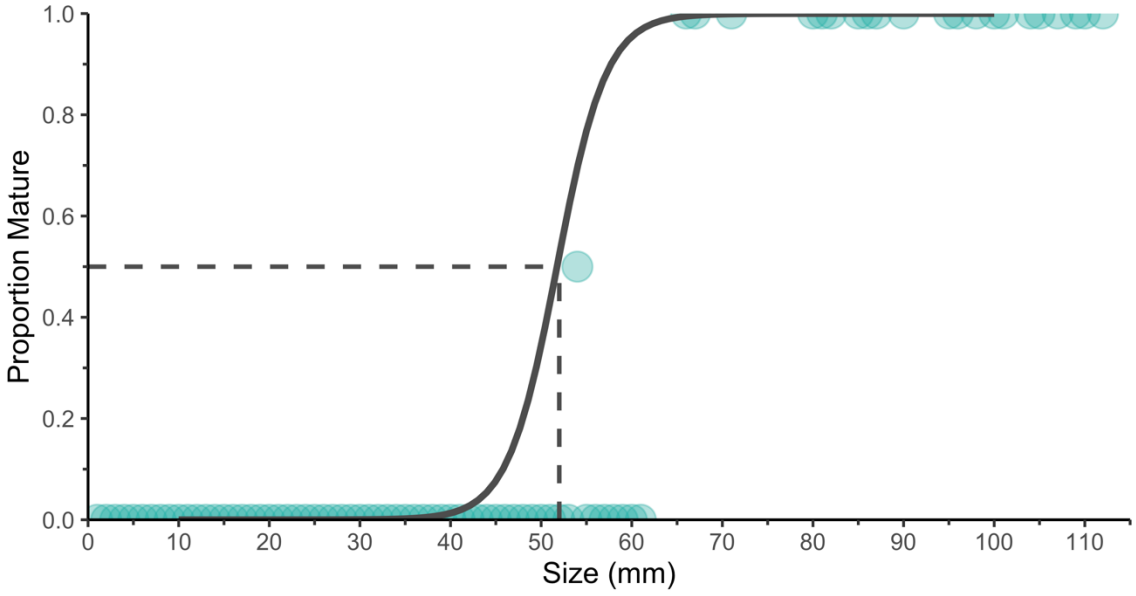

Figure 5.13 Maturity by size. Combined proportion of mature *A. islandica* collected in 2017 from Georges Bank and Long Island (Mann unpublished). The populations were 50% maturity at a mean size of 52 mm, with a 95% confidence interval of 50.4-53.0 mm.

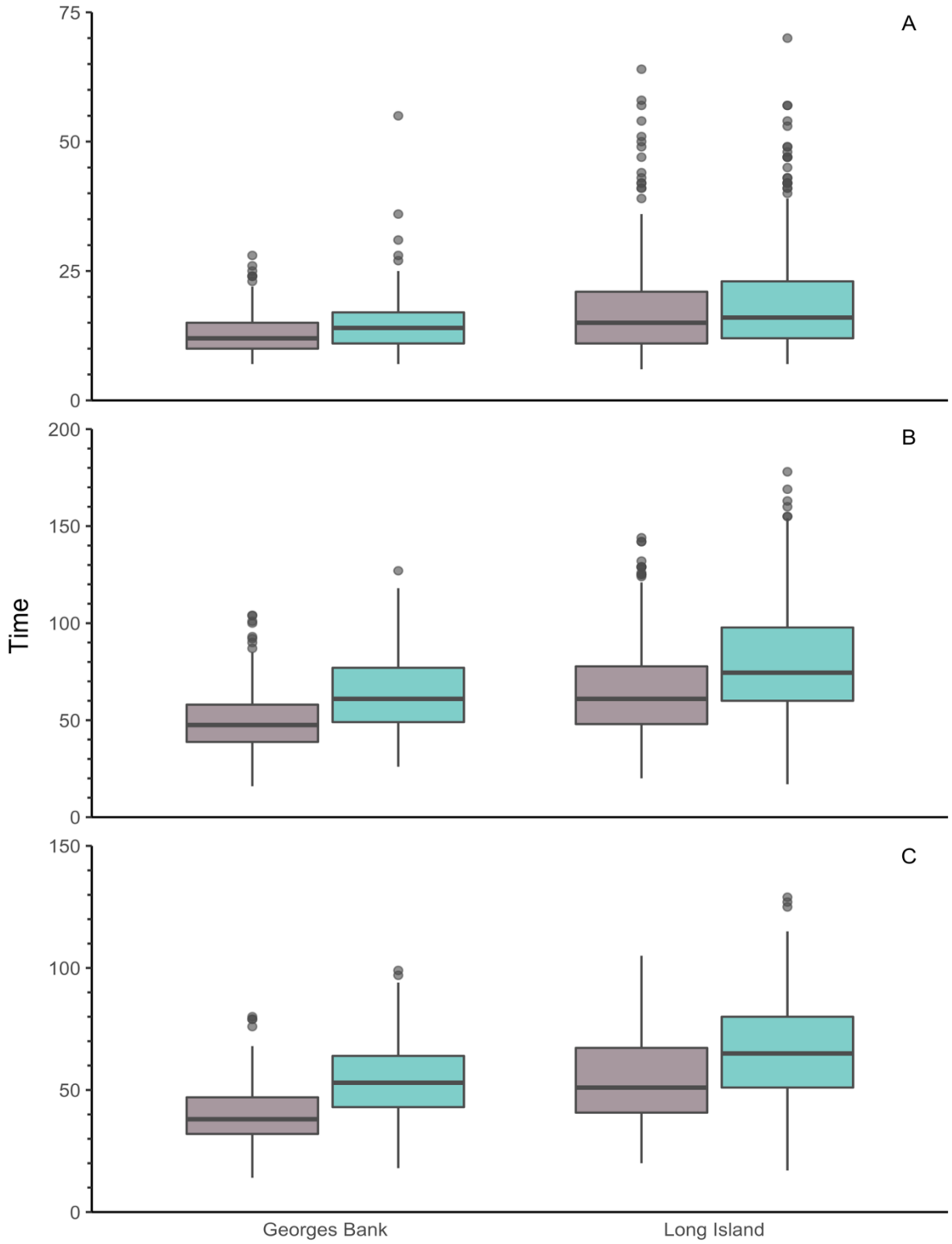

Figure 5.14 Growth rates by sex and site. Female (dark mauve, left) and male (green, right) growth rates within a site for (A) time to 50% maturity, (B) time to fishable size, (C) time (years) of reproduction. Box represents the interquartile range (IQR) with 50th percentile bar (median), whiskers represent 15*IQR, and points are outliers.

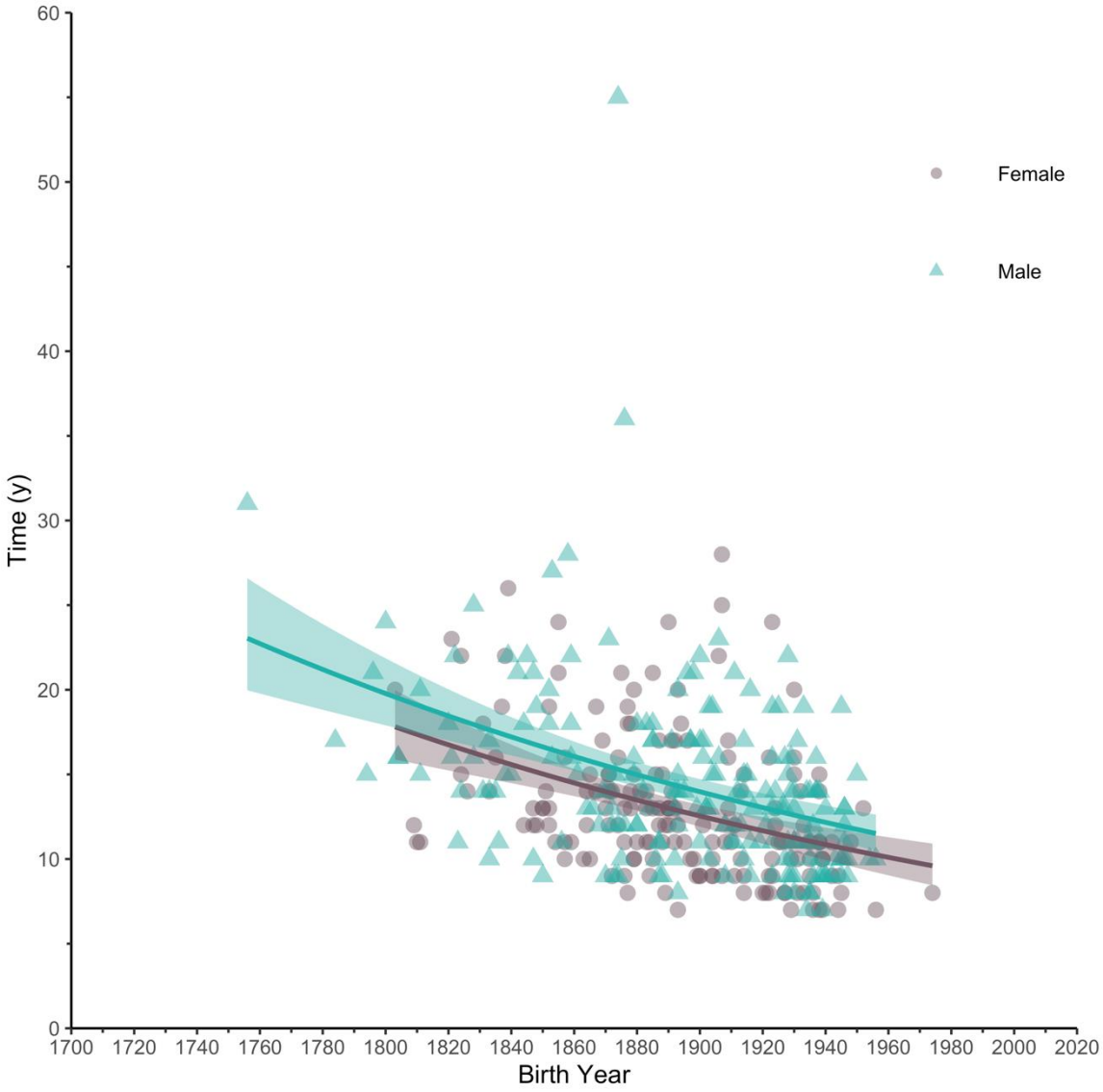

Figure 5.15 Georges Bank time to 50% maturity by birth year. Individual time to 52 mm and negative exponential regression with 95% confidence intervals.

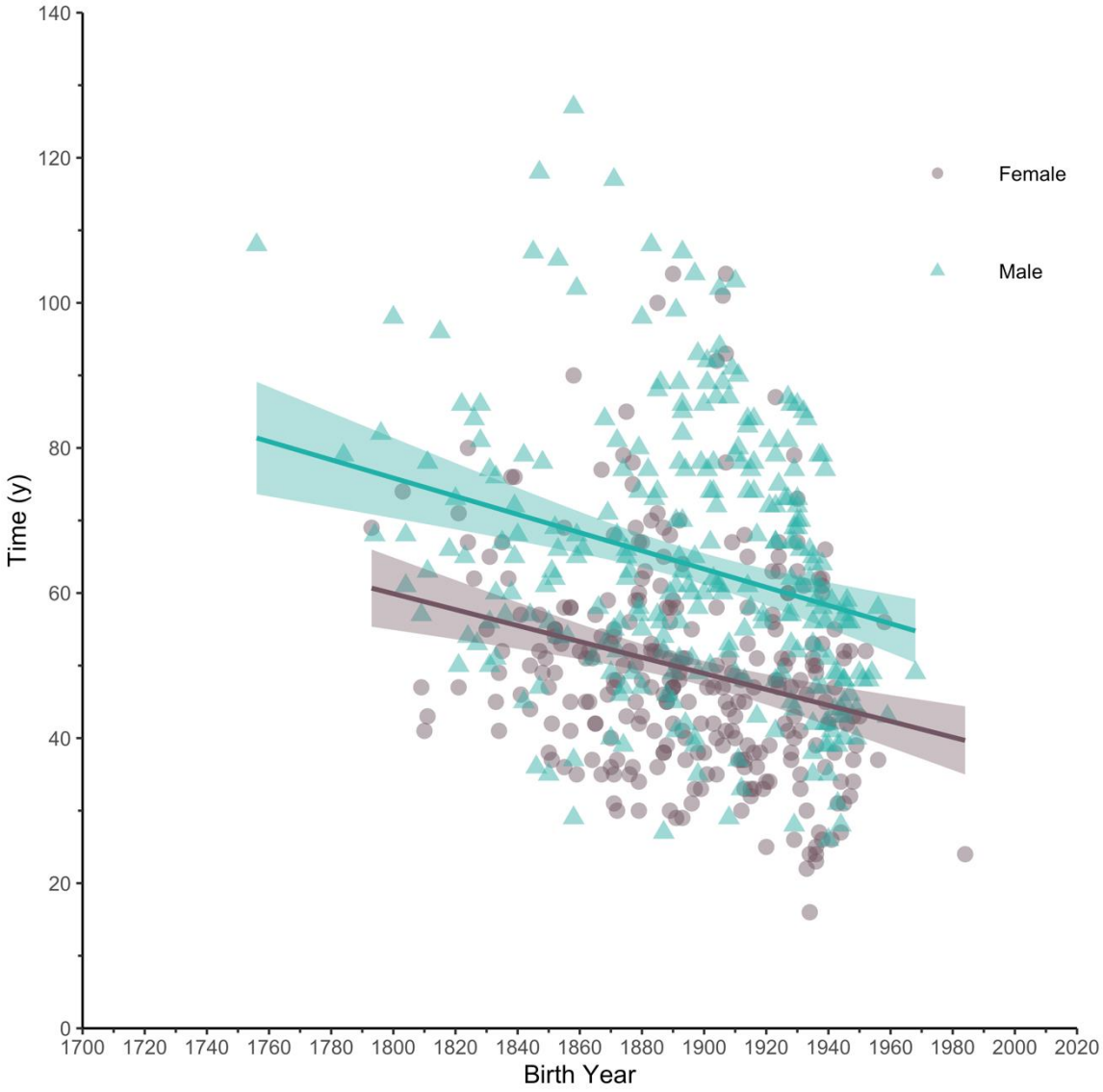

Figure 5.16 Georges Bank time to fishable size by birth year. Individual time to 80 mm and linear regression with 95% confidence intervals.

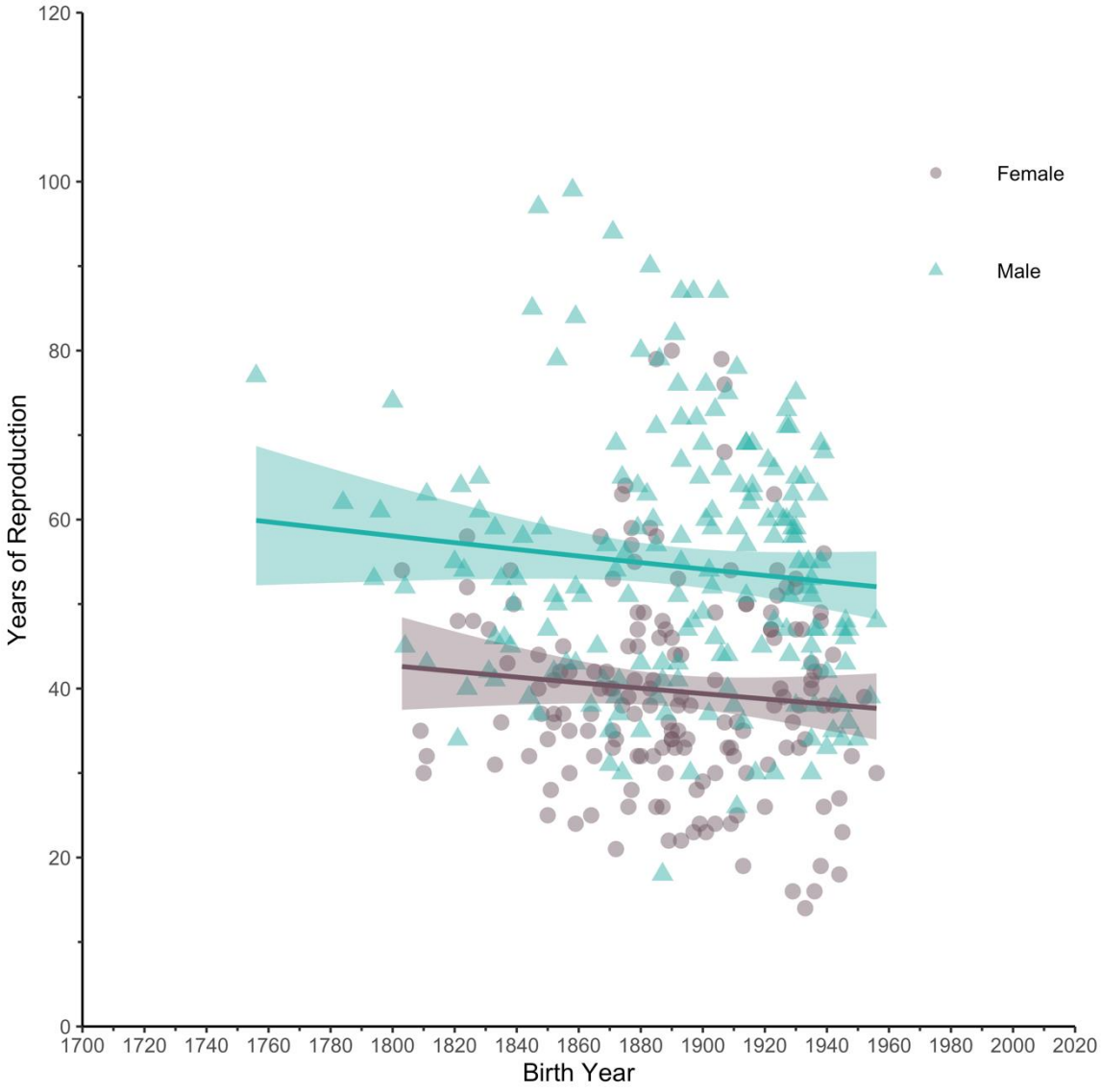

Figure 5.17 Georges Bank estimated years of reproduction by birth year. Individual time from 52-80 mm and negative exponential regression with 95% confidence intervals.

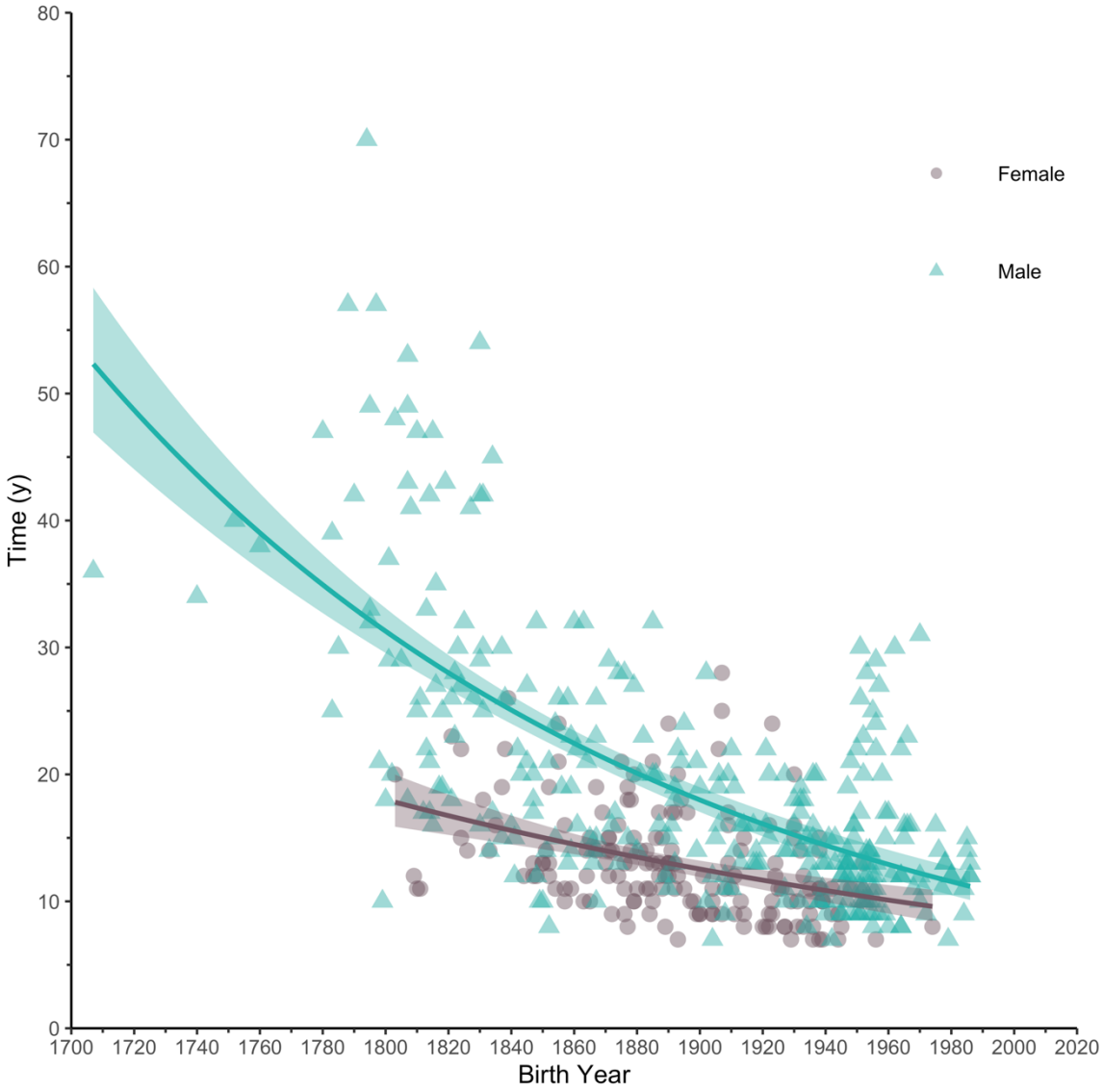

Figure 5.18 Long Island time to 50% maturity by birth year. Individual time to 52 mm and negative exponential regression with 95% confidence intervals.

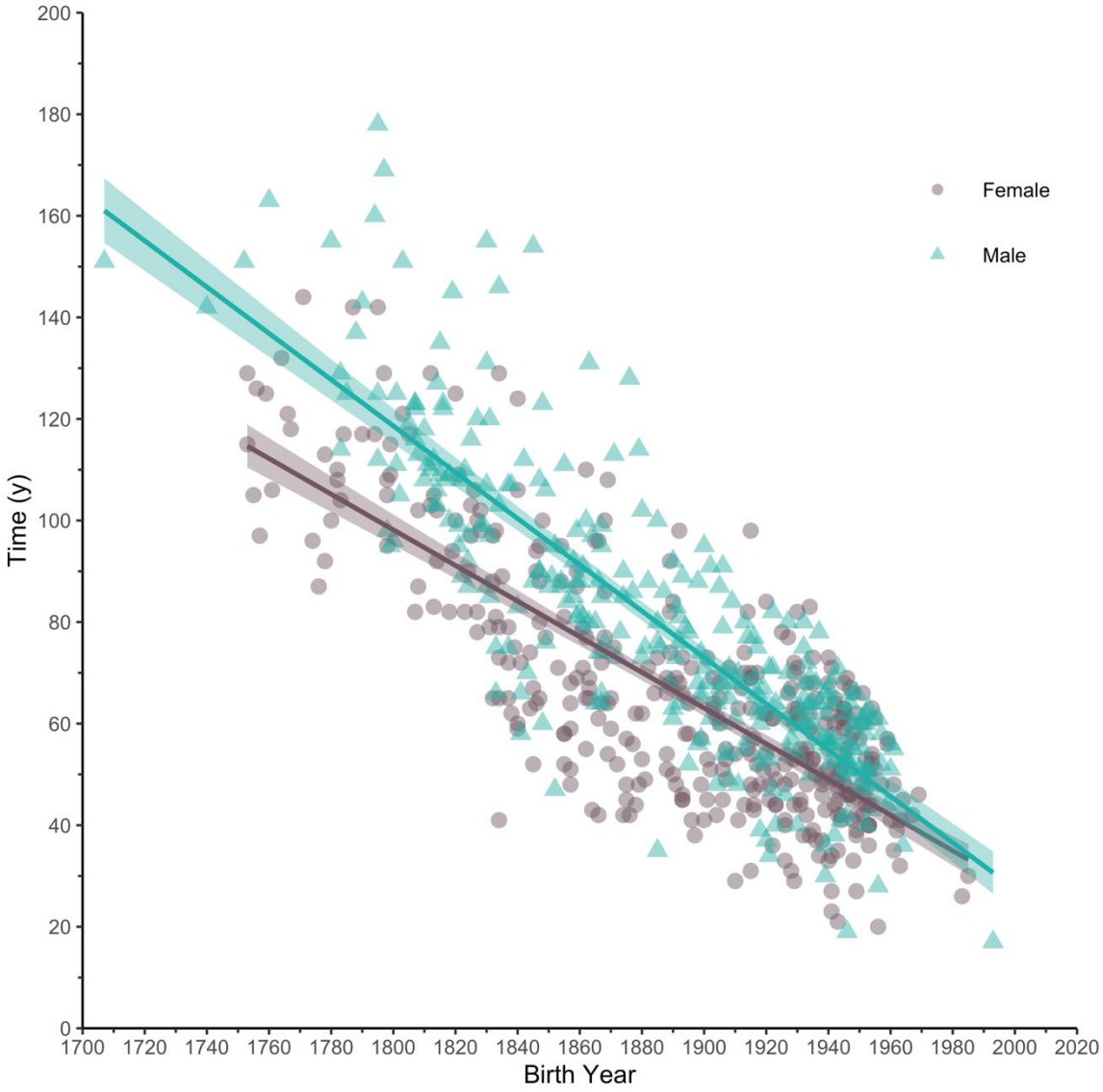

Figure 5.19 Long Island time to fishable size by birth year. Individual time to 80 mm and linear regression with 95% confidence intervals.

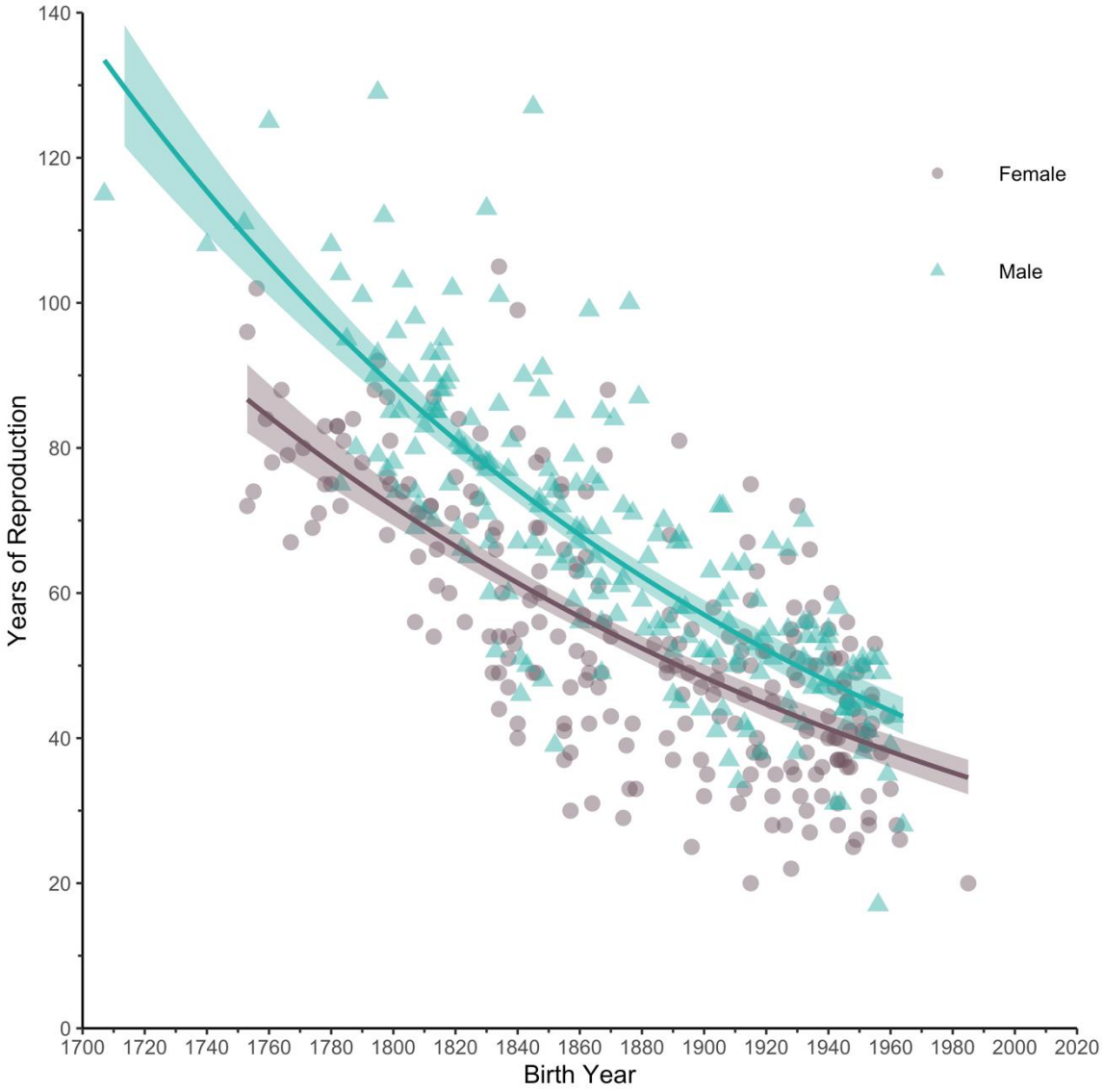

Figure 5.20 Long Island estimated years of reproduction by birth year. Individual time from 52-80 mm and negative exponential regression with 95% confidence intervals.

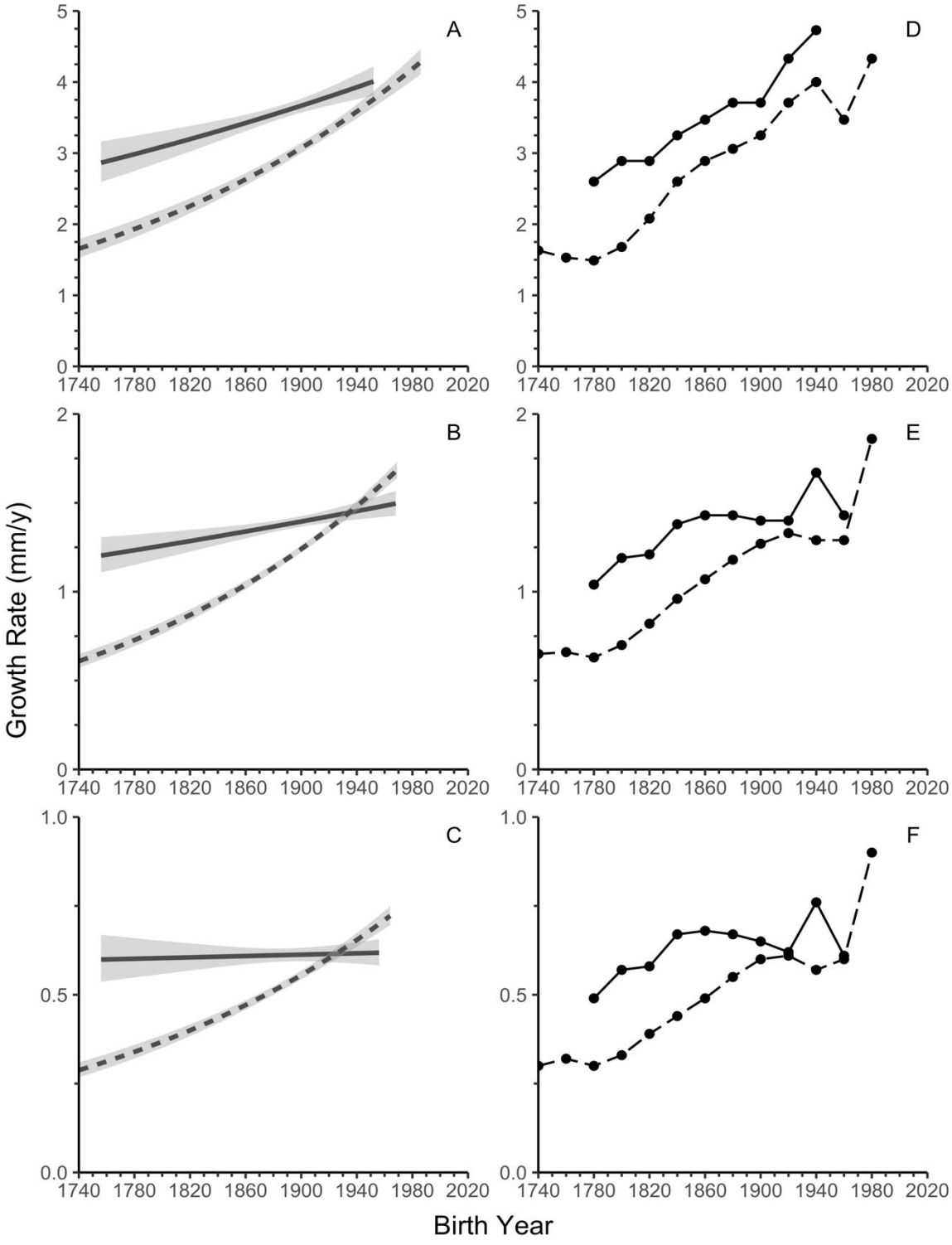

Figure 5.21 Regional growth rates by birth year. Regression model (A-C) and Modified Tanaka model (D-F) growth rate estimates for Georges Bank (solid) and Long Island (dashed) to size milestones: (A, D) size of 50% maturity - 52 mm; (B, E) to fishable size - 80 mm; (C, F) between 50% maturity and fishable size - 28 mm. Grey shading (A-C) represent standard error of regression models.

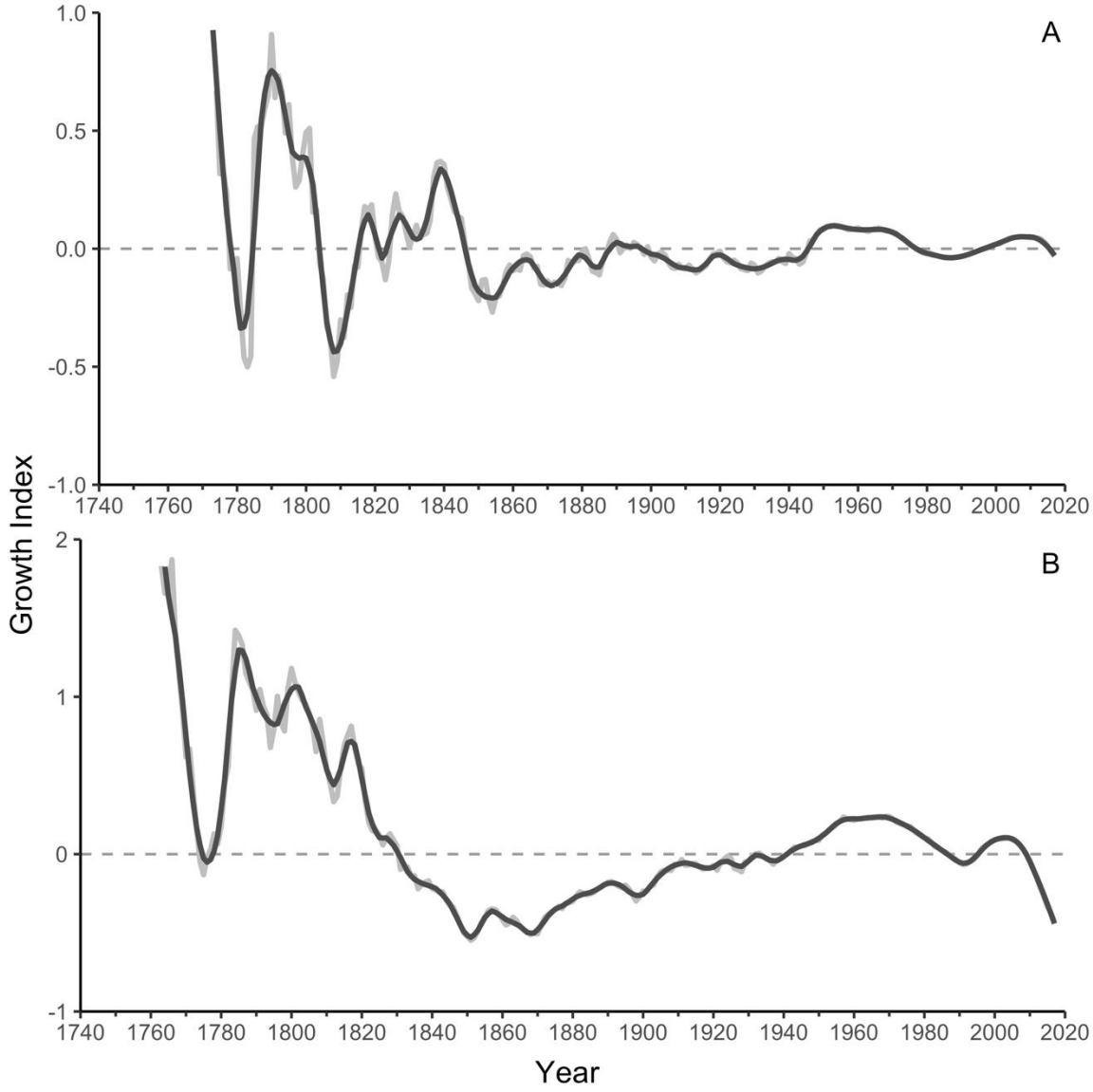

Figure 5.22 Regional population indexed growth over time. (A) Georges Bank and (B) Long Island growth indices (light grey line), and growth indices with a 15-y loess smoother (black line).

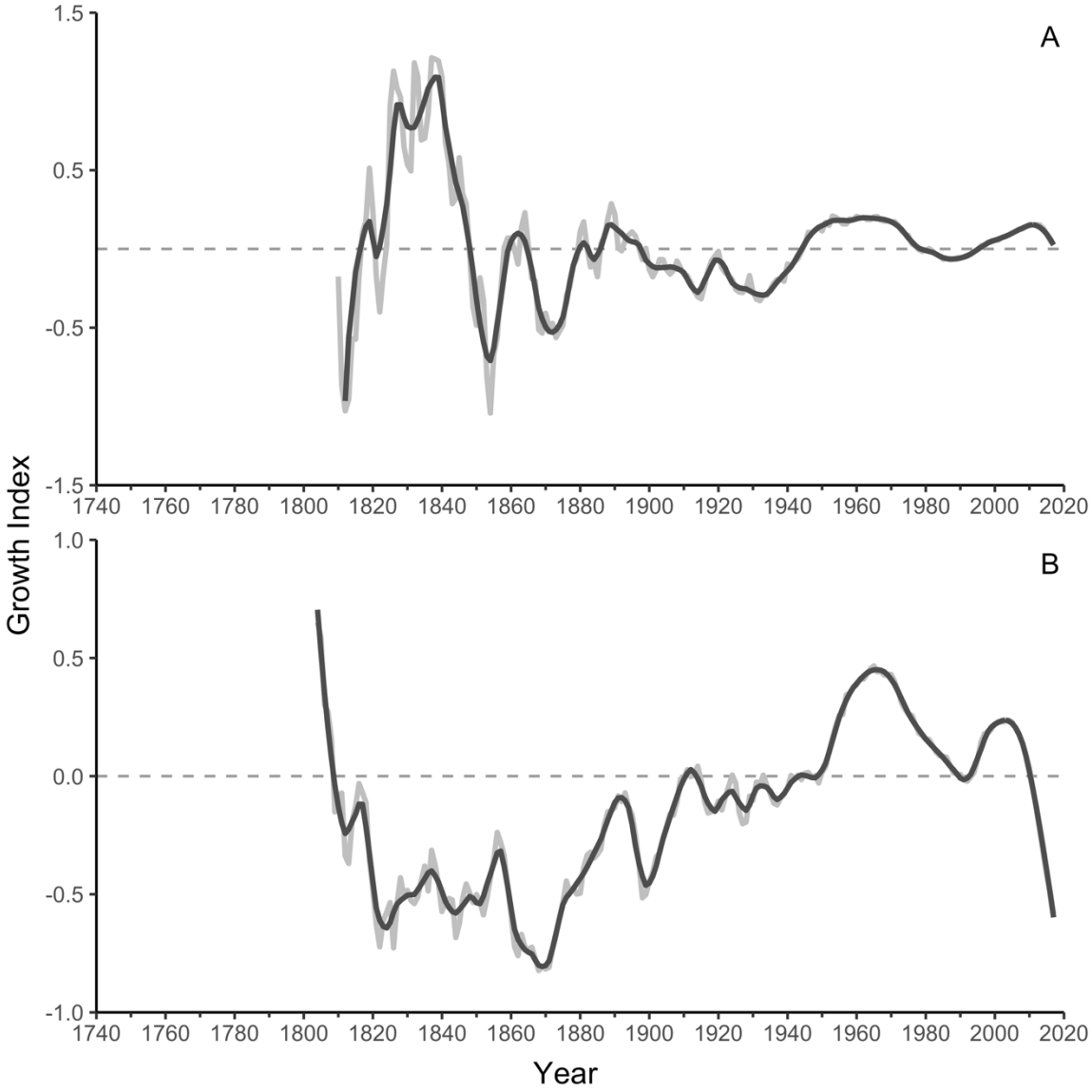

Figure 5.23 Female indexed growth over time. (A) Georges Bank and (B) Long Island growth indices (light grey line) and growth indices with a 15-y loess smoother (black line).

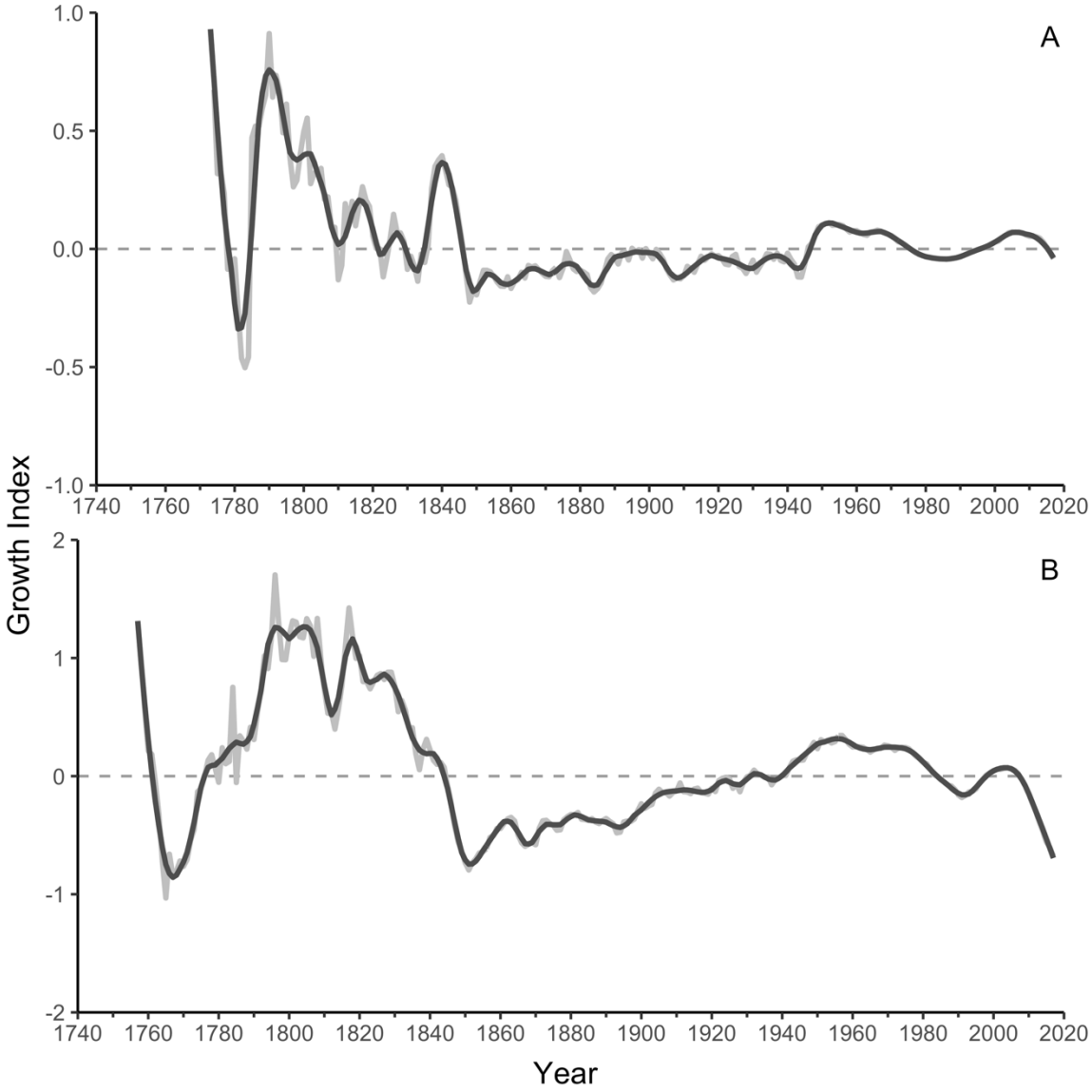

Figure 5.24 Male indexed growth over time. (A) Georges Bank and (B) Long Island growth indices (light grey line) and growth indices with a 15-y loess smoother (black line).

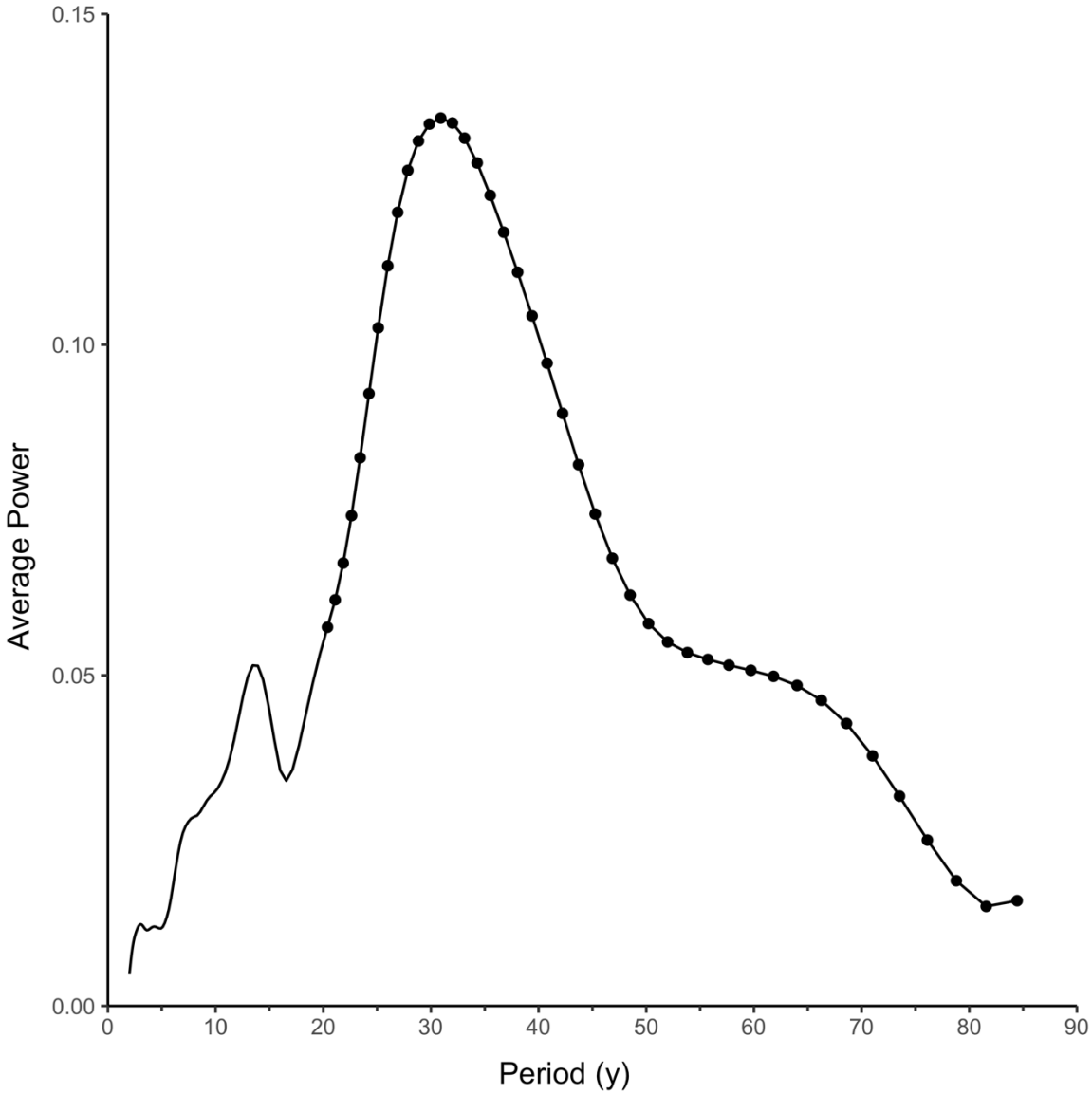

Figure 5.25 Within-region cross wavelet analysis. Georges Bank-Long Island population growth indices analyzed for average frequency power by time period. Significance represented by black points (alpha=0.10).

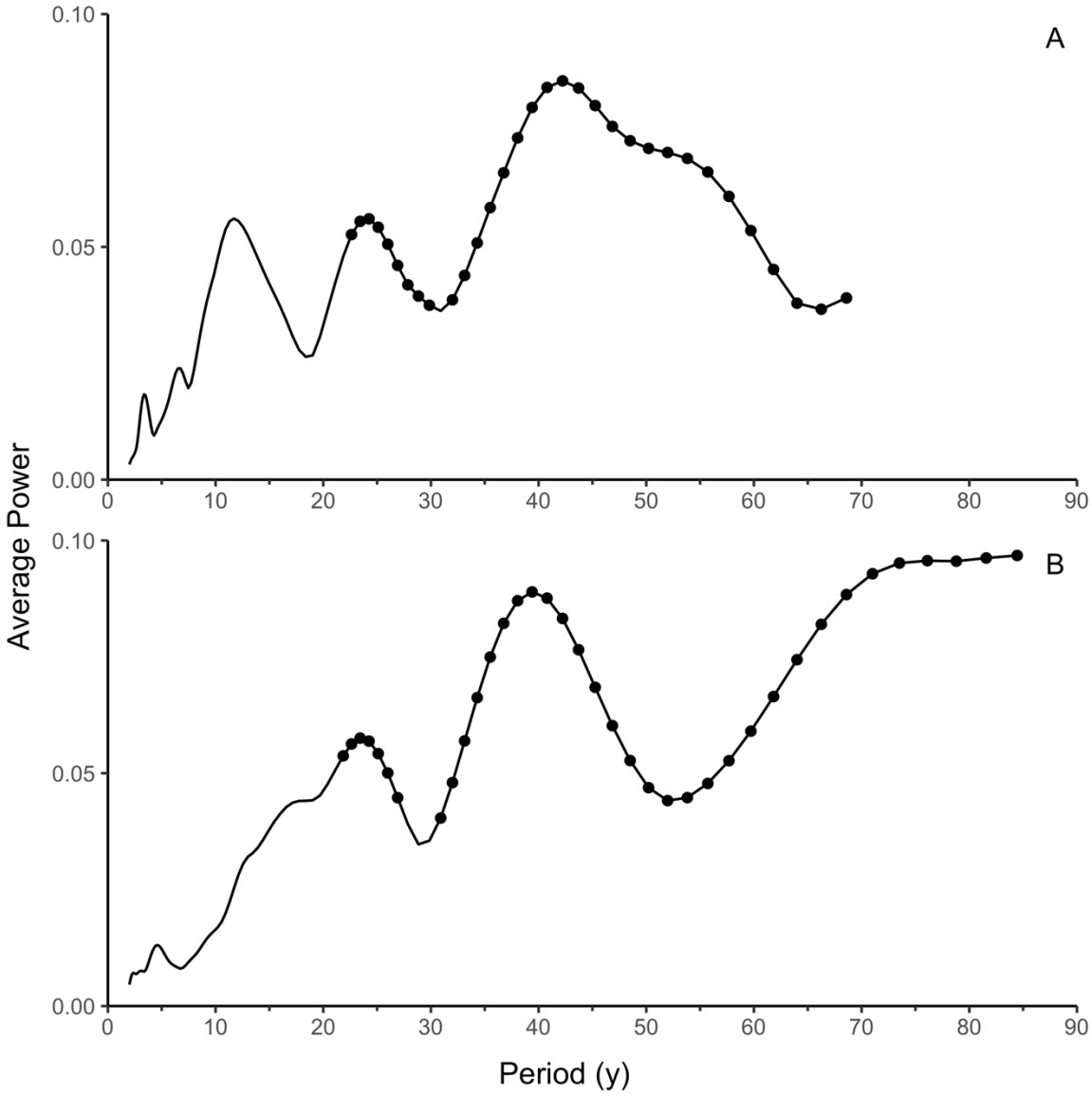

Figure 5.26 Within-sex cross wavelet analysis. (A) Female-female growth indices, and (B) male-male growth indices, analyzed for average frequency power by time period. Significance represented by black points (alpha=0.10).

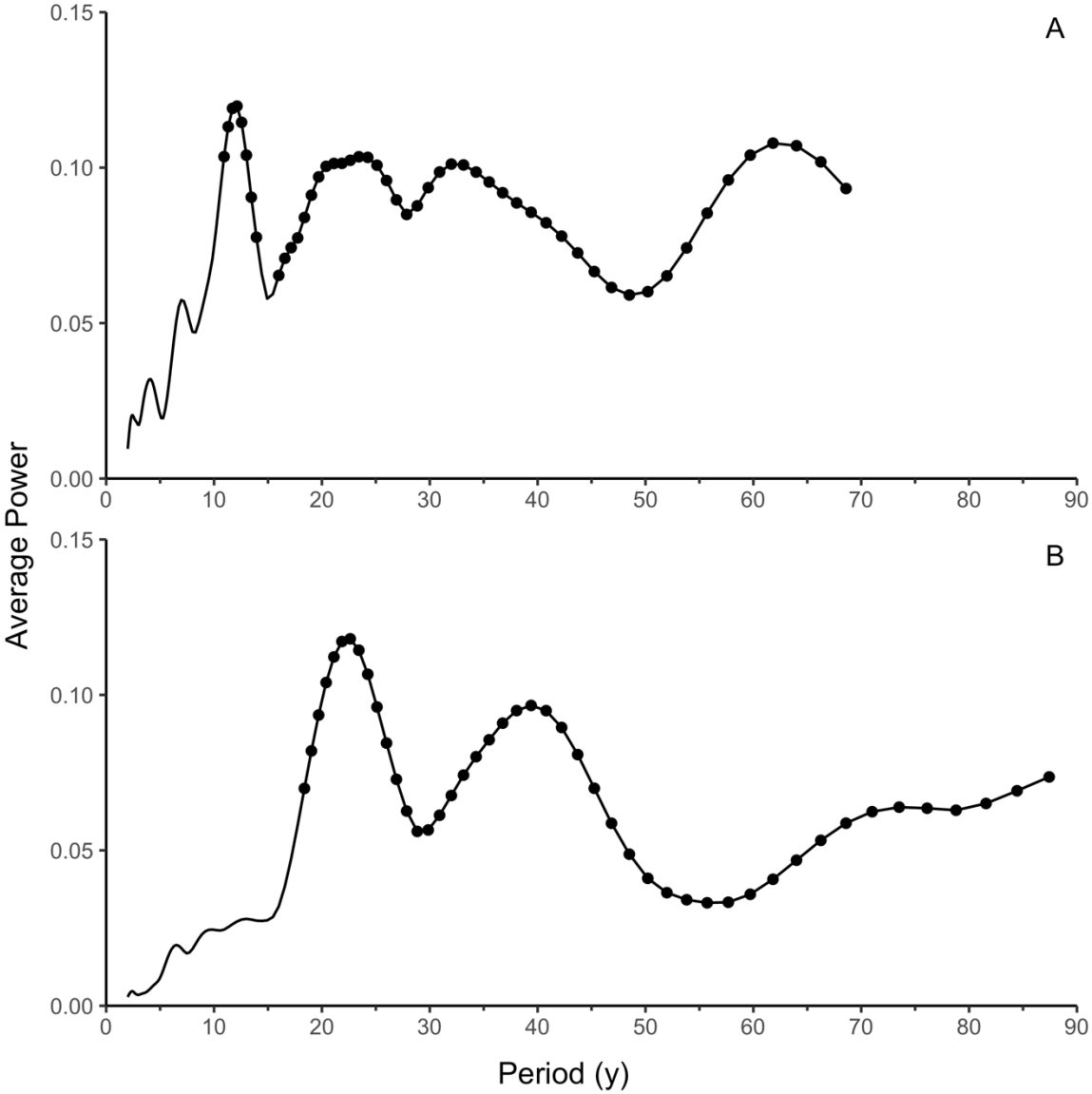

Figure 5.27 Within-site cross wavelet analysis. (A) Georges Bank male-female growth indices, and (B) Long Island male-female growth indices, analyzed for average frequency power by time period. Significance represented by black points (alpha=0.10).

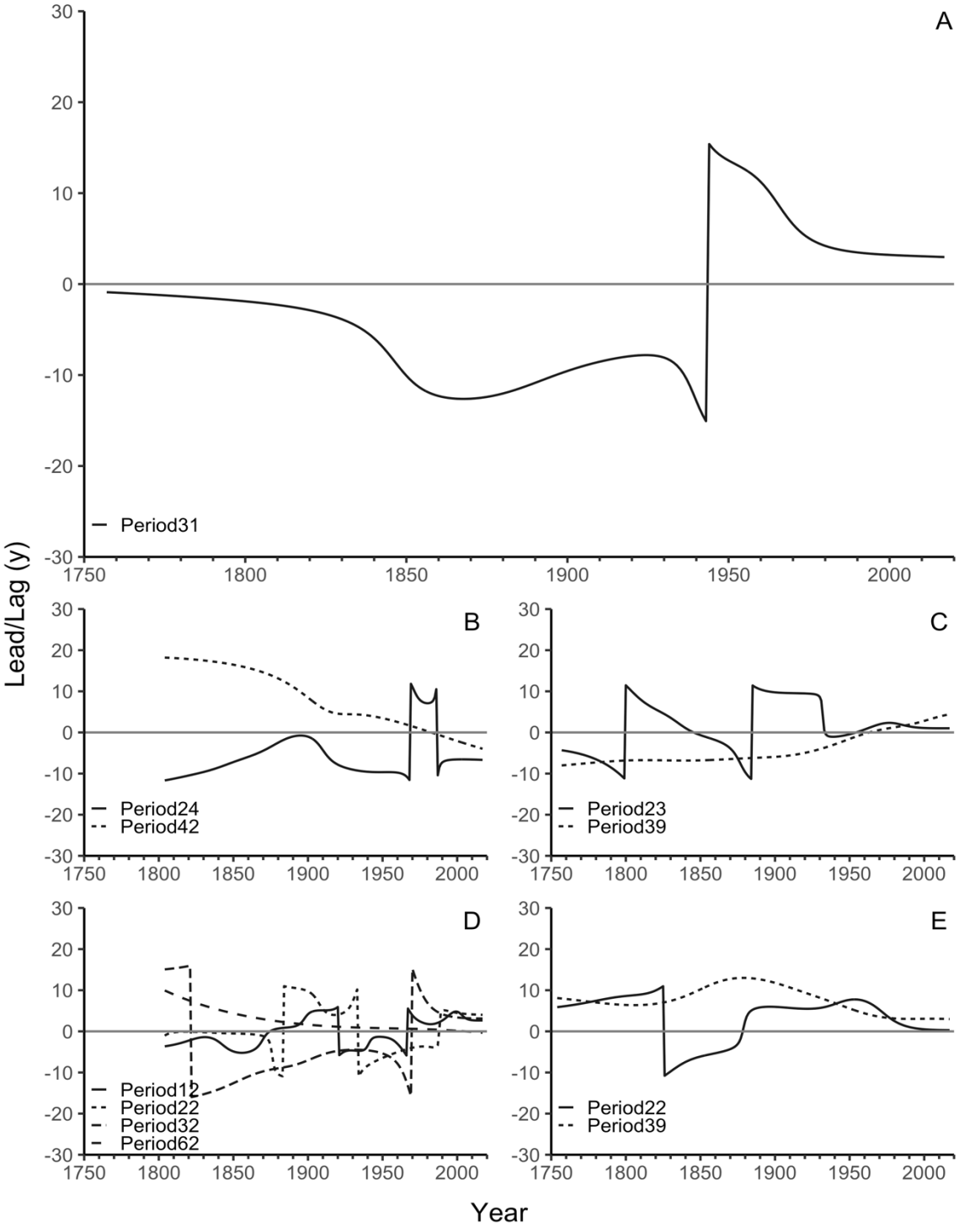

Figure 5.28 Lead/lag of growth periodicities. (A) Within-region comparison of Georges Bank "over" Long Island; (B) within-sex female comparison of Georges Bank "over" Long Island; (C) within-sex male comparison of Georges Bank "over" Long Island; (D) within-site of Georges Bank male "over" female; (E) within-site of Long Island male "over" female. Variable "over" leads when y values are positive and lags the alternative variable when y values are negative.

5.7 References

Ballesta-Artero I, Janssen R, van der Meer J, Witbaard R (2018) Interactive effects of temperature and food availability on the growth of *Arctica islandica* (Bivalvia) juveniles. Mar Environ Res 133:67

Black BA, Gillespie DC, MacLellan SE, Hand CM (2008) Establishing highly accurate production-age data using the tree-ring technique of crossdating: a case study for Pacific geoduck (*Panopea abrupta*). Can J Fish Aquat Sci 65:2572-2578

Flinn SA, Midway SR (2021) Trends in growth modeling in fisheries science. Fishes 6:1

Grissino-Mayer HD (2001) Evaluating crossdating accuracy: A manual and tutorial for the computer program COFECHA. Tree Ring Res 57:205-221

Harding JM, King SE, Powell EN, Mann R (2008) Decadal trends in age Structure and recruitment patterns of ocean quahogs *Arctica islandica* from the Mid-Atlantic Bight in relation to water temperature. J Shellfish Res 27:667-690

Hixon MA, Johnson DW, Sogard SM (2014) BOFFFFs: on the importance of conserving old-growth age structure in fishery populations. ICES J Mar Sci 71:2171-2185

Kilbourne KH, Alexander MA, Nye JA (2014) A low latitude paleoclimate perspective on Atlantic multidecadal variability. Journal of Marine Systems 133:4-13

Kirby JF (2005) Which wavelet best reproduces the Fourier power spectrum? Comput Geosci 31:846-864

Knudsen MF, Jacobsen BH, Seidenkrantz M-S, Olsen J (2014) Evidence for external forcing of the Atlantic Multidecadal Oscillation since termination of the Little Ice Age. Nat Commun 5:3323

Machu E, Ferret B, Garçon V (1999) Phytoplankton pigment distribution from SeaWiFS data in the subtropical convergence zone south of Africa: A wavelet analysis. Geophys Res Lett 26:1469-1472

Marali S, Schöne BR (2015) Oceanographic control on shell growth of *Arctica islandica* (Bivalvia) in surface waters of Northeast Iceland — implications for paleoclimate reconstructions. Palaeo Palaeo Palaeo 420:138-149

McShane PE, Anderson OF (1997) Resource allocation and growth rates in the sea urchin *Evechinus chloroticus* (Echinoidea: Echinometridae). Mar Biol 128:657-663

Moore GWK, Halfar J, Majeed H, Adey W, Kronz A (2017) Amplification of the Atlantic Multidecadal Oscillation associated with the onset of the industrial-era warming. Sci Rep 7:40861

NEFSC (2017) Report of the 63rd Northeast Regional Stock Assessment Workshop (63rd SAW). Northeast Fisheries Science Center. NEFSC Ref Doc 17-10, 414 pp

NEFSC (2020) Stock assessment of the ocean quahog for 2020. Woods Hole, MA: Northeast Fisheries Science Center. NEFSC Ref Doc 20-XXXX. 210 pp

Neves A, Vieira AR, Sequeira V, Silva E, Silva F, Duarte AM, Mendes S, Ganhão R, Assis C, Rebelo R, et al. 2022. Modelling Fish Growth with Imperfect Data: The Case of Trachurus picturatus. Fishes 7:52

Nye JA, Baker MR, Bell R, Kenny A, Kilbourne KH, Friedland KD, Martino E, Stachura MM, Van Houtan KS, Wood R (2014) Ecosystem effects of the Atlantic Multidecadal Oscillation. J Mar Syst 133:103-116

Pace SM, Powell EN, Mann R, Long MC (2017a) Comparison of age-frequency distributions for ocean quahogs *Arctica islandica* on the western Atlantic US continental shelf. Mar Ecol Prog Ser 585:81-98

Pace SM, Powell EN, Mann R, Long MC, Klinck JM (2017b) Development of an age—frequency distribution for ocean quahogs (*Arctica islandica*) on Georges Bank. J Shellfish Res 36:41-53

Pace SM, Powell EN, Mann R (2018) Two-hundred year record of increasing growth rates for ocean quahogs (*Arctica islandica*) from the northwestern Atlantic Ocean. J Exp Mar Biol Ecol 503:8-22

Peharda M, Vilibić I, Black BA, Markulin K, Dunić N, Džoić T, Mihanović H, Gačić M, Puljas S, Waldman R (2018) Using bivalve chronologies for quantifying environmental drivers in a semi-enclosed temperate sea. Sci Rep 8:5559

Powell EN, Stanton Jr RJ (1985) Estimating biomass and energy flow of molluscs in paleo-communities Palaeontology 28:1-34

Roesch A, Schmidbauer H (2018). WaveletComp: Computational Wavelet Analysis. R package version 1.1. https://CRAN.R-project.org/package=WaveletComp

Rothschild BJ, Mullen AJ (1985) The information content of stock-and-recruitment data and its non-parametric classification. ICES J Mar Sci 42:116-124

Schöne BR, Houk SD, Castro ADF, Fiebig J, Oschmann W, Kröncke I, Dreyer W, Gosselck F (2005) Daily growth rates in shells of *Arctica islandica*: sssessing sub-seasonal environmental controls on a long-lived bivalve mollusk. Palaios. 20:78-92

Sebens KP (1987) The ecology of indeterminate growth in animals. Annu Rev Ecol Syst 18:371-407

Seip KL, Grøn Ø, Wang H (2019) The North Atlantic oscillations: cycle times for the NAO, the AMO and the AMOC. Climate 7:43

Soniat TM, Klinck JM, Powell EN, Hofmann EE (2006) Understanding the success and failure of oyster populations: climatic cycles and *Perkinsus marinus*. J Shellfish Res 25:83-93

Tanaka, M (1982) A new growth curve which expresses infinite increase. Pub Amakusa Mar Biol Lab 6:167-177

Tanaka, M (1988) Eco-physiological meaning of parameters of ALOG growth curve. Pub Amakusa Mar Biol Lab 9:103-106

Thompson I, Jones DS, Dreibelbis D (1980a) Annual internal growth banding and life history of the ocean quahog *Arctica islandica* (Mollusca: Bivalvia). Mar Biol 57:25-34

Thompson I, Jones DS, Ropes JW (1980b) Advanced age for sexual maturity in the ocean quahog *Arctica islandica* (Mollusca: Bivalvia). Mar Biol 57:35-39

Thorarinsdóttir G, Steingrímsson S (2000) Size and age at sexual maturity and sex ratio in the ocean quahog, *Arctica islandica* (Linnaeus, 1767), off Northwest Iceland. J Shellfish Res 19:943-947

Torrence C, Compo GP (1998) A practical guide to wavelet analysis. Bull Amer Meteor Soc 79:61-78

Velázquez-Abunader I, Monsreal-Vela K, Poot-López GR (2016) Model selection for determining the growth of juveniles and sub-adults of two species of shrimp (Decapoda, Penaeidae) in a tropical coastal lagoon. Crustaceana 89:29-45

von Bertalanffy L (1938) A quantitative theory of organic growth. Hum Biol 10:181–213

Xu H, Kim H-M, Nye JA, Hameed S (2015) Impacts of the North Atlantic Oscillation on sea surface temperature on the Northeast US Continental Shelf. Cont Shelf Res 105:60-66

Zaklan, SD, Ydenber R (1997) The body size-burial depth relationship in the infaunal clam *Mya arenaria*. J Exp Mar Biol Ecol 215:1-17

CHAPTER VI CONCLUSIONS

6.1 Age-Reader Error

A 3-fold error study indicated that the 610-sample *Arctica islandica* age dataset from Georges Bank (GB) met the predetermined error thresholds for bias (conditionally because of significant and nonsignificant results), precision (average coefficient of variation less than 7%), and error frequency (less than 10%). Pending improved age-validation data for this species, particularly for the younger animals entering the fishery, these age data are within acceptable error bounds proposed in this study to be used for age compositions and suggest that the reader aging protocol can be used in future age-structure studies. These analyses also establish the degree of uncertainty associated with age compositions for integration into fisheries assessment models. The representativeness of the GB population for error applications generally is, as yet, unknown, though published growth rates on GB are thought to be higher than other locations at similar latitudes. Also unclear is the degree to which these higher growth rates might provide reduced precision relative to animals aged from other regions, as lower precision in this study was associated with periods of higher growth rate. Regardless, the degree of uncertainty places a detection limit on identifying the shortest detectable period of low recruitment, a consideration of some importance, given the population dynamics of this species. Age frequencies derived are, in effect, smoothed by this degree of error and pose a limitation on the interpretation of fine-scale variations in the inferred cohort dynamics within the population.

Given the cost of processing and the number of aged animals required to provide an adequate age-at-length relationship across many ages wherein high variability exists in

age at length, attention to increasing precision is necessary and may result in the reduction of required sample size. The differential error rate between males and females provides a possible opportunity to reduce age determination bias by focusing on females. Precision was clearly greater and bias less for females. The tendency for females to be larger than males would suggest some bias in the sex ratio of landings as well, which would support the preferential use of female SSB in an assessment. Although a number of studies have examined *A. islandica* aging methods in the Mid-Atlantic region, a focus on the increased uncertainty in age determination at small size, which is conflated with the number of males in those size classes, has not occurred. Nonetheless, this study suggests that a focus on females would reduce uncertainty in the age frequency and possibly reduce the required sample number to produce a reliable age-length key (ALK) and subsequent population age-frequency distribution.

6.2 Georges Bank Population Dynamics

Because GB provides a virgin-stock proxy, age and length data are not fishery biased and represent natural mortality and recruitment processes. Sex-based demographics are different in regard to length frequencies and derived ALKs, growth rates, and estimated natural mortality and longevity. The reliability of constructed ALKs has long been debated for an animal with such extreme age-length data variability, and this study discovered that a large age sample can produce reliable ALKs for the modal section of an age frequency when sex-specific ALKs are used. Assumptions of prolonged lapses in recruitment were not substantiated for the GB population and yearly cohorts were observed for the past century; however, depressed recruitment was observed at somewhat regular intervals averaging as 8-y cyclicities. Regular recruitment and

expanded longevity than previously documented for GB indicates that this species is capable of rebuilding, but periods of reduced recruitment and population expansion at the turn of the 1900s support hypotheses that recruitment and mortality of this species are highly responsive to environmental conditions.

This study evaluated sex-based population dynamics from a substantial age sample; however, data were collected from a single sampling site. Additional samples from GB are needed to ensure this dataset is representative of the entire GB area and that population dynamics are homogenous across GB. Assuming representativeness, these data can supply age-based assessments with sex-specific ALKs, longevity estimates, and natural mortality rates. As fishery managers move towards age-based models for this species, it would also be critical to understand age compositions of young animals that have not yet recruited to the fishery, ensure consistent recruitment from recent decades not present in this fishery sample, and identify the size at which sexual dimorphism originates. In addition, understanding the deviation in sex-based mortality could be supported by a more thorough understanding of *A. islandica* behavior in terms of sex-based burrowing rates, burrowing depths, and burrowing responses to adverse environmental factors and the real possibility of an increased cost of reproduction in females as an outcome of their larger size increasing vulnerability to temperature extremes. Understanding the processes that drive sex-based demographics, whether life-history tactics or behavioral responses, would greatly inform recruitment potential and stability of this species when confronted with fluctuating climatic and fishery effects.

6.3 Long Island Population Dynamics

Long Island (LI) *A. islandica* population dynamics support findings from the GB population dynamics study that *A. islandica* are sexually dimorphic. Females at LI are significantly offset to larger size classes than males, and females represent the maximum observed lengths. Sex-ratio at size clearly indicated that males dominated small size classes $<$ 80 mm, while females dominated large size classes $\geq$ 95 mm. Age-length data also suggested that females grow faster than males, because females are generally younger at size compared to their male counterparts. The population ALK was reliable at reproducing the modal section of the population age frequency derived from an extremely large age dataset 100% of the time, and the distribution was only offset from the true distribution 16% of the time (alpha = 0.05). A reliable population ALK offers fishery managers the option to maintain the LI assessment as a non-sex-differentiated model, particularly since the population-scale total mortality estimates were equal between population, females, and males. This decision would be both time and cost effective.

Maximum ages at LI are higher than previously reported for the US Mid-Atlantic region with a male *A. islandica* visually aged to 310 y. Age-reader error is high for LI males, and some flexibility is expected in the true age of these organisms, but the age is still remarkable even with error considered. Continued age validation of animals located in the Cold Pool, and for young, male *A. islandica* whose error is particularly high, would resolve many questions in regard to accurate aging methods and improve our confidence in age demographics for this species, as even isotope dating inherits substantial age error.

6.4 Regional Growth Dynamics

Arctica islandica is a challenging commercial species to manage as ALKs to this point have been unreliable and age estimates derived from traditional von Bertalanffy growth models have been inaccurate in recent studies of Mid-Atlantic populations. A sample of 569 animals from GB, and 865 animals from LI demonstrated that the Modified Tanaka growth model is the best fit for the indeterminate growth observed at old ages and large size classes. Modified Tanaka and growth rate results also revealed that *A. islandica* at GB generally grow faster than at LI, and that females grow faster than males regardless of population. Growth curves are also highly dependent on the birth year of the animal, where growth rates of mature animals entering the fishery are 104% faster at GB for animals born in the 1980s compared to animals born in the 1860s, and 48% faster at LI for animals born in the 1980s compared to the 1860s.

Whether to model growth for a single stock versus by population and cohort, is an important decision for federal fishery biologists because if birth year is ignored, model parameters do not reflect contemporary growth of upcoming generations. Inaccurate growth estimates would likely underestimate stock biomass projections, and also overestimate the number of spawning years prior to *A. islandica* recruitment to the fishery. Additionally, understanding how these growth relationships correlate with environmental cycles will assist in accurate forecasts of future growth conditions and growth responses to anomalous temperatures. The continuation of cross wavelet analyses between *A. islandica* growth indices with both basin-wide (e.g., AMO, NAO, Atlantic Meridional Overturning Circulation) and local temperature variability (Cold Pool

strength, ENSO), will provide insight into fishery milestone timing and conditions necessary for successful growth and recruitment.

6.5 Regional Fishery Dynamics

The US *A. islandica* stock is divided into two distinct area-specific assessment models. One model evaluates the northern region of the stock at GB, while the other model assesses a much larger area spanning the continental shelf west of GB southeast to southern Virginia. Two sites were evaluated in this study, GB located in the northern management area and LI located in the center of the southern management area. The GB site is relatively unfished and represents a pseudo-virgin population, whereas LI represents the greatest stock landings in the US Mid-Atlantic fishery. Currently, the assessment models applied to the active fishery in the southern region incorporates length-based data, but with capacity to apply age-based data if chosen.

Similarities between LI and GB include sexually dimorphic growth, a population sex ratio that is biased towards males, and relatively coherent recruitment cycles that occur in 8-y periods. However, that is where the likenesses end. The modes of the length frequencies were offset by sex and site, with GB length frequency central tendencies generally larger than those of the LI length frequencies. Growth rates were faster at GB than LI, and female growth rates were faster than males. Not surprisingly, the ALKs at GB and LI were not interchangeable due to the above-mentioned age and length relationships and at least two independent keys are needed for the Mid-Atlantic stock. Female growth rates are divergent from males and aging only females at a site to reduce aging error would not be sufficient to replicate the population ALK and subsequent population age frequency, both male and female ages are required. Instantaneous

mortality rates at GB were approximately double those at LI, and GB appeared to have a higher female mortality rate than males; although, GB had a smaller sample size than LI and mortality may be inflated due to the absence of rare very-old animals at GB. Finally, the transition from male to female dominance by size class occurred across different size ranges dependent on the population, and this metric may interfere with predicted spawning-stock biomass estimates if the sex proportions are not designated correctly across a length sample by site.

Evidence listed herein assert that the GB and LI sites require different ALKs, mortality estimates, and sex ratios at size. It is also still unknown if the LI population dynamics are comparable to other *A. islandica* populations within the southern management area, or if models should be developed latitudinally or in reference to location in the Cold Pool footprint. Furthermore, additional data are needed to understand how patchy the age-length demographics are within and between populations, and if replication of the modal section of the age-frequency distribution is sufficient for the purposes of the assessment model, or if the tails need to be resolved in the ALK analyses.

Interpretation of an age-frequency distribution is a confounding task as an age frequency can be evaluated through either a mortality or recruitment lens. For instance, are the peaks and troughs of an age distribution the result of fluctuating morality that periodically removed animals from a population, or the product of successful recruitment over time that systematically added animals to a population? Each option assumes that the other variable is held constant through time. In reality, both mortality and recruitment rates likely change over time and survival and mortality are intrinsically linked, particularly for benthic invertebrates that are highly dependent on external conditions for

suitable habitat and reproductive success. When considering the age frequency of *A. islandica*, is the long tail of old animals born prior to 1890 the result of 1) low mortality rates long ago that allowed such old animals to persevere for centuries, 2) low recruitment during 1700-1890 at the initiation of a range expansion into the Mid-Atlantic 200-300 y ago followed by a population explosion in the 1880s, or 3) are these lingering extremely old animals the product of successful genotypes that have optimal functionality within these environments? Understanding conditions that drive mortality and recruitment in recent generations, can facilitate our collective interpretation of Mid-Atlantic shelf ecology in prior centuries as well as the concurrent multi-centenarians still living in the modern fishery.